Generalized Parton Distributions of Pions. Spin Structure of Hadrons.

PhD Thesis
Author: Aurore Courtoy
Advisor: Santiago Noguera
Departamento de Física Teórica
Universidad de Valencia

Tout homme est fou, mais qu'est-ce qu'une destinée humaine sinon une vie d'effort pour unir ce fou à l'Univers.

Malraux

Max (ou encore Nicole), comme beaucoup d'autres physiciens qui font des choses très impalpables et abstraites au possible, pensait qu'il n'y avait plus de questions encore sans réponse en QCD; que l'on connaissait tout; que l'on maîtrisait et savait déjà jouer avec la structure des petits hadrons comme on joue aux Legos.

Voilà comment, un vendredi après-midi, j'ai tenté de lui expliquer que la physique hadronique était un sujet passionant, au même titre que ses bien aimés trous noirs.

PS: Je m'en suis, bien évidemment, tenue à l'Introduction.

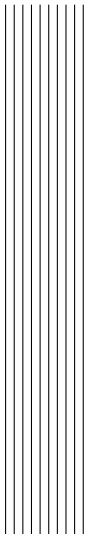

Contents

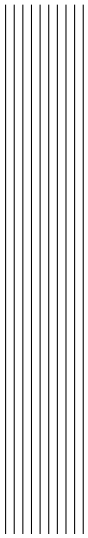

Distribuciones Generalizadas de Partones en Piones. Estructura de Espín de Hadrones.

Introducción

Una de las preguntas de física a la que aún no hemos contestado es entender como se construyen los hadrones a partir de los quarks y gluones. Efectivamente, la idea que los quarks son los elementos constituyentes de los hadrones viene del año 1964 cuando Gell-Mann y Zweig publicaron sus famosos artículos [96, 207]. En 1973 Fritzsch, Gell-Mann y Leutwyler [95] propusieron la formulación de la CromoDinámica Cuántica (QCD) como la teoría de la interacción fuerte entre quarks. A pesar de que QCD haya sido formulada hace unos 35 años y que esta teoría haya sido verificada a altas energías, no hemos sido capaces de desvelar la estructura detallada de los hadrones. Uno se podría preguntar porqué todavía no lo hemos logrado. La respuesta es que las proprias características de las interacciones fuertes hacen que esta tarea sea muy intrincada.

A alta energía, el tratamiento perturbativo de QCD, que se justifica por la libertad asintótica [106, 169], permite que expliquemos los fenómenos hadrónicos. Los ingredientes básicos que describen los hadrones son las *Distribuciones de Partones*. Esas distribuciones pueden ser determinadas experimentalmente a un valor relativamente alto de la transferencia de momento Q^2. Entonces, la QCD perturbativa dicta la evolución de esas distribuciones con la transferencia de momento, con lo cual podemos dar predicciones para los observables.

En cambio, a baja energía (tipicamente por debajo de ~ 1 GeV), un tal tratamiento perturbativo de la QCD no está justificada. Entonces, ya no podemos describir a través de QCD los observables que son relevantes a baja energía. En este régimen, los modelos hadrónicos así como las teorías efectivas entran en juego. En estos esquemas, los parámetros vienen fijados por la fenomenología.

Ahora bien, no existe una clara y definida frontera entre estos dos regímenes. Tampoco existen unas conexiones definidas entre los grados de libertad relevantes : aunque sean los grados de libertad elementares de la QCD, los quarks y gluones libres nunca han sido observados. Este hecho nos indicó que los quarks eran confinados en los hadrones. Por otro lado, una otra característica

importante de las interacciones fuertes está relacionada con la simetría quiral. En el límite en él que los quarks no tienen masa, la simetría quiral, una propriedad del lagrangiano de QCD, se realiza a la Goldstone, o sea : está espontaneamente rota. El papel fundamental jugado por esa simetría y su realización ha sido confirmado por la masa pequeña del pión así como por las propriedades de los procesos fuertes a energía intermedia. Citamos, como ejemplo, la Conservación Parcial de la Corriente Axial (PCAC) o los teoremas de piones blandos (Soft Pion Theorems). Por lo tanto, la estructura de los hadrones tiene que surgir de los efectos combinados del confinamiento y de la realización de la simetría quiral. En particular, el régimen energético en el que podamos reunir información sobre la estructura de las hadrones se encuentra exactamente en la frontera entre estos dos regímenes que acabamos de describir. En otras palabras, situamos el régimen de energía que nos interesa en la región donde suponemos que tanto el confinamientocomo la simetría quiral entran en juego.

Una manera de conectar los mundos *perturbativo* y *no perturbativo* sería el estudio de las Distribuciones de Partones a través de modelos. El esquema que se propone es : construimos modelos cuyas caracteristícas "imitan" de algún modo las propriedades de la QCD que son relevantes en el rango de energía que estamos considerando ($\sim$ 1 GeV); evaluamos las Distribuciones de Partones en este modelo y, finalmente, evolucionamos esas distribuciones a la escala de los experimentos para poder comparar nuestros resultados con los datos.

Las reacciones que permiten el acceso a los diferentes tipos de Distribuciones de Partones han recibido mucha atención de parte de la comunidad de física hadrónica. Esas reacciones son tal que permiten mirar con una buena resolución el interior de los hadrones, resolviendo distancias muy pequeñas, i.e. configuraciones muy pequeñas de quarks y gluones. Como que, a cortas distancias, las interacciones entre quarks se hacen debiles, esta parte del proceso se puede describir a través de la QCD perturbativa. Una resolución a tan cortas distancias se obtiene con la ayuda de sondas que no interactuan fuertemente. Una tal sonda, tipicamente un fotón, viene proporcionada por "reacciones duras", como la difusión profundamente inelástica (DIS), DIS semi-inclusiva, Deeply Virtual Compton Scattering,.... En este esquema, las distribuciones de partones reflejan como el blanco reacciona a la sonda, o cómo los quarks y gluones están distribuidos dentro del blanco. Los elementos para entender la estructura de los hadrones se encuentran en esta etapa: la gran virtualidad del fotón intercambiado, Q^2, involucrado en estos procesos permite la factorización entre las contribuciones dura (perturbativa) y blanda (no perturbativa) de sus amplitudes. Es exactemente esa parte *blanda/soft* de los procesos lo que nos va a interesar a lo largo de esta tesis.

Los primeros pasos hacia la comprensión de las estructura de los hadrones fueron dados estudiendo las secciones eficaces totales de procesos totalmente inclusivos o asimetrías longitudinales. Esas cantidades se interpretan facilmente en el marco de modelos de partones [113].

Desde un punto de vista teórico, las distribuciones de partones están relacionadas con elementos de matriz de operadores bilocales en el cono de luz entre estados hadrónicos inicial y final iguales, es decir la misma partícula con el mismo momento. Esas distribuciones tienen una interpretación probabilistica sencilla. Para quarks colineales, las distribuciones de partones $q(x)$ reciben el nombre de densidades de número porqué reflejan la densidad de probabilidad de encontrar un quark con una fracción x del momento longitudinal del hadrón padre, independietemente de la orientación de su espín. De la misma manera, surgió la definición de otras cantidades muy interesantes tal como la distribución de helicidad (polarización longitudinal) o también la más misteriosa distribución

de transversidad. Ahora bien, la distribución de polarización transversa no se puede observar en procesos totalmente inclusivos. Por lo tanto, esta distribución requiere el análisis de otros procesos duros como, por ejemplo, procesos semi-inclusivos.

Una primera proliferación de distribuciones vino como consequencia de tener en cuenta quarks no colineales. Básicamente, eso significa que el movimiento intrínseco de los quarks no puede entenderse completamente si sólo nos fijamos en las tres cantidades previamente definidas. Hoy en día, las distribuciones de partones que dependen del momento transverso de los quarks $\vec{k}_T$ (TMD PDs) están siendo examinadas minuciosamente en el marco de lo que conocemos como Física del Espín. Dado que contienen un grado de libertad interno adicional, esas distribuciones están involucradas en correlaciones no triviales con el espín por lo que podrían conducir a una mejor comprensión de la estructura de espín de los hadrones.

En estos días, las instalaciones experimentales permiten el acceso a no sólo procesos inclusivo como difusión profundamente inelástica sino también procesos duros exclusivos como la difusión Compton virtual profundamente inelástica (DVCS) $\gamma^* p \to \gamma p$ o la producción dura e exclusiva de mesones (HEMP) $\gamma^* p \to Mp$. El primer proyecto de una instalación dedicada al estudio de procesos exclusivos en el régimen de "scaling" fue el proyecto ELFE [18, 129], que lamentablemente no tuvo éxito. En los últimos años, se han ido obteniendo datos experimentales relacionados con la estructura de los hadrones, como las asimetrías y las secciones eficaces de DVCS o HEMP en diferentes colaboraciones. Mencionamos las colaboraciones HERMES, por ejemplo [4], así como H1, por ejemplo [6], y ZEUS, por ejemplo [55], en DESY; la colaboración CLAS, por ejemplo [191], en el Hall B de JLab.

La descripción teórica de estos procesos exige la extensión de las Distribuciones de Partones a las Distribuciones de Partones Generalizadas [117, 148, 173]. Estas distribuciones son elementos de matriz de distribuciones no diagonales, a saber, aquellas que tienen un estado final con momento diferente que el inicial (para revista veáse, por ejemplo, Refs. [30, 36, 81, 101, 120]). Las Distribuciones de Partones Generalizadas describen elementos de matriz de corrientes bilocales en el cono de luz con transferencia de momento bno nula. Miden la respuesta de la estructura interna de los hadrones a las sondas en los procesos mencionados. Estas nuevas distribuciones han demostrado ser unas interesantes herramientas teóricas para el estudio de los hadrones : se conectan, mediante las reglas de suma, a los Factores de Forma hadrónicos, su límite hacia adelante conecta con las distribuciones de Partones habituales. Presentamos las propiedades de esos elementos de matriz que se deducen de su análisis a partir de primeros principios en el Capítulo 1. Esas propiedades se utilizan como limitaciones en el procedimiento de modelización que ha sido descrito anteriormente para las Distribuciones de Partones.

Las predicciones de algunos modelos fenomenológicos ya han sido verificadas, estando de acuerdo con los datos experimentales mencionados anteriormente. Ese éxito se interpretó como un signo alentador de que el marco de procesos exclusivos profundamente inelásiticos era adaptado a nuestros objetivos. Sin embargo, un mapa detallado así como la extracción de GPDs de los experimentos requerirá más datos para constringir los modelos. En un futuro próximo, esperamos nuevos datos sobre DVCS de las colaboraciones CLAS y HERMES (mirar las referencias de propuestas en [108]). La mejora hasta 12 GeV del acelerador CEBAF en JLAB prevista para 2012 [54] ya implica a la mayor parte de la comunidad de física hadronica en propuestas para el acceso de las distribuciones involucradas como un modo de explorar la estructura de los hadrones. Lo mismo esperamos del experimento COMPASS en el CERN.

Las colisiones de un fotón verdadero y un fotón sumamente virtual también pueden ser un instrumento útil para estudiar los aspectos fundamentales de QCD. Dentro de esta clase de procesos, la producción exclusiva de pares de mesones en la difusión $\gamma^*\gamma$ ha sido analizada en la Ref. [165], introduciendo una nueva clase de amplitudes de distribución, llamada Amplitud de Distribución de Transición (TDA). Representan una generalización de las distribuciones de partones al caso donde estados incial y final corresponden a partículas diferentes. Por motivos prácticos obvios, las primeras transiciones que han sido estudiadas son las que corresponden a la TDA (mesoníca) de pión a fotón, gobernando alternativamente procesos como $\pi^+\pi^- \to \gamma^*\gamma$ o $\gamma^*\pi^+ \to \gamma\pi^+$ en el régimen cinemático donde el fotón virtual es sumamente virtual, pero con una transferencia de momento pequeña. Sin embargo, las TDAs bariónicas también han sido introducidas en la Ref. [165] y han sido analizadas para la transición $\pi \to N$ en la Ref. [135].

Amplitudes de Distribución de Transición

Esta tesis es una contribución en la comprensión de la estructura de los hadrones profundizando en el conocimiento presente sobre las Amplitudes de Distribución de Transición de pión a fotón.

Para conseguir este objetivo, presentamos los resultados para las TDAs de pión a fotón en un esquema de teoría cuántica de campos que trata el pión como un estado ligado en una manera totalmente covariante usando la ecuación de Bethe-Salpeter, con la estructura del pión descrita por el modelo de Nambu - Jona Lasinio (NJL) [67, 68, 69]. El modelo de NJL es el modelo más realista para el pión, basado en una teoría cuántica de campos local construida con quarks. Respeta las realizaciones de la simetría quiral y da una descripción buena de la física de baja energía del pión [125]. El modelo de NJL es una teoría de campos non-renormalizable y por lo tanto debe introducirse un procedimiento de "corte" (cut-off). Hemos escogido el procedimiento de regularización de Pauli-Villars respetando así la invariancia gauge. El modelo de NJL junto con su procedimiento de regularización, puede verse como una teoría efectiva de QCD. En términos de los procesos físicos, el modelo de NJL se usa para describir la parte blanda (no perturbativa) de los procesos profundos, mientras, para la parte dura, la QCD perturbativa convencional se debe usar.

Por claridad, desarrollaremos este asunto paso a paso, siguiendo las mejoras teóricas descritas arriba. A saber, para ilustrar el marco de las Distribución Partones así como el formalismo desarrollado para calcular tales cantidades, presentamos, en el Capítulo 2, el cálculo detallado de las Amplitudes de Distribución del pión en el modelo de NJL. En el mismo Capítulo, se muestra el enlace entre la Amplitud de Distribución del pión y la Distribución de Partones a través del teorema de piones blandos. También mostramos la consistencia del modelo que usamos acentuando que, una vez incluida la evolución de QCD, se alcanza un buen acuerdo entre la Distribución de Partones calculada y la experimental.

Siguiendo el mismo esquema, ampliamos nuestras consideraciones a la Distribución de Partones Generalizada del pión en el Capítulo 3. Mostramos los resultados para el cálculo de ésta última en el formalismo de Capítulo 2 [153]. Uno se podría preguntar si los resultados, aunque constringidos por las propiedades encontradas por primeros principios, son compatibles con otros formalismos. Con aquella pregunta en mente, mostramos la parameterización de las GPDs por las llamadas "Distribuciones Dobles". El último paso del análisis es el uso de las ecuaciones de evolución de QCD. El efecto de la evolución sobre la GPD del pión calculado en el modelo de NJL se ha estudiado

en [45], cuyos resultados trataremos en detalle.

Estos desarrollos anteriores permiten una mejor prensión de la Amplitudes de Distribución de Transición como objetos no perturbativos, correspondiendo a algunas restricciones muy bien conocidas. Una particularidad de estas transiciones consiste en la conexión de su estructura con la del proceso de desintegración radiativa del pión $\pi^+ \to \gamma e^+ \nu$ [46, 147], que pone de manifiesto la importancia del papel jugado por la Conservación Parcial de la Corriente Axial. En el Capítulo 4 presentamos un análisis detallado del elemento de la matriz de corriente bilocal definiendo las TDAs de pión a fotón. En este capítulo estudiamos las propiedades de las TDAs, y damos los resultados del cálculo en el modelo de NJL.

Se han realizado diferentes estudios de las TDAs de pión a fotón axial y vector usando diferentes modelos quarks [44, 67, 127, 199]. Hemos presentado una comparación cualitativa así como la parameterización por Dobles Distribuciones, lo cuál nos permite concluir que hay un acuerdo cualitativo, y en muchos casos cuantitativo, entre los diferentes enfoques.

Una aplicación directa de los resultados obtenidos para las TDAs a la fenomenología es la estimación de la sección eficaz para los procesos que ellos gobiernan. El Capítulo 5 está dedicado al estudio de las secciones eficaces para la producción exclusiva de mesones en difusión $\gamma^*\gamma$ [70, 131], donde, en Ref. [70], se tiene en cuenta la evolución de la TDA.

Hasta este punto, nuestro objetivo ha sido estudiar la estructura del pión. Dentro del estudio de la estructura de los hadrones que hemos realizado, hemos querido ampliar nuestros análisis a la estructura de espín del protón. Por eso relatamos brevemente algunas mejoras recientes de la física de espín. Gracias a la fenomenología, sabemos que el DIS semi-inclusivo sobre un blanco polarizado transversalmente muestra asimetrías azimutales, p.ej. [5, 7], que se podrían entender por correlaciones no triviales entre el movimiento intrínseco de los quarks y el espín transverso. Se podría obtener información de como está hecha la estructura de espín del protón gracias a la comprensión de la modulación de la densidad de número de quarks no polarizados en un protón polarizado. Esta modulación viene de la correlación entre el momento intrínseco transverso de los quarks y la componente transversa del espín del protón. Los resultados para esta función llamada función de Sivers, calculada en dos modelos diferentes [66, 72], se exponen en el Capítulo 6.

Para resumir lo que se ha mostrado en esta tesis, podemos recapitular los resultados generales obtenidos a partir de las Distribuciones de Partones para a continuación explicitar los resultados originales de esta tesis. Esos últimos se relacionan con las Amplitudes de Distribución de Transición así como con la función de Sivers.

Como ya hemos dicho, la Difusión Profundamente Inelástica proporciona nuestra fuente principal de información sobre la estructura interna del pión y del nucleón. El DIS no polarizado ha revelado las distribuciones partonicas de los hadrones. Esto ha mostrado que los quarks llevaban sólo aproximadamente la mitad del momento total del hadrón. El DIS polarizado ha proporcionado información sobre las distribuciones de espín, diciéndonos que sólo una pequeña fracción del espín del protón era llevada por el espín intrínseco de los quarks.

Durante la última década se ha desarrollado un tratamiento teórico de reacciones profundamente

inelásticas semi-inclusivas así como exclusivas, aumentando de esta forma nuestro conocimiento sobre la estructura de los hadrones.

Por ejemplo, la Difusión Profundamente Inelástica y Semi-Inclusiva permite obtener información sobre Distribuciones de Partones impares bajo quiralidad. En un hadrón transversalmente polarizado, la distribución de transversidad nos dice cuál es la densidad de número de quarks con polarización paralela a la del hadron, menos la densidad de número de quarks con polarización antiparalela. Además, el estudio completo de las características del hadrón producido en SIDIS requiere que tengamos en cuenta el movimiento transverso de los quarks. Los instrumentos teóricos para la descripción de este proceso son, por lo tanto, las Distribuciones de Partones Dependiente del Momento Transverso. Entre esta clase de distribuciones, la función de Sivers ha sido el objeto de estudios teóricos importantes ya que ha sido propuesta para explicar las asimetrías de espín en SIDIS.

Por otra parte, la electroproducción exclusiva de fotones (DVCS) ha sido el proceso más estudiado. En las condiciones de virtualidad grande Q^2 del fotón intercambiado y de transferencia de momento baja t, por ejemplo cerca de la dirección hacia adelante, la amplitud de la reacción se factoriza en una parte dura y una parte blanda. Esta parte blanda abre nuevas ventanas sobre la estructura de los hadrones.

Los instrumentos teóricos para la comprensión de estos procesos son las *Distribuciones de Partones Generalizadas*. Las GPDs se relacionan en límites diferentes a otras cantidades físicas conocidas : en el límite de transferencia de momento baja, $t \to 0$, conectan con las Distribuciones de Partones habituales. Integrado sobre la fracción de momento del quark, las GPDs conducen a los Factores de Forma electromagnéticos de hadrones. Además, por la regla de suma de Ji, una combinación particular de los momentos de las GPDs puede ser relacionada con el espín del protón.

Podemos asumir que la amplitud de la reacción de producción exclusiva de hadron en la difusión $\gamma^*\gamma$ a pequeña transferencia de momento y a grande masa invariante también factoriza en partes duras y blandas, veáse Fig. 4.1. La parte blanda nos proporciona información adicional sobre la estructura de los hadrones a través de las *Amplitudes de Distribución de Transición* como ya hemos mencionado.

En esta tesis, hemos considerado algunas de las distribuciones de las que acabamos de describir. A lo largo de los Capítulos 2, 3, 4 y 5, la estructura partonica del pión ha sido analizada bajo la visión de Nambu - Jona-Lasinio del pión. En los Capítulos 2 y 3, hemos repasado la situación anterior; mientras que, en los Capítulos 4 y 5, hemos presentado nuestros resultados sobre las Amplitudes de Distribución de Transición.

En el Capítulo 2, se han presentado las Amplitudes de Distribución del pión, junto con su relación, por los teoremas de piones blandos, a las Funciones de Distribución de Partones del pión. El estudio de estas cantidades conocidas ha permitido plantar el escenario para la parte subsecuente y original del manuscrito. Para ser específico, más que una simple ilustración del formalismo en el que ibamos a trabajar, el cálculo de la DA del pión ha permitido hacer una primera evaluación de la elección del modelo de NJL. Esto se ha hecho, entre otras cosas, determinando la escala de validez Q_0 de este modelo quark, evolucionando según las ecuaciones de evolución de QCD. En particular, la Función de Distribución de Parton del pión obtenida está en un acuerdo sorprendentemente bueno con los datos, una vez evolucionados al orden dominante (Leading-Order). También hemos considerado la evolución al "Next-to-Leading-Order", alcanzando la conclusión de que el efecto de

la evolución al NLO ha sido compensado al LO en la adaptación de la baja escala del modelo Q_0. Por otra parte, las Amplitudes de Distribución del pión calculadas en el modelo de NJL están en un buen acuerdo, aunque menos impresionante, con los datos.

El análisis de la PDF y la DA del pión también permite sacar conclusiones acerca de la propiedad de soporte así como acerca del comportamiento de los end-points. Primero, concluimos que la conservación de covariancia sobre el cono de luz debe ser un rasgo imprescindible del modelo que escogamos para los análisis de las funciones de distribución. De hecho, hemos aprendido que la propiedad de soporte se relaciona estrechamente con esta simetría, que se respeta en el modelo de NJL. Segundo, enfatizamos la importancia de QCD cuando vamos hacia energías más altas, en las cuales se realizan los experimentos. Por lo tanto abogamos que desechar algunos modelos sólo debe hacerse después de haber evolucionado sus resultados a una escala perturbativa.

Considerando las simetrías que respeta y los resultados buenos a los que ha conducido, el modelo de NJL, con todas sus ventajas y defectos, puede ser considerado como un modelo realista para el pión no sólo para observables de baja energía, pero también para la determinación de las Distribuciones de Partones. La imagen que emerge para el pión es que su estructura queda básicamente determinada por la simetría quiral.

El Capítulo 3 se ha dedicado a las *Distribuciones de Partones Generalizadas* del pión. En concreto, se han presentado los resultados de las Ref. [153], junto a la parameterización de las GPDs vía Dobles Distribuciones [171]. Se han obetenido el soporte esperado y la propiedad de polinomialidad para la GPD del pión. No hay ninguna discrepancia relevante entre estos resultados obtenidos en el modelo de NJL y otros cálculos, p.ej. [45, 171], tanto antes como después de la evolución de QCD. El acuerdo después de la evolución nos da confianza sobre el código de evolución [94] que hemos usado.

En el Capítulo 4, hemos presentado nuestros resultados para las *Amplitudes de Distribución de Transición* de pión a fotón vector y axial, respectivamente $V(x,\xi,t)$ y $A(x,\xi,t)$ [67, 68, 69]. Hemos usado el formalismo desarrollado en el Capítulo 2: la amplitud de Bethe-Salpeter para el pión se construye con la función de vértice quark-pión que viene del modelo de Nambu-Jona Lasinio. Esta técnica nos permite dar predicciones numéricas. También hemos aplicado el procedimiento de regularización de Pauli-Villars para conservar la invariancia gauge.

La definición de estas TDAs de pión a fotón la hemos dado en la Sección 4.2. La Conservación Parcial de la Corriente Axial nos dice que la corriente axial se acopla al pión. Por lo tanto, para definir correctamente la TDA axial, a saber con toda la estructura del hadrón entrante incluido en $A\left(x,\xi,t\right)$, la contribución del polo del pión debe ser extraída. Haciendo esto, encontramos que la TDA axial tiene, en el modelo de NJL y en la aproximación de diagramas de tipo "bolso de mano" (handbag), dos contribuciones diferentes: la primera se relaciona con un acoplamiento directo de la corriente axial a un quark del pión entrante y a un quark acoplado al fotón saliente. La segunda se relaciona con la parte no resonante de un par de quark-antiquark acoplado con los números cuánticos del pión. La presencia de esa última contribución garantiza la invariancia gauge de la TDA axial.

El hecho de usar un enfoque totalmente covariante Lorentz e invariante gauge garantiza que todas las propiedades fundamentales de las TDAs serán recuperadas. De este modo, obtenemos el soporte correcto, $x \in [-1,1]$. Las reglas de suma, junto con el desarrollo en polinomios, también se recuperan. Queremos hacer hincapié en que estas tres propiedades no son condiciones impuestas por nosotros al modelo sino resultados que surgen de nuestro cálculo [67]. El valor que se obtiene en el modelo de NJL para el Factor de Forma vectorial está de acuerdo con el resultado experimental

proporcionado en el Grupo de Datos de Partículas [11], mientras que el valor encontrado para el Factor de Forma axial es dos veces más grande que él encontrado en el PDG [11]. Esta discrepancia es un rasgo común de los modelos quark, y aparece en los diferentes cálculos de las TDAs [44, 127]. También, describimos bien el Factor de Forma vectorial del pión neutro $F_{\pi\gamma^*\gamma}(t)$, reproduciendo el valor dado por la anomalía [39]. Estos resultados nos permiten suponer que el modelo de NJL da una descripción razonable de la física de aquellos procesos en este régimen de energía.

Ahora nos vamos a concentrar en el desarrollo en polinomios de las TDA. Hemos mostrado que para la TDA vectorial y en el límite quiral, sólo los coeficientes de las potencias pares en ξ son no nulos [67]. No hemos obtenido ninguna restricción similar para la TDA axial. Sin embargo, obtenemos, en el modelo de NJL, expresiones simples para los coeficientes del desarrollo en polinomios en el límite quiral, dados en la ecuación (4.43).

Hemos obtenido unas formas bastante distintas para las TDAs vectorial y axial. Eso es en parte debido, por lo menos en la región llamada DGLAP, a la relación de isospín

$$V(x,\xi,t) = -\frac{1}{2}V(-x,\xi,t)\,, \qquad A(x,\xi,t) = \frac{1}{2}A(-x,\xi,t)\,, \qquad\qquad |\xi| < x < 1 \quad .$$

La diferencia de forma se debe también a la parte no resonante del diagrama para el par interactuando qq para la TDA axial en la región ERBL. Es interesante preguntarse sobre del dominio de validez de las relaciones anteriores. Estas relaciones se obtienen a partir del cálculo de la traza de isospín que viene del diagrama central de la Fig. 4.8. Debido a la simplicidad de la función de onda de isospín del pión, estos resultados son más generales que el modelo de NJL. Por lo tanto, podemos intuir que esos resultados son más generales que resultando de los diagramas que hemos considerado, que son la contribución más sencilla de diagramas de tipo de "bolso".

Existen otros cálculos en otros modelos así como enfoques fenomenológicos de las TDAs de pión a fotón [44, 127, 131, 199], por lo que debemos hacer una comparación con nuestros resultados. Esto hemos hecho en la Sección 4.7. En dicha sección también hemos definido las Distribuciones Dobles para TDAs. Hemos concluido que no hay ningún desacuerdo entre los diferentes estudios que conciernen las TDAs π-γ, a pesar de algunas ambigüedades en la definición de la variable ξ, llamada "skewness variable".

Las TDAs, calculadas, como primer paso, para transiciones de pión a fotón, nos ha llevado a estimaciones interesantes para la sección eficaz asociada a la producción exclusiva de pares de mesones en difusión $\gamma^*\gamma$ que implican transiciones de fotón a pión para la parte blanda. También hemos mostrado las simetrías que relacionan las diferentes transiciones pudiendo pasar de las TDAs $\pi^+ \to \gamma$ a las TDAs $\gamma \to \pi^-$.

En el Capítulo 5 hemos presentado nuestros resultados para esta aplicación fenomenológica de las TDAs [70]. Hemos examinado cuál sería la sección eficaz esperada para a producción exclusiva de π-π y π-ρ en difusión $\gamma^*\gamma$ en la región cinemática hacia adelante, usando modelos realistas para la descripción del pión. En primer lugar, confirmamos las estimaciones anteriores para la producción de ρ obtenida en la Ref. [131], aunque nuestros resultados para la sección eficaz son más grandes de un factor 2. En segundo lugar, en comparación con la evaluación anterior de las secciones eficaces, hemos mejorado nuestro resultado anterior, considerando el efecto de la evolución de QCD sobre la corriente vectorial. Haciendo esto, aparece un factor 5 adicional en la región de ξ pequeñas, llevando a una sección eficaz para la producción de ρ de un orden de magnitud más grande que en las estimaciones de la Ref. [131]. También hemos mejorado el resultado previo para la produccción de π-π, al incluir el término de polo del pión en la descomposición tensorial de la corriente axial.

Encontramos así un factor de realce aún más grande, de aproximadamente 60 en este caso, para la sección eficaz para la producción de piones. El término de interferencia se hace más grande por un factor 15 con respecto a la contribución pura de la TDA, haciendo la TDA axial más accesible experimentalmente.

Además de la estructura del pión, también hemos estado interesados en procesos semi-inclusivos que implican las Distribuciones de Partones del protón. Ya que las características del protón son bastante diferentes de las del pión, la descripción del protón requiere que usemos modelos cuyas propiedades son adecuadas para aquel problema. En particular, hemos usado dos modelos para el protón que no incluyen la realización de la simetría quiral, sino el confinamiento: el modelo de quarks constituyentes no relativista de Isgur-Karl así como el modelo de saco del MIT.

En el Capítulo 6 hemos presentado nuestros resultados para el cálculo de la función de Sivers en los dos modelos descritos encima. El formalismo que hemos desarrollado en la Ref. [66] para la evaluación de la función de Sivers es general ya que puede ser usado en cualquier modelo de quarks constituyentes. El ingrediente crucial de nuestro cálculo es la reducción No Relativista de la parte leading-twist del diagrama de One-Gluon-Exchange (intercambio de un gluón) en el estado final, veáse Fig. 6.6. Hemos mostrado que el modelo de Isgur-Karl, basado también en una contribución de tipo OGE al hamiltoniano, es un marco apropiado para la estimación de la función de Sivers. Los resultados obtenidos muestran un efecto importante, con un signo opuesto para los sabores u y d. Este resultado está en acuerdo con el patrón encontrado en el análisis de las GPDs dependiente del parámetro de impacto en el mismo modelo de IK. Eso permite que se cumpla la regla de suma de Burkardt (6.10)

$$\sum_{\mathcal{Q}=u,d,s,g..} \langle k_y^{\mathcal{Q}} \rangle = -\int_0^1 dx \int d\vec{k}_T \frac{k_y^2}{M} f_{1T}^{\perp \mathcal{Q}}(x, k_T) = 0 \quad .$$

Más precisamente, esta regla de suma se verifica con una precisión de unos pocos por ciento. La conexión de la función de Sivers con las GPDs dependiente del parámetro de impacto merece un análisis cuidadoso y será tratada en otra parte.

Hemos rehecho el estudio de la función de Sivers en el modelo de saco del MIT [72], y, ahora cumple la regla de suma de Burkardt a un nivel de 5%. Comparando este resultado alentador con él del CQM, uno puede decir que la regla de suma de Burkardt se cumple mejor en el CQM. Esto tiene que ver probablemente con el hecho de que la regla de suma de Burkardt se asocia a la conservación del momento transverso.

Queremos hacer hincapié en el hecho de que hemos establecido, por primera vez, los marcos correctos para los cálculos en modelos de la función de Sivers, proporcionando unas interpretaciones fenomenológicas acertadas y compatibles entre ellos

Conclusión

Concluimos esta tesis diciendo que las posibilidades de aprender algo más sobre la estructura partonica de los piones y protones parecen ser infinitas Esperamos que seremos capaces de desvelar muchos secretos de la estructura de espín de los hadrones realizando, en un primer lugar, cálculos simples e intuitivos, que pueden ser puestos en práctica por intuiciones fenomenológicas.

Introduction

One of the main open question in physics is the understanding of the hadrons as constituted of quarks and gluons. In effect, the idea that quarks are the building blocks of hadrons goes back to 1964, when Gell-Mann and Zweig published their famous papers [96, 207]. In 1973, the formulation of Quantum ChromoDynamics (QCD), as the theory of the strong interaction between quarks, was proposed by Fritzsch, Gell-Mann and Leutwyler [95]. But despite the fact that QCD has been adopted 35 years ago and even though this theory has been verified at high energy, we have not been able to reveal the detailed structure of hadrons. One might wonder why we have not achieved this aim yet. The answer is that the peculiar features of the strong interactions renders such a task very intricate.

At high energy, the perturbative treatment of QCD, which is justified by asymptotic freedom [106, 169], allows for the explanation of the hadronic phenomena, whose basic ingredients are the *Parton Distributions*. These distributions can be experimentally determined for a relatively high value of the momentum transfer Q^2. Therefore, we are able to evolve those quantities and give predictions for different values of Q^2.

At low energy (typically below $\sim$ 1 GeV), there is no justification for such a perturbative treatment of QCD and, therefore, we do not longer have a description of the relevant low energy observables from QCD. In this regime, hadronic models and effective theories come into play. In these schemes, the parameters are fixed by phenomenology.

There exists no clear and definite frontier between these two energy regimes. Neither do exist definite connections between the relevant degrees of freedom: even though they are the elementary degrees of freedom of QCD, free quarks and gluons have never been observed. This fact has revealed that quarks and gluons were confined in hadrons. On the other hand, another important feature of the strong interactions is related to the chiral symmetry. In the limit of massless quarks, chiral symmetry, which is a property of the QCD lagrangian, is realized in the Goldstone mode, i.e. is spontaneously broken. The fundamental rôle played by this symmetry and its realization has been confirmed by the small mass of the pion as well as properties of the strong processes at

intermediate energies like the Partial Conservation of the Axial Current or the Soft Pion Theorems. Therefore, the structure of a hadron arises from an interplay between these two important properties of QCD, namely, confinement and the realization of the chiral symmetry. The energy regime from which we can gather information on the hadron structure resides in the frontier between the two regimes described above, where both confinement and chiral symmetry are supposed to be into play.

A way of connecting the perturbative and non-perturbative *worlds* is the study of Parton Distributions using models. The scheme that has been proposed runs as follows: we build models, whose characteristics somehow mimic the QCD's properties that are relevant at the energy range we are considering (~ 1 GeV); we then evaluate the Parton Distributions in these models; finally, we evolve these distributions to the scale of the experiment in order to compare with the data.

The reactions allowing to access the different types of Parton Distributions have been receiving great attention from the hadronic physics community. These reactions are such that they enable us to look with a good resolution inside the hadron and allow us to resolve the very short distances, i.e. small configurations of quarks and gluons. Since at short distances the interactions between quarks and gluons become weak, this part of the process is described through *perturbative* QCD. A resolution of such short distances is obtained with the help of non-strongly interacting probes. Such a probe, typically a photon, is provided by hard reactions, like Deep Inelastic Scattering, Semi-Inclusive Deep Inelastic Scattering, Deeply Virtual Compton Scattering, ... In that scheme, the Parton Distributions reflect how the target reacts to the probe, or how the quarks and gluons are distributed inside the target. The insight into the structure of hadrons is reached at that stage: the large virtuality of the photon, Q^2, involved in such processes allows for the factorization of the hard (*perturbative*) and soft (*non-perturbative*) contributions in their amplitudes. It is this *non-perturbative* part of the process that will interest us all along this thesis.

The first steps towards the understanding of the structure of hadrons were taken by studying the total cross sections of fully inclusive processes or longitudinal asymmetries, which receive simple interpretations in parton models [113].

From a theoretical point of view, Parton Distributions are related to diagonal matrix elements of a bilocal operator on the light-cone from the initial hadron state to the same final hadron state, i.e. the same particle with the same momentum. They have simple probabilistic interpretations. For collinear quarks, the Parton Distributions $q(x)$ receive the name of number densities because they reflect the probability density of finding a quark with a fraction x of the longitudinal momentum of the parent hadron, regardless of its spin orientation. Also, the definition of other appealing quantities arise, such as the helicity distribution (i.e. longitudinal polarization), as well as the more mysterious transversity distribution. Now, the distribution of transverse polarization is not observable in fully inclusive processes, thus, it requires the analyses from other hard processes, e.g. semi-inclusive processes.

A first proliferation of distributions was the consequence of considering non-collinear quarks. It basically means that the intrinsic motion of quark could hardly be understood through the three previous densities. Nowadays, Transverse Momentum, $\vec{k}_T$, Dependent parton distributions are being thoroughly examined in the context of Spin Physics. Since they embody an additional internal degree of freedom, they can be involved in non-trivial correlations with spin that might lead to a deeper understanding of the spin structure of hadrons.

In these days, the experimental facilities allow to access not only inclusive processes like Deep Inelastic Scattering but also exclusive deep processes like the Deeply Virtual Compton Scattering (DVCS) $\gamma^* p \to \gamma p$ or Hard Exclusive Meson (M) Production (HEMP) $\gamma^* p \to M p$. The first project of a facility devoted to the study of exclusive processes in the scaling regime was proposed as the ELFE project [18, 129], which unfortunately did not succeed. In the last few years, experimental data related to the structure of hadrons, like asymmetries and DVCS or HEMP cross sections, have been obtained from different collaborations. We mention the HERMES, e.g. [4], as well as the H1, e.g. [6], and the ZEUS, e.g. [55], collaborations at DESY; the CLAS collaboration, e.g. [191], at the Hall B of JLab.

The theoretical description of these processes requires the generalization of the Parton Distributions to *Generalized Parton Distributions* [117, 148, 173]. These distributions are matrix elements of non-diagonal distributions, namely, those which have a final state with different momentum than the initial one (for reviews, see, e.g., Refs. [30, 36, 81, 101, 120]). The Generalized Parton Distributions describe non-forward matrix elements of bilocal operators on the light-cone. They measure the response of the internal structure of the hadrons to the probes in the above-mentioned processes. These *new* distributions have been shown to be interesting theoretical tools for the study of hadrons; they connect, through sum rules, to the hadronic Form Factors. Also their forward limit connects to the usual Parton Distributions. The properties of such matrix elements that ensue from their analysis from *first principles* are presented in Chapter 1. Those properties are used as constraints on the modeling procedure that has been described above for the Parton Distributions.

Already the prediction of some phenomenological models have been verified to be in agreement with the data mentioned above. This was taken as an encouraging sign that the framework of exclusive deep processes was adapted to our purposes. However, a detailed mapping as well as the extraction of GPDs from the experiments will require more data in order to constrain the models. In a near future, we expect new data on DVCS from the CLAS and HERMES collaborations (see references of proposals in [108]). The improvement up to 12 GeV of the CEBAF accelerator at JLab foreseen for 2012 [54] is already involving much of the hadronic physics community in proposals for the access of the involved distributions as a way to explore the structure of the hadrons. So is the COMPASS experiment at CERN.

Also, collisions of a real photon and a highly virtual photon can be an useful tool for studying fundamental aspects of QCD. Inside this class of processes, the exclusive meson pair production in $\gamma^*\gamma$ scattering has been analyzed in Ref. [165] introducing of a new kind of distribution amplitudes, called *Transition Distribution Amplitude* (TDA). They represent a generalization of parton distributions to the case where the initial and final states correspond to different particles. For obvious practical reasons, the first transitions that have been studied are the (mesonic) pion-photon TDA, alternatively governing processes like $\pi^+\pi^- \to \gamma^*\gamma$ or $\gamma^*\pi^+ \to \gamma\pi^+$ in the kinematical regime where the virtual photon is highly virtual but with small momentum transfer. Nevertheless, it has also been proposed in Ref. [165] baryonic TDAs that have been analyzed for the $\pi \to N$ transition in Ref. [135].

This thesis aims to contribute to the understanding of the hadron structure by gathering the present knowledge on the pion-photon *Transition Distribution Amplitudes*.

For that purpose, we present the results for the pion-photon TDAs in a field theoretic scheme treating the pion as a bound state in a fully covariant manner using the Bethe-Salpeter equation, with the pion structure described by the Nambu - Jona Lasinio (NJL) model [67, 68, 69]. Actually, the NJL model is the most realistic model for the pion, based on a local quantum field theory built with quarks. It respects the realizations of chiral symmetry and gives a good description of the low energy physics of the pion [125]. The NJL model is a non-renormalizable field theory and therefore a cut-off procedure has to be defined. The Pauli-Villars regularization procedure has been chosen because of the symmetries it respects. Also, the NJL model together with its regularization procedure, is regarded as an effective theory of QCD.
In terms of the physical processes, the NJL model is used to describe the soft (non perturbative) part of the deep processes, while for the hard part conventional perturbative QCD must be used.

For the sake of clarity, we will develop this topic step by step, following the theoretical improvements described above. Namely, in order to illustrate the framework of Parton Distributions as well as the formalism developed to calculate such quantities, the detailed calculation of the pion *Distribution Amplitudes* in the NJL model is presented in Chapter 2. In the same Chapter, the link between pion Distribution Amplitudes and Parton Distributions are displayed through the Soft Pion Theorem. We also show the consistency of the model we use by emphasizing that, once QCD evolution is taken into account, a good agreement is reached between the calculated Parton Distributions and the experimental one.

According to the same scheme we extend our considerations to the pion *Generalized Parton Distributions* in Chapter 3. The results for the calculation of the latter in the formalism of Chapter 2 are shown [153]. One could wonder whether the results, even if constrained by the *first principles* properties, are consistent with other formalisms. With that question in mind, we display the parameterization of the GPDs through the so-called *Double Distributions*. The last step of the analysis is the application of the QCD evolution equations. The effect of evolution on the pion GPD calculated in the NJL model has been studied in [45], whose results we will be discussed in detail.

These previous developments enable a better prehension of the Transition Distribution Amplitudes as non-perturbative objects matching with some well-known constraints. A peculiarity of these transitions consists in the connection of their structure with the one given by the pion radiative decay $\pi^+ \to \gamma e^+ \nu$ process [46, 147], which stresses the importance of the rôle played by the Partial Conservation of the Axial Current. A detailed analysis of the matrix element of bilocal current defining the pion-photon TDAs is presented in Chapter 4. Their properties are displayed and studied. The results of the calculation in the NJL model are subsequently given.
Different studies of the axial and vector pion-photon TDA have been performed using different quark models [44, 67, 127, 199]. A qualitative comparison as well as the parameterization through Double Distributions are also presented, which allow us to conclude that there is a qualitative agreement between all the different approaches.

The direct application of the results obtained for the TDAs to phenomenology is obviously the estimation of the cross section for the processes they govern. Chapter 5 is devoted to the study of the cross sections for the exclusive meson production in $\gamma^*\gamma$ scattering [70, 131], where, in Ref. [70], the evolution of the TDA is taken into account.

Up to this point, we have proposed to consider, in this thesis, the structure of the pion. Within the study of the hadron structure that we have carried out, we wanted to extend our analyses to the spin structure of the proton. This is why we briefly report some recent improvements in Spin Physics. From the phenomenology, it is known that Semi-Inclusive DIS off a transversely polarized target shows azimuthal asymmetries, e.g. [5, 7], that could be understood through non-trivial correlations between intrinsic motion of the quarks and transverse spin. A hint on the spin structure of the proton could be given through the understanding of the modulation of the number density of unpolarized quarks in a polarized proton. This modulation is due to the correlation between the intrinsic transverse momentum of the quarks and the transverse component of the proton spin. The results for this so-called Sivers function, calculated in two different models [66, 72], are exposed in Chapter 6.

In the final Chapter, we conclude by gathering all the questions and all the ideas that emerged in this work, which represent good starting points for future research.

1 Hadron Structure from Distribution Functions

An intuitive approach of parton distribution can be provided in the context of the parton model. Feynman [90] introduced the parton distributions as phenomenological quantities describing the properties of the nucleon in high-energy scattering. Actually a nucleon moving at the speed of light can be seen as made of noninteracting massless and collinear partons. In such a scheme the parton distributions are the density of partons as a function of the fraction of the nucleon longitudinal momentum they carry.

Nevertheless the nucleon does not exactly consits of free partons. Knowledge of the internal structure of the nucleon, or the pion, is required in order to properly study the parton distributions as a nonperturbative object.

From the phenomenological point of view, the study of Deep Inelastic Scattering processes, where individual partons are resolved, revealed itself to be an essential tool in this context. The unpolarized parton distributions have been extracted with good precision from various high-energy scattering data [98, 130]. Those distributions have provided important clues about the hadron structure but yet important pieces of information are missed out in these quantities.

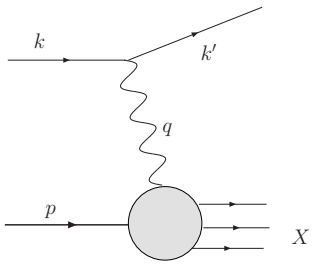

Figure 1.1: DIS: Kinematics of lepton-hadron scattering.

In order to study the properties of hadrons we will examine the properties of the hadronic matrix element defining them. The adapted framework for these purposes is any Deep Inelastic Process, characterized by the Bjorken limit. The cross section for those processes 1.1 can be separated into a leptonic $l_{\mu\nu}$ and a hadronic tensors $W^{\mu\nu}$. While the leptonic tensor is known completely, $W^{\mu\nu}$, which describes the internal structure of the nucleon, depends on non perturbative strong interaction dynamics. It is expressed as the com-

mutator of two currents J^μ defined at 2 different space-time points,

$$W^{\mu\nu} = \frac{1}{4\pi}\int d^4z\, e^{iq\cdot z}\langle p,S|[J^\mu(z),J^\nu(0)]|p,S\rangle \quad , \tag{1.1}$$

and can be related to the imaginary part of the forward Virtual Compton Scattering through the Optical Theorem.

1.1 On the Light Cone

Without loss of generality, any 4-vector could be expressed as, see Appendix. A,

$$a^\mu = (a^+,\vec{a}^\perp,a^-) \quad , \tag{1.2}$$

with $\vec{a}^\perp=(a^1,a^2)$ and with the components $a^\pm=\frac{1}{\sqrt{2}}(a^0\pm a^3)$.

We define two vectors whose norm is zero

$$\begin{aligned} \bar{p}^\mu &= \frac{p^+}{\sqrt{2}}(1,0,0,1)=p^+(1,\vec{0}^\perp,0) \quad , \\ n^\mu &= \frac{1}{p^+\sqrt{2}}(1,0,0,-1)=\frac{1}{p^+}(0,\vec{0}^\perp,1) \quad . \end{aligned} \tag{1.3}$$

Those vectors follow the properties (A.9).
The Sudakov decomposition for a vector

$$\begin{aligned} a^\mu &= \alpha\bar{p}^\mu + a^{\perp\mu} + \beta n^\mu \quad , \\ &= (a.n)\bar{p}^\mu + a^{\perp\mu} + (a.\bar{p})n^\mu \quad , \end{aligned}$$

with $a^{\perp\mu}=(0,\vec{a}^{\perp\mu},0)$, can be adopted for the vectors q,z, with q constrained by the DIS kinematics. In terms of the Sudakov vectors, the nucleon momentum p and the momentum of the virtual photon q can be written as

$$\begin{aligned} p^\mu &= \bar{p}^\mu + \frac{M^2}{2}\,n^\mu \quad , \\ q^\mu &\xrightarrow{Bj} (p\cdot q)\,n^\mu - x\,\bar{p}^\mu \quad , \end{aligned}$$

with $x\equiv Q^2/2p\cdot q$ the Bjorken variable.

One could inquire about the restriction imposed by the kinematical regime of DIS on the domain of validity of the expression of the hadronic tensor (1.1). The argument of the exponential is crucial. For a generic 4-vector $z^\mu=\alpha_z\bar{p}^\mu+z^{\perp\mu}+\beta_z n^\mu$, the product $q\cdot z$ reads, in the Bjorken limit,

$$q\cdot z \xrightarrow{Bj} (p\cdot q)\,\alpha_z - x\,\beta_z \quad ,$$

When $(p\cdot q)$ goes to infinity, the oscillations produced by the exponential term in (1.1) imply that $\alpha_z \lesssim 1/(p\cdot q)$. Also, causality implies that the commutator $[J^\mu(z),J^\nu(0)]$ vanishes unless $z^2>0$, therefore $\vec{z}^{\perp 2}\lesssim 2\,\alpha_z\beta_z$. These two restrictions together imply that the hadronic tensor (1.1) in the

Bjorken regime is dominated by light-like distances, i.e. $z^2 \sim 0$.

Since the dominant contribution to DIS comes from the light-cone, it is natural to consider a dynamical formulation in which the light-cone plays a special rôle, namely: the light-cone dynamical form [34, 126]. [1] The vector decomposition (1.2) actually corresponds to the light-cone decomposition, with the light-like vectors (1.3).

1.2 Ordering

The domain of validity of the approach has been defined. So has been the treatment of the dynamics on the light-cone. We can now start to investigate on the consequences/advantages of these definitions by analyzing the operator describing the hadronic tensor, $W^{\mu\nu}$ (1.1).

Since DIS processes are light-cone dominated, [2] we can apply the Wilson's Operator Product Expansion (OPE). A product of local operators $\hat{A}(x)$ and $\hat{B}(y)$ at short distance, i.e. $x - y \sim 0$, can be expanded in a serie of well-defined local operators $\hat{O}_i(x)$ with singular c-number coefficients $C_i(x)$ for $(i = 0, 1, 2, 3, \ldots)$ [150]

$$\hat{A}(x)\hat{B}(y) \quad = \quad \sum_{i=0}^{\infty} C_i(x-y)\hat{O}_i(\frac{x+y}{2}) \quad . \tag{1.4}$$

The OPE basically represents a separation between short-distance, i.e. the singular coefficients, and large-distance, i.e. the local operators, objects. It is a formal step towards the factorization property. For instance, the Operator Product Expansion Eq. (1.4) of simple bilocal currents is, see for example [150],

$$j(z)j(0) \quad = \quad \sum_{i,n} C_n^{(i)}(z^2)\, z^{\mu_1} \ldots z^{\mu_n}\, \mathcal{O}_{\mu_1 \ldots \mu_n}(0) \quad , \tag{1.5}$$

with $C_n^{(i)}(z^2)$ singular c-numbers called Wilson coefficients. The terms in the expression (1.5) are arranged in the order of decreasing singularity, the leading contribution being the first term, providing for an expansion parameter.

The strength of light-cone singularity can be found by simple dimensional analysis. If we call d_j the dimension of the currents, $d_{\mathcal{O}}^{(i)}(n)$ the dimension of the operator $\mathcal{O}_{\mu_1 \ldots \mu_n}(0)$ and n the spin, the dimension of the singular coefficients is

$$C_n^{(i)}(z^2) \quad \sim \quad (z^2)^{-d_j + \frac{d_{\mathcal{O}}^{(i)}(n)}{2} - \frac{n}{2}} \quad . \tag{1.6}$$

The strength of the singularity is then governed by $\tau_n^i \equiv d_{\mathcal{O}}^{(i)}(n) - n$ and we call τ_n^i the twist. The smaller the value of the twist, the higher the light-cone singularity: we can use the twist as an

[1] Following Dirac [84] there are three independent parameterizations of space and time, namely, three different forms of dynamics which are completely equivalent; namely the instant, front and point forms. The most familiar form is the *instant form*, where the quantization is specified on a space-time hypersurface at a given *instant time* $x^0 = 0$. In the light-cone approach, called the *front form*, the theory is quantized at a particular value of the light-cone time x^+. The quantization conditions are specified on a hypersurface that is a tangent plane to the light-cone defined at a light-cone time $x^+ = 0$.

[2] Light-cone dominated does not mean short distance, but the light-cone domination can be led to short distances.

expansion parameter. In QCD the lowest twist operator has $\tau_n^i = 2$. A more informal definition of the twist is often used [114]. The twist is the order in M/Q, M being the target mass, at which an operator contributes to DIS processes. In other words we have $(M/Q)^{\tau_n^i - 2}$.

An alternative way of isolating the leading-twist contribution of the hadronic tensor $W^{\mu\nu}$ (1.1) is obtained by decomposing the hard and soft parts like in Ref. [114]. The vector current associated with a fermion field is

$$J^\mu(z) \quad = \quad : \bar\psi(z)\gamma^\mu\psi(z) : \quad .$$

with $: \hat O :$ the normal ordering. We will need the identity $\left[\bar\psi_1\psi_1, \bar\psi_2\psi_2\right] = \bar\psi_1\{\psi_1, \bar\psi_2\}\psi_2 - \bar\psi_2\{\psi_2, \bar\psi_1\}\psi_1$, as well as the following one, for massless fields,

$$\{\psi(z), \bar\psi(0)\} \quad = \quad \frac{1}{2\pi}\, \not\partial\, \epsilon(z_0)\, \delta(z^2) \quad .$$

The commutator of two currents appearing in (1.1) can be expressed in terms of bilocal operators

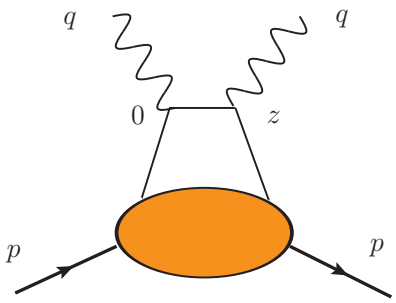

Figure 1.2: Handbag diagram. Most of the Feynman diagrams in this thesis have been drawn using JaxoDraw [33].

$$\begin{aligned}[J^\mu(z), J^\nu(0)] \quad = \quad & -\frac{1}{4\pi}\left(\partial_\rho\epsilon(z_0)\,\delta(z^2)\right)\Big[\frac{1}{2}\mathrm{tr}\left(\gamma^\mu\gamma^\rho\gamma^\nu\gamma^\alpha\right)\left(\bar\psi(z)\,\gamma_\alpha\,\psi(0) - \bar\psi(0)\,\gamma_\alpha\,\psi(z)\right) \\ & -i\epsilon^{\mu\rho\nu\alpha}\left(\bar\psi(z)\,\gamma_\alpha\,\gamma_5\,\psi(0) + \bar\psi(0)\,\gamma_\alpha\,\gamma_5\,\psi(z)\right)\Big] \quad . \end{aligned} \tag{1.7}$$

The hadronic matrix element, decomposed in the following way,

$$\begin{aligned} W^{\mu\nu} \quad = \quad & -\left(\frac{1}{4\pi}\right)^2 \int d^4z\, e^{iq\cdot z}\, \partial_\rho\left(\delta(z^2)\varepsilon(z^0)\right) \\ & \Big[\mathrm{tr}\left(\gamma^\mu\gamma^\rho\gamma^\nu\gamma^\alpha\right)\,\langle p,S|\bar\psi(z)\,\gamma_\alpha\,\psi(0)|p,S\rangle + \ldots\Big] \quad , \end{aligned} \tag{1.8}$$

with the ellipses representing the other terms present in (1.7), gives rise to the *handbag* diagram depicted on Fig. 1.2. The hard part comes from the quark propagator between 0 and z, whereas the soft part is parameterized through a bilocal matrix element represented by the lower blob. The latter object is related to the *Parton Distributions*.

The expression (1.8) has been shown without writing explicitly the color indices. However, the latter are implicit and, in order to preserve gauge invariance, one has to take into account the propagation of the quarks in the gluon background by linking the two quark fields through the *Wilson link*, i.e.

$$\bar\psi(z)\,\Gamma\psi(0) \longrightarrow \bar\psi(z)\,\mathcal{P}\,\left(\exp i\int_0^z d\zeta^\mu\, A_\mu(\zeta)\right)\Gamma\psi(0) \quad .$$

Since the δ-function in (1.8) selects the light-cone, we can expand the gauge link and keep only the leading-twist contribution. In the usual parton distribution, the leading-twist contribution involves the plus-component of the gauge field. An appropriate choice of the gauge reduces the Wilson link to unity: the light-cone gauge $A^+ = 0$ is chosen that allows the interpretation of the parton

distributions as probability densities. [3]

We assume that the handbag diagram contribution to the hadronic tensor is dominated by small values of the transverse momentum of the quark. We therefore consider collinear quarks. Hence, to leading-twist, the (unpolarized) Parton Distributions read

$$\int \frac{dz^-}{2\pi}\, e^{iz^-p^+x}\, \langle p|\bar{\psi}(0,z^-,\vec{0}_\perp)\,\gamma^+\psi(0)|p\rangle \;=\; \frac{1}{p^+}q(x) \quad . \tag{1.9}$$

1.3 Deeply Virtual Compton Scattering

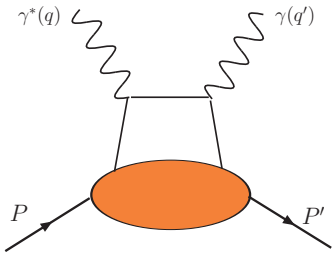

Figure 1.3: Virtual Compton Scattering

The Forward Virtual Compton Scattering (FVCS) is related to the hadronic part of DIS through the optical theorem. What generally refers to as Virtual Compton Scattering (VCS) is any process where 2 photons are involved and where at least one of them is virtual. Virtual Compton Scattering in the Bjorken region was proposed by Ji [117] and Radyushkin [173] as a tool to extract new structure functions of the nucleon. Since in this limit the momentum transfer is large, we will refer to VCS in the Bjorken region as Deeply-Virtual Compton Scattering (DVCS). The DVCS provides for a new ground to explore the quark and the gluon structure of the nucleon.

A new kind of distributions, namely non-diagonal distributions, called off-forward, skewed or generalized parton distributions (GPDs), were introduced by Ji [117] and Radyushkin [173] from the DVCS amplitude

$$T^{\mu\nu}(P+P',q,P-P') \;=\; i\int d^4z\, e^{-iq.z}\langle P'|Tj^\mu(z)j^\nu(0)|P\rangle \qquad , \tag{1.10}$$

whose sum rule are related to the Form Factors of the target.

Following the example of the analysis of DIS in the previous Section, we would like to determine the dominant contributions to DVCS.

1.3.1 Definition of the Generalized Parton Distributions

The kinematics are similar to the DIS case. Nevertheless the off-forward nature of the new distributions requires an additional variable for the description of the initial and final parton states, called the skewness variable, ξ, which reflects the longitudinal momentum asymmetry. Hence the Generalized Parton Distributions are functions of two more variables in comparison to the usual Parton Distribution Functions, namely they depend on x, in this context the variable x is just the Fourier variable of the light-cone distance, ξ and the four-momentum transfer (squared) t.
In this work, we choose to follow Ji's notations instead of Radyushkin's[4]. Hence we introduce the

[3] The light-cone gauge is not always the most adapted choice. For instance, leading-twist Final State Interactions, i.e. the exchange of a gluon between the active quark and one of the "spectator", after scattering by the virtual photon would rather be studied in a non-singular gauge [29]. This comment will make sense in Chapter 6.

[4] For a comparison of the variables see [103].

average 4-momentum $p^\mu = (P + P')^\mu/2$ which has to be collinear to q^μ in the z direction. The decomposition on the light-cone is [107]

$$\begin{aligned} p^\mu &= \bar{p}^\mu + \frac{1}{2}\left(M^2 - \frac{t}{4}\right) n^\mu \quad , \\ q^\mu &= -2\xi\, \bar{p}^\mu + \frac{Q^2}{4\xi} n^\mu \quad , \\ \Delta^\mu &= -2\xi\, \bar{p}^\mu + \xi\left(M^2 - \frac{t}{4}\right) n^\mu + \Delta^\mu_\perp \quad . \end{aligned} \tag{1.11}$$

The skewness variable is defined as $\xi \simeq Q^2/(4\,p\cdot q)$ and is related to the Bjorken variable x in the Bjorken limit. Here the momentum transfer $t = \Delta^2$ is negative.

Similarly to the expression (1.8) obtained for the DIS process, factorization for DVCS can be studied [119]. Therefore the DVCS amplitude Eq. (1.10) fulfills its rôle in being expressed as a convolution of hard and soft parts [117]

$$\begin{aligned} T^{\mu\nu}(p,q,\Delta) &= -\frac{1}{2}(p^\mu n^\nu + p^\nu n^\mu - g^{\mu\nu}) \int_{-1}^{1} dx \left(\frac{1}{x-\xi+i\epsilon} + \frac{1}{x+\xi+i\epsilon}\right) \\ &\quad \left[H(x,\xi,t)\bar{u}(P')\not{n}u(P) + E(x,\xi,t)\bar{u}(P')\frac{i\sigma^{\alpha\beta}n_\alpha\Delta_\beta}{2M}u(P)\right] \\ &\quad -\frac{i}{2}\epsilon^{\mu\nu\alpha\beta}p_\alpha n_\beta \int_{-1}^{1} dx \left(\frac{1}{x-\xi+i\epsilon} - \frac{1}{x+\xi+i\epsilon}\right) \\ &\quad \left[\tilde{H}(x,\xi,t)\bar{u}(P')\not{n}\gamma_5 u(P) + \tilde{E}(x,\xi,t)\frac{\Delta\cdot n}{2M}\bar{u}(P')\gamma_5 u(P)\right] \quad , \end{aligned} \tag{1.12}$$

with $u(P)$ the nucleon spinor.
This decomposition corresponds to the *handbag* diagram depicted on Fig. 1.3. The dominant subprocess Fig. 1.4 consists on a virtual photon with momentum q^μ absorbed by a single quark with momentum k^μ. Subsequently the quark radiates a real photon, whose momentum is now $q^\mu - \Delta^\mu$, and falls back with a resulting momentum $k^\mu + \Delta^\mu$ in the nucleon. The momentum of the recoil nucleon is $P'^\mu = P^\mu + \Delta^\mu$.

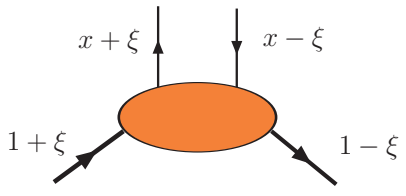

Figure 1.4: Kinematics of the Deeply-Virtual Compton Scattering [117].

The four distributions $H(x,\xi,t)$, $E(x,\xi,t)$, $\tilde{H}(x,\xi,t)$ and $\tilde{E}(x,\xi,t)$ represent the soft part, namely the *Generalized Parton Distributions*. They are defined through the matrix elements of

quark operators at a light-like separation. To leading twist, we have

$$\begin{aligned}
&\frac{1}{2}\int \frac{dz^-}{2\pi} e^{ixz^-p^+} \langle P'|\bar{\psi}(-\frac{z}{2})\gamma^+\psi(\frac{z}{2})|P\rangle\Big|_{z^+=\vec{z}^\perp=0} \\
&= \frac{1}{2p^+}\Big[H(x,\xi,t)\bar{u}(P')\gamma^+u(P) + E(x,\xi,t)\bar{u}(P')\frac{i\sigma^{+\nu}\Delta_\nu}{2M}u(P)\Big] \quad , \\
&\frac{1}{2}\int \frac{dz^-}{2\pi} e^{ixz^-p^+} \langle P'|\bar{\psi}(-\frac{z}{2})\gamma^+\gamma_5\psi(\frac{z}{2})|P\rangle\Big|_{z^+=\vec{z}^\perp=0} \\
&= \frac{1}{2p^+}\Big[\tilde{H}(x,\xi,t)\bar{u}(P')\gamma^+\gamma_5u(P) + \tilde{E}(x,\xi,t)\bar{u}(P')\frac{\gamma_5\Delta^+}{2M}u(P)\Big] \quad . \qquad (1.13)
\end{aligned}$$

The two distributions $H(x,\xi,t)$ and $\tilde{H}(x,\xi,t)$ conserve the nucleon helicity while the two others are said to be (nucleon) helicity-flipping.

1.3.2 Properties

Let us overview the properties of these new objects that follow from the analysis from *first principles*.

Support

The support in x of the GPDs is $[-1,1]$. A negative momentum fraction would correspond to an antiquark. In Fig. 1.4, the active quark has a (+)-component momentum fraction $x+\xi$. From the definition of the skewness variable,

$$\xi = \frac{P^+ - P'^+}{P^+ + P'^+} = -\frac{\Delta^+}{2p^+} \quad , \qquad (1.14)$$

and from the fact that (+)-momenta of physical states cannot be negative, it follows that the physical region for ξ is the interval $[-1,1]$. However, from the light-cone decomposition, we find that ξ is bounded by

$$0 \leq \xi \leq \frac{\sqrt{-t}}{2\sqrt{M^2 - \frac{t}{4}}} < 1 \quad . \qquad (1.15)$$

Given the intervals in x and in ξ, we can distinguish 3 regions in x,

- In the region $x \in [\xi, 1]$ both momentum fractions $x+\xi$ and $x-\xi$ are positive. In this region the GPD describes the emission and reabsorption of a quark.
- The behavior is similar in the region $x \in [-1, -\xi]$. Both momentum fractions $x+\xi$ and $x-\xi$ are negative and therefore the GPD describes the emission and reabsorption of an antiquark, respectively with momentum fractions $\xi - x$ and $-\xi - x$. This is shown on the extreme sides of Fig. 1.5.
- In the third region, i.e. $x \in [-\xi, \xi]$, one has that $x+\xi$ is positive but $x-\xi$ negative. This can be interpreted as the emission of a quark with momentum fraction $x+\xi$ and the emission of an antiquark with momentum fraction $\xi - x$ both emitted from the initial nucleon.

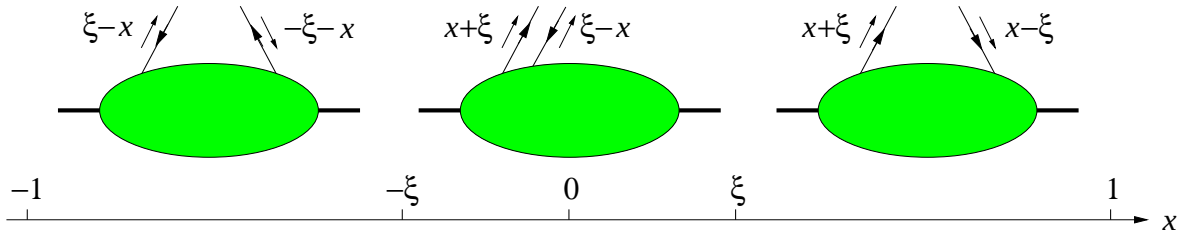

Figure 1.5: The support of the GPDs. The parton interpretation of GPDs in the x-intervals $[-1,-\xi]$, $[-\xi,\xi]$ and $[\xi,1]$. Figure taken from Ref. [81].

Forward Limit

When $P' = P$, the skewness variable ξ is equal to zero. As a consequence GPDs, in the regions corresponding to emission/reabsorption of a quark or an antiquark, i.e. $[-1,-\xi]$ and $[\xi,1]$, have an equivalence with usual PDFs. This is not true for the region of emission of a quark and an antiquark since the interval $[-\xi,\xi]$ reduces to zero in the same limit. This means that, in the forward limit, when the initial and final states are equal, i.e. equal helicities and $P' = P$, Generalized Parton Distributions as defined in Eq. (1.13) are expected to reduce to ordinary Parton Distributions Eq. (1.9),

$$\begin{aligned} H^q(x,0,0) &= q(x) \quad , \\ H^q(x,0,0) &= -\bar{q}(-x) \quad , \end{aligned} \tag{1.16}$$

for $x > 0$ and $x < 0$ respectively.

When considering the hadronic tensor in DIS (1.8) we have omitted the spin dependent distribution function as well as the gluon distribution functions. However it seems useful to notice that, in the forward limit, the second helicity-conserving distribution is related to the spin dependent parton distribution: $\tilde{H}(x,0,0) = \Delta q(x)$ for $x > 0$.

Symmetries

Time reversal interchanges P with P' and its invariance ensures the distribution will not change. By so doing we change the sign of ξ and find that the GPDs are symmetric in ξ

$$H(x,\xi,t) = H(x,-\xi,t) \quad . \tag{1.17}$$

Quark distributions are neither even nor odd in x.

Sum Rules

On the other hand, forming the first moment of the GPDs by integrating over the momentum fraction x, we get the sum rules

$$\begin{aligned} \int dx\, H(x,\xi,t) &= F_1(t) \qquad \int dx\, E(x,\xi,t) = F_2(t) \quad , \\ \int dx\, \tilde{H}(x,\xi,t) &= g_A(t) \qquad \int dx\, \tilde{E}(x,\xi,t) = g_P(t) \quad , \end{aligned} \tag{1.18}$$

where the dependence on ξ drops out. The integration over x of the matrix element Eq. (1.13) removes all reference to the particular light-cone direction with respect to which ξ is defined. As a consequence the Form Factors are ξ-independent.

The Form Factors $F_1(t)$ and $F_2(t)$ are respectively the Dirac and Pauli Form Factors

$$\langle P'|\bar{\psi}(0)\gamma^\mu\,\psi(0)|P\rangle \;=\; \bar{u}(P')\Big[F_1(t)\gamma^\mu + F_2(t)\frac{i\sigma^{\mu\alpha}\Delta_\alpha}{2M}\Big]u(P) \qquad , \tag{1.19}$$

and $g_A(t)$ and $g_P(t)$ the axial and pseudoscalar ones

$$\langle P'|\bar{\psi}(0)\gamma^\mu\gamma_5\,\psi(0)|P\rangle \;=\; \bar{u}(P')\Big[g_a(t)\gamma^\mu\gamma_5 + g_p(t)\frac{\gamma_5\Delta^\mu}{2M}\Big]u(P) \qquad , \tag{1.20}$$

defined for each separate flavor.

Gluon Distributions and the Ji's Sum Rule

We can define the gluon GPDs in a similar way as the quark GPDs

$$\begin{aligned}
&\frac{1}{p^+}\int\frac{dz^-}{2\pi}e^{ixz^-p^+}\langle P'|G^+_\mu(-\frac{z}{2})\;G^+_\mu(\frac{z}{2})|P\rangle\Big|_{z^+=\vec{z}^\perp=0}\\
=\;&\frac{1}{2p^+}\Big[H^g(x,\xi,t)\bar{u}(P')\gamma^+u(P)+E^g(x,\xi,t)\bar{u}(P')\frac{i\sigma^{+\nu}\Delta_\nu}{2M}u(P)\Big] \qquad ,\\
&\frac{-i}{p^+}\int\frac{dz^-}{2\pi}e^{ixz^-p^+}\langle P'|G^+_\mu(-\frac{z}{2})\;\tilde{G}^+_\mu(\frac{z}{2})|P\rangle\Big|_{z^+=\vec{z}^\perp=0}\\
=\;&\frac{1}{2p^+}\Big[\tilde{H}^g(x,\xi,t)\bar{u}(P')\gamma^+\gamma_5u(P)+\tilde{E}^g(x,\xi,t)\bar{u}(P')\frac{\gamma_5\Delta^+}{2M}u(P)\Big] \qquad .
\end{aligned} \tag{1.21}$$

An interesting sum rule concerns the quark and gluon spin contribution to the nucleon spin as it has been one of the main motivation for GPDs. The second moment of both $H(x,\xi,t)$ and $E(x,\xi,t)$, the helicity conserving distributions as well as the first moments of the same gluonic distributions are directly related to the total angular momentum contribution to the nucleon spin J [117]

$$\begin{aligned}
\langle J^3\rangle \;&=\; \langle J^3_q\rangle + \langle J^3_g\rangle \quad ,\\
\frac{1}{2} \;&=\; \frac{1}{2}\sum_q\int_{-1}^{1}dx\,x\,[H^q(x,\xi,0)+E^q(x,\xi,0)] + \frac{1}{2}\int_0^1 dx\,[H^g(x,\xi,0)+E^g(x,\xi,0)]
\end{aligned} \tag{1.22}$$

As a consequence, the total angular momentum carried by the quarks or the gluons inside a proton could be known if one takes the particular value of the desired Form Factors at the forward limit $t = 0$. Since the spin part of the angular momentum is found through the helicity distributions $\Delta q(x)$, the Ji's sum rule enables to access the orbital angular momentum of the quarks and gluons.

1.3.3 Polynomiality

By writing down the most general expression in terms of relevant vectors, the first moments are immediately related to their Form Factors. The higher-moments of the GPDs are accessed through the tower of twist-2 operators, generalization of the current, of the type

$$O_V^{\mu\mu_1\cdots\mu_{n-1}} \;=\; \bar\psi\gamma^{\{\mu}\, i\overset{\leftrightarrow}{\mathcal{D}}^{\mu_1}\ldots i\overset{\leftrightarrow}{\mathcal{D}}^{\mu_n\}}\,\psi \quad , \tag{1.23}$$

where the action of $\{\ldots\}$ on Lorentz indices produces the symmetric, traceless part of the tensor. In a general way, the matrix element of towers of twist-two operators appear in the operator product expansion.

Using symmetries, we can write down the general form for the matrix element of the latter tower between states of unequal momenta. All possible Form Factors therefore arise, and for the vector operator, we obtain [120]

$$\begin{aligned}\langle P'|O_V^{\mu\mu_1\cdots\mu_{n-1}}|P\rangle &= \bar u(P')\gamma^{\{\mu}u(P)\sum_{i=0}^{[\frac{n-1}{2}]}A_{n,2i}(t)\,\Delta^{\mu_1}\ldots\Delta^{\mu_{2i}}p^{\mu_{2i+1}}\ldots p^{\mu_{n-1}\}}\\ &+ \bar u(P')\frac{i\sigma^{\{\mu\alpha}\Delta_\alpha}{2M}u(P)\sum_{i=0}^{[\frac{n-1}{2}]}B_{n,2i}(t)\,\Delta^{\mu_1}\ldots\Delta^{\mu_{2i}}p^{\mu_{2i+1}}\ldots p^{\mu_{n-1}\}}\\ &+ C_n(t)\,\frac{1}{2}(1+(-1)^n)\,\frac{1}{M}\,\bar u(P')u(P)\Delta^{\{\mu}\Delta^{\mu_1}\ldots\Delta^{\mu_{n-1}\}} \quad .\end{aligned} \tag{1.24}$$

Time-reversal invariance imposes that only even powers in Δ appears.

We project the result (1.24) on the light-front by multiplying by $n_\mu n_{\mu_1}\ldots n_{\mu_{n-1}}$ and define the off-forward parton distributions through the Form Factors

$$n_\mu n_{\mu_1}\ldots n_{\mu_{n-1}}\,\langle P'|O_V^{\mu_1\cdots\mu_n}|P\rangle \;=\; \bar u(P')\gamma^+u(P)\,H_n(\xi,t)\;+\;\bar u(P')\frac{i\sigma^{+\alpha}\Delta_\alpha}{2M}u(P)\,E_n(\xi,t) \tag{1.25}$$

with $H_n(\xi,t)$ and $E_n(\xi,t)$ the moments of the helicity-conserving quark GPDs which are defined as

$$\begin{aligned}H_n(\xi,t) &= \int_{-1}^{1}dx\,x^{n-1}H(x,\xi,t)\\ &= \sum_{i=0}^{[\frac{n-1}{2}]}A_{n,2i}(t)\,(-2\xi)^{2i}+C_n(t)\,\frac{1}{2}(1+(-1)^n)\,(-2\xi)^n \quad ,\\ E_n(\xi,t) &= \int_{-1}^{1}dx\,x^{n-1}E(x,\xi,t)\\ &= \sum_{i=0}^{[\frac{n-1}{2}]}B_{n,2i}(t)\,(-2\xi)^{2i}-C_n(t)\,\frac{1}{2}(1+(-1)^n)\,(-2\xi)^n \quad .\end{aligned} \tag{1.26}$$

Basically it means that the moments of the GPDs are polynomials of the skewness variable ξ of order at most n.

We have here presented the properties of the bilocal matrix elements defining the GPDs of the proton. The latter can be easily adapted to, e.g., the pion.

1.4 Transverse Momentum Dependent Distribution Functions

All along this Chapter the quantities have been defined considering only collinear quarks.

Let us now account for the transverse motion of quarks [27]. The number of Parton Distributions at leading-twist increases from the three usual (i.e. number density $q(x)$, helicity density $\Delta q(x)$ and transversity $\Delta_T q(x)$) to eight distributions;

$$q, \Delta q, \Delta_T q \,, \overbrace{g_{1T}, h_{1L}^{\perp}, h_{1T}^{\perp} \underbrace{f_{1T}^{\perp}, h_1^{\perp}}_{T\text{-odd}}}^{k_T\text{-dependent}}$$

For the description of the quark content of the proton, the following quantity [5] is relevant,

$$\Phi_{ij}(x, \vec{k}_T) = \int \frac{dz^- d^2\vec{z}_T}{(2\pi)^3} \; e^{i(xp^+z^- - \vec{k}_T\cdot\vec{z}_T)} \, \langle p, S|\overline{\psi}_j(0)\, \psi_i(0, z^-, \vec{z}_T)|p, S\rangle \quad , \tag{1.27}$$

depending on the light-cone fraction of the quark momentum, $x = k^+/p^+$ and the transverse momentum component $\vec{k}_T$. Using Lorentz invariance, hermiticity, and parity invariance one finds that up to leading order in $1/Q$ [35]

$$\begin{aligned} \Phi(x, \vec{k}_T) \;=\; & \frac{1}{2}\Bigg\{ q(x, k_T) \;\not{n}_+ + f_{1T}^{\perp}(x, k_T) \, \frac{\epsilon_{\mu\nu\rho\sigma}\gamma^\mu n_+^\nu k_T^\rho S_T^\sigma}{M} + g_{1s}(x, k_T)\, \gamma_5 \not{n}_+ \\ & + \Delta_T q(x, k_T)\, i\sigma_{\mu\nu}\gamma_5 n_+^\mu S_T^\nu + h_{1s}^{\perp}(x, k_T)\, \frac{i\sigma_{\mu\nu}\gamma_5 n_+^\mu k_T^\nu}{M} + h_1^{\perp}(x, k_T)\, \frac{\sigma_{\mu\nu} k_T^\mu n_+^\nu}{M} \Bigg\}, \end{aligned} \tag{1.28}$$

where S is the spin of the proton target. The quantities g_{1s} and $h_{1s}^{\perp}$ are shorthand for

$$\begin{aligned} g_{1s}(x, k_T) \;&=\; \lambda\, \Delta q(x, k_T) + \frac{\vec{k}_T \cdot \vec{S}_T}{M}\, g_{1T}(x, k_T)\,, \\ h_{1s}^{\perp}(x, k_T) \;&=\; \lambda\, h_{1L}^{\perp}(x, k_T) + \frac{\vec{k}_T \cdot \vec{S}_T}{M}\, h_{1T}^{\perp}(x, k_T), \end{aligned} \tag{1.29}$$

with M the mass of the proton, $\lambda = M\, S^+/p^+$ the light-cone helicity, and $\vec{S}_T$ the transverse spin of the target hadron.

The three distribution functions $q(x, k_T), \Delta q(x, k_T), \Delta_T q(x, k_T)$ reduce to their analogs under integration over k_T, whereas the 5 others vanish if integrated over the transverse momentum.

The two *naïvely T-odd* distribution functions $f_{1T}^{\perp}, h_1^{\perp}$ are respectively the Sivers and the Boer-Mulders functions. Their rôle in the left-right asymmetries as well as their contribution to the understanding of the spin structure of hadrons will be highlighted in Chapters 6 & 7.

[5] It is given in the light-cone gauge $A^+ = 0$.

2 Pion Distribution Amplitude

This Chapter is devoted to the pion Distribution Amplitude (DA). The DA ϕ is the probability amplitude for finding, in the pion, the valence quarks sufficiently near the light cone. Its behavior as well as its evolution in Q^2 has been extensively studied in Refs. [45, 140]. We also study the pion Parton Distribution Function (PDF). Nowadays accurate experimental data allow for a comparison from the model calculations.

Since there are a well-known quantities, the pion DA and PDF represent a perfect framework for illustrating our approach. Also, the properties of the pion DA and PDF are placed under scrutiny. We consider sum rules, support and soft pion theorem; the latter linking the DA to the PDF or to the Generalized Distribution Amplitudes. The discrete symmetries as well as isospin relation are used to relate the different pion DAs. We draw the way to QCD evolution of the DA and the PDF. We eventually give the expression of the electromagnetic Form Factor and its well-known asymptotic limit; namely the Brodsky-Lepage Form Factor.

2.1 The Pion DA in the NJL Model

In this Section, we illustrate our approach by performing the complete calculation of a simple quantity: the pion DA $\phi(x)$. This will fix the conventions and allow us to give the parameters of the model. Also, the result of the calculation will tell us whether the model is appropriate for the calculation of such quantity. In particular, in the next Sections, we will see that the normalization condition as well as the support in x are respected.

By definition, the pion DA is, as depicted in Fig. 2.1,

$$\int \frac{dz^-}{2\pi} e^{i(x-\frac{1}{2})p^+z^-} \left\langle 0\right| \bar{q}\left(-\frac{z}{2}\right) \not{n} \gamma_5 \tau^- q\left(\frac{z}{2}\right) \left|\pi\left(p\right)\right\rangle \Big|_{z^+=\vec{z}^\perp=0} = \frac{1}{p^+} i\sqrt{2} f_\pi \phi\left(x\right) \quad . \tag{2.1}$$

The DA has a support in $x \in [0,1]$ and obeys the normalization condition

$$\int_0^1 dx\, \phi(x) \quad = \quad 1 \quad . \tag{2.2}$$

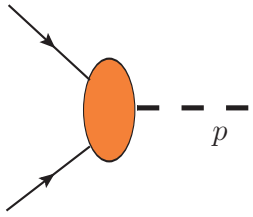

Figure 2.1: The pion DA.

The field theoretical approach we propose to use here has been first developed in Ref. [153]. The pion is described as a bound state in the sense of Bethe-Salpeter. In order to have an exact solution for the bound state, the kernel has to be chosen carefully. The Nambu - Jona-Lasinio interaction being point-like, it leads to such a solution. Furthermore, as it is extensively explained in Appendix C, the NJL model respects all the required symmetries of the problem. The pions appear to be the three Goldstone modes coming from the chiral symmetry (dynamical) breaking.
The shortcomings of the model are the absence of confinement and the non-renormalizability due to the point-like interaction. A regularization scheme should be chosen indeed. Also, the choice of this scheme defines the model per se. The NJL model completed with its regularization scheme is considered as an effective theory of QCD; even if built with quarks. Lorentz covariance and gauge invariance will assure the recovering of the properties of the parton distributions; so that the Pauli-Villars scheme is chosen that fulfills these conditions (see Section C.2). The regularization parameters, namely the cutoff Λ as well as the coupling strength G, are determined by calculating the pion decay constant f_π and the quark condensate. For $f_\pi = 93$ MeV and $\langle \bar{u}u \rangle = \langle \bar{d}d \rangle = -(250\,\mathrm{MeV})^3$, we obtain [125]

$$\Lambda = 859 \quad \mathrm{MeV} \qquad , \qquad G\Lambda^2 = 2.84 \quad . \tag{2.3}$$

From the gap equation Eq. (C.9), we also fix the value of the constituent quark mass to

$$m = 241 \quad \mathrm{MeV} \quad . \tag{2.4}$$

This model for the pion is used in the description of the bound state. The Bethe-Salpeter (BS) amplitude for the bound state π with four-momentum p is given by

$$\vec{\chi}_{\beta\alpha}(x_1, x_2; p) \quad = \quad \langle 0 | T q_\beta(x_1) \bar{q}_\alpha(x_2) | \vec{\pi}(p) \rangle \qquad . \tag{2.5}$$

The NJL model contains a four-fermion interaction. Direct and exchange diagrams are related to each other by a Fierz transformation. Since they go like $1/N_c$, the exchange diagrams are subleading and we may only consider direct diagrams. We also work in the ladder approximation, which consists in considering the iteration of the simplest closed loop with the kernel given by the model. The NJL interaction, giving rise to the kernel

$$V_{\alpha\beta,\delta\gamma}(k, k'; p) \quad = \quad 2iG(i\,\gamma_5 \vec{\tau}^\pi)_{\delta\gamma}(i\,\gamma_5 \vec{\tau}^\pi)_{\alpha\beta} \quad , \tag{2.6}$$

renders the BS equation for the bound state easy to handle.
Precisely, the integral equation generated by the chain of diagrams is the Bethe-Salpeter equation [112] for the bound state. Solving the Bethe-Salpeter equation in the ladder approximation with the kernel $V(k, k'; p)$,[1] we find the expression for the Bethe-Salpeter (BS) amplitude

$$\vec{\chi}\,(k; p) = iS\left(k + \frac{p}{2}\right)\, \vec{\Phi}\,(k, p)\; iS\left(k - \frac{p}{2}\right) \quad , \tag{2.7}$$

[1] See Eqs. (C.18, C.19) in Appendix C.

with $S^{-1}(k) = \not{k} - m$. The quark-pion vertex function is

$$\vec{\Phi}(k,p) \;=\; i\, g_{\pi qq}\, i\gamma_5\, \vec{\tau}^{\,\pi} \quad , \tag{2.8}$$

with the quark-pion coupling constant $g_{\pi qq}$ determined by the standard normalization of the BS equation.

In the theoretical scheme defined above, the pion DA is evaluated by developing the matrix element on the r.h.s. of Eq. (2.1) and rearrange it in such a way that we can identify the BS amplitudes $\chi(k;p)$. Therefore the Eq. (2.1) becomes

$$\begin{aligned} i\frac{\sqrt{2}f_\pi}{p^+}\phi(x) &= -\int \frac{dz^-}{2\pi}\, e^{ip^+(x-\frac{1}{2})z^-} \langle 0|q_\beta\left(\frac{z}{2}\right)\bar{q}_\alpha\left(-\frac{z}{2}\right)|\pi(p)\rangle \left(\not{n}\,\gamma_5\tau^-\right)_{\alpha\beta} \quad ; \\ &= -\int \frac{dz^-}{2\pi}\, e^{ip^+(x-\frac{1}{2})z^-} \chi_{\beta\alpha}\left(\frac{z}{2},-\frac{z}{2}\right)\left(\not{n}\,\gamma_5\tau^-\right)_{\alpha\beta} \quad . \end{aligned} \tag{2.9}$$

We define the Fourier transform, Ref. [153],

$$\vec{\chi}_P(x_1,x_2) \;=\; e^{-iPX}\int \frac{d^4k}{(2\pi)^4}\, e^{-ik\cdot r}\vec{\chi}(k,P) \quad , \tag{2.10}$$

with the center of mass and relative coordinates $X = \mu_1 x_1 + \mu_2 x_2$ and $r = x_1 - x_2$ and where $\mu_{1,2} = m_{1,2}/(m_1+m_2)$. So that

$$\begin{aligned} i\frac{\sqrt{2}f_\pi}{p^+}\phi(x) &= -\int \frac{dz^-}{2\pi}\, e^{ip^+(x-\frac{1}{2})z^-} \int \frac{d^4k}{(2\pi)^4} e^{-ik\cdot z}\mathbb{T}\mathrm{r}[\chi(k,p)\,\not{n}\,\gamma_5\tau^-] \quad , \\ &= -(-ig_{\pi qq})N_c\int \frac{dz^-}{2\pi}\, e^{ip^+(x-\frac{1}{2})z^-} \\ &\quad \int \frac{d^4k}{(2\pi)^4} e^{-ik\cdot z}\mathrm{tr}[S(k+\frac{p}{2})i\gamma_5\tau^{\pi^+}S(k-\frac{p}{2})\,\not{n}\,\gamma_5\tau^-] \quad . \end{aligned} \tag{2.11}$$

The symbol $\mathbb{T}\mathrm{r}$ at the first line is the trace over the Dirac, isospin, flavor and color spaces. Going one step further in the calculation, we perform the trace over isospin for a π^+. By making the change of variable $k \to -k + p/2$, we find

$$\begin{aligned} & i\,\sqrt{2}f_\pi\,\phi^{\pi^+}(x) \\ & = -i(-4m)p^+\,(-ig_{\pi qq})N_c\sqrt{2}\int \frac{d^4k}{(2\pi)^4}\,\frac{\delta(p^+(x-1)+k^+)}{((-k)^2-m^2+i\epsilon)\,((-k+p)^2-m^2+i\epsilon)}\,. \end{aligned} \tag{2.12}$$

The δ-function imposes a decomposition on light-cone components in order to perform the d^4k integral

$$\int \frac{d^4k}{(2\pi)^4} = \frac{1}{(2\pi)^2}\int\frac{d^2k^\perp}{(2\pi)^2}\int dk^-\int dk^+ \quad .$$

The integral over dk^+ is trivial: the δ-function imposes the $+$-component of the momentum carried by the outgoing quark. The remaining integral over $d^2k^\perp$ in Eq. (2.12) is divergent. Since it

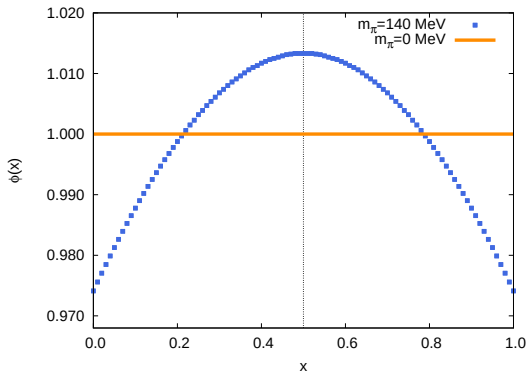

Figure 2.2: The pion DA in NJL. The dotted blue line represents the DA for the physical value of the pion mass while the plain orange line represents the chiral limit.

has been obtained with the NJL model interaction, the integral over $d^2k^\perp$ has to be consistently regularized using the Pauli-Villars regularization, which is part of the model.

The result Eq. (2.12) is proportional to the two-propagator integral $\tilde{I}_{2,P}(x,\xi)$ defined by Eq. (E.11)

$$i\sqrt{2}f_\pi\,\phi^{\pi^+}(x) \quad = \quad -4m\,ig_{\pi qq}\,N_c\sqrt{2}\,\tilde{I}_{2,P}(x,0) \quad . \tag{2.13}$$

In doing so, the normalization condition of the DA Eq. (2.2) is recovered for any value of the pion mass.

The result in the NJL model is shown on Fig. 2.2 for both the physical pion mass and the chiral limit. In the latter case, the pion DA is a constant which is equal to 1. This result is obtained by plugging f_π as given in Eq. (C.45) into Eq. (2.13). In the physical case, the DA deviates by less than 3% from 1. [2] The distribution amplitude does manifestly not vanish at the end points for none of the pion masses. This result is obviously characteristic of the model within which the calculation has been performed. It is not a QCD result, and in fact, QCD evolution, as will be shown later on, will push the DA to zero at the end points.

2.2 Symmetries

In the previous paragraph, we have considered the case of a π^+. Using discrete symmetries we can relate, in a model-independent way, the π^+ DA to the, e.g., π^- DA.

For a generic particle $\mathcal{P}$ with momentum $\vec{p}$, spin projection s_z and charge Q_i, we write the particle state $|\mathcal{P}(\vec{p},s_z,Q_i)\rangle$. Parity, time reversal invariance and charge conjugation act on this generic state in the following way

$$\begin{aligned}
P|\mathcal{P}(\vec{p},s_z,Q_i)\rangle &= \eta_P|\mathcal{P}(-\vec{p},s_z,Q_i)\rangle \quad , \\
T|\mathcal{P}(\vec{p},s_z,Q_i)\rangle &= \eta_T\,(-1)^{s-s_z}|\mathcal{P}(-\vec{p},-s_z,Q_i)\rangle \quad , \\
C|\mathcal{P}(\vec{p},s_z,Q_i)\rangle &= \eta_C|\mathcal{P}(\vec{p},s_z,-Q_i)\rangle \quad ,
\end{aligned} \tag{2.14}$$

[2] Mind the scale in Fig. 2.2!

with η_P, η_T, η_C the respective phases. For the π^+, which is $J^{PC} = 0^{-+}$, are $\eta_P = \eta_T = -1, \eta_C = 1$. In the light-front, the T symmetry as defined by the second expression of Eq. (B.1) changes x^+ to $-x^-$ and vice versa. It is therefore useful to define the V symmetry has the combination $P_z T$, what gives

$$V|\mathcal{P}(\vec{p}, s_z, Q_i)\rangle \;=\; \eta_V\,(-1)^{s-s_z}|\mathcal{P}(\vec{p}, -s_z, Q_i)\rangle \quad , \tag{2.15}$$

with $\eta_V = \eta_P\,\eta_T$.

In Appendix B are developed in details the symmetry relations for any type of distributions. We here relate such relations for the pion DA as given by Eq. (2.1). Using the relations Eq. (B.1), Time reversal invariance leads to

$$\Big(\phi^{\pi^+}(x)\Big)^* \;=\; \phi^{\pi^+}(x) \quad ; \tag{2.16}$$

charge conjugation to

$$\phi^{\pi^-}(x) \;=\; \phi^{\pi^+}(1-x) \quad ; \tag{2.17}$$

and CPT to

$$\Big(\phi^{\pi^-}(1-x)\Big)^* \;=\; \phi^{\pi^+}(x) \quad . \tag{2.18}$$

As perfectly illustrated on Fig. 2.2, the pion DA is symmetric around $x = 1/2$ so that $\phi(x) = \phi(1-x)$ as required by isospin: it is easily seen from Eq. (2.26) that it is implied by the fact that the quarks carry the same constituent mass. By Eq. (2.17), it means that there is no difference between the DA for a π^+ or a π^-. This also corresponds to the isospin relation: the distribution amplitude for a u-quark is related by the change $x \to 1-x$ to the amplitude for a d-quark.

Those relations remain unchanged under evolution.

2.3 The Pion Parton Distribution Function

The nomenclature of distribution functions includes a huge variety of transitions. As overviewed in the Introduction, the names are mostly related to the nature of the final and initial states. For instance, the DA is a transition from a physical state to the vacuum. Also, by definition, the pion Parton Distribution Function is the probability density to find a quark carrying a fraction x of the parent pion's momentum, i.e.

$$\int \frac{dz^-}{2\pi}\, e^{i\,(x-\frac{1}{2})\,z^-p^+}\,\langle\pi^+(p)|\bar{q}\left(-\frac{z}{2}\right)\,\not{n}\,\frac{1}{2}(1+\tau^3)\;q\left(\frac{z}{2}\right)|\pi^+(p)\rangle \;=\; \frac{1}{p^+}\,q(x) \quad , \tag{2.19}$$

as illustrated on Fig. 2.3. In the NJL model we obtain

$$q(x) \;=\; 4\,N_c g_{\pi qq}^2\left[-\frac{1}{2}\tilde{I}_{2,P'} - \frac{1}{2}\tilde{I}_{2,P}(x,0) + m_\pi^2\,x\,\tilde{I}_3^{GPD}(x,0,0)\right] \quad , \tag{2.20}$$

with the 2- and 3-propagator integrals defined Eqs. (E.10, E.11, E.13). In the chiral limit, $q(x)$ is equal to 1. The NJL model has been applied to the study of pion Parton Distribution in different occasions [76, 77, 179]. More elaborated studies of pion Parton Distribution have been performed

in the Instanton Liquid Model [14], and in lattice calculation inspired nonlocal Lagrangian models [155, 156], which confirm that the result obtained in the NJL model for the Parton Distribution is a good approximation.

A low-energy theorem based on PCAC[3] links the pion DA and the distributions of two physical pion states.
Following the same steps as in Ref. [86], we hereafter derive this relation between the pion DA $\phi(x)$ and the pion PDF $q(x)|_{p^\mu_{\pi_2}\to 0}$, which leads to the particularly interesting result

$$\phi_\chi(x) = q_\chi(x) \quad , \tag{2.21}$$

where χ means $m_\pi = 0$ MeV for the pion under scrutiny.

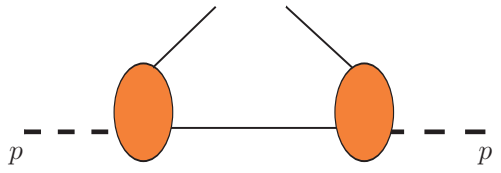

Figure 2.3: The pion Parton Distribution Function. The orange blobs represent the pions.

Let us take the matrix element of a pion-pion transition with momentum transfer $p_1 - p_2$; we call it f^{ab}. Such a matrix element obeys the following isospin decomposition [170]

$$f^{ab} \;=\; \delta^{ab}\, f^{I=0} + \frac{1}{2}\,\mathrm{tr}([\tau^a,\tau^b]\,\tau^c)\, f^{I=1} \quad .$$

It is related to the $u-$ and $d-$quarks distributions by $f^u + f^{\bar{d}}$. We consider the isovector contribution of such a matrix element

$$\left\langle \pi^b(p_2) \left| \bar{q}(x)\,\hat{n}\,\frac{\tau^3}{2}\,q(0) \right| \pi^a(p_1) \right\rangle \quad . \tag{2.22}$$

Using the Lehmann-Symanzik-Zimmermann reduction formula we can write

$$\begin{aligned}
&\langle \pi^b(p_2)|\bar{q}(x)\,\hat{n}\,\frac{\tau^3}{2}\,q(0)|\pi^a(p_1)\rangle \\
&= i\int d^4x\, e^{-ip_2\cdot x}\,\left(\Box_y^2 + m_\pi^2\right)\,\langle 0|\,T\left\{\pi^b(y)\,\bar{q}(x)\,\hat{n}\,\frac{\tau^3}{2}\,q(0)\right\}|\pi^a(p_1)\rangle \quad ,
\end{aligned}$$

where $\pi^j(x)$ is the pion interpolating field and is given by PCAC, Eq. (C.42). We now integrate twice by parts and use the relation for the derivative of the Time-ordered product $\partial_{t'}T\{\varphi(x')\varphi^\dagger(x)\} = T\{(\partial_{t'}\varphi(x'))\varphi^\dagger(x)\} + \delta(t'-t)\,[\varphi(x'),\varphi^\dagger(x)]$.
Taking the soft pion limit, i.e. $p_2^\mu \to 0$, the matrix element (2.22) becomes

$$\begin{aligned}
&\lim_{p_2^\mu\to 0}\langle \pi^b(p_2)|\bar{q}(x)\,\hat{n}\,\frac{\tau^3}{2}\,q(0)|\pi^a(p_1)\rangle \\
&\qquad = \frac{-i}{f_\pi}\int d^4x\,\Big[\delta(y_0-x_0)\langle 0|[A^{0b}(y),\bar{q}(x)]\,\hat{n}\,\frac{\tau^3}{2}\,q(0)|\pi^a(p_1)\rangle \\
&\qquad\qquad +\delta(y_0)\langle 0|\bar{q}(x)\,\hat{n}\,\frac{\tau^3}{2}\,[A^{0b}(y),q(0)]|\pi^a(p_1)\rangle\Big] \quad .
\end{aligned} \tag{2.23}$$

[3]Partial Conservation of the Axial Current; see Section C.4 in Appendix C.

The axial current gives rise to the axial charge $Q_5^a = \int d^4x\, \delta(x_0) A_0^a(x)$ with the equal-time commutators obeying $[Q_5^a, q(x)] = i/2\, \tau^{\pi^a}\, \gamma_5\, q(x)$.
The expression (2.23) becomes

$$\begin{aligned}\lim_{p_2^\mu \to 0} \langle \pi^b(p_2)|\bar{q}(x)\, \hat{n}\, \frac{\tau^3}{2}\, q(0)|\pi^a(p_1)\rangle &= \frac{1}{f_\pi}\Big[\langle 0|\bar{q}(x)\, \sqrt{2}\frac{\tau^b}{2}\gamma_5\, \hat{n}\, \frac{\tau^3}{2}\, q(0)|\pi^a(p_1)\rangle \\ &\qquad + \langle 0|\bar{q}(x)\, \hat{n}\, \frac{\tau^3}{2}\, \sqrt{2}\frac{\tau^b}{2}\gamma_5\, q(0)|\pi^a(p_1)\rangle\Big] \quad , \\ &= \frac{i\, \epsilon^{3bc}}{f_\pi}\, \langle 0|\bar{q}(x)\, \hat{n}\, \sqrt{2}\frac{\tau^c}{2}\gamma_5\, q(0)|\pi^a(p_1)\rangle \quad , \end{aligned} \tag{2.24}$$

where we have used the algebra $[\tau^3/2\,,\, \tau^b/2] = i\, \epsilon^{3bc}\, \tau^c/2$.

In order to go to the pion Distribution Functions, we Fourier transform Eq. (2.22) for quarks at a light-light separation and replace p_1 by p and make the transition diagonal in isospin and in momentum. In the soft pion limit, the isovector pion PDF is exactly the pion DA

$$\begin{aligned}&\lim_{p_{\pi_2}^\mu \to 0} \int \frac{dz^-}{2\pi}\, e^{i\,(x-\frac{1}{2})\, z^- p^+}\, \langle \pi_2^+(p)|\bar{q}\left(-\frac{z}{2}\right)\, \gamma^+\, \frac{\tau^3}{2}\, q\left(\frac{z}{2}\right)|\pi_1^+(p)\rangle \\ &\qquad = \frac{-i}{\sqrt{2}\, f_\pi} \int \frac{dz^-}{2\pi}\, e^{i\,(x-\frac{1}{2})\, z^- p^+}\, \langle 0|\bar{q}\left(-\frac{z}{2}\right)\, \gamma^+\gamma_5\, \tau^-\, q\left(\frac{z}{2}\right)|\pi_1^+(p)\rangle \quad , \end{aligned} \tag{2.25}$$

what corresponds to the definition of the pion DA, Eq. (2.1). This results takes all its physical meaning in the chiral limit $m_{\pi_1} = m_{\pi_2} = 0$, where both pions are chosen to have zero mass by consistency. The PDF actually has to be diagonal in state. If one of the pion is massless ($p_{\pi_2}^\mu \to 0$ implies that $p_{\pi_2}^2 = 0$), the other pion has to be massless as well. We find the expected result of Eq. (2.21).

2.4 Towards the Support Problem

We now focus on the support property that is easy to illustrate in the context of 2-propagator integrals. Nevertheless the discussion that follows is extended to 3-propagator integrals.

The support in x is determined by the pole structure in k^- of the function given in Eq. (2.13). Developping this integral, Eq. (E.11), leads to

$$\begin{aligned}&i\sqrt{2} f_\pi \phi(x) \\ &= -i\, 4m\, p^+\, i g_{\pi qq} N_c \sqrt{2}\, \frac{1}{(2\pi)^2} \int \frac{d^2\vec{k}_\perp}{(2\pi)^2}\, dk^- \\ &\qquad \frac{1}{2p^+(1-x)\left(k^- - \frac{\vec{k}_\perp^2 + m^2}{2p^+(1-x)} - \frac{i\epsilon}{2p^+(1-x)}\right)\, 2p^+ x\left(p^- - k^- - \frac{(\vec{p}_\perp - \vec{k}_\perp)^2 + m^2}{2p^+ x} + \frac{i\epsilon}{2p^+ x}\right)} \quad . \end{aligned} \tag{2.26}$$

The integral over dk^- is performed in the complex plane making use of the Cauchy's theorem. Would $x \notin [0,1]$, both the poles would be on the same side of the real axis and the integral would be identically zero. The definition Eq. (2.1) therefore leads to the required support in x, i.e. $x \in [0,1]$.

It is true as long as the regularization scheme that we use is covariant. This condition is necessary but not sufficient: the regularization procedure should preserve the symmetries of the light-cone instead. Regularizing Eq. (2.26) through a 3-momentum cutoff would break covariance, spoiling the required support. However, it is obvious that a cutoff of the type $\vec{\Lambda} = (\Lambda^-, \vec{\Lambda}_\perp)$, with $\Lambda^- < \infty$ prevent us from closing the contour in the complex plane of k^-. This leads to support corrections of the order of $1/\Lambda^-$. Therefore the loss of light-cone invariance here produces the loss of the correct support.

Many calculations of PDFs show problems with the support properties. In particular, the support problem occurs in calculations performed in non relativistic (NR) Constituent Quark Models (CQM), e.g. Ref. [200]. In such NR calculations, the light-cone coordinates are defined from the 3-momentum and the energy, $k_0^2 = m^2 + \vec{k}^2$, so that the dependence on k^- is not the genuine one. A slight support violation is observed. In the same Reference [200], the inclusion of Final State Interactions is proposed to restore translational invariance and therefore the support, which in turn will restore the number of particle conservation. A trivial solution to the support problem would be to change the normalization in order to rescale the support to compensate for the problem. In the same line, we also mention that a slight violation of the support is found in the MIT bag model e.g. Ref. [188].

Let us now comment on the role of the interaction on the support problem, staying in the description of the hadron as a bound state in the sense of Bethe-Salpeter.

The vertex function $\Phi(k,p)$ defines the BS amplitudes, which are afterwards plugged into the distribution in the BS approach (2.9). The former is defined within a model with its given symmetries; whereas the latter requires covariance on the light-cone. It is important to realize that, in order to preserve the support property, one has to go to the light-front without breaking its covariance [156], a constraint that is respected by NJL model.

The BS equation for the pion has been studied using different vertices, e.g., [57, 58, 195, 196, 197, 204]. In the five first References, use has been made of a reduction of the BS amplitudes to light-cone wave functions by projecting on the light-cone. In Refs. [57, 58], the light-front BS vertex functions were replaced by wave functions obtained in a light-front CQM. In Refs. [195, 196, 197], the scalar Wick-Cutkosky model was adopted and successfully applied to the calculation of scalar meson GPDs. The correct support has been found. It is however not the case in Ref. [203, 204] where the calculation is performed in a covariant CQM, i.e., the Bonn model. Once more, the problem is initially non covariant but the authors attempted to restore Lorentz invariance by applying a boost; attempt which was nonetheless either too schematic or incomplete. In Ref. [202] a detailed study of the problem suggests that the dependence upon the energy, k^-, of the vertex is responsible for the introduction of additional dynamical poles. As a counter example we mention the non-local Lagrangian [155] used to calculate PDFs in Ref. [155, 156]. The non-locality of the interaction obviously leads to a k^--dependent vertex, whose definition is chosen consistently with the definition of the mass $m(p)$, given there by lattice QCD. The problem is totally covariant and the support is recovered in the physical cases. Since the calculation in non-local models is performed in the Euclidean space, it is the Wick rotation that, in this case, might spoil the support property.

It is therefore tempting to explain the fulfillment of the support property by the conservation of covariance on the light-cone.

2.5 QCD Evolution

In a previous Section, we have proven that the pion DA and the PDF coincide in the chiral limit. Nevertheless this result based on PCAC must be strongly broken by QCD evolution when we move from low to high Q^2. We will now discuss how evolution changes the PDFs and the DAs. Our first objective will be to determine the scale of the model, which can be fixed from our knowledge of PDFs.

The Parton Distributions here obtained are valid at a low scale where scaling still holds and our model is still defined. However, one would like to link the results of a model calculation with QCD. In other words, one would like to know the corrections when going to higher energy. The start of the scaling violations is given by the so-called evolution equations, which schematically describe the dependence of the distribution functions on Q^2

$$\phi(x) \stackrel{?}{\longrightarrow} \phi(x,Q) \quad .$$

The pioneer works on the behavior of Parton Distribution Functions (PDFs) with Q^2 were done by Dokshitzer [85], Gribov and Lipatov [104, 141] as well as by Altarelli and Parisi [9]. The QCD evolution of the Distribution Amplitudes has been studied by Efremov and Radyushkin [88] as well as by Brodsky and Lepage [140]. This gave rise to the so-called ERBL evolution equations.

The rôle of the model calculations is to provide for the initial conditions to the evolution equations.

The initial scale from the NJL calculation

The scale of validity of the model calculation is still to be found. One needs to fix the value of Q_0 for which the quark distributions obtained in the NJL model are considered to be a good approximation of the QCD quark distributions. For the purpose of evolving the parton distributions, we use the code of Freund and McDermott [94].

The only information we have at hand is the momentum sum rule. Obviously momentum conservation holds and we know that the sum of the momentum fractions carried by each constituent, namely the valence quarks (v), the gluons (g) and the sea quarks (s), i.e. the second moment of the PDF $f(x,Q)$

$$\langle x \rangle_y(Q) \equiv \int_0^1 dx\, x\, f(x,Q) \tag{2.27}$$

has to be conserved. In the models we are interested in, only valence quarks are taken into account, so that,

$$\langle x \rangle_v(Q_0) = 1 \quad , \qquad \langle x \rangle_s(Q_0) + \langle x \rangle_g(Q_0) = 0 \quad . \tag{2.28}$$

To leading order (LO), scaling violations are manifested in a logarithmical dependence, of the PDFs, on the scale through the running coupling constant

$$\alpha(Q^2) \;=\; \frac{4\pi}{\beta \ln(Q^2/\Lambda^2)} \quad , \tag{2.29}$$

with $\beta = 11/3\,N_c - 2/3\,N_f$ and Λ is the scale of QCD. In order to find the value of Q_0, we need to fix the value of Λ consistently with the evolution code; i.e. we choose $\Lambda = 0.174\,\mathrm{GeV}$. Following the NLO evolution, one is to use $\Lambda = 0.246\,\mathrm{GeV}$.

Knowing that the momentum fraction of each valence quark at $Q = 2$ GeV is 0.235 [192], we fix the initial point of the evolution in such a way that the evolution of the second moment of the pion Parton Distribution reproduces this result. This condition is fulfilled at a rather low value, i.e.

$$\begin{aligned} Q_0 &= 0.29\mathrm{GeV} \quad , \quad \text{for the LO evolution}\,; \\ Q_0 &= 0.43\mathrm{GeV} \quad , \quad \text{for the NLO evolution}\,. \end{aligned} \tag{2.30}$$

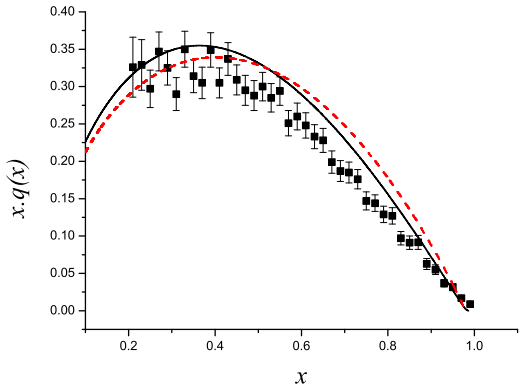

Figure 2.4: Pion parton distribution. See text.

The first result that we obtained is that the PDF resulting from the NLO evolution is basically unimproved with respect to the one evolved to LO. In order to illustrate the latter statement, we have depicted the pion PD evolved at both LO and NLO in Fig. 2.4. The solid (black) line of the Figure corresponds to the LO evolution of the NJL model prediction while the dashed (red) line represents the NLO. Both evolved results are compared to the experimental data [65]. The agreement with the data is not better in one or the other case. The effect of the NLO evolution is compensated in the LO evolution going to a lower value of Q_0, a result that has already been noticed in proton Parton Distributions [200]. It is therefore obvious that, for numerical reasons, we will prefer to evolve the distributions to LO.

The method used here is also applied by the authors of Ref. [103]. There exists other ways of fixing the scale, using different data or comparing with lattice data. They are reviewed in the latter Reference.

The QCD evolution of the Pion DA

The Distribution Amplitudes have a logarithmic dependence in Q which is completely determined by the QCD evolution equations derived in Ref. [138, 139, 140]. The QCD evolution equations for the distribution amplitudes can be expressed, to leading order, in terms of Gegenbauer polynomials

$$\phi(x,Q) \;=\; x(1-x)\sum_{\substack{n=0\\ even}}^{\infty} a_n\, C_n^{3/2}(2x-1)\left(\ln\frac{Q^2}{\Lambda^2}\right)^{-\gamma_n} \quad , \tag{2.31}$$

where only even n contribute since $\phi(x,Q) = \phi(1-x,Q)$ is required by isospin. The anomalous dimensions are

$$\gamma_n \;=\; \frac{C_F}{\beta}\left(1 + 4\sum_{2}^{n+1}\frac{1}{k} - \frac{2}{(n+1)(n+2)}\right) \quad , \tag{2.32}$$

where $C_F = (N_c^2 - 1)/(2N_c)$ and $\beta = 11/3\, N_c - 2/3\, N_f$.
The evolution equations would be completely known if the coefficients a_n were determined. These coefficients can be determined from the initial conditions which are provided by the model calculation. The evaluation of the DA in the model provides us for the $\phi(x_i, Q_0)$. By using this initial distribution together with the orthogonality relations for the Gegenbauer polynomials,

$$a_n \left(\ln\frac{Q_0^2}{\Lambda^2}\right)^{-\gamma_n} = 4\,\frac{2n+3}{(n+1)(n+2)} \int_0^1 dx\, C_n^{3/2}(2x-1)\,\phi(x,Q_0) \quad , \quad n = \text{even} \quad , \tag{2.33}$$

one might be able to find the a_n coefficients, namely, to determined the evolution equations.

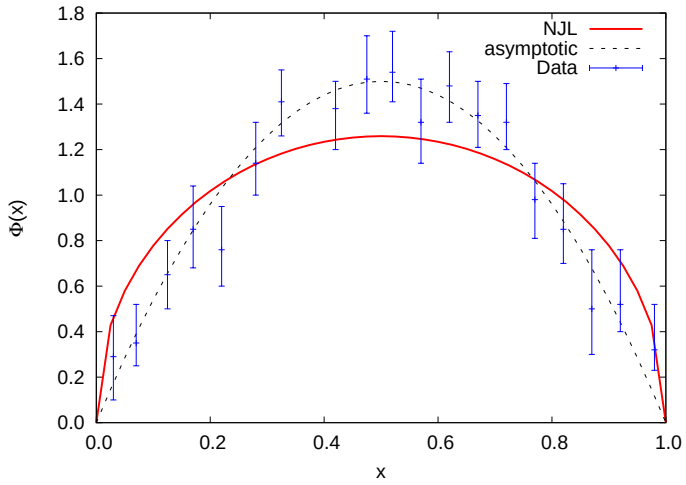

Figure 2.5: The pion DA in the NJL model evolved to the scale $Q = 2$ GeV (red curve) and compared to E971 di-jet measurement [3] after proper normalization of the data Ref. [45]. The dashed line represent the asymptotic DA.

All the model calculations, after evolution, should agree with the theoretical asymptotic behavior of the DA, that is given by Eq. (2.31) with $Q^2 \to \infty$. Since $\gamma_0 = 0$ and $\gamma_n > 0$ for positive n, only the first term, i.e. $n = 0$, survives

$$\phi(x,Q) \overset{Q^2\to\infty}{=} a_0\, x(1-x) \quad . \tag{2.34}$$

Using the orthogonality relations for the Gegenbauer polynomials Eq. (2.33) and the renormalization of the charged weak current, it is found in Ref. [140] that $a_0 = 6$. We can find the other coefficients through the initial conditions given by our result in the NJL model. As mentioned in Section 2.1, in the chiral limit, the pion DA is a constant normalized to 1

$$\phi(x,Q_0) \;=\; 1 \quad , \tag{2.35}$$

what holds at the scale of the model, Q_0. It is then easy to apply the above-described formalism and determine the a_n for our model calculation. Plugging Eq. (2.35) into the relation (2.33), we find[4]

$$\phi(x,Q) \;=\; 4\,x(1-x) \sum_{\substack{n=0\\ even}}^{\infty} \frac{2n+3}{(n+1)(n+2)}\, C_n^{3/2}(2x-1) \left(\frac{\ln(Q^2/\Lambda^2)}{\ln(Q_0^2/\Lambda^2)}\right)^{-\gamma_n} \quad . \tag{2.36}$$

[4] $\int_0^1 dx\, C_n^{3/2}(2x-1) = 1$ for $n =$ even.

At a scale Q_0, the series of the previous result should give 1. However, it must be realized that this result is reached for $n \to \infty$ which is numerically not feasible. At a low scale $Q_0 < Q \lesssim 1$ GeV, where changes due to evolution are more important, one should include a high number of terms of the series. As proven by Fig. 2.6, the desired result is reached by increasing the n value. It nevertheless takes an infinite number of terms to compensate for 0 going to 1 at the end-points.

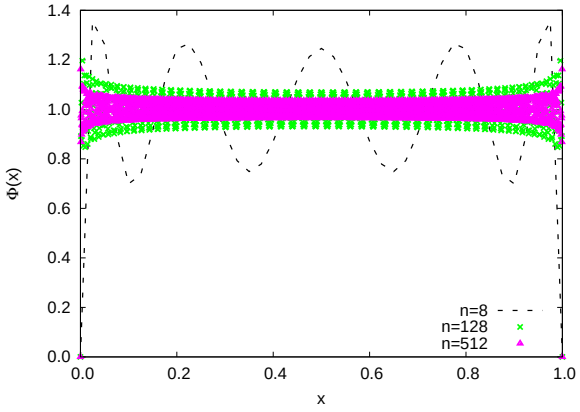

Figure 2.6: The truncated series (2.36) for the pion DA in the NJL model at Q_0.

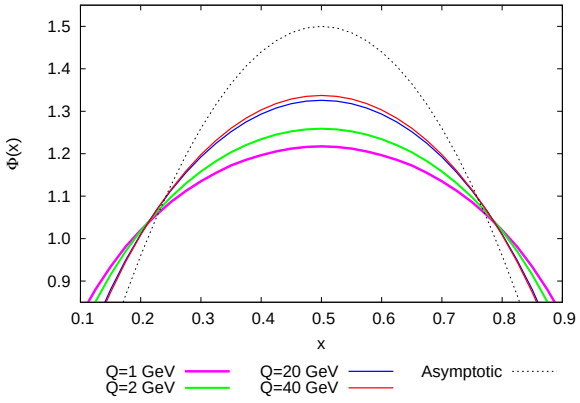

Figure 2.7: The pion DA in the NJL model evolved to the scales $Q = 1, 2, 20\,\&\,40$ GeV as well as the asymptotic form.

On the other hand, once QCD is switched on, the end-point problems for the pion DA calculated in the NJL model in the chiral limit is solved, showing the need for QCD evolution.

The pion DA evolved to a scale of $Q = 2$ GeV is shown in Fig. 2.5 for the NJL model with Pauli-Villars regularization. It is compared to the data of the E791 measurement [3] once properly normalized [45]. The asymptotic DA is also plotted that seems to be in a better agreement with the data.

In our version of the NJL model, the scale of the model is found to be as low as $Q_0 = 290$ MeV at LO, see Eq. (2.30). At high Q, one could take into account only the 4th first terms of the series. This approximation is justified by the fact that the coefficients a_n decrease with increasing n and by the asymptotic behaviour in Q. However, for a better resolution and smoothness of the plots, we choose to truncate the series at $n = 512$.
In order to illustrate the result obtained in Eq. (2.36), we plot the series in Fig. 2.7 for different, high values of Q. For Q higher than 1 GeV (pink curve), the effect of evolution starts being less important. The green, blue and red lines represent the LO order evolved at, respectively, $Q = 2$ GeV, $Q = 20$ GeV and $Q = 40$ GeV. The result changes slowly showing that no big improvement to reach the asymptotic value can be done by this model calculation at least at LO evolution. One can however easily check that the analytical asymptotic behavior for the series. (2.36) is $\phi(x, Q) = 6\,x(1-x)$, as required.

2.6 End-points

Although its rôle seems to be only that it provides for the initial conditions, a model calculation is a calculation that has a physical meaning. As a consequence, the results in the model are supposed to obey all the properties of the initial object. Turning the problem over: the results of model calculations are not complete until evolution is performed and most of the properties of Parton Distributions that were respected at the quark-model scale, e.g. isospin relations, will still be after evolution. On the other hand, we will show that other intrinsic properties can be restored.

In particular, one could evoke the problem of the distribution functions at the end-points. Effectively, in the free parton model, PDFs are expected to vanish at the boundaries, i.e. $x = 0, 1$. For on-shell particles, at $x = 1$ one of the quarks carries the whole (+)-component of the momentum and the other quark has zero (+)-component of the momentum, i.e. on-shellness implies an infinite (−)-component of the momentum. Since the (−)-component of the momentum appears in the propagator, the PDF vanishes. Also, this end-point behavior has been analytically predicted in perturbative QCD, e.g. [40].

It is however not what happens for the results in lots of models such as the NJL model illustrated in, e.g., Fig. 2.2. This *unwelcome* behavior comes from the misunderstanding of the Nature of the quarks beyond the naïve parton model. It is effectively unclear how the constituent quarks of the quark models can be linked to the current quarks of QCD. We are willing phenomenological evidences to shed some light on the constituent density distributions. The scenario suggested by Altarelli, Cabibbo, Maiani and Petronzio (ACMP) [8] pictures the constituent quark as a complex system of point-like partons. This ansatz is so far one of the only for those distributions. A variation of this scenario has been applied in, e.g., Refs. [154, 156, 186, 187], showing a huge improvement.

As for the calculation in the NJL model, the end-point problem shows the limits of validity of our model calculation. The simple considerations given above do not hold for the bound-state quarks in the NJL model; and as a matter of fact we cannot expect the Parton Distributions to vanish at the boundary. This behavior has been shown to arise in a regularization-independent way as they appear in both the results of Refs. [45, 153].

Turning our attention to the chiral limit, the question could also be formulated as follows: what is, in the NJL model, the probability density of finding -massless(current)- quarks with momentum x inside a massless pion? The quarks can, a priori, not carry a particular fraction of the massless pion momentum, so that the probability density does not depend on x, explaining at the same time the end-point behavior and the result $q(x) = 1$. This problem is the opposite of the zero bounding energy problem, where the mass of the pion is chosen to be twice that of the constituent quarks. In that case, the distribution is rather peaked in $x = 1/2$ as shown by a quick analysis of the kinematics.

As for the treatment of the quarks in the calculation given here, our choice has been to maintain consistency with the model in itself. The relation between the current quarks of the NJL model, with mass m_0, and the constituent quarks, carrying a mass m, is the one given by the Bogoliubov-Valatin transformation which is proper to the model. [5] Therefore an additional convolution of the type ACMP is not necessary.

We conclude by highlighting the fact that the obtained values about $q(x) = 1$ in the vicinity of $x = 0, 1$ enable a good reproduction of the evolved PDF at the end-points, see Fig. 2.4. On the

[5] See Appendix C.

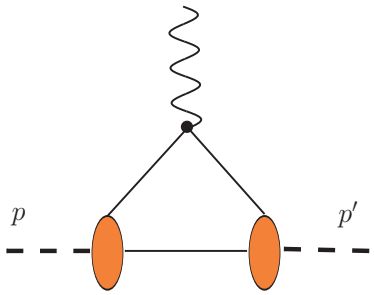

Figure 2.8: The Feynman diagram representing the elastic scattering.

other hand, similar considerations for the pion DA, e.g. Fig. 2.5, indicate that the obtained DA is too high at the end-points.

2.7 The Pion Electromagnetic Form Factor

In this Chapter we have examined the meson Distribution Amplitudes as an illustration of the method we will use throughout this thesis. The DAs contribute to both elastic and deep inelastic processes, what made the example interesting. In particular, they can contribute to the elastic scattering process Fig. 2.8. It is, however, not the simplest situation for the study of elastic processes: The simplest objects that allow for the study of hadron properties are not the meson DAs but the elastic Form Factors. In effect, the Form Factor is the amplitude for the, e.g., pion to absorb large transverse momentum while remaining intact. In this Section, we aim to link both quantities and to discuss the asymptotic - and model-independent - limits of the pion electromagnetic Form Factor.

For a charged pion π^+ the electromagnetic Form Factor F_π is defined as

$$\langle \pi^+(p')|J_\mu^{elm}(0)|\pi^+(p)\rangle \quad = \quad (p+p')_\mu \, e \, F_\pi(q^2) \quad ,$$

with $q^2 = (p'-p)^2$; and its charge radius by

$$\langle r^2 \rangle_\pi \quad = \quad -6 \frac{d^2 F_\pi(q^2)}{dq^2}\Big|_{q^2=0} \quad .$$

We evaluate the diagram on Fig. 2.8 in the NJL model, with both incoming and outgoing particles being pions as well as its crossed version, applying the technique of the Section 2.1. We find

$$F_\pi(q^2) \quad = \quad \frac{4\, N_c \, g_{\pi qq}^2}{m_\pi^2 + p\cdot p'} \left(-m_\pi^2 \, I_2(p) - p\cdot p' \, I_2(p-p') + m_\pi^4 \, I_3(p,p') \right) \quad , \tag{2.37}$$

with the 2- and 3-propagator integrals defined in Appendix E. The charge radius evaluated in the NJL model is found to be $\langle r^2 \rangle_\pi = 0.31\,\mathrm{fm}^2$, which has to be compared to the experimental value of 0.44 fm^2. It must be realized that our model does not include the vector mesons, which also contribute to the charge radius of the pion, see e.g. [87].

Here, we have used an effective theory of QCD in order to calculate the electromagnetic quantity. The expression (2.37) is a useful check for the sum rules for GPDs and will be used in the next Chapter.

The Asymptotic Limit: the Brodsky-Lepage Form Factor

The electromagnetic Form Factor can also be seen as the convolution of three probability amplitudes. Basically, those probability amplitudes are the probability of finding a 2-quark valence state in the incoming pion, i.e. the pion DA ϕ; a hard amplitude T_H for this 2-quark-state to scatter with the photon and, therefore, to produce 2 quarks which can reform in similar 2-quark state [140]. The latter is described by a pion DA ϕ^*;[6]

$$F_\pi(Q^2) \;=\; \int_0^1 dx_i\, dy_i\, \delta(1-\Sigma_i x_i)\, \delta(1-\Sigma_i y_i)\, \phi^*(y_i,Q)\, T_H(x_i,y_i,Q)\, \phi(x_i,Q) \quad , \tag{2.38}$$

where T_H contains all the 2-particle irreducible amplitude for $\gamma^* + q\bar{q} \to q\bar{q}$. This approach is similar to the previous one in that the pion DA is well-described by the Bethe-Salpeter amplitude on the light-front. However, the pion DA calculated within this formalism does not explicitly depend on the scale unless we switch on QCD. Now, the effects of QCD evolution need to be taken into account into the convolution (2.40), so that we need the evolved pion DA.

Using the light-cone perturbation theory together with the light-cone gauge, Brodsky and Lepage [138, 139] obtained the evolution equations of Section 2.5. Those equation can in turn be applied to the calculation of the Form Factors. The hard amplitude gives the behavior in powers of Q^2. For instance, plugging Eq. (2.31) with T_H evaluated in the same light-cone perturbation theory, they found, to leading logarithmic corrections

$$F_\pi(Q^2) \;=\; \frac{4\pi\, C_F\, \alpha_s(Q^2)}{Q^2} \left| \sum_{n=0}^{\infty} \frac{a_n}{2} \frac{f_\pi}{\sqrt{N_c}} \left(\log \frac{Q^2}{\Lambda^2} \right)^{-\gamma_n} \right|^2 \left[1 + \mathcal{O}\left(\alpha_s(Q^2), m/Q \right) \right] \quad , \tag{2.39}$$

which shows the most important dynamical feature of the Form Factors, namely, their power-law fall-off. The asymptotic limit is given by Eq. (2.34) with known a_0

$$\begin{aligned} F_\pi(Q^2) &\overset{Q^2\to\infty}{=} \frac{4\pi\, C_F\, \alpha_s(Q^2)}{Q^2} \frac{9\, f_\pi^2}{N_c} \quad , \\ &\overset{Q^2\to\infty}{=} 16\,\pi \alpha_s(Q^2) \frac{f_\pi^2}{Q^2} \quad , \end{aligned} \tag{2.40}$$

with $N_c = 3$.

[6] $-q^2 = Q^2$.

3 Pion Generalized Parton Distributions

The adjective *generalized* in the name Generalized Parton Distributions (GPDs) appeared in the early nomenclature of distribution functions [117, 118]. Their introduction through the factorization theorems for deep exclusive processes demonstrated the wide applicability of the diagonal transitions obtained with inclusive processes. Deep exclusive processes have also been discussed in terms of *off-forward* parton distributions [173] for they are non-diagonal in momentum, i.e. there is a momentum transfer between the initial and final states. The off-forward distributions are univocally related to the GPDs. The initial and final states we will nevertheless consider as corresponding to the same quantum numbers when referring to *Generalized* Parton Distributions. Such distributions, with states not corresponding to the same particles, are called Transition GPDs or Transition Distribution Amplitudes. The study of the latter quantities is actually the main topic of this thesis and will be fully developed in Chapter 4.

In Chapter 1 we have introduced the Generalized Parton Distributions for the nucleons. Nevertheless such bilocal matrix elements can also be defined for mesonic states, e.g. pions. Let us now focus on the study of the pion GPDs applying the rules developed in the NJL model which have been given in the previous Chapter about the Pion Distribution Amplitude.

The set of distributions proposed for the proton in Refs. [79, 82] is adapted to the pion case including both the chiral-even and the chiral-odd GPDs. The tensorial structure for the $\gamma^*\pi \to \gamma\pi$ process allows a single twist-2 chiral-even GPD. In the light-front, the tensorial decomposition of this GPD is found, using the recipe of Ref. [15, 79], from the vector current

$$\begin{aligned} F^\pi(x,\xi,t) &= \frac{1}{2}\int \frac{dz^-}{2\pi}\, e^{ixz^-p^+} \left\langle \pi(P') \left| \bar{q}\left(-\frac{z}{2}\right) \gamma^+ q\left(\frac{z}{2}\right) \right| \pi(P) \right\rangle |_{\vec{z}^\perp = z^+ = 0} \quad , \\ &= \frac{1}{2\,p^+} H^\pi(x,\xi,t)\ (P+P')\cdot n = \frac{1}{p^+} H^\pi(x,\xi,t) \quad , \end{aligned} \tag{3.1}$$

with $q(x)$ the quark field and where $2p^\mu = (P'+P)^\mu$. On the other hand, the axial current gives

rise to a twist-3 GPD, involving the $\gamma^\perp\gamma_5$ current. [1] This distribution function will not be studied in this thesis. The effect of twist-3 distributions is small but, for nucleons, their inclusion is useful for the restoration of electromagnetic gauge invariance in DVCS, e.g. Ref. [15]. In the pion case, the twist-3 GPD can be associated to a Single-Spin Asymmetry [12].

Taking into account chiral-odd, namely helicity-flip, GPDs makes the number of twist-2 pion GPDs increase. This case will be overviewed in the *Future Perspectives* in Chapter 7.

In the literature, different approaches of the non-diagonality -in momentum- have been proposed for the hadronic matrix element

$$\left\langle \pi(P') \left| \bar{q}\left(-\frac{z}{2}\right) \Gamma^\mu \, q\left(\frac{z}{2}\right) \right| \pi(P) \right\rangle \quad . \tag{3.2}$$

One bases its analysis of the longitudinal asymmetry on the kinematics of the process. Since the dependence upon the skewness variable is hence explicit, this approach leads to the so-called *skewed* parton distributions [117, 118, 173, 174]. Another approach is to write the spectral decomposition of the matrix element of the bilocal operator at a light-like distance without kinematical assumptions on the skewness variable, allowing one to make statements about this very dependence. This second approach leads to the so-called Double Distributions (DD), which have been proposed in Refs. [148, 173, 174].

The Nambu - Jona-Lasinio model is an appropriate choice in the context of model calculation of both the pion *skewed* PDs and DDs. As above-mentioned the pion can be treated as a bound-state in a fully covariant manner following the Bethe-Salpeter approach inside the NJL model. Given the tools exposed in Chapter 2 we are now able to extend the application of the model for the pion to the definition of GPDs. So, in this Chapter we will aim to analyze the twist-2 pion *skewed* PD following the lines of Ref. [153] and link it to the DD approach [45]. In particular, semi-kinematical approaches deriving from the original DD as well as the resonance exchange contribution will be investigated. The QCD evolution already described in the context of Distribution Amplitudes will be overviewed.

3.1 Kinematics for Skewed Parton Distributions

We define the kinematics of the GPDs following the conventions of Ref. [107]. As it has been explained in Chapter 1, the momenta in deep processes are expressed in light-cone coordinates.

The GPDs depend on three kinematical variables: the Fourier transform variable x, the momentum transfer t and the longitudinal momentum asymmetry, also called skewness variable, ξ.

[1] The tensor structure of the twist-3 GPD is given by

$$\begin{aligned} \tilde{F}^\pi(x,\xi,t) &= \frac{1}{2}\int \frac{dz^-}{2\pi}\, e^{ixz^-p^+} \left\langle \pi(P') \left| \bar{q}\left(-\frac{z}{2}\right) \gamma^\perp\gamma_5 \, q\left(\frac{z}{2}\right) \right| \pi(P) \right\rangle |_{\vec{z}^\perp = z^+ = 0} \quad , \\ &= \frac{1}{2\,p^+} \frac{i\epsilon^{\perp\nu\rho\sigma} p_\nu n_\rho \Delta_\sigma}{m_\pi^2} \tilde{H}^\pi(x,\xi,t) \quad , \end{aligned}$$

where by $\perp$ we understand the component 1 or 2.

The latter is defined, for an incoming momentum P and outgoing one P', by

$$\xi = \frac{P^+ - P'^+}{P^+ + P'^+} \quad .$$

The momentum P of the incoming pion and the momentum P' of the outgoing pion are therefore defined, see Fig. 3.1,

$$\begin{aligned} P^\mu &= (1+\xi)\,\bar{p}^\mu - \frac{\Delta^{\perp\mu}}{2} + \frac{1-\xi}{2}\bar{M}^2\,n^\mu \quad , \\ P'^\mu &= (1-\xi)\,\bar{p}^\mu + \frac{\Delta^{\perp\mu}}{2} + \frac{1+\xi}{2}\bar{M}^2\,n^\mu \quad , \end{aligned} \tag{3.3}$$

with

$$\bar{M}^2 = \frac{1}{1-\xi^2}\left(m_\pi^2 + \frac{\Delta^{\perp 2}}{4}\right) = m_\pi^2 - \frac{t}{4} \quad ,$$

and where we have used the on-shellness conditions $P^2 = P'^2 = m_\pi^2$. Δ^μ is related to the momentum transfer t by $\Delta^2 = t$, and defined as follows

$$\begin{aligned} \Delta^\mu = (P'-P)^\mu &= -2\xi\,\bar{p}^\mu + \Delta^{\perp\mu} + \xi\bar{M}^2\,n^\mu \quad , \\ t &= -4\,\xi^2\,\bar{M}^2 - \Delta^{\perp 2} \quad ; \\ p^\mu = \frac{(P+P')^\mu}{2} &= \bar{p}^\mu + \frac{\bar{M}^2}{2}\,n^\mu \quad . \end{aligned} \tag{3.4}$$

From the relation (3.4) and the fact that $\Delta^{\perp 2}$ is a positive quantity, we can deduce the interval of kinematically allowed values for the skewness variable ξ

$$0 \leq \xi \leq \frac{\sqrt{-t}}{2\sqrt{\bar{M}^2}} \quad . \tag{3.5}$$

Figure 3.1: u and d-quark contributing diagrams to the GPD in the NJL model.

3.2 The Chiral-Even Pion GPD

The calculation of H^π in the NJL model has been performed in Ref. [153]. In this Section, we comment these results.

For the π^+, the two contributing diagrams are depicted in Fig. 3.1. The bilocal u-quark current in the BS approach is given by

$$\begin{aligned}\langle \pi^j(P')|\bar{u}\left(x'\right)\,\gamma^\mu\,u\left(x\right)|\pi^j(P)\rangle \\ = \int d^4x_2\,\mathbb{T}\mathrm{r}\left\{\bar{\chi}^j_{P'}(x',x_2)\frac{1}{2}(1+\tau_3)\,\gamma^\mu\Big[\chi^j_P(x,x_2)(i\overleftarrow{\partial}^{\,(2)}-m_2)\Big]\right\} \\ +\int d^4x_1\mathbb{T}\mathrm{r}\Big\{\bar{\chi}^j_{P'}(x_1,x)(i\overrightarrow{\partial}^{\,(1)}-m_1)\chi^j_P(x_1,x')\frac{1}{2}(1+\tau_3)\gamma_\mu\Big\}\quad,\end{aligned}\tag{3.6}$$

the j index selects the isospin: $j=\pi^+,\pi^-$ or π^0. Here the projector $\frac{1}{2}(1+\tau_3)$ selects the contributions from the u-quark present in Eq. (3.6). The two terms on the r.h.s. correspond each one to one of the 2 components of the bound-state, namely the u or d-quark, as active quark. [2]

We now set the quark masses equal to the constituent quark mass, i.e. $m_1=m_2=m$. For the first diagram of Fig. 3.1, namely the active u-quark, the variables become $p_1=P-k$ and $p_2=k$ while for the active d-quark the variables are $p_1=-P+k$ and $p_2=-k$. That is, due to isospin symmetry also, we can relate both diagrams

$$H_u^{\pi^\pm}(x,\xi,t) \;=\; -H_d^{\pi^\pm}(-x,\xi,t)\quad.\tag{3.7}$$

We can then concentrate on the calculation of the u-quark distribution. The GPD (3.1) becomes

$$\begin{aligned}&H_u^{\pi^+}(x,\xi,t)\\ &=\frac{1}{2}\int\frac{d^4k}{(2\pi)^4}\;\delta\left(x-1+\frac{k^+}{p^+}\right)\,\mathbb{T}\mathrm{r}\left\{\bar{\chi}^{\pi^+}_{P'}(P'-k)\,\frac{1}{2}(1+\tau_3)\,\gamma^+\,\chi^{\pi^+}_P(P-k)(-\not{k}-m)\right\}\quad.\end{aligned}\tag{3.8}$$

The BS amplitudes are replaced by their expression in terms of Feynman propagators and the pion-quark vertex function Eq. (C.20).

After having performed the traces and integrating over k^+, we can analyze the poles in k^- similarly to the case of 2-propagator integrals in Section 2.4. In the present case it is the interplay between 3 poles that defines the support property: the integral is non-vanishing if there are poles on both sides. Thus, two kinematical regions are found that correspond to a GPD for the u-quark of supports $x\in[\xi,1]$ and $x\in[-\xi,\xi]$. From Fig. 1.5, it is easily seen that the u-quark GPD contributes to the region of emission and reabsorption of a quark as well as to the region of emission of a quark-antiquark pair.

We obtain a combination of 3-propagator, as it might be expected, as well as 2-propagator integrals;

$$\begin{aligned}H_u^{\pi^+}(x,\xi,t) \;=\; 4\;N_c\;g^2_{\pi qq}\Big[&-\frac{1}{2}(1+\xi)\tilde{I}_{2,P}(x,\xi)-\frac{1}{2}(1-\xi)\tilde{I}_{2,P'}-x\tilde{I}_{2,\Delta}(x,\xi,t)\\ &+(m_\pi^2x+\frac{t}{2}(1-x))\tilde{I}_3^{\mathrm{GPD}}(x,\xi,t)\Big]\quad,\end{aligned}\tag{3.9}$$

[2] We refer to Section 2.1 for the details of the technique.

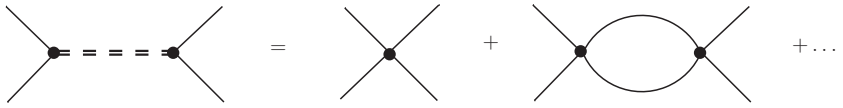

Figure 3.3: Effective interaction in the Random Phase Approximation where only the direct terms are considered.

with the light-front integrals given in Appendix E.

For the pion GPD, one should take into account the isoscalar meson-exchange in the t-channel: in the ERBL region, the two quarks can couple with quantum numbers corresponding to the σ-meson. Since the NJL model describes the pion as well as the σ-meson, the diagrams 3.1 may already contain this particular exchange. Moreover, in the region $-\xi \leq x \leq \xi$, a new diagram Fig. 3.2 should be considered as the model's expression of this σ-exchange. This meson-exchange, which is an explicit manifestation of chiral symmetry, can be calculated in the Random Phase Approximation;

$$\begin{aligned} iU(k^2) &= \Big[2iG + 2iG(-i\Pi_s(k^2))2iG + \dots\Big] \quad , \\ &= \frac{2iG}{1 - 2G\Pi_s(k^2)} \quad , \end{aligned} \tag{3.10}$$

where $\Pi_s(k^2)$ is the scalar proper polarization given in Eq. (C.35). Notice that the expression of the interaction is similar to the one obtained with the Bethe-Salpeter equation in the ladder approximation Eq. (C.31). The central part of Fig. 3.2 is given exactly by Eq. (3.10).

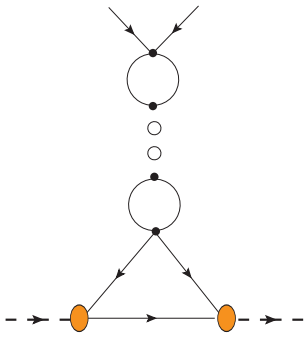

Figure 3.2: u-quark diagram contributing to the GPD in the NJL model coming from the σ coupling to the two photons in the $-\xi < x < \xi$ region. The corresponding diagram for the d-quark must be taken into account.

The second contribution to the GPD for the u-quark is then

$$H^{\pi^+}_{u\,\sigma}(x,\xi,t) = 4N_c g^2_{\pi qq}\, x\, \tilde{I}_{2,\Delta}(x,\xi,t)\, C(t) \quad , \tag{3.11}$$

with

$$\begin{aligned} &C(t) \\ &= (-4m^2)\, \frac{P.P' I_3(m,P,P') - I_2(m,-\Delta)}{m_\pi^2 I_2(m,m_\pi^2) + (4m^2 - t)\, I_2(m,\Delta)} \quad . \end{aligned}$$

We automatically find that the resonance exchange obeys

$$H^{\pi^+}_{\sigma}(x,\xi,t) = -H^{\pi}_{\sigma}(-x,\xi,t) \quad , \tag{3.12}$$

what corresponds to the symmetry imposed by Time-reversal and hermiticity.

As it will be shown, the σ-exchange term contributes to both the sum rule and the polynomiality property. Such a resonance exchange should always be taken into account. It reflects the interpretation of GPDs as depending on the interval in x. In the ERBL region, the GPD can no longer be considered as a pure quark or an antiquark distribution but rather as a combination of

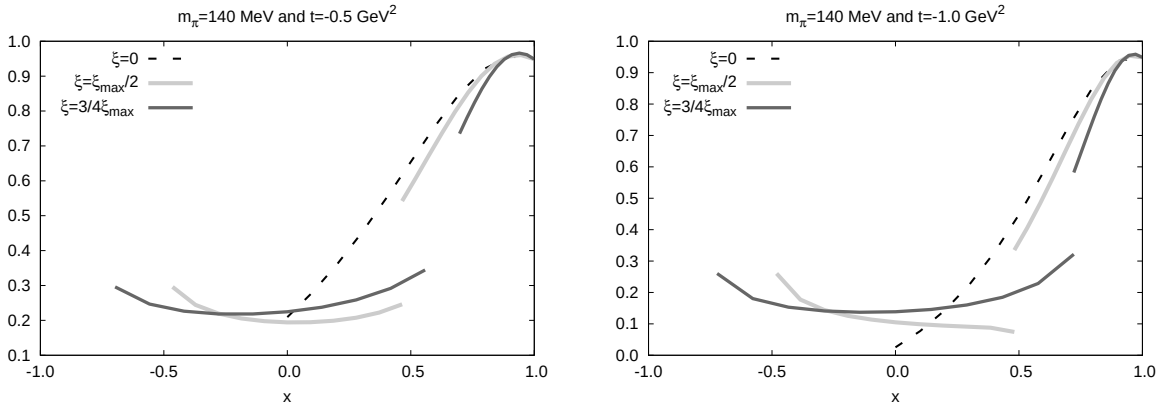

(a) (b)

Figure 3.4: Total GPD for the u-quark in the NJL model in the case where, respectively, (a) $t = -0.5$ GeV^2 and (b) $t = -1$ GeV^2 .

a q or $\bar{q}$ distribution as well as a meson Distribution Amplitude; what arises naturally from the diagrammatic description of the *skewed* parton distributions, i.e. Fig. 1.5.

The total distributions for the u- and d-quarks are then

$$\begin{aligned} H_u^{\pi^+\,\mathrm{tot}}(x,\xi,t) &= H_u^{\pi^+}(x,\xi,t) + H_\sigma^{\pi^+}(x,\xi,t) \quad , \\ H_d^{\pi^+\,\mathrm{tot}}(x,\xi,t) &= H_d^{\pi^+}(x,\xi,t) - H_\sigma^{\pi^+}(-x,\xi,t) = -H_u^{\pi^+\,\mathrm{tot}}(-x,\xi,t) \quad , \end{aligned} \tag{3.13}$$

with the u-distribution being defined with the support $x \in [-\xi, 1]$ and the d-distribution $x \in [-1, \xi]$, as required. The support property has been brought up in Section 2.4. So was the discussion about the support violation; therefore we do not need to develop this argument here.

Isospin Decomposition

As it was the case for the PDFs, the total π^+ distribution can be decomposed in an isoscalar and an isovector parts. The two terms are correspondingly defined as, in terms of operators,

$$\begin{aligned} \delta_{ab}\, H^{I=0}(x,\xi,t) &= \int \frac{dz^-}{4\pi}\, e^{ixp^+z^-} \langle \pi^a(P')|\bar{q}\left(-\frac{z}{2}\right) \gamma^+ q\left(\frac{z}{2}\right)|\pi^b(P)\rangle|_{z^\perp=z^+=0} \quad , \\ i\epsilon_{3ab}\, H^{I=1}(x,\xi,t) &= \int \frac{dz^-}{4\pi}\, e^{ixp^+z^-} \langle \pi^a(P')|\bar{q}\left(-\frac{z}{2}\right) \gamma^+ \tau_3\, q\left(\frac{z}{2}\right)|\pi^b(P)\rangle|_{z^\perp=z^+=0} \quad , \end{aligned} \tag{3.14}$$

with the pion field $|\pi^{+,-}\rangle = \left(|\pi^1\rangle \pm i|\pi^2\rangle\right)/\sqrt{2}$ and $|\pi^0\rangle = |\pi^3\rangle$.

Using the isospin relation (3.7) and Eq. (3.13) it is easily seen that the σ-meson exchange does only contribute to the isoscalar pion GPD. Effectively, the isoscalar decomposition is antisymmetric

in x

$$H^{I=0}(x,\xi,t) \;=\; H_u^{\pi^+}(x,\xi,t) - H_u^{\pi^+}(-x,\xi,t) + 2\,H_{u\,\sigma}^{\pi}(x,\xi,t) = -H^{I=0}(-x,\xi,t) \quad . \tag{3.15}$$

Also, the isovector decomposition is hence symmetric in x and corresponds to the valence quark distribution

$$H^{I=1}(x,\xi,t) \;=\; H_u^{\pi^+}(x,\xi,t) + H_u^{\pi^+}(-x,\xi,t) = H^{I=1}(-x,\xi,t) \quad . \tag{3.16}$$

We obtain the corresponding relation for the pions

$$\begin{aligned} H_u^{\pi^0}(x,\xi,t) &= \frac{1}{2}\,H^{I=0}(x,\xi,t) \quad , \\ H_u^{\pi^+}(x,\xi,t) &= \frac{1}{2}\left(H^{I=0}(x,\xi,t) + H^{I=1}(x,\xi,t)\right) \quad , \\ H_u^{\pi^-}(x,\xi,t) &= \frac{1}{2}\left(H^{I=0}(x,\xi,t) - H^{I=1}(x,\xi,t)\right) \quad . \end{aligned} \tag{3.17}$$

Let us now comment on the numerical results for the pionic GPDs in the NJL model. The GPD for the u-quark in the NJL model is discontinuous at $x = \xi$, see Fig. 3.4. So that the isoscalar GPD is discontinuous at $x = -\xi$ and ξ. The $|\xi|$ discontinuity comes from the formulation of the σ-exchange in the NJL model, as a realization of the chiral symmetry. This could be understood by considering the σ-exchange as a separate DA. In effect, the Distribution Amplitude in the NJL model calculation does not vanish at the end-points unlike its asymptotic form, leading to discontinuities at its end-points. This result has also been obtained in the Chiral Soliton Quark Model when the dependence of the dynamical quark mass is not taken into account [171], a situation that is similar to the one presented here. However, this peculiarity of the model calculation will disappear when switching on QCD just like for the Distribution Amplitudes as it has been discussed in Section 2.6.

Sum Rule and Polynomiality

We can now check that the properties of GPDs are respected in this model calculation. The sum rule for the isovector GPD reads [3]

$$\int_{-1}^{1} dx \sum_q Q_q H_q^{\pi^+}(x,\xi,t) = \int_{-1}^{1} dx\, H^{I=1}(x,\xi,t) \;=\; 2\,F_\pi(t) \quad , \tag{3.18}$$

with $F_\pi(t)$ the electromagnetic Form Factor given by Eq. (2.37). This sum rule is respected and has been analytically verified. Regarding the isoscalar combination, the sum rule involves the gravitational Form Factors of the pion $\theta_{1,2}(t)$ in the following way,

$$\int_{-1}^{1} dx\, x\, H^{I=0}(x,\xi,t) \;=\; \theta_1(t) - \xi^2\,\theta_2(t) \quad . \tag{3.19}$$

[3] The association $\int_{-1}^{1} dx \sum_q Q_q H_q^{\pi^+}(x,\xi,t) = \int_{-1}^{1} dx\, H^{I=1}(x,\xi,t)$ is valid under the integral over dx only.

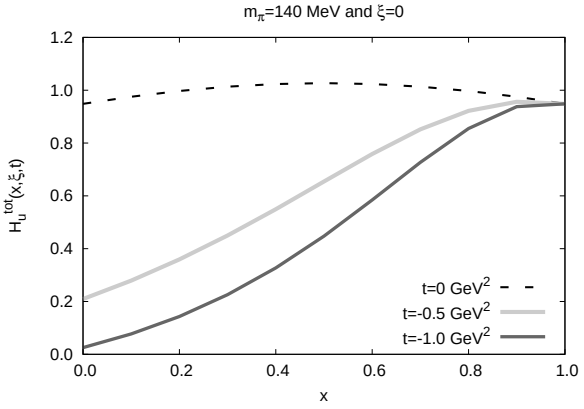

Figure 3.5: GPDs in the NJL model in the case $m_\pi = 140$ MeV and $\xi = 0$.

Since this sum rule refers to the momentum carried by each quark when taken at $t = 0$ GeV^2, we expect, in the chiral limit, $\theta_1(0) = \theta_2(0) = 1$. This condition has been fulfilled as it can be seen in Table 3.1.[4]

The polynomiality property is also respected,

$$\begin{aligned} \int_{-\xi}^{1} dx\, x^{n-1}\, H_u^{\pi\,\mathrm{tot}}(x,\xi,t) &= F_N(\xi,t) \quad , \\ &= \sum_{i=0}^{[\frac{n}{2}]} A_{n,2i}(t)\, \xi^{2i} \quad , \end{aligned} \tag{3.20}$$

where at the second line we have explicitly expressed the $F_N(\xi,t)$ as polynomials in ξ of order not higher than n. On virtue of the relation

$$H_q(x,\xi,t) = H_q(x,-\xi,t) \quad ,$$

given by Time-reversal invariance, only even powers in the skewness variable are allowed in the previous expansion in polynomials. The numerical results for the coefficients in both cases $m_\pi = 0$ MeV and $m_\pi = 140$ MeV are given in Table 3.1.

The chiral limit, where $m_\pi = 0$, and with zero momentum transfer, is perfectly defined in a regularization-independent way. It makes sense to study separately the ξ dependence of the contributions coming from the *direct* and *crossed* diagrams of Fig. 3.1 and the σ-exchange of Fig. 3.2;

$$\begin{aligned} H_u^{\pi}(x,\xi,0) &= \frac{1}{2}\left(1-\frac{x}{2\xi}\right)\theta(\xi-x)\theta(\xi+x) + \theta(x-\xi)\theta(1-x) \quad , \\ H_{u\,\sigma}^{\pi}(x,\xi,0) &= \frac{1}{2}\,\frac{x}{2\xi}\,\theta(\xi-x)\theta(\xi+x) \quad . \end{aligned} \tag{3.21}$$

The total GPD for the u-quark in a π^+ reads

$$H_u^{\pi\,\mathrm{tot}}(x,\xi,0) = \frac{1}{2}\,\theta(\xi-x)\theta(\xi+x) + \theta(x-\xi)\theta(1-x) \quad . \tag{3.22}$$

[4]Notice that Table 3.1 is given $H_u^{\pi^+ tot}$ which is defined between $[-\xi,1]$ so that the results have to be mutliplied by 2 when considering $H^{I=0}$ and we extend the integral to $[-1,1]$.

n	1	2		3		4		
	$A_{1,0}(t)$	$A_{2,0}(t)$	$A_{2,2}(t)$	$A_{3,0}(t)$	$A_{3,2}(t)$	$A_{4,0}(t)$	$A_{4,2}(t)$	$A_{4,4}(t)$
$m_\pi = 0$								
$t = 0$	1.	0.5	-0.5	0.333	0.	0.25	0.	-0.25
$t = -1$	0.487	0.336	-0.240	0.257	-0.049	0.208	-0.030	-0.113
$t = -10$	0.091	0.119	-0.093	0.118	-0.058	0.111	-0.046	-0.044
$m_\pi = 140$								
$t = 0[-10^{-5}]$	1.	0.5	$[-0.473]$	0.332	$[0.005]$	0.247	$[0.005]$	$[-0.236]$
$t = -1$	0.482	0.332	-0.230	0.253	-0.045	0.203	-0.026	-0.109
$t = -10$	0.090	0.116	-0.088	0.114	-0.055	0.108	-0.043	-0.042

Table 3.1: Coefficients of the polynomial expansion. The pion mass is expressed in MeV and t is expressed in GeV^2. Values between brackets correspond to $t = -10^{-5}$ GeV^2 [153].

Evaluated for the *skewed* PD, the expression of the σ-resonance is model dependent. However, since the interpretation of the σ-exchange is unique in the limit $m_\pi \to 0$, chiral symmetry implies that the diagram 3.2 cancels out the "σ-exchange like" contribution contained in H^q_π. In other words, we recover the result $H^{I=0}(x,1,0) = 0$ predicted by the chiral symmetry [171]. Also, the isoscalar and isovector combinations read

$$\begin{aligned} &H^{I=0}(x,\xi,0) \\ &= -\theta(-x-\xi)\theta(1+x) + \theta(x-\xi)\theta(1-x) \quad , \end{aligned}$$

$$\begin{aligned} &H^{I=1}(x,\xi,0) \\ &= \theta(-x-\xi)\theta(1+x) \\ &+ \theta(\xi-x)\theta(\xi+x) + \theta(x-\xi)\theta(1-x) \quad , \end{aligned}$$

what is consistent with previous results [171]. This result is illustrated on Fig. 3.6.

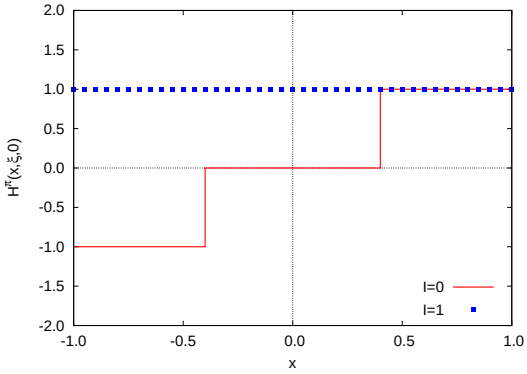

Figure 3.6: Chiral limit for $\xi = 0.4$.

We notice also that, in the forward limit, i.e. for $\xi = t = 0$, we find the quark distribution function

$$H_u^{\pi\,\mathrm{tot}}(x,0,0) \quad = \quad q(x) = 1 \quad ,$$

where, as expected, the σ-exchange does not contribute.

To this point, we have presented the calculation of the chiral-even twist-2 GPD of the pion in the NJL model using a fully covariant Bethe-Salpeter approach. The only approximation employed has been the ladder approximation. We have solved the BS equation exactly thanks to the point-like interaction of the NJL model. The usual properties of GPDs have been recovered. Nevertheless discontinuities are encountered, at the boundaries and are associated to the off-shellness of the constituent quark. Also the expression of the σ-exchange in the NJL model introduces discontinuities at the x values $-\xi$ and ξ.

3.2.1 Double Distributions and the D-term

An alternative way to describe the hadronic matrix elements defining the GPDs is through the so-called Double Distribution (DD) parameterization. By Lorentz invariance the matrix element (3.2) can only depend on the two independent variables $p\cdot z$ and $\Delta\cdot z$. Hence the pion DD [173, 174] is defined as a 2-dimensional Fourier transform in these two independent variables. The analysis of diagrams of the type 3.1 & 3.2 yields the behavior of these variables;

$$\begin{aligned}\mathcal{M}_q^\pi\left(p\cdot z,\Delta\cdot z;t\right) &= \langle\pi^+(P')|\,\bar{q}\left(-\frac{z}{2}\right)\not{z}\;q\left(\frac{z}{2}\right)|\pi^+(P)\rangle \\ &= 2\left(p\cdot z\right)\int_{-1}^{1}d\beta\int_{-(1-|\beta|)}^{1-|\beta|}d\alpha\, e^{-i\beta(p\cdot z)+i\alpha(\Delta\cdot z)/2}\,\mathcal{F}_q^\pi(\beta,\alpha,t) \\ &\quad -(\Delta\cdot z)\int_{-1}^{1}d\alpha\, e^{i\alpha(\Delta\cdot z)/2}\,\mathcal{D}_q^\pi(\alpha,t)\quad , \end{aligned} \tag{3.23}$$

for the whole matrix element.

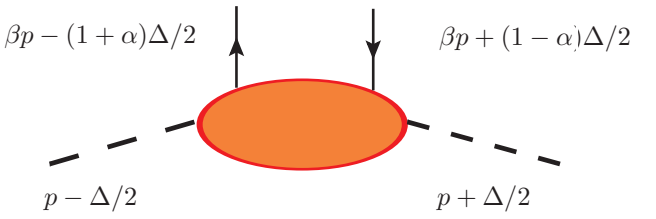

Figure 3.7: Momenta associated with the quarks and hadrons in the Double Distribution parameterization.

Since the variables $p\cdot z$ and $\Delta\cdot z$ are treated as independent, the DD refers to fixed momentum transfer t but with unfixed individual hadron momenta P and P'. In other words, these momenta do not depend on the skewness variable. The interpretation of the latter being process dependent, one can say that the matrix element on the r.h.s. of Eq. (3.23) contains a process-independent information and, hence, has a quite general nature.

The dependence on β is of the parton distribution type, while the one on the parameter α resembles the dependence of a distribution amplitude. This feature is illustrated in Fig. 3.7.

From the naïve analysis of GPDs as parameterized through the DD, one would write the whole contribution coming from diagrams such as 3.1 or 3.7 in the form $f_q^\pi(\beta,\alpha,t)$; i.e. (3.23). From our experience in model calculations, we know that diagrams of this type may contain a resonance exchange in the t-channel whose tensorial structure corresponds exactly to the one of the remaining non-resonant part of the diagram. The behavior of this meson-exchange contribution with respect to the two independent variables $p\cdot z$ and $\Delta\cdot z$ is manifestly different.

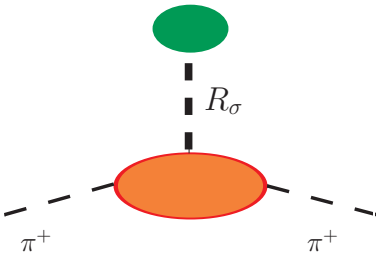

Figure 3.8: The D-term as a σ-resonance in the t-channel.

As a matter of fact, it has been shown in Ref. [171] that another twist-2 "DD structure" has to be considered indeed. The origin of this new structure is the subtraction from the matrix element

of those resonances in the t-channel (Fig. 3.8). Namely they are terms depending solely on the $\Delta \cdot z$ variable, i.e. non-vanishing terms in the limit

$$p \cdot z \to 0 \quad . \tag{3.24}$$

The function $\mathcal{D}(\alpha; t)$ is therefore defined taking the latter limit and subtracting this result from the $p \cdot z$-dependent contribution, i.e.

$$\mathcal{M}_q^\pi \left(p \cdot z, \Delta \cdot z; t\right) \;=\; \underbrace{\mathcal{M}_q^\pi \left(p \cdot z \neq 0, \Delta \cdot z; t\right) - \mathcal{M}_q^\pi \left(0, \Delta \cdot z; t\right)}_{\to \mathcal{F}_q^\pi(\beta,\alpha;t)} + \underbrace{\mathcal{M}_q^\pi \left(0, \Delta \cdot z; t\right)}_{\to \mathcal{D}_q^\pi(\alpha;t)} \quad .$$

The meson-exchanges must have the characteristics of Distribution Amplitudes so that we expect them to be parametrized by α. In terms of DD, we call the corresponding function the D-term [171]. The D-term is uniquely defined for a given hadronic matrix element.

When applying the limit (3.24) to the matrix element as expressed in the NJL model calculation (3.6) taking into account all diagrams, this resonance exchange corresponds in part to the term going like $\tilde{I}_{2,\Delta}$ of the integral decomposition (3.9) as well as to the term coming from the second diagram Fig. 3.2. The whole resonance exchange also includes a x-odd part of the $\tilde{I}_{2,P}$ as well as of the $\tilde{I}_3$ integrals in (3.9).

The Double Distributions can be reduced to the usual *skewed* parton distribution by taking a one-dimensional cut, i.e. imposing a relation between $p \cdot z$ and $\Delta \cdot z$. This reduction formula reads

$$H_q^\pi(x, \xi, t) \;=\; \int_{-1}^{1} d\beta \int_{-(1-|\beta|)}^{1-|\beta|} d\alpha \, \delta(x - \beta - \xi\alpha) \mathcal{F}_q^\pi(\beta, \alpha, t) + \mathrm{sgn}(\xi) D_q^\pi\left(\frac{x}{\xi}, t\right) \quad . \tag{3.25}$$

The D-term obeys the symmetries of an isoscalar resonance (3.12). Therefore it contributes solely to the isoscalar GPD as expected.

The parameterization through Double Distribution applies at the level of the Fourier transform of the matrix element. This renders the evaluation of the DD model independent. Nonetheless this statement is quite misleading in the sense that the relevant diagrams depend on the model considered. So, from a technical point of view, one has to evaluate the diagrams that apply, and, with the Feynman rules resulting from the features of the model. The GPDs appear to be a combination of two- and three-point functions, e.g. in the NJL model Eqs. (3.9, 3.11), which, in turn, can be expressed in terms of Double Distributions through the reduction formula. An explicit example would be the expression of the 3-propagator integral

$$\tilde{I}_3(x, \xi, t) \;=\; \int_{-1}^{1} d\beta \int_{-(1-|\beta|)}^{1-|\beta|} d\alpha \, \delta\left(x - \beta - \alpha\xi\right) \mathcal{I}_3(\beta, \alpha, t) \quad ; \tag{3.26}$$

with $\mathcal{I}_3$ a Double Distribution given in (F.6). The 2-propagator integrals that do not behave like DAs can also be included in the form $\mathcal{I}(\beta, \alpha, t)$. This reduction is totally model independent.

The model's description of the σ-exchange, illustrated in Fig. 3.2, also accounts for a formal and general description on the form of the r.h.s. of Eq. (3.23). In particular, it is of a pure D-term structure. The total description of the matrix element simply results from the sum of the two contributions; namely H_q^π as given by the reduction formula (3.25) plus the corresponding formula for $H_{q\,\sigma}^\pi$.

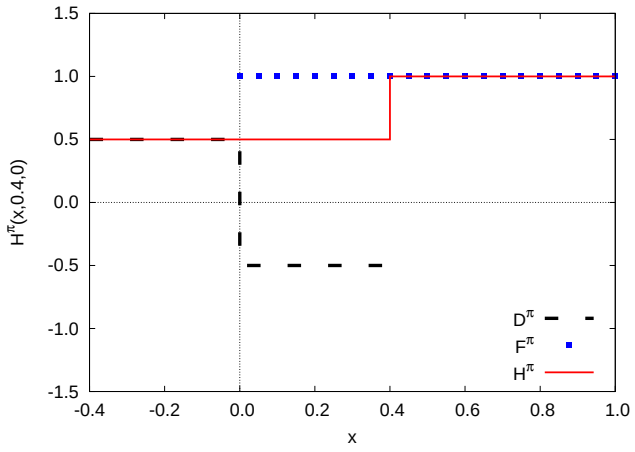

Figure 3.9: The contributions from the double distribution F^π (blue dotted line), from the D-term (dashed line) and the total distribution H^π (red curve).

As already mentioned in Section 2.1, the difference between the quark models is manifest in the regularization scheme. The chosen regularization scheme is an integrant part of the model since it depends on the model's interaction and conveniences for the adaptation to the problem under scrutiny. Concretely the Double Distributions are reduced to the physical propagator integrals by imposing a regularization scheme. In the NJL model as presented in the previous Chapter 2, it would mean that the propagator integrals follow, in the case of 3-propagator integrals, the expression (3.26) to which we impose the Pauli-Villars regularization scheme, i.e. Eq. (C.15).

In Ref. [45] the Double Distributions of the pion in the NJL model are given using a Pauli-Villars regularization in the twice-subtracted version of Ref. [180], as well as in the Spectral Quark Model [181]. Both calculations yield results comparable to the calculation of Ref. [153].

One of the main advantages of the DD parameterization is that the expression (3.25) manifestly leads to the correct polynomiality properties of the GPDs. Effectively, when taking the Mellin moments of the reduction formula, one immediately finds

$$\begin{aligned}&\int_{-1}^{1} dx\, x^{n-1}\, H_q^\pi(x,\xi,t)\\ &= \int_{-1}^{1} dx\, x^{n-1}\Big[\int_{-1}^{1} d\beta \int_{-(1-|\beta|)}^{1-|\beta|} d\alpha\, \delta(x-\beta-\xi\alpha)\mathcal{F}_q^\pi(\beta,\alpha,t) + \mathrm{sgn}(\xi) D_q^\pi\left(\frac{x}{\xi},t\right)\Big] \quad ,\end{aligned} \tag{3.27}$$

where the first term on the r.h.s. is a polynomial at a power of order at most $n-1$ of the skewness variable ξ. The D-term instead gives the highest power in ξ, i.e. n. [5]

Concerning the chiral limit, the DD approach yields the same results (3.21) as the *skewed* PD evaluation [171]. In this limit, the D-term is therefore reduced to the zeroth order term of the resonance exchange coming from the $\tilde{I}_{2,P}$ term.

[5] The latter statement can be visualized by performing the change of variable $x/\xi = \nu$; which carries a ξ^n outside the integral over, then, ν.

Let us illustrate the previous statements. In the chiral limit, the D-term reads, for the u-quark,

$$D_u^\pi\left(\frac{x}{\xi},0\right) \;=\; \frac{1}{2}\,\theta\left(x+\xi\right)\theta\left(-x\right)-\frac{1}{2}\,\theta\left(x-\xi\right)\theta\left(x\right) \quad . \tag{3.28}$$

The remaining part is found through the reduction formula, providing that

$$H_u^\pi(x,\xi,t) \;=\; F_u^\pi(x,\xi,t)+D_u^\pi\left(\frac{x}{\xi},t\right) \quad . \tag{3.29}$$

Using (3.22), we obtain

$$F_u^\pi(x,\xi,0) \;=\; \theta\left(x\right)\theta\left(1-x\right) \quad ,$$

which can obviously not satisfy the polynomiality property. By inserting the D-term (3.28), we obtain the expression for the total GPD (3.29). In particular, we recover the expression (3.22) which, in turn, fulfills the required conditions. These results are illustrated in Fig. 3.9.

There is considerable freedom in the tensorial decomposition of the matrix element $\mathcal{M}_q^\pi$. An alternative decomposition to the expression (3.23) is given in Ref. [198],

$$\begin{aligned}\mathcal{M}_q^\pi\left(p\cdot z,\Delta\cdot z;t\right) &= \langle\pi^+(P')|\,\bar{q}\left(-\frac{z}{2}\right)\not{z}\;q\left(\frac{z}{2}\right)|\pi^+(P)\rangle \\ &= 2\left(p\cdot z\right)\int_{-1}^{1}d\beta\int_{-(1-|\beta|)}^{1-|\beta|}d\alpha\,e^{-i\beta(p\cdot z)+i\alpha(\Delta\cdot z)/2}\,\mathcal{K}_q^\pi(\beta,\alpha,t) \\ &\quad -(\Delta\cdot z)\int_{-1}^{1}d\beta\int_{-(1-|\beta|)}^{1-|\beta|}d\alpha\,e^{-i\beta(p\cdot z)+i\alpha(\Delta\cdot z)/2}\,\mathcal{G}_q^\pi(\beta,\alpha,t) \quad ,\end{aligned} \tag{3.30}$$

with the function $\mathcal{K}_q^\pi(\beta,\alpha,t)$ even in α and the function $\mathcal{G}_q^\pi(\beta,\alpha,t)$ α-odd, as a consequence of Time-reversal invariance. The corresponding reduction formula reads

$$H_q^\pi(x,\xi,t) \;=\; \int_{-1}^{1}d\beta\int_{-(1-|\beta|)}^{1-|\beta|}d\alpha\,\delta(x-\beta-\xi\alpha)\left[\mathcal{K}_q^\pi(\beta,\alpha,t)+\xi\,\mathcal{G}_q^\pi(\beta,\alpha,t)\right] \quad . \tag{3.31}$$

The sum rule for $\mathcal{K}^\pi$ gives the electromagnetic pion Form Factor, as expected; whereas the sum rule for $\mathcal{G}^\pi$ gives 0 since it is an odd function of α.

One could relate the above given expression to the *usual* DD decomposition by writing all the β dependence of $\mathcal{G}_q^\pi(\beta,\alpha,t)$ as a $\mathcal{K}_q^\pi(\beta,\alpha,t)$, leaving a pure $\Delta\cdot z$ in the second term. The decomposition (3.30) is however calculationally the most useful, since it does not evoke the cumbersome limit (3.24). On the other hand the expression of the meson-exchanges is less explicit.

The distribution amplitude character of the D-term implies it obeys to the ERBL evolution equations, that has been introduced in the previous Chapter. The total GPD does however not have the same behavior when going the higher Q^2. From Fig. 1.5, we have defined the three regions as DGLAP-regions for the support in x being either $[\xi,1]$ or $[-1,-\xi]$ and ERBL-region for the $x\in[-\xi,\xi]$ region. Those regions were named after the evolution equations they obey.

3.2.2 QCD Evolution

The form of the Leading-Order (LO) QCD evolution has been given, for the standard PDF evolution, by Dokshitzer [85], Gribov and Lipatov [104, 141] as well as by Altarelli and Parisi [9]. It gave rise to the DGLAP equations, whose evolution will be followed by the two regions of emission and reabsorption of a quark or antiquark, respectively. On the other hand, the equations describing the evolution of the distribution amplitudes were given by Efremov and Radyushkin [88] as well as by Brodsky and Lepage [140].

The form of the integral-equation defining the evolution equations depend upon the nature of the distributions. In Eqs. (3.15, 3.16), the singlet or sea distribution have been defined as well as the non-singlet or valence distribution

$$H^S(x,\xi,t) = \sum_q H_q^{I=0}(x,\xi,t) \quad ; \tag{3.32}$$

$$H_q^{NS}(x,\xi,t) = H_q^{I=1}(x,\xi,t) \quad . \tag{3.33}$$

Still, one main ingredient of QCD evolution has to appear: the gluon distribution, obeying the following symmetry

$$xH_g(x,\xi,t) = -xH_g(-x,\xi,t) \quad ;$$

with the gluon distribution being zero at the scale of the model, i.e. $H_g(x,\xi,t,Q_0^2) = 0$.
It is important to notice that the non-singlet distribution does not mix with the singlet under LO evolution. However, the singlet and gluon distribution do mix under evolution.

The explicit form of the LO QCD evolution equations for the GPDs can be found in Refs. [103, 118, 123, 124, 148, 174]. The effect of LO evolution on the non-singlet, singlet and gluon distributions is depicted on Fig. 3.10. The evolution code of Freund and McDermott [94] has been used with the value for Q_0 and Λ as given in (2.30) and in the paragraph preceding the latter expression. On both panels the LO evolution is performed for the initial scale given by NJL model as given by the expression (2.30). The results presented here are in agreement with the evolution for the NJL model as introduced in Ref. [45].

The initial distributions are represented by the thin pink curves. We can see that the isovector GPD (on the top) differs in the ERBL-region from the isoscalar distribution (middle of the panel), where the D-term, or σ-resonance, contributes due to its antisymmetry.

On the left panel, the thick green lines represent the distributions evolved at $Q = 4$ GeV. One is immediately struck by the fact that evolution changes completely the end-point behavior as well as smoothes the discontinuities between the two regions, i.e. at $x = \pm\xi$. Even if the evolution seems strong here, it is mentioned in Ref. [45] that the desired continuity of the functions at the end-points is achieved already at values of Q infinitesimally larger than Q_0. Once more, we refer to the case of the distribution amplitude where a numerical analysis of the truncation of the solution of the evolution equation has been driven, see Fig. 2.6.

An important feature of the evolution in Q^2 of the GPDs is that the evolution equations in the ERBL-region depend on the value of the GPDs in both the ERBL-region and the DGLAP-region, while the DGLAP evolution equation do only depend on the value of the GPDs in its very own region. In other words, the GPDs in the DGLAP-regions feed the ERBL-region. Moreover, as for

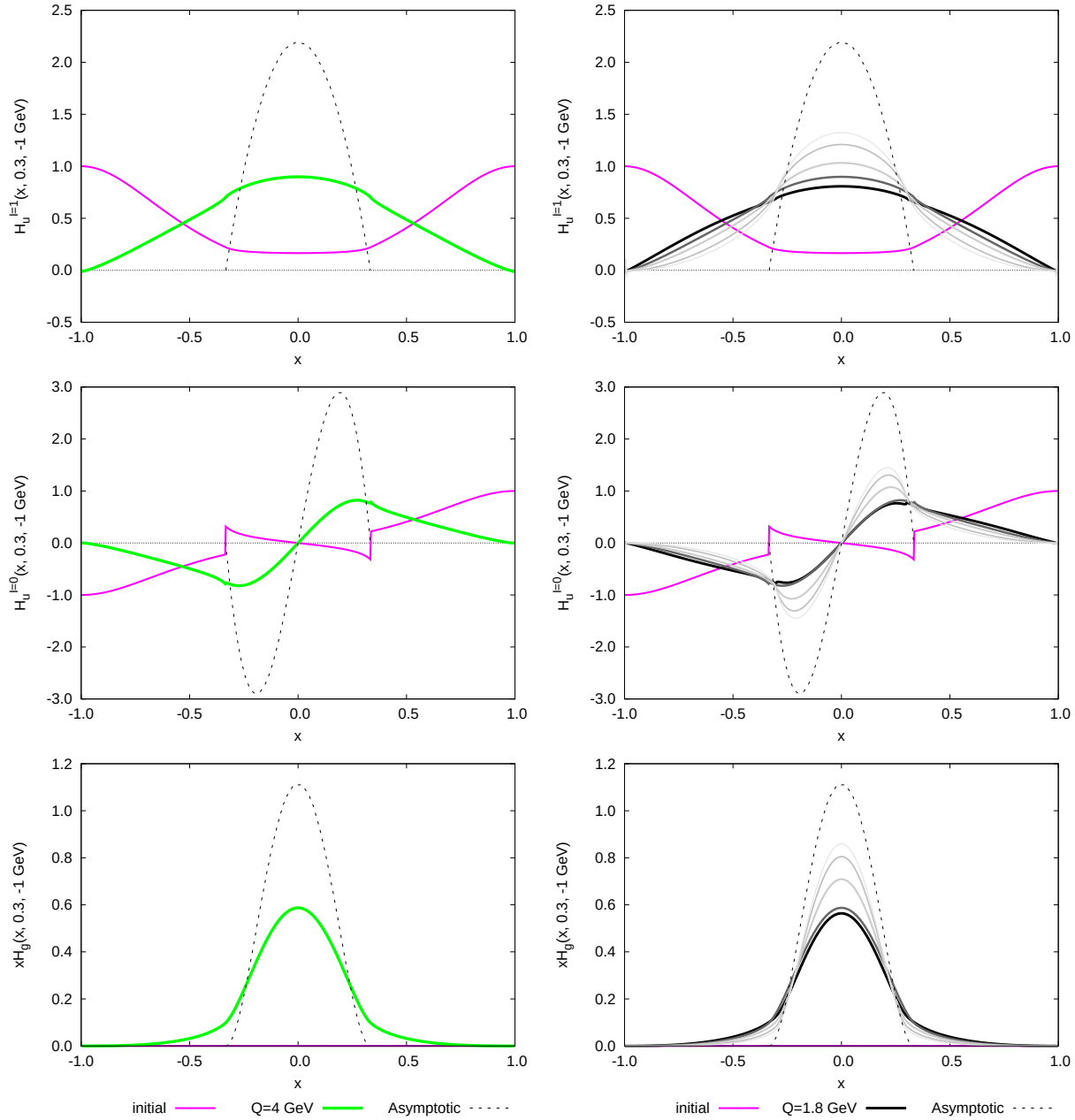

Figure 3.10: Results of the LO QCD evolution from the NJL model for several values of $t = -1$ GeV^2 and for $\xi = 1/3$. From top to bottom, respectively, the non-singlet, the singlet and the gluon distributions. The solid pink lines represent the initial conditions. Left panel: The thick green lines are the evolved result to $Q = 4$ GeV and the dashed lines the asymptotic forms. Right panel: The grey lines are the evolved result to different values of Q $(1, 8;$ 4; 10; 100 and 1000 GeV) and the dotted red line the asymptotic form.

the DA, evolution pushes the distributions towards low x's. This can be observed in both the left and right panels of Fig. 3.10.

As a matter of fact the asymptotic forms for the evolved distributions are solely defined in the ERBL-region. The (anti)symmetry of the distributions around the point $x = 0$ shown in Eqs. (3.32, 3.33) remains unchanged under evolution. The analytic asymptotic solutions were found in Ref. [174]. We adopt the forms given in Ref. [45]

$$\begin{aligned} H_q^{NS}(x,\xi) &= \frac{3}{2\,\xi}\frac{\xi^2-x^2}{\xi^2}\,F_\pi(t) \quad , \\ H^S(x,\xi) &= \frac{15}{2\,\xi^2}\,\frac{N_f}{4C_F+N_f}\,\frac{x}{\xi}\,\frac{\xi^2-x^2}{\xi^2}\,\frac{1}{2}\left[\theta_1(t)-\xi^2\,\theta_2(t)\right] \quad , \\ xH^g(x,\xi) &= \frac{15}{8\,\xi}\,\frac{4\,C_F}{4C_F+N_f}\left(\frac{\xi^2-x^2}{\xi^2}\right)^2\,\frac{1}{2}\left[\theta_1(t)-\xi^2\,\theta_2(t)\right] \quad , \end{aligned} \tag{3.34}$$

for $-\xi \le x \le \xi$ as well as for fixed t-values. The t-behavior is given by the sum rules (3.18, 3.19); a first principles property that remains unchanged after evolution. The presence of the gluon distribution nevertheless affects the isoscalar sum rule (3.19)

$$\int_{-1}^{1} dx\,\left(x\,H^S(x,\xi,t,Q^2)+x\,H_g(x,\xi,t,Q^2)\right) = \theta_1(t,Q^2)-\xi^2\,\theta_2(t,Q^2) \quad . \tag{3.35}$$

The values of the gravitational Form Factors for different t values are given in Table 3.1.

The asymptotic behavior described by Eqs. (3.34) is illustrated on Fig. 3.10 by the dashed lines. On the right panel, it is clearly shown that the evolution is slow in reaching the solution for $Q \to \infty$ of the GPDs. On the other hand, the evolution is faster at low values of Q. This result we could expect as it happens for the pion DA, which obeys the ERBL evolution equations. In Fig. 2.7 is depicted the slow evolution of the pion DA at high Q-values.

Also, in order to improve in reaching the asymptotic behavior, one should start the evolution from a different value of Q_0. However, as it has been explained in Section 2.5, the scale is fixed by the model's results for the second moment of the PDFs. Even going to the NLO could not change such a peculiarity of the model calculations. Effectively, the initial scale for a NLO evolution is found to be higher than for the LO one. However, this lower Q_0 for the LO evolution compensates for the effect of NLO evolution: the results are consistent one to the other.

3.2.3 From the Experimental Side

From the experimental point of view the GPDs of the pion are difficult to determine. Pions decay into muons or photons and therefore the pion Distribution Functions cannot be obtained from direct DIS experiments. Rather they have been inferred from Drell-Yan process [26, 31, 65] and direct photon production [21] in pion-nucleon and pion-nucleus collisions. In a near future, the CLAS++ detector with the CEBAF accelerator at 12 GeV at JLab should allow the observation of pion GPDs through large angle Compton scattering [54].

It has been recently proposed, in Ref. [10], to access the pion GPDs by studying the DVCS on a virtual pion that is emitted by a proton, i.e. the process $e\,p \to e\,\gamma\,\pi^+\,n$.

4 Transition Distribution Amplitudes

Here comes the heart of the thesis. The study of Generalized Parton Distribution is extended to distribution amplitudes for transitions.

Collisions of a real photon and a highly virtual photon are an useful tool for studying fundamental aspects of QCD. Inside this class of processes, the exclusive meson pair production in $\gamma^*\gamma$ scattering,

$$\gamma_L^*\gamma \to \pi^+\pi^- \quad , \quad \gamma_L^*\gamma \to \rho^+\pi^- \quad , \tag{4.1}$$

has been analyzed in Ref. [131, 165]. This process is particularly interesting since it implies, in different kinematical regions, different mechanisms.

At small momentum transfer t and in the kinematical regime where the photon is highly virtual, a separation between the perturbative and the nonperturbative regimes is assumed to be valid. Through the factorization theorems the amplitude for such reactions can be written as a convolution of a hard part M_h, a meson Distribution Amplitude ϕ_M and another soft part, describing the photon-pion transition by means of the *Transition Distribution Amplitudes*.

On the other hand, at small s, the factorization corresponds to the GDA's mechanism. The interplay between the two mechanisms in the kinematical region $s, t \ll Q^2$ may lead to an interesting *duality* property. This will be considered in the Future Perspectives. Also, the kinematical regime where both $t, s \sim Q^2$ corresponds to large angle scattering *à la* Brodsky-Lepage and will not be considered here.

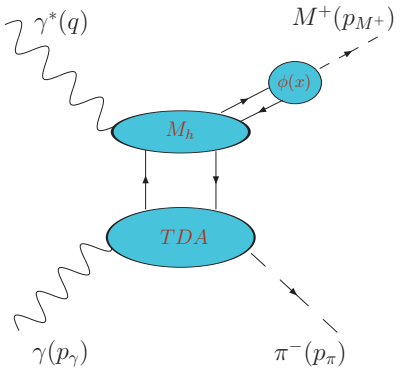

Figure 4.1: Factorization diagram defining the TDA for the process $\gamma^*\gamma \to \pi M$ at small momentum transfer, $t = (q - p_M)^2$, and large invariant mass, $s = (p_\gamma + q)^2$.

The accurate definition of these objects was first presented for the mesonic TDAs, by simplicity. In particular, it has been first analyzed for the pion-photon transitions [165] involved in related processes, like hadron annihilation into two photons $\pi^+\pi^- \to \gamma^*\gamma$ and backward virtual Compton scattering $\gamma^*\pi^+ \to \gamma\pi^+$.

The concept of transition distribution was first introduced by Frankfurt, Polyakov, Strikman and Pobylitsa [91, 92] as a study of the transitions $\gamma^* + p \to Baryon + Meson$ through *Skewed* Distribution Amplitudes.

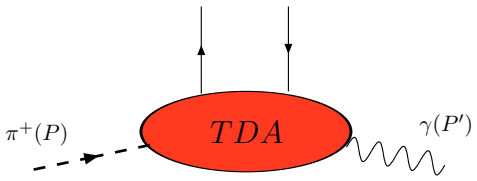

Figure 4.2: The $\pi^+ \to \gamma$ Transition Distribution Amplitude.

In this Chapter, we compile the results of our publications on mesonic Transition Distribution Amplitudes calculated in the NJL model [67, 69].

We establish the connection between the TDA and the vector and axial pion Form Factors, F_V and F_A. The definition of the $\pi \to \gamma$ TDAs are amplified to $\gamma \to \pi$ transitions. The calculation and the results in the NJL model are given in details for the *skewed* distribution approach. The way to Double Distributions is given that enables us to compare our results with both phenomenological parameterizations and other model calculations.

In the next Chapter, as an application of the numerical results, we will use the defined quantities to estimate the cross sections for exclusive meson production in $\gamma^*\gamma$ scattering (4.1) in the same kinematical regime.

4.1 The Pion Transition Form Factors

The pion-photon TDAs are connected, through sum rules, to the vector and axial-vector pion Form Factors, F_V and F_A. Before giving a proper definition of the TDAs let us recall the definition of these Form Factors. They appear in the vector and axial vector hadronic currents contributing to the decay amplitude of the process $\pi^+ \to \gamma e^+ \nu$ depicted in Figs. 4.3 & 4.4. The precise definition of these currents is [147, 46],

$$\langle \gamma\,(p_\gamma)|\,\bar{q}\,(0)\,\gamma_\mu \tau^-\, q\,(0)\,|\pi\,(p_\pi)\rangle = -i\,e\,\varepsilon^\nu\,\epsilon_{\mu\nu\rho\sigma}\,p_\gamma^\rho\,p_\pi^\sigma\,\frac{F_V\,(t)}{m_\pi}\ , \tag{4.2}$$

$$\begin{aligned}\langle \gamma\,(p_\gamma)|\,\bar{q}\,(0)\,\gamma_\mu\gamma_5 \tau^-\, q\,(0)\,|\pi\,(p_\pi)\rangle &= e\,\varepsilon^\nu\,(p_{\gamma\,\mu}\,p_{\pi\,\nu} - g_{\mu\nu}\,p_\gamma\cdot p_\pi)\,\frac{F_A\,(t)}{m_\pi} \\ &+ e\,\varepsilon^\nu\left((p_\gamma - p_\pi)_\mu\,p_{\pi\,\nu}\frac{2\sqrt{2}f_\pi}{m_\pi^2 - t} - \sqrt{2}f_\pi\,g_{\mu\nu}\right)\ ,\end{aligned} \tag{4.3}$$

with $f_\pi = 93\,\mathrm{MeV}$, $\varepsilon^{0123} = 1$ and $\tau^- = (\tau_1 - i\,\tau_2)/2$ as given in Appendix A. All the structure of the decaying pion is included in the Form Factors F_V and F_A. We observe that the vector current only contains a Lorentz structure associated with the F_V Form Factor. On the other hand, the axial current is composed of two terms. The first one, defining F_A, gives the structure of the pion

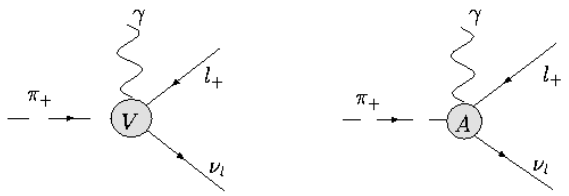

Figure 4.3: Diagrams contributing to the process $\pi^+ \to \gamma e^+ \nu$: the structure-dependent contributions governed, respectively, on the l.h.s. by the vector and, on the r.h.s., the axial Form Factor.

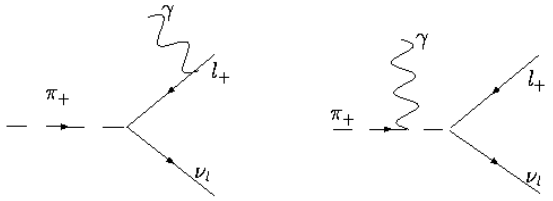

Figure 4.4: Diagrams contributing to the process $\pi^+ \to \gamma e^+ \nu$: the electron (l.h.s.) and the pion (r.h.s.) inner Bremsstrahlung. The electron Bremsstrahlung does not contribute to the $\pi \to \gamma$ hadronic current.

and is gauge invariant. The second one corresponds to the axial current for a point-like pion and is not gauge invariant. This term coming from the pion inner Bremsstrahlung has, in turn, two different contributions. The first one corresponds to a point-like coupling between the incoming pion, the outgoing photon and a virtual pion which is coupled to the axial current. It is depicted in the diagram of Fig. 4.5 and can be seen as a result of PCAC, because the axial current must be coupled to the pion. It isolates the pion pole contribution from the axial current in a model independent way. The second contribution of this term, proportional to $f_\pi \, g_{\mu\nu}$, corresponds to a pion-photon-axial current contact term. With these definitions, all the structure of the pion remains in the Form Factor F_A. The total gauge invariance of the amplitude for the pion radiative decay is ensured by the electron Bremsstrahlung contribution, whose amplitude does not contribute to the hadronic currents (4.2,4.3).

4.2 From Hadronic Currents to Transition Distribution Amplitudes

Let us go now to TDAs.
For their definition we introduce the light-cone coordinates as defined in Appendix A.

The skewness variable describes the loss of plus momentum of the incident pion, i.e.

$$\xi \;=\; \frac{(p_\pi - p_\gamma)^+}{2p^+} \quad , \tag{4.4}$$

with $p^+ = (p_\pi + p_\gamma)^+ /2$.

The explicit expressions for the pion and photon momenta in terms of the light-front vectors are

$$p_\pi^\mu = (1+\xi)\,\bar{p}^\mu - \frac{1}{2}\,\Delta^{\perp\mu} + \frac{1}{2}\left[p^2\,(1-\xi) + \frac{1}{2}\,m_\pi^2\right]\,n^\mu \quad ,$$
$$p_\gamma^\mu = (1-\xi)\,\bar{p}^\mu + \frac{1}{2}\,\Delta^{\perp\mu} + \frac{1}{2}\left[p^2\,(1+\xi) - \frac{1}{2}\,m_\pi^2\right]\,n^\mu \quad . \tag{4.5}$$

Here we have

$$p^2 = [(p_\pi + p_\gamma)/2]^2 = m_\pi^2/2 - t/4\,, \qquad \Delta^\mu = (p_\gamma - p_\pi)^\mu \quad ,$$
$$\Delta^{\perp\mu} = \left(0, \Delta^1, \Delta^2, 0\right) = \left(0, \vec{\Delta}^\perp, 0\right)\,, \qquad \Delta^2 = t \quad . \tag{4.6}$$

Given the kinematics here above, it is easy to determine $\vec{\Delta}^{\perp 2}$

$$\vec{\Delta}^{\perp 2} = 2\,\xi\,(1-\xi)\,m_\pi^2 \;-\; (1-\xi^2)\,t \quad , \tag{4.7}$$

which gives the expression for t

$$t \;=\; \frac{2\xi(1-\xi)m_\pi^2 - \vec{\Delta}^{\perp 2}}{1-\xi^2} \quad . \tag{4.8}$$

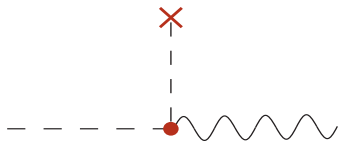

Figure 4.5: Pion pole contribution between the axial current (represented by a cross) and the photon-external pion vertex associated to the last contribution of Eq. (4.3).

The value of the skewness variable is constrained to range between

$$\frac{t}{(2m_\pi^2 - t)} < \xi < 1 \quad . \tag{4.9}$$

Actually there is no symmetry relating the distributions for negative and positive ξ which could have constrained the values of the skewness variable to be positive, like for GPDs.

The polarization vector of the real photon, ε, must satisfy the transverse condition,

$$\varepsilon.p_\gamma = 0 \quad ,$$

as well as an additional gauge fixing condition. When going from the hadronic currents to the parton distribution amplitudes, we need $\varepsilon.n = \varepsilon^+/p^+$ to kinematically become higher-twist, i.e.

$$\varepsilon.n \to 0 \quad \text{when} \quad p^+ \to \infty \quad .$$

The standard gauge fixing conditions, namely $\varepsilon^0 = 0$ or $\varepsilon^+ = 0$, both satisfy the previous requirement. In fact, all what we need is that the components of the polarization vector remain finite when p^+ goes to infinity.

A general expression for ε is

$$\varepsilon \;=\; \vec{\varepsilon}^{\perp} + \alpha\frac{\bar{p}}{p^+} + \beta\,p^+\,n \quad . \tag{4.10}$$

The transverse condition for the real photon polarization provides us for a first constraint, e.g. on β,

$$\beta\, p^+ \;=\; \frac{1}{1-\xi}\left[\frac{1}{2}\,\vec{\varepsilon}^{\perp}\cdot\vec{\Delta}^{\perp} - \frac{\alpha}{2\,p^+}\left(\frac{m_\pi^2}{2}\xi - \frac{t}{4}\,(1+\xi)\right)\right] \quad .$$

Therefore the scalar product $\varepsilon\cdot\Delta$ is

$$\varepsilon\cdot\Delta \;=\; -\frac{\vec{\varepsilon}^{\perp}.\vec{\Delta}^{\perp}}{1-\xi} + \mathcal{O}\left(\frac{\alpha}{p^+}\right) \quad , \tag{4.11}$$

where the gauge dependence inclosed in α is kinematically higher-twist, i.e. goes like $1/p^+$. Also, the decomposition $\varepsilon\cdot\Delta$ depends on the kinematics, what is explicit through the $1-\xi$ in the latter expression. Henceforth the tensor decomposition would rather be chosen to be $\vec{\varepsilon}^{\perp}.\vec{\Delta}^{\perp}$.

The vector and axial TDAs are the Fourier transform of the matrix element of the bilocal currents separated by a light-like distance

$$\bar{q}\,(-z/2)\,\gamma_\mu\,[\gamma_5]\,q\,(z/2) \quad .$$

Then, they are directly related to the currents defined in Eqs. (4.2-4.3) through the sum rules

$$\begin{aligned}&\int_{-1}^{1} dx \int \frac{dz^-}{2\pi} e^{ixp^+z^-}\;\langle\gamma\,(p_\gamma)|\,\bar{q}\left(-\frac{z}{2}\right)\gamma_\mu\,[\gamma_5]\,\tau^-\,q\left(\frac{z}{2}\right)|\pi\,(p_\pi)\rangle\Big|_{z^+=z^\perp=0}\\ &= \frac{1}{p^+}\,\langle\gamma\,(p_\gamma)|\,\bar{q}\,(0)\,\gamma_\mu\,[\gamma_5]\,\tau^-\,q\,(0)\,|\pi\,(p_\pi)\rangle \quad .\end{aligned} \tag{4.12}$$

With this connection we can introduce the leading-twist decomposition of the bilocal currents. For that we need the light-front vectors $\bar{p}^\mu$ and n^μ defined in Eq. (A.8), which leads to the expressions (4.5-4.6).
To leading-twist, the $\pi^+\to\gamma$ TDAs are defined

$$\begin{aligned}&\int \frac{dz^-}{2\pi} e^{ixp^+z^-}\;\langle\gamma\,(p_\gamma)|\,\bar{q}\left(-\frac{z}{2}\right)\not{n}\tau^-\,q\left(\frac{z}{2}\right)|\pi^+\,(p_\pi)\rangle\Big|_{z^+=z^\perp=0}\\ &= \frac{i}{p^+}\,e\,\varepsilon^\nu\,\epsilon_{\mu\nu\rho\sigma}\,n^\mu\,p^\rho\,\Delta^\sigma\,\frac{V^{\pi^+}\,(x,\xi,t)}{\sqrt{2}f_\pi} \quad ,\end{aligned} \tag{4.13}$$

$$\begin{aligned}&\int \frac{dz^-}{2\pi} e^{ixp^+z^-}\;\langle\gamma\,(p_\gamma)|\,\bar{q}\left(-\frac{z}{2}\right)\not{n}\gamma_5\tau^-\,q\left(\frac{z}{2}\right)|\pi^+\,(p_\pi)\rangle\Big|_{z^+=z^\perp=0}\\ &= \frac{1}{p^+}e\,\left(\vec{\varepsilon}^{\perp}\cdot\vec{\Delta}^{\perp}\right)\frac{A^{\pi^+}\,(x,\xi,t)}{\sqrt{2}f_\pi} + \frac{1}{p^+}e\,(\varepsilon\cdot\Delta)\,\frac{2\sqrt{2}f_\pi}{m_\pi^2-t}\,\epsilon\,(\xi)\;\phi\left(\frac{x+\xi}{2\xi}\right) \quad ,\end{aligned} \tag{4.14}$$

where $\epsilon\,(\xi)$ is equal to 1 for $\xi>0$, and equal to -1 for $\xi<0$. Here $V\,(x,\xi,t)$ and $A\,(x,\xi,t)$ are

respectively the vector and axial TDAs. They are defined as dimensionless quantities. From the condition (4.12) we observe that they obey the following sum rules,

$$\int_{-1}^{1} dx\ V^{\pi^+}(x,\xi,t) = \frac{\sqrt{2}f_\pi}{m_\pi} F_V(t)\ , \tag{4.15}$$

$$\int_{-1}^{1} dx\ A^{\pi^+}(x,\xi,t) = \frac{\sqrt{2}f_\pi}{m_\pi} F_A(t)\quad . \tag{4.16}$$

In the second term of Eq. (4.14), we have introduced the pion Distribution Amplitude (DA) $\phi(x)$, whose expression in given by Eq. (2.1). The pion DA $\phi(x)$ vanishes outside the region $x \in [0,1]$ and satisfies the normalization condition (2.2).

This second term has been introduced in order to isolate the pion pole contribution of the axial current in a model independent way, as we have done in Eq. (4.3) for the $\pi^+ \to \gamma e^+ \nu$ process. Therefore, all the structure of the pion remains in the TDA $A(x,\xi,t)$. It can be seen as a result of PCAC, because the axial current must be coupled to the pion. Therefore, this term is not a peculiarity of the pion-photon TDAs. A similar pion term will be present in the Lorentz decomposition in terms of distribution amplitudes of the axial current for any pair of external particles. We emphasize that it is a model independent definition, because we have defined the numerator of the pion pole term as the residue at the pole $t = m_\pi^2$. With this definition, all the structure dependence related to the outgoing $\pi^\pm$ is included in $A(x,\xi,t)$. Moreover, the pion pole contribution can be estimated in a phenomenological way, as we will see later on.

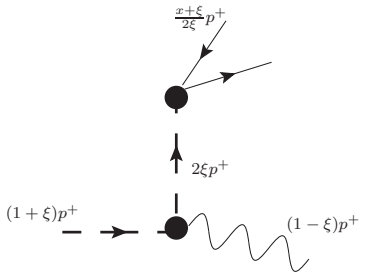

Figure 4.6: Pion pole contribution to the axial bilocal current corresponding to the last term of equation (4.14).

A pion exchange contribution was analyzed in [145, 160] for the axial helicity-flip GPD and, in [199], a similar structure for the axial current was obtained using different arguments. This term we have represented in Fig. 4.6 is only non-vanishing in the ERBL region, i.e. the $x \in [-\xi,\xi]$ region. The kinematics of this region allow the emission or absorption of a pion from the initial state, which is described through the pion DA. And it can be seen from Fig. 4.6 that positive values of ξ corresponds to an outcoming virtual pion, whereas negative values of ξ describe an incoming virtual pion. The latter is related to the matrix element $\langle \pi(p_\pi)| \bar{q}\not{n}\gamma_5\tau^- q\,|0\rangle$, instead of the one present in Eq. (2.1), what gives rise to the minus sign included in $\epsilon(\xi)$.

In order to make possible the connection with other works, it must be realized that the axial TDA must be defined from an electromagnetic gauge independent tensorial structure. As abovementioned, the product $\varepsilon \cdot \Delta$ contains gauge dependent terms. Since the TDAs are gauge independent quantities, the tensorial structure defining them has to be itself gauge independent. The only possibility is hence, see Eq. (4.14),

$$\vec{\varepsilon}^{\perp}.\vec{\Delta}^{\perp}\quad , \tag{4.17}$$

which is equal to, e.g., $(1-\xi)\,(\varepsilon.\Delta)$ in the $\varepsilon^0 = 0$ gauge we have chosen to work in.

In many papers present in the literature, the r.h.s. of Eq. (4.14) contains only the A term. In a general case the A term and the pion pole terms have different tensor structures as shown by Eq. (4.3). However we can fix the gauge convention and the frame conventions in such a way that these two tensorial structures coincide. In other words, should we have chosen another gauge and a frame in which all the transverse component is in the pion momentum, i.e. $\vec{p}_\gamma^{\,\perp} = 0$, the tensorial structure of the axial TDA and the pion pole would have coincided: we have the freedom to choose ε_μ with only transverse component. In that case,

$$\varepsilon \cdot \Delta \quad = \quad -\vec{\varepsilon}^{\,\perp} \cdot \vec{\Delta}^{\perp} \quad .$$

Only with this particular definition, we can change our definition of the axial TDA to

$$\begin{aligned} &\int \frac{dz^-}{2\pi} e^{ixp^+z^-} \left\langle \gamma\left(p_\gamma \varepsilon\right)\right| \bar{q}\left(-\frac{z}{2}\right) \gamma^+\gamma_5\, \tau^-\, q\left(\frac{z}{2}\right) \left|\pi^+\left(p_\pi\right)\right\rangle \Big|_{z^+=z^\perp=0} \\ &= \quad \frac{1}{p^+}\left[\, e\left(\vec{\varepsilon}^{\,\perp} \cdot \left(\vec{p}_\gamma^{\,\perp} - \vec{p}_\pi^{\,\perp}\right)\right) \frac{\bar{A}^{\pi^+\to\gamma}(x,\xi,t)}{\sqrt{2} f_\pi}\right] , \end{aligned} \tag{4.18}$$

with

$$\bar{A}^{\pi^+\to\gamma}(x,\xi,t) = A^{\pi^+\to\gamma}(x,\xi,t) - \frac{4 f_\pi^2}{m_\pi^2 - t}\, \epsilon(\xi)\, \phi^\pi\left(\frac{x+\xi}{2\xi}\right) \quad . \tag{4.19}$$

The latter expression shows that the pion pole contribution to the axial TDA is closely related to the D-term of the Generalized Parton Distributions [171]. However it must be realized that in this case it gives an explicit contribution to the sum rule

$$\int_{-1}^{1} dx\; \bar{A}^{\pi^+\to\gamma}\left(x,\xi,t\right) = \frac{\sqrt{2}\; f_\pi}{m_\pi}\; F_A\left(t\right) - \frac{4 f_\pi^2}{m_\pi^2 - t}\; \left(p_\gamma - p_\pi\right) \cdot n \quad . \tag{4.20}$$

In what follows, the definitions derived from the tensorial decomposition (4.13, 4.14) of the hadronic matrix element for the pion radiative decay will mainly be used.

4.3 A Field Theoretical Approach to the Pion-Photon TDA

In Chapter 2.1 we have defined a method of calculation for the pion DA in a field theoretical scheme, treating the pion as a bound state of quarks and antiquarks in a fully covariant manner using the Bethe-Salpeter equation. We then applied the same method for evaluating the pion GPDs in Chapter 3. The same is done here for the evaluation of the pion-photon TDAs [67]. This method has enormous advantages because it preserves all the physical invariances of the problem. Therefore, any property as sum rules or polynomiality is expected to be preserved.

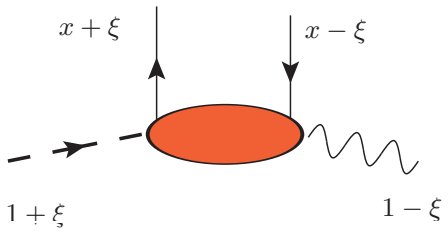

Figure 4.7: Diagram representing the $\pi \to \gamma$ TDAs.

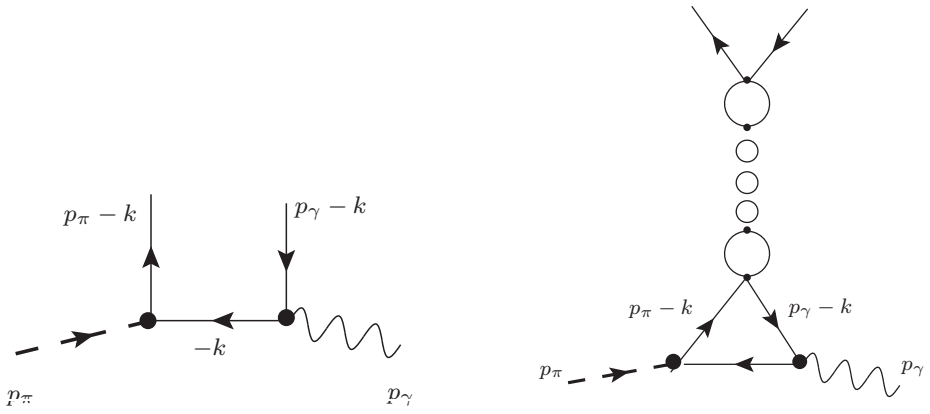

Figure 4.8: Diagrams contributing to the TDA. We have depicted diagrams in which a quark u is changed into a quark d by the bilocal current. There are similar diagrams in which the antiquark $\bar{d}$ is changed into a $\bar{u}$

As usual, we consider that the process is dominated by the handbag diagram. Each TDA has two related contributions, depending on which quark (u or d) of the pion is scattered off by the deeply virtual photon. In Fig. 4.8 we have depicted the diagrams in which the photon scatters off the u-quark. We observe that there are two kinds of contributing diagrams. In the first one the d-antiquark appears as the intermediate state, while in the second the bi-local current couples to a quark-antiquark pair coupled in the pion channel. The latter is present only for the axial current and includes the pion pole contribution.

The details of the method of calculation are given in Ref. [153]. In the present case we obtain, from the first kind of diagram of Fig. 4.8, the following contributions [67]

$$\begin{aligned}
&\int \frac{dz^-}{2\pi} e^{ixp^+z^-} \left\langle \gamma\left(p_\gamma,\varepsilon\right) \left| \bar{q}\left(-\frac{z}{2}\right) \gamma^\mu \left[\gamma_5\right] \tau^- q\left(\frac{z}{2}\right) \right| \pi^+\left(p_\pi\right) \right\rangle \Big|_{z^+=z^\perp=0} \\
&= -e \int \frac{d^4k}{\left(2\pi\right)^4} \varepsilon_\nu \left\{ -\delta\left(xp^+ - \frac{1}{2}\left(p_\gamma^+ + p_\pi^+ - 2k^+\right)\right) \right. \\
&\quad \mathbb{T}\mathrm{r}\left[\frac{1}{2}\left(\frac{1}{3} + \tau_3\right) \gamma^\nu\, iS\left(p_\gamma - k\right) \gamma^\mu \left[\gamma_5\right] \tau^- iS\left(p_\pi - k\right) \Phi^{\pi^+}\left(k, p_\pi\right) iS\left(-k\right) \right] \\
&\quad - \delta\left(xp^+ - \frac{1}{2}\left(2k^+ - p_\pi^+ - p_\gamma^+\right)\right) \\
&\quad \left. \mathbb{T}\mathrm{r}\left[\frac{1}{2}\left(\frac{1}{3} + \tau_3\right) \gamma^\nu\, iS\left(k\right) \Phi^{\pi^+}\left(k, p_\pi\right) iS\left(k - p_\pi\right) \gamma^\mu \left[\gamma_5\right] \tau^- iS\left(k - p_\gamma\right) \right] \right\} \quad , \qquad (4.21)
\end{aligned}$$

where $S\left(k\right)$ is the Feynman propagator of the quark and $\Phi^{\pi^+}\left(k, p_\pi\right)$ is the Bethe-Salpeter amplitude for the pion. Here $\mathbb{T}\mathrm{r}()$ represents the trace over spinor, color, flavor and Dirac indices.

The first contribution in Eq. (4.21) is the one depicted in the first diagram of Fig. 4.8. The second contribution corresponds to a similar diagram but changing quarks u and d. In the NJL model, $\Phi^{\pi^+}\left(k, p_\pi\right)$ is as simple as,

$$\Phi^{\pi^+}\left(k, p_\pi\right) = ig_{\pi qq}\, i\gamma_5\, \tau^{\pi^+} \quad , \qquad (4.22)$$

where $g_{\pi qq}$ is the pion-quark coupling constant defined in Eq.(C.30).

4.3.1 Vector TDA

The vector TDA has contribution only from this first kind of diagrams. We can express $V(x,\xi,t)$ as the sum of the active u-quark and the active d-quark distributions. The first contribution will be proportional to the d's charge, and the second contribution to the u's charge. Therefore, we can write

$$V^{\pi^+}(x,\xi,t) = Q_d v^{\pi^+}_{u\to d}(x,\xi,t) + Q_u v^{\pi^+}_{\bar{d}\to\bar{u}}(x,\xi,t) \quad . \tag{4.23}$$

Isospin relates these two contributions,

$$\begin{aligned} v^{\pi^+}_{u\to d}(x,\xi,t) &= v(x,\xi,t) \quad , \\ v^{\pi^+}_{\bar{d}\to\bar{u}}(x,\xi,t) &= v(-x,\xi,t) \quad . \end{aligned}$$

A direct calculation gives

$$v(x,\xi,t) = 8\, N_c\, f_\pi\, g_{\pi qq}\, m\, \tilde{I}_{3v}(x,\xi,t) \quad , \tag{4.24}$$

with

$$\begin{aligned} &\tilde{I}_3^{TDA}(x,\xi,t) \\ &= i\int \frac{d^4k}{(2\pi)^4}\,\delta\left(x-1+\frac{k^+}{p^+}\right)\frac{1}{(k^2-m^2+i\epsilon)\left[(p_\gamma-k)^2-m^2+i\epsilon\right]\left[(p_\pi-k)^2-m^2+i\epsilon\right]} \quad , \end{aligned} \tag{4.25}$$

given by the expression (E.15) in Appendix.

In this integral, we first perform the integration over k^-. The pole structure of the integrand fixes two non-vanishing contributions to $v(x,\xi,t)$, the first one in the region $\xi < x < 1$, corresponding to the quark contribution, and the second in the region $-\xi < x < \xi$, corresponding to a quark-antiquark contribution. Given the relation (4.23), the support of the entire vector TDA, $V^{\pi^+}(x,\xi,t)$, is therefore $x \in [-1,1]$. The analytical expression for (4.25) is given by Eqs. (E.15-E.17).

For the $\pi^0 \to \gamma^*\gamma$ process, the contributions of the first type of diagram (Fig. 4.8) can be related to $v(x,\xi,t)$

$$\begin{aligned} V_u^{\pi^0} &= \frac{Q_u}{\sqrt{2}}\left(v(x,\xi,t) + v(-x,\xi,t)\right) \quad , \\ V_d^{\pi^0} &= \frac{Q_d}{\sqrt{2}}\left(v(x,\xi,t) + v(-x,\xi,t)\right) \quad . \end{aligned} \tag{4.26}$$

4.3.2 Axial TDA

Turning our attention to the axial TDA, we find a new contribution arising from the second diagram of Fig. 4.8. This second contribution comes from the re-scattering of a $q\bar{q}$ pair in the pion channel. Therefore

$$\begin{aligned} &\int \frac{dz^-}{2\pi} e^{ixp^+z^-}\left\langle \gamma(p_\gamma,\varepsilon)\left|\bar{q}\left(-\frac{z}{2}\right)\gamma^\mu\gamma_5\tau^- q\left(\frac{z}{2}\right)\right|\pi^+(p_\pi)\right\rangle\Big|_{z^+=z^\perp=0} \\ &= (4.21) + \sum_i M^i \frac{2ig}{1-2g\Pi_{ps}(t)} N^i \quad , \end{aligned} \tag{4.27}$$

where i is an isospin index,

$$M^i = -e\int \frac{d^4k'}{(2\pi)^4}\varepsilon_\nu \left\{ -\mathbb{T}\mathrm{r}\left[\phi^{\pi^+}\left(k',p_\pi\right)\, iS\left(-k'\right)\frac{1}{2}\left(\frac{1}{3}+\tau_3\right)\gamma^\nu\, iS\left(p_\gamma-k'\right)\, i\gamma_5\tau^i\, iS\left(p_\pi-k'\right)\right]\right.$$
$$\left. -\mathbb{T}\mathrm{r}\left[\phi^{\pi^+}\left(k',p_\pi\right)\, iS\left(k'-p_\pi\right)\, i\gamma_5\tau^i\, iS\left(k'-p_\gamma\right)\frac{1}{2}\left(\frac{1}{3}+\tau_3\right)\gamma^\nu\, iS\left(k'\right)\right]\right\}\ , \tag{4.28}$$

$$N^i = -\int \frac{d^4k}{(2\pi)^4}\delta\left(xp^+ - \frac{1}{2}\left(p_\gamma^+ + p_\pi^+ - 2k^+\right)\right)\mathbb{T}\mathrm{r}\left[iS\left(p_\gamma-k\right)\,\gamma^\mu\gamma_5\tau^-\, iS\left(p_\pi-k\right)\, i\gamma_5\tau^i\right]\quad , \tag{4.29}$$

and Π_{ps} is the pseudoscalar polarization, see Fig C.3, described by Eq. (C.23),

$$\Pi_{ps}\left(\Delta^2\right) = -i\int\frac{d^4k}{(2\pi)^4}\left\{\mathbb{T}\mathrm{r}\left[i\gamma_5\, iS\left(k\right)\, i\gamma_5\, iS\left(\Delta-k\right)\right]\right. \quad ; \tag{4.30}$$

We can now evaluate the axial current in a straightforward way. [1] Nevertheless, in order to extract the axial TDA we must subtract the pion pole contribution. We need for that the pion amplitude studied in Chapter 2.1. In the NJL model, the pion DA is given by Eq. (2.13) in the $[-\xi,\xi]$ region,

$$\frac{1}{2\xi}\,\phi\left(\frac{x+\xi}{2\xi}\right) \;=\; -\frac{g_{\pi qq}\,4N_c m}{\sqrt{2}f_\pi}\,\tilde{I}_{2,\Delta}(x,\xi,m_\pi^2)\quad . \tag{4.32}$$

The trace over the Dirac space involves a k-dependent 3-propagator integral that renders a bit more tricky the calculation. After a long but direct calculation, we obtain the expression for $A\left(x,\xi,t\right)$. As the vector TDA, $A\left(x,\xi,t\right)$ can be expressed as a sum of the contributions coming from the active u-quark and the active $\bar{d}$-quark. The first one will be proportional to the d's charge and the second to the u's charge,

$$A^{\pi^+}\left(x,\xi,t\right) = Q_d\, a^{\pi^+}_{u\to d}\left(x,\xi,t\right) + Q_u\, a^{\pi^+}_{\bar{d}\to\bar{u}}\left(x,\xi,t\right)\quad . \tag{4.33}$$

Isospin relates these two contributions,

$$\begin{aligned} a^{\pi^+}_{u\to d}\left(x,\xi,t\right) &= a\left(x,\xi,t\right)\quad , \\ a^{\pi^+}_{\bar{d}\to\bar{u}}\left(x,\xi,t\right) &= -a\left(-x,\xi,t\right)\quad , \end{aligned}$$

where the minus sign is originated in the change in helicity produced by the γ_5 operator. The expression for $a^{\pi^+}_{u\to d}\left(x,\xi,t\right)$ depends on the sign of ξ.

[1] The pion pole structure of this contribution can be explicitly understood if we observe that

$$\sum_i M^i\frac{2ig}{1-2g\Pi_{ps}\left(t\right)}N^i|_{t\simeq m_\pi^2} \;=\; -8N_c\, f_\pi g_{\pi qq}\, m\,\frac{4\xi}{1-\xi}\frac{1}{m_\pi^2-t}\,\tilde{I}_{2,\Delta}(x,\xi,t)\quad . \tag{4.31}$$

In the $|\xi| < x < 1$ region we have

$$a\,(x,\xi,t) = -8\,N_c\,f_\pi\,g_{\pi qq}\,m\left\{\left(1+\frac{m_\pi^2\,(x-\xi)+(1-x)\,t}{2\xi m_\pi^2-t\,(1+\xi)}\frac{1+\xi}{1-\xi}\right)\tilde{I}_{3v}\,(x,\xi,t)\right.$$
$$\left.+\,\frac{1}{2\xi m_\pi^2-t\,(1+\xi)}\,\frac{1+\xi}{1-\xi}\frac{1}{16\pi^2}\sum_{i=1}^{2}c_i\left[\log\frac{m^2\left(m_i^2-\bar{z}\,m_\pi^2\right)}{m_i^2\left(m^2-\bar{z}\,m_\pi^2\right)}\right]\right\}\quad, \tag{4.34}$$

with the abbreviations $\bar{z}=(1-x)\,(\xi+x)\,/\,(1+\xi)^2$. And in the $-|\xi| < x < |\xi|$ region we have

$$a\,(x,\xi,t) = -8\,N_c\,f_\pi\,g_{\pi qq}\,m\left\{\left(1+\frac{m_\pi^2\,(x-\xi)+(1-x)\,t}{2\xi m_\pi^2-t\,(1+\xi)}\frac{1+\xi}{1-\xi}\right)\tilde{I}_{3v}\,(x,\xi,t)\right.$$
$$+\,\frac{\epsilon\,(\xi)}{1-\xi}\frac{1}{16\pi^2}\sum_{i=1}^{2}c_i\left[\frac{1+\xi}{2\xi m_\pi^2-t\,(1+\xi)}\log\frac{\left(4\xi^2m^2-\bar{x}\,t\right)\left(m_i^2-\bar{y}\,m_\pi^2\right)}{\left(4\xi^2m_i^2-\bar{x}\,t\right)\left(m^2-\bar{y}\,m_\pi^2\right)}\right.$$
$$\left.\left.+\,\frac{2}{t-m_\pi^2}\log\frac{\left(4\xi^2m^2-\bar{x}\,t\right)\left(4\xi^2m_i^2-\bar{x}\,m_\pi^2\right)}{\left(4\xi^2m_i^2-\bar{x}\,t\right)\left(4\xi^2m^2-\bar{x}\,m_\pi^2\right)}\right]\right\}\quad, \tag{4.35}$$

where $\bar{x}=\left(\xi^2-x^2\right)$ and $\bar{y}=\bar{z}$ for $\xi>0$ and $\bar{y}=0$ for $\xi<0$.

4.3.3 The Chiral Limit

The expressions for both the vector and axial TDAs in the chiral limit, i.e. $m_\pi = 0$, are well defined. In particular, for $t=0$, we find the following simple expression for $v(x,\xi,t)$

$$v(x,\xi,0) = \sqrt{2}\,f_\pi\,6\,F_V^{\pi^+\chi}(0)\,\left[\theta(\xi^2-x^2)\,\frac{x+|\xi|}{2\,|\xi|\,(1+|\xi|)}\,+\,\theta(x-|\xi|)\theta(1-x)\frac{1-x}{1-\xi^2}\right]\quad, \tag{4.36}$$

where $F_V^{\pi^+\chi}(0)$ is the chiral limit of the vector pion form factor at zero momentum transfer

$$F_V^{\pi^+\chi}(0) = \lim_{m_\pi\to 0}\frac{F_V^{\pi^+}(0)}{m_\pi} = 0.17\,\mathrm{GeV}^{-1}\quad.$$

A similar expression is obtained for $a(x,\xi,t)$ in the chiral limit for $t=0$

$$a(x,\xi,0) = -\sqrt{2}\,f_\pi\,6\,F_A^{\pi^+\chi}(0)\,\left[\theta(\xi^2-x^2)\,\epsilon\,(\xi)\,\frac{(\xi-x)}{4\xi^2(1+|\xi|)}\left(x+\xi+(x-\xi)\,\frac{|\xi|-\xi}{(1+|\xi|)}\right)\right.$$
$$\left.+\,\theta(x-|\xi|)\theta(1-x)\frac{(1-x)(x-\xi)}{(1-\xi^2)(1-\xi)}\right]\quad, \tag{4.37}$$

with $F_A^{\pi^+\chi}(0)$ the axial Form Factor at $t=0$ in the chiral limit

$$F_A^{\pi^+\chi}(0) = \lim_{m_\pi\to 0}F_A^{\pi^+}(0)/m_\pi = F_V^{\pi^+\chi}(0)\quad.$$

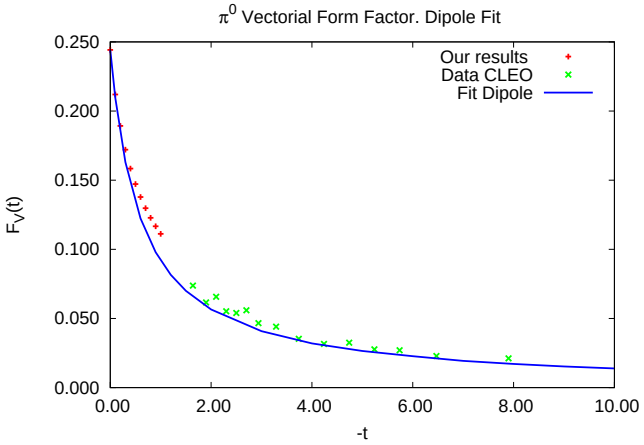

Figure 4.9: The vector Form Factor for the π^0 compared to the experimental data and to the dipole parameterization based on it [105].

4.3.4 Sum Rules and Polynomiality

The vector TDA of the π^+ must obey the sum rule given in Eq. (4.15) with the expression of the vector pion Form Factor in the NJL model given by Eq. (D.1). We have numerically recovered the sum rule for different t values. In particular we obtain the value $F_V^{\pi^+}(0) = 0.0242$ for the vector Form Factor at $t = 0$, which is in agreement with the experimental value

$$F_V(0) = 0.017 \pm 0.008 \quad ,$$

given in [11].

The π^0 distribution must satisfy the following sum rule [165]

$$\int_{-1}^{1} dx \, \Big(Q_u \, V_u^{\pi^0}(x,\xi,t) - Q_d \, V_d^{\pi^0}(x,\xi,t) \Big) = \sqrt{2} \, f_\pi \, F_{\pi\gamma^*\gamma}(t) \qquad . \tag{4.38}$$

A theoretical prediction of the π^0 Form Factor value is given in Ref. [39]. In particular, at $t = 0$, the value $F_{\pi\gamma^*\gamma}(0) = 0.272$ GeV^{-1} is found. The neutral pion Form Factor is directly related to the π^+ vector Form Factor so that the sum rule is satisfied. We obtain the value $F_{\pi\gamma^*\gamma}(0) = 0.244$ GeV^{-1}. The difference with the well-known result from the anomaly is due to the regularization parameters, see (D.4). In Ref. [105], a dipole parameterization based on experimental data is proposed for the t-dependence of $F_{\pi\gamma^*\gamma}(t)$,

$$F_{\pi\gamma^*\gamma}(t) \quad = \quad \frac{F_{\pi\gamma^*\gamma}(0)}{1 - t/\Lambda^2} \quad ,$$

obtaining for the dipole mass $\Lambda = 0.77$ GeV. In Fig. 4.9 are shown the experimental results of the CLEO experiment [105] (green diagonal crosses) obtained for higher values of t than our calculation allows. [2] On the same plot, the red crosses represent our results for the neutral pion Form Factor.

[2] Notice that the recent measurements of the BABAR collaboration for $Q^2 > 10$ GeV^2 show surprising results [2]: the measured neutral pion Form Factor exceeds the asymptotic limit f_π/Q^2 and contradicts most of the models for the pion DA.

We have found that, for small values of t, the NJL neutral pion Form Factor can be parametrized in a dipole form with $\Lambda = 0.81$ GeV. The blue line represents the fit with the latter value for the free parameter.

The axial TDA obeys the sum rules given by Eq. (4.16) with the axial Form Factor given in the NJL model by Eq. (D.2). This sum rule is satisfied for different t values. The numerical results also coincide. In particular we obtain $F_A^{\pi^+}(0) = 0.0239$ for the axial Form Factor at $t = 0$, which is about twice the value

$$F_A^{\pi^+}(0) = 0.0115 \pm 0.0005 \quad ,$$

given by the Particle Data Group [11].

We expect TDAs to obey the polynomiality condition. However no time reversal invariance enforces the polynomials to be even in the Δ-momenta like for GPDs. That means that the polynomials should be "complete", i.e. they should include all powers in ξ,

$$\int_{-1}^{1} dx\, x^{n-1}\, V(x,\xi,t) = \sum_{i=0}^{n-1} C_{n,i}(t)\, \xi^i \quad . \tag{4.39}$$

We have numerically tested the polynomiality and obtained it. We observe that, for the vector TDA, the coefficients for the odd powers in ξ are of one order of magnitude smaller than those for the even powers in ξ. In particular we have numerically proved that, in the chiral limit, the polynomials only contain even powers in ξ for any value of t,

$$\int_{-1}^{1} dx\, x^{n-1}\, [\lim_{m_\pi \to 0} V(x,\xi,t)] = \sum_{i=0}^{[\frac{n-1}{2}]} C^{\chi}_{n,2i}(t)\, \xi^{2i} \quad . \tag{4.40}$$

We have analytically found that the odd powers in ξ go to zero for the polynomial expansion of the vector TDA. A study of the polynomiality in the limit given in Eq. (4.36) leads to the following analytical expression for the coefficients $C^{\chi}_{n,2i}(t)$

$$C^{\chi}_{n,2i}(0) = \sqrt{2}\, f_\pi\; 2\, F_V^{\pi^+\chi}(0)\; \left(-1 + 2(-1)^{n-1}\right) \left(\frac{1}{n} - \frac{1}{n+1}\right) \quad . \tag{4.41}$$

Notice they do not depend on i. The coefficients in the chiral limit, Eq. (4.40), as well as the coefficients for $m_\pi = 140$ MeV, Eq. (4.39), we numerically obtained are given in Table 4.1.

The ξ-dependence of the moments of the axial TDA also has a polynomial form. Those polynomials contain all the powers in ξ, i.e. even and odd,

$$\int_{-1}^{1} dx\, x^{n-1}\, A(x,\xi,t) = \sum_{i=0}^{n-1} C'_{n,i}(t)\, \xi^i \quad . \tag{4.42}$$

An analytic study of the polynomiality in the limit given in Eq. (4.37) confirms that all the powers in ξ have to be present. The analytic values for the coefficients in this specific limit are

$$\begin{aligned} C'^{\chi}_{n,2i}(0) &= \sqrt{2}\, f_\pi\; 2\, F_A^{\pi^+\chi}(0)\; \left(1 + 2(-1)^{n-1}\right) \frac{n-2i}{n(n+1)(n+2)} \quad , \\ C'^{\chi}_{n,2i+1}(0) &= \sqrt{2}\, f_\pi\; 2\, F_A^{\pi^+\chi}(0)\; \left(1 + 2(-1)^{n-1}\right) \frac{-2(i+1)}{n(n+1)(n+2)} \quad , \end{aligned} \tag{4.43}$$

n	1	2		3			4			
	$C_{1,0}(t)$	$C_{2,0}(t)$	$C_{2,1}(t)$	$C_{3,0}(t)$	$C_{3,1}(t)$	$C_{3,2}(t)$	$C_{4,0}(t)$	$C_{4,1}(t)$	$C_{4,2}(t)$	$C_{4,3}(t)$
$m_\pi = 0$										
$t = 0$	22.6	-22.6	0.0	3.77	0.0	3.77	-6.7	0.0	-6.7	0.0
$t = -0.5$	13.7	-16.3	0.0	3.00	0.0	2.43	-5.7	0.0	-4.9	0.0
$t = -1.0$	10.4	-13.4	0.0	2.57	0.0	1.90	-5.0	0.0	-4.0	0.0
$m_\pi = 140$										
$t = 0$	22.7	-22.9	0.44	3.80	-0.10	3.67	-6.8	0.19	-6.8	0.12
$t = -0.5$	13.7	-16.4	0.25	3.00	-0.06	2.43	-5.7	0.13	-4.9	0.08
$t = -1.0$	10.3	-13.4	0.19	2.57	-0.05	1.87	-5.0	0.11	-4.0	0.06

Table 4.1: Coefficients of the polynomial expansion for the vector TDA. The pion mass is expressed in MeV and t is expressed in GeV^2. Notice that the coefficients have to be multiplied by 10^{-3}.

which is in agreement with those numerically obtained. The coefficients of the polynomial expansions in the chiral limit are very close to those obtained for the physical values of the pion mass. In Table 4.2, the coefficients $C'_{n,i}(t)$ are therefore shown only for $m_\pi = 140\,\mathrm{MeV}$.

The polynomiality property of the term containing the pion DA can also be studied. The t-dependence only comes from the pion pole and it is divergent at the chiral limit when $t = 0$. We have numerically found

$$\int_{-\xi}^{\xi} dx\, x^{n-1}\, \frac{4\, f_\pi^2}{m_\pi^2 - t}\, \frac{1}{2\xi}\, \phi\left(\frac{x+\xi}{2\xi}\right) \;=\; \frac{1}{2}\left(1 + (-1)^{n+1}\right)\, C^{\diamond}_{n-1}(t)\, \xi^{n-1} \qquad , \tag{4.44}$$

which is true for both $m_\pi = 0$ and 140 MeV. The even moments in x disappear due to the pion distribution amplitude is an even function in the interval $[-\xi, \xi]$.

Calling the l.h.s. of Eqs. (4.42-4.44), respectively, $A_n(\xi, t)$ and $\Phi_n(\xi, t)$, and using the *alternative* tensorial decomposition (4.18), we tend to write a general relation about the polynomiality property of the whole axial bilocal matrix element, in the fashion of the *alternative* sum rule (4.20). In the $\varepsilon^+ = 0$ gauge, it reads

$$\begin{aligned}
&\int_{-1}^{1} dx\, x^{n-1} \int \frac{dz^-}{2\pi}\, e^{ix\,p^+ z^-}\, \langle \gamma(p_\gamma) | \bar{q}\left(-\frac{z}{2}\right)\, \not{n}\, \gamma_5\, \tau^-\, q\left(\frac{z}{2}\right) | \pi(p_\pi) \rangle\, |_{z^+ = z^\perp = 0} \\
&= \frac{1}{p^+}\, e\, \left(\vec{\varepsilon}^{\,\perp} \cdot \vec{\Delta}^\perp\right)\, \frac{1}{\sqrt{2} f_\pi}\, \Big[A_n(\xi, t) - (2\xi)\, \Phi_n(\xi, t) \Big] \qquad , \\
&= \frac{1}{p^+}\, e\, \left(\vec{\varepsilon}^{\,\perp} \cdot \vec{\Delta}^\perp\right)\, \frac{1}{\sqrt{2} f_\pi}\, \Big[\sum_{i=0}^{n-1} C'_{n,i}(t)\, \xi^i \,-\, 2\, \frac{1}{2}\left(1 + (-1)^{n+1}\right)\, C^{\diamond}_{n-1}(t)\, \xi^n \Big] \quad .
\end{aligned} \tag{4.45}$$

We can therefore write a general relation about the polynomiality property of the whole axial bilocal matrix element

$$\begin{aligned}
&\int_{-1}^{1} dx\, x^{n-1} \int \frac{dz^-}{2\pi}\, e^{ix\,p^+ z^-}\, \langle \gamma(p_\gamma) | \bar{q}\left(-\frac{z}{2}\right)\, \not{n}\, \gamma_5\, \tau^-\, q\left(\frac{z}{2}\right) | \pi(p_\pi) \rangle\, |_{z^+ = z^\perp = 0} \\
&= \frac{1}{p^+}\, e\, \left(\vec{\varepsilon}^{\,\perp} \cdot \vec{\Delta}^\perp\right)\, \frac{1}{\sqrt{2} f_\pi}\, \sum_{i=0}^{n} C^{\star}_{n,i}(t)\, \xi^i \quad ,
\end{aligned} \tag{4.46}$$

with the highest power in ξ given by the pion pole contribution. The latter result is the expected one from Lorentz invariance, e.g. for the GPDs (1.26).

4.4 Symmetries

In the previous Section we have defined the TDAs in the particular case of a transition from a π^+ to a photon, parameterizing processes like hadron annihilation into two photons and backward VCS in the kinematical regime where the virtual photon is highly off-shell but with small momentum transfer t

$$H\bar{H} \to \gamma^*\gamma \to e^+e^-\gamma \quad \text{and} \quad \gamma^* H \to H\gamma \quad , \tag{4.47}$$

n	1	2		3		
	$C'_{1,0}(t)$	$C'_{2,0}(t)$	$C'_{2,1}(t)$	$C'_{3,0}(t)$	$C'_{3,1}(t)$	$C'_{3,2}(t)$
$m_\pi = 140$						
$t = 0$	22.4	-3.77	4.00	6.8	-4.9	2.3
$t = -0.5$	16.1	-2.97	2.57	5.7	-3.5	1.7
$t = -1.0$	13.2	-2.53	1.97	5.0	-2.8	1.3

Table 4.2: Coefficients of the polynomial expansion for the axial TDA. The pion mass is expressed in MeV and t is expressed in GeV^2. Notice that the coefficients have to be multiplied by 10^{-3}.

with H a hadron. Symmetries relate the latter distributions to TDAs involved in other processes. For instance, we could wish to study the γ-π^- TDAs entering the factorized amplitude of the process

$$\gamma_L^* \gamma \to M^\pm \pi^\mp \quad ,$$

M being either ρ_L or π; in the same kinematical regime.

By consistency with the processes that we are considering, we choose to change the definitions of the kinematical variables. The momentum transfer is $\Delta = p_\pi - p_\gamma$, therefore $p^2 = m_\pi^2/2 - t/4$ and $t = \Delta^2$. The skewness variable describes the loss of plus momentum of the incident photon, i.e.

$$\xi \;=\; (p_\gamma - p_\pi)^+ / 2p^+ \quad , \tag{4.48}$$

and its value ranges between

$$-1 < \xi < \frac{-t}{(2m_\pi^2 - t)} \quad . \tag{4.49}$$

Since the skewness variable defined for $\pi-\gamma$ transitions is minus the one defined for $\gamma-\pi$ transitions, we should hence consider the results corresponding to the results for negative ξ is a previous Section.

Within these conventions, we define the γ-$\pi^\pm$ TDAs

$$\begin{aligned}
\int \frac{dz^-}{2\pi} e^{ixp^+z^-} \qquad & \left\langle \pi^\pm(p_\pi) \right| \bar{q}\left(-\frac{z}{2}\right) \gamma^+ \tau^\pm q\left(\frac{z}{2}\right) \left|\gamma(p_\gamma \varepsilon)\right\rangle \Big|_{z^+ = z^\perp = 0} \\
&= \frac{1}{p^+} i\, e\, \varepsilon_\nu\, \epsilon^{+\nu\rho\sigma}\, P_\rho\, (p_\pi - p_\gamma)_\sigma\, \frac{V^{\gamma\to\pi^\pm}(x,\xi,t)}{\sqrt{2} f_\pi} \quad , \\
\int \frac{dz^-}{2\pi} e^{ixp^+z^-} \qquad & \left\langle \pi^\pm(p_\pi) \right| \bar{q}\left(-\frac{z}{2}\right) \gamma^+ \gamma_5 \tau^\pm q\left(\frac{z}{2}\right) \left|\gamma(p_\gamma \varepsilon)\right\rangle \Big|_{z^+ = z^\perp = 0} \\
&= \pm \frac{1}{p^+} \Big[- e \left(\vec{\varepsilon}^{\,\perp} \cdot (\vec{p}_\pi^{\,\perp} - \vec{p}_\gamma^{\,\perp})\right) \frac{A^{\gamma\to\pi^\pm}(x,\xi,t)}{\sqrt{2} f_\pi} \\
&\quad + e\, (\varepsilon \cdot (p_\pi - p_\gamma)) \frac{2\sqrt{2} f_\pi}{m_\pi^2 - t}\, \epsilon(\xi)\, \phi\left(\frac{x+\xi}{2\xi}\right) \Big] \quad .
\end{aligned} \tag{4.50}$$

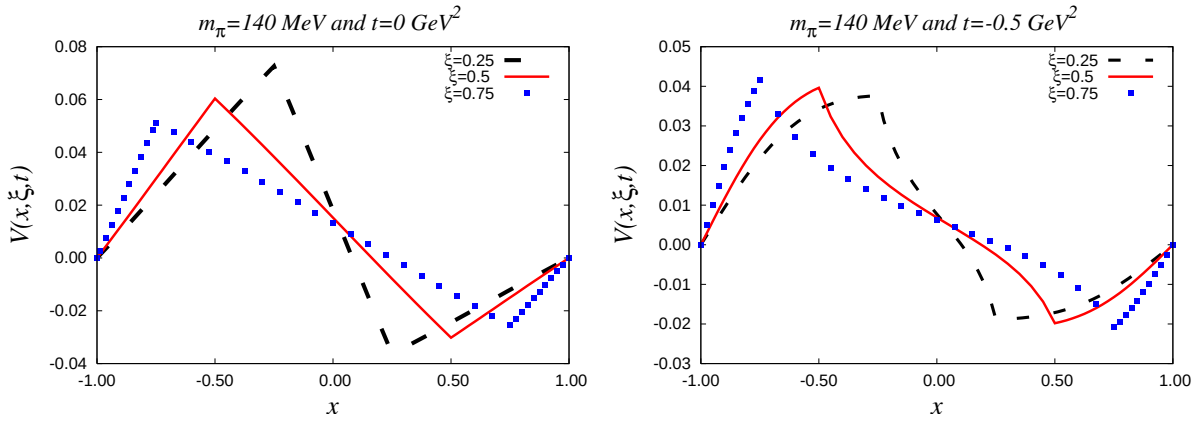

Figure 4.10: The vector TDA in the case $m_\pi = 140$ MeV and, respectively, (a) $t = 0$ and (b) $t = -0.5$ GeV^2.

With the help of Appendix B, we find the following relations. Time-reversal relates the π^+-γ TDAs to γ-π^+ TDAs in the following way

$$D^{\pi^+\to\gamma}(x,\xi,t) \;=\; D^{\gamma\to\pi^+}(x,-\xi,t) \quad , \tag{4.51}$$

where $D = V, A$. And CPT relates the presently calculated TDAs to their analog for a transition from a photon to a π^-

$$D^{\pi^+\to\gamma}(x,\xi,t) \;=\; D^{\gamma\to\pi^-}(-x,-\xi,t) \quad . \tag{4.52}$$

4.5 Pion-Photon TDAs in the Nambu-Jona Lasinio Model

In Figs. 4.10 and 4.11, the vector and axial $\pi^+ \to \gamma$ TDAs obtained in the NJL model are plotted in function of x for several values of ξ and t. In these figures, the u-quark contributes to the TDAs in the region of x going from $-|\xi|$ to 1 and the d-antiquark going from -1 to $|\xi|$. Therefore, for $x \in [|\xi|, 1]$ ($x \in [-1, -|\xi|]$) only u-valence quarks (d-valence antiquarks) are present (DGLAP regions). Besides, TDAs in the $-|\xi| < x < |\xi|$ region (ERBL region) receive contributions from both type of quarks. For the vector TDA, we observe in Fig. 4.10 that the position of the maxima is given by the ξ value, separating explicitly the ERBL region from the DGLAP regions. The vector TDA is positive (negative) for negative (positive) values of x with the change of sign occurring around $x = 0$. This change in the sign of the vector TDA is originated in the presence of the electric charge of the quarks in Eq. (4.23).

The process involved in the calculation of the TDAs allows negative values of the skewness variable. In the chiral limit, the skewness variable goes from $\xi = -1$ to $\xi = 1$, for any value of t. In the chiral limit, the vector TDA for a negative value of ξ is equal to the vector TDA for $|\xi|$. This can be seen from the polynomiality expansion in this limit, Eq. (4.40), which has only even powers of ξ. For the physical value of the pion mass, negative values of ξ are bounded by $t/\left(2m_\pi^2 - t\right) < \xi$. For each allowed value of ξ, we found that the numerical value of $V(x, -|\xi|, t)$ is close to $V(x, |\xi|, t)$, due to the smallness of the coefficients of the odd powers of ξ in the polynomial expansion (4.39).

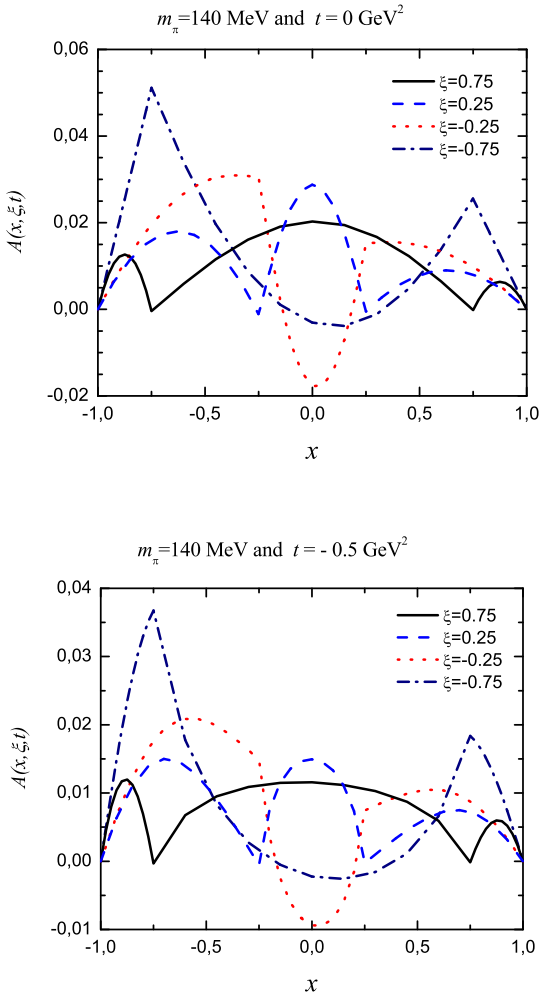

Figure 4.11: The axial TDA in the case $m_\pi = 140$ MeV and, respectively, (a) $t = 0$ and (b) $t = -0.5$ GeV^2.

Analyzing the axial TDAs, plotted in Fig. 4.11, we observe two different behaviors depending on the sign of ξ. For positive ξ, the position of the minima is given by the value of the skewness variable while the position of the maxima is always $x \simeq 0$ in the ERBL region and $x \simeq \pm(1+\xi)/2$ in the DGLAP regions. For negative ξ, the value of the axial TDA at $x = \pm\xi$ is important and in some cases is a maximum and, in the ERBL region, $A(x,\xi,t)$ presents a minimum near $x = 0$. As we have previously shown, the axial TDA in the ERBL region receives contributions from two different diagrams, depicted in Fig. 4.8. In the second of these diagrams, a virtual quark-antiquark interacting pair in the pion channel appears. The pion pole, contained in this diagram, has been subtracted but the remaining non-resonant part contributes to the axial TDA. We observe that the latter contribution is the dominant one and produces the maxima around $x = 0$ for positives ξ (Fig. 4.16). Now, the axial TDA does not change the sign when we go from negative to positive values of x. In the axial TDA the change of sign originated in the presence of the electric charge of the quarks in equation (4.33) is compensated by the change of sign between quark and antiquark contributions generated by the γ_5 operator present in the axial current.

By comparing the plots in Figures 4.10 and 4.11 for different values of the momentum transfer, it is observed that the amplitudes are lower for higher $(-t)$ values, as it can be inferred from the decreasing of the Form Factors with $(-t)$, connected to the TDAs through the sum rules. In the case of the vector TDA, by increasing the $(-t)$ value, not only the width and the curvature of the TDAs are changed but we also observe that higher values of ξ are preferred, i.e. the sign of the derivative of the collection of maxima changes passing from a zero momentum transfer to a non-zero one.

Isospin relates the value of the vector and axial TDAs in the DGLAP regions,

$$V(x,\xi,t) = -\frac{1}{2}V(-x,\xi,t)\,, \qquad A(x,\xi,t) = \frac{1}{2}A(-x,\xi,t)\,, \qquad |\xi| < x < 1 \quad , \tag{4.53}$$

being the factor 1/2 the ratio between the charge of the u and d quarks. We observe in Figs. 4.10 and 4.11 that our TDAs satisfy these relations. It must be realized that the relation (4.53) cannot

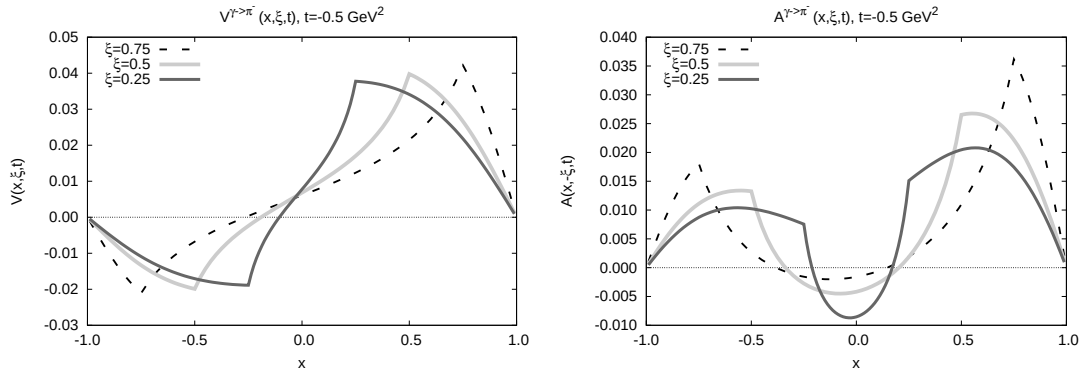

(a) (b)

Figure 4.12: The functions (a) $V^{\gamma\to\pi^-}(x,\xi,t)$ and (b) $A^{\gamma\to\pi^-}(x,\xi,t)$ for different values of the skewness variable ξ and for $t=-0.5$ GeV^2.

be changed by evolution.

Regarding the chiral limit, we observe that both the vector and axial TDAs do not significantly change going from a non-zero pion mass to the physical mass, except for the change in the lower bound of ξ.

In Fig. 4.12 are illustrated the vector and axial TDA for the transition $\gamma\to\pi^-$, whose expressions have been given in (4.52).

4.6 Polynomiality and Double Distributions

In the previous Section, the definition of the pion-photon transition has been given from the tensorial structure of the pion radiative decay. This structure for the hadronic matrix element leads to the identification of the vector and axial TDAs as well as the pion pole contribution.

Generalized Parton Distributions can also be studied through their moments [120]. In this Section, we build up the vector and axial-vector pion-photon transition distributions by considering matrix elements of towers of twist-two operators. This manifestly Lorentz-covariant approach leads us to define the Transition Distribution Amplitudes in terms of Double Distributions.

The Mellin moments in x lead to derivative operators between the light-like separated fields. Such derivative operators correspond to the local twist-2 operators defined in Eq. (1.23) that, sandwiched between two hadronic states, give generalized Form Factors.

The pion-photon matrix elements of vector twist-2 operators can be decomposed in a fully Lorentz covariant fashion in terms of various twist-2 Form Factors $C_{nk}(t)$ similarly to Eq. (1.24) adapted to the tensorial structure (4.2). Namely [199]

$$\begin{aligned}&\langle\gamma(p_\gamma)|\bar\psi(0)\,\tau^-\,\gamma^{\{\mu}\,i\overset{\leftrightarrow}{\mathcal{D}}^{\mu_1}\dots i\overset{\leftrightarrow}{\mathcal{D}}^{\mu_{n-1}\}}\,\psi(0)|\pi^+(p_\pi)\rangle\\&=-\frac{i\,e}{f_\pi}\,\varepsilon_\nu\,p_\rho\Delta_\sigma\epsilon^{\nu\rho\sigma\{\mu}\sum_{k=0}^{n-1}\frac{(n-1)!}{k!\,(k-n-1)!}\,C_{nk}(t)\,p^{\mu_1}\dots p^{\mu_{n-1-k}}\left(-\frac{\Delta}{2}\right)^{\mu_{n-k}}\dots\left(-\frac{\Delta}{2}\right)^{\mu_{n-1}\}}\quad,\end{aligned}\tag{4.54}$$

where the action of $\{\ldots\}$ on Lorentz indices produces the symmetric, traceless part of the tensor. The polynomiality property immediately follows.

The generalized moments can be written as a Double Distribution $\mathcal{W}(\beta,\alpha;t)$ which is the generating function of the twist-2 Form Factors,

$$C_{nk}(t) \;=\; \int_{-1}^{1} d\beta \int_{-(1-|\beta|)}^{1-|\beta|} d\alpha\, \beta^{n-1-k}\, \alpha^{k}\, \mathcal{W}(\beta,\alpha;t) \quad . \tag{4.55}$$

It is exactly this step from the tower of twist-2 Form Factors as generated by the double distribution that ensures the fulfillment of the polynomiality property when evaluating the distribution through this parameterization. [3] By definition [173, 174], the matrix element of bilocal vector operator is written in terms of DD in the following way

$$\begin{aligned}
&\langle \gamma\,(p_\gamma)|\,\bar{q}\left(-\frac{z}{2}\right) \not{z} \tau^{-} q\left(\frac{z}{2}\right)|\pi^{+}\,(p_\pi)\rangle \\
&= -i\,\frac{e}{\sqrt{2}\,f_\pi}\,\varepsilon_\nu\, p_\rho \Delta_\sigma \epsilon^{\nu\rho\sigma\,\mu} z_\mu \int_{-1}^{1} d\beta \int_{-(1-|\beta|)}^{1-|\beta|} d\alpha\, e^{-i\beta(p\cdot z)+i\alpha(\Delta\cdot z)/2}\, \mathcal{W}(\beta,\alpha;t) \quad .
\end{aligned} \tag{4.56}$$

From the definition of the vector TDA (4.13) and the skewness variable (4.4), we find the reduction formula

$$V^{\pi^+}(x,\xi,t) \;=\; \int_{-1}^{1} d\beta \int_{-(1-|\beta|)}^{1-|\beta|} d\alpha\, \delta(x-\beta-\xi\alpha)\, \mathcal{W}^{\pi^+}(\beta,\alpha;t) \quad . \tag{4.57}$$

The analysis of the axial matrix element is quite similar to the analysis of the vector one. Nonetheless, it is worth reminding that the structure dependent tensorial form is not the only contribution. There is, actually, also the pion inner Bremsstrahlung to be separated out from the TDA. As already mentioned in Section 4.1, we adopt the tensorial decomposition (4.3) given in Ref. [46, 147], required in order to ensure electromagnetic gauge invariance is pointed out.

Thus, an appropriate tensorial decomposition for the definition of the Double Distributions would be

$$\begin{aligned}
&\langle\gamma(p_\gamma)|\bar{\psi}(0)\,\tau^{-}\,\gamma^{\{\mu}\gamma_5\, i\overset{\leftrightarrow}{\mathcal{D}}^{\mu_1}\ldots i\overset{\leftrightarrow}{\mathcal{D}}^{\mu_{n-1}\}}\,\psi(0)|\pi^{+}(p_\pi)\rangle \\
&= e\;(\varepsilon\cdot\Delta)\;\sqrt{2}\,f_\pi\,\frac{\Delta^{\{\mu}}{t-m_\pi^2}\,\phi^{(n-1)}\;(-\Delta)^{\mu_1}\ldots(-\Delta)^{\mu_{n-1}\}} \\
&+\frac{e}{2}\,\left(\vec{\varepsilon}^{\perp}\cdot\vec{\Delta}^{\perp}\right)\left[\frac{2\,p^{\{\mu}}{\sqrt{2}\,f_\pi}\;\sum_{k=0}^{n-1}\frac{(n-1)!}{k!\,(k-n-1)!}\,C'_{nk}(t)\,p^{\mu_1}\ldots p^{\mu_{n-1-k}}\,\left(-\frac{\Delta}{2}\right)^{\mu_{n-k}}\ldots\left(-\frac{\Delta}{2}\right)^{\mu_{n-1}\}}\right. \\
&\qquad\left.+\;\frac{\Delta^{\{\mu}}{\sqrt{2}\,f_\pi}\;B_n(t)\left(-\frac{\Delta}{2}\right)^{\mu_1}\ldots\left(-\frac{\Delta}{2}\right)^{\mu_{n-1}\}}\right] \quad ,
\end{aligned} \tag{4.58}$$

where we have chosen to decompose the second term on the r.h.s. in such a way that it does explicitly not depend on the gauge choice. Also, since there is a large freedom in the way of

[3] In Appendix F, the polynomiality property is derived from the expression of the Double Distribution in the α-representation of the propagator.

writing down this decomposition, we have chosen to isolate the highest power of ξ, in the third line. However, the generalized Form Factor $B_n(t)$ could perfectly be included into $C'_{nk}(t)$. This is more *naturally* seen if we adopt the tensorial decomposition $\varepsilon_\nu\, p_\gamma^\mu\, p_\pi^\nu$.

Time-reversal invariance does not imply any symmetry on either term. The polynomiality property immediately follows.

The decomposition of the axial twist-2 matrix element (4.58) leads to a relation in agreement with the general relation Eq. (4.45). From the polynomiality property in the NJL calculation, we know that the pion pole term yields the highest power of ξ for odd moments in x (4.44). In particular, in the NJL model calculation, no B-like term is present.

The moments of the pion DA are expressed in terms of

$$\phi^{(n)} \;=\; \int_0^1 dx\, \left(x-\frac{1}{2}\right)^n \phi(x) \quad ,$$

with n even; what corresponds to the expression (4.44) to which we have extracted the t-dependence to keep trace of the pion pole.

The generalized moments can be written as Double Distributions following (3.23). These DD's are the generating functions of the twist-2 Form Factors. The term depending on both p and Δ is expressed as $\mathcal{W}'(\beta,\alpha;t)$,

$$C'_{nk}(t) \;=\; \int_{-1}^1 d\beta \int_{-(1-|\beta|)}^{1-|\beta|} d\alpha\, \beta^{n-1-k}\, \alpha^k\, \mathcal{W}'(\beta,\alpha;t) \quad . \tag{4.59}$$

On the other hand, we have extracted the pure Δ-dependent generalized moments whose expression is therefore

$$B_n(t) \;=\; \int_{-1}^1 d\alpha\, \alpha^{n-1}\, \mathcal{B}(\alpha,t) \quad . \tag{4.60}$$

After all these considerations, we can write down the light-like separated matrix element

$$\begin{aligned}
&\langle \gamma\,(p_\gamma)|\, \bar q\left(-\frac{z}{2}\right) \not{z}\, \gamma_5\, \tau^- q\left(\frac{z}{2}\right) |\pi^+\,(p_\pi)\rangle \\
&= e\;(\varepsilon\cdot\Delta)\;\sqrt{2}\, f_\pi\, \frac{\Delta\cdot z}{t-m_\pi^2}\; \int_{-1}^1 d\alpha\, e^{i\alpha\,(\Delta\cdot z)/2}\, \phi\left(\frac{\alpha+1}{2}\right) \\
&+\frac{e}{2}\left(\vec{\varepsilon}^{\,\perp}\cdot\vec{\Delta}^{\,\perp}\right)\left[\frac{1}{\sqrt{2}\, f_\pi}\; 2\, p\cdot z\; \int_{-1}^1 d\beta \int_{-(1-|\beta|)}^{1-|\beta|} d\alpha\, e^{-i\beta(p\cdot z)+i\alpha(\Delta\cdot z)/2}\, \mathcal{W}'(\beta,\alpha;t)\right. \\
&\qquad\left. +\frac{1}{\sqrt{2}\, f_\pi}\, \Delta\cdot z\; \int_{-1}^1 d\alpha\, e^{i\alpha\,(\Delta\cdot z)/2}\, \mathcal{B}(\alpha,t)\right] \quad ,
\end{aligned} \tag{4.61}$$

where the pion resonance structure has been subtracted.

From the definition of the axial TDA (4.14), we find the reduction formula

$$A^{\pi^+}(x,\xi,t) \;=\; \int_{-1}^1 d\beta \int_{-(1-|\beta|)}^{1-|\beta|} d\alpha\, \delta(x-\beta-\xi\alpha)\, \mathcal{W}'^{\pi^+}(\beta,\alpha,t) + \mathrm{sgn}(\xi)\, B\left(\frac{x}{\xi},t\right) \quad . \tag{4.62}$$

The Fourier transform of the first term on the r.h.s. of Eq. (4.61) manifestly reduces to the pion pole term parameterization of Eq. (4.14) as expected.

A D-term was introduced in the matrix elements defining the GPDs. This new term is necessary in order to modify the tensorial structure to reproduce the correct behavior with the two independent variables $p \cdot z, \Delta \cdot z$. We therefore interpret the D-term in the context of TDAs as the minimal contribution that we are compelled to introduce in order to restore gauge invariance in the tensorial structure adapted from the axial vector hadronic current involved in the pion radiative decay (4.3). In other words, the equivalent of the D-term is the pion pole contribution in the language of Double Distribution parameterization.

4.7 Pion-Photon TDAs in Other Approaches

Other studies of pion-photon TDAs have already been undertaken [199, 44, 127]. We also mention the phenomenological approach, coming from the GPD analysis, used in Ref. [131]. All these calculations have been performed using the Double Distributions described in Section 3.2.1.

In this Section, we aim to compare the (x, ξ, t) dependencies as obtained by different methods and models in order to give a critical point of view of our results.

4.7.1 The α-Representation of the DD for the TDAs

In this Section, we consider the α-representation of the propagators in the kinematics of the pion-photon transition described in Section 4.2. This technique leads to the identification of the Double Distributions defined here above. Nevertheless and as it is been highlighted before, the model imposes the integral decomposition as well as the relevant diagrams to be considered. The forthcoming considerations aim to be general and applicable to the model calculations whose results will be given in a further Section.

In the vector current case, the trace over the Dirac indices yields to the exact tensorial structure (4.13). As a consequence, the 3-point function corresponds exactly to the vector TDA for the u-quark up to an overall factor g coming from the trace over isospin, flavor, color and Dirac spaces. [4] In terms of Double Distribution, it reads

$$\begin{aligned} v(x,\xi,t) &= g\,\tilde{I}_3(x,\xi,t) \quad , \\ &= \frac{1}{(4\,\pi)^2}\int_0^1 d\beta \int_{-1+|\beta|}^{1-|\beta|} d\alpha\,\delta\left(x-\beta-\alpha\xi\right)\,\mathcal{I}_3(\beta,\alpha,t) \quad , \end{aligned} \tag{4.63}$$

with the Double Distribution in the same kinematics being

$$\mathcal{I}_3(\beta,\alpha,t) = g\,\frac{\theta\left(1-\alpha-\beta\right)}{m^2 - m_\pi^2\,\frac{1}{2}\,\beta(1-\beta-\alpha) - \frac{t}{4}\,(1+\alpha-\beta)(1-\alpha-\beta)} \quad . \tag{4.64}$$

A detailed derivation of this result is given in Appendix F. The total DD for the vector TDA $\mathcal{W}(\beta,\alpha,t)$ is obtained applying the previous result to the isospin decomposition (4.23). The support property follows from the β-integration (F.11, F.12).

[4] In the very particular case of the NJL model calculation, the factor is $g = 8N_c\,f_\pi\,g_{\pi qq}$, e.g. Eq. (4.24).

From the DD (4.64), one can easily see that the limit $m_\pi^2 \to 0$ implies that

$$\mathcal{I}_3(\beta,\alpha,t) \;=\; \mathcal{I}_3(\beta,-\alpha,t) \quad .$$

This so-called α-symmetry reflects the appearance of only even powers of ξ in the polynomiality expansion of the vector TDA; a result that has been obtained in the calculation of *skewed* PDs in the NJL model (4.40).

The trace over the Dirac space for the axial current involves 2- and 3-propagator integrals. Besides the terms proportional to the external momenta, the trace evaluation of the diagram of the type (a) of Fig. 4.8 yields a factor $-2\varepsilon\cdot k\, p_\pi^\mu$. This renders the calculation slightly more complicated but the k^ν-dependent integral can be reduced to the same 3-propagator integral as for the vector one.

The evaluation of the Double Distributions is similar to the one undertaken for the 3-propagator integral of the vector TDA. The subsequent steps are as described in Appendix F, and the result for the k^ν-dependent integral is

$$\varepsilon\cdot\tilde{I}_3(x,\xi,t) \;=\; \frac{\varepsilon\cdot\Delta}{(4\,\pi)^2}\int_0^1 d\beta \int_{-1+|\beta|}^{1-|\beta|} d\alpha\,\delta\left(x-\beta-\alpha\xi\right)\,(1+\alpha-\beta)\,\mathcal{I}_3(\beta,\alpha,t) \quad , \quad (4.65)$$

with the same double distribution $\mathcal{I}_3(\beta,\alpha,t)$ defined by Eq. (4.64).

4.7.2 Phenomenological Parameterizations of TDAs

Phenomenological parameterizations of the (x,ξ,t) dependence of the parton distributions constitute a good alternative and/or complementary approach of the diagrammatic analysis of the Double Distributions. In what follows, we report a fully phenomenological t-independent parameterization and a semi-kinematical approach improved by phenomenological considerations.

It is easier to start describing the (x,ξ) dependency by setting $t=0$. Hence, we will, in a first time, consider the t-independent Double Distributions, entering the reduction formulae (4.57, 4.62).

In the DVCS framework, the suggestion has been made by Radyushkin [175, 176] to parameterize the GPDs in such a way that the forward limit, i.e.

$$\int_{-1+|\beta|}^{1-|\beta|} d\alpha\,\mathcal{F}^q(\beta,\alpha) \;=\; q(\beta) \quad ,$$

is ensured. The function $q(\beta)$ is hence related to the parton distribution for the flavor q. Basically, the phenomenological forward quark distribution as measured from DIS can be used as an input in the parameterization.

The TDA do not obey any forward limit, but it has nevertheless been proposed to apply the DIS phenomenology as a first approach [131]. Hence, for the TDAs, we will use the same form as for the GPDs, i.e.

$$\mathcal{F}^q(\beta,\alpha) \;=\; h(\beta,\alpha)\,q(\beta) \quad , \quad (4.66)$$

for $\mathcal{F}^q$ corresponding either to the vector or axial DD, namely $\mathcal{W}$ or $\mathcal{W}'$ respectively. The function $h(\beta,\alpha)$ denotes a profile function, that can be parameterized through a one-parameter ansatz, following Refs. [175, 176, 177],

$$h(\beta,\alpha) \;=\; \frac{\Gamma(2b+2)}{2^{2b+1}\Gamma^2(b+1)}\,\frac{\left[(1-|\beta|)^2-\alpha^2\right]^b}{(1-|\beta|)^{2b+1}} \quad . \tag{4.67}$$

The profile function is normalized to 1.

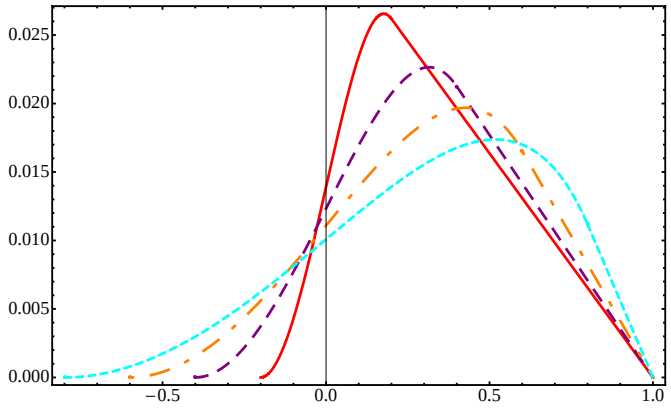

Figure 4.13: The TDA v^π as described in Ref. [131] through the ansatz for the profile function (4.67); for values of the ξ variable $0.2, 0.4, 0.6$ & 0.8, respectively, the plain red, the dashed purple, the dashed-dotted orange and the short-dashed cyan curves.

The parameter b in (4.67) characterizes the strength of the ξ-dependence of the resulting GPD. The limiting case $b \to \infty$ corresponds to the ξ-independent ansatz for the GPD, namely $H(x,\xi) = q(x)$. The power in b is a free parameter for both the valence and sea distributions. They can be used as fit parameters in the extraction of GPDs from the experiments. For instance, the twist-2 DVCS predictions of Ref. [201] corresponds to the choice

$$b = b_{val} = b_{sea} = 1 \quad .$$

This mild dependence on ξ is followed by the authors of Ref. [131] for the parameterization of the pion-photon TDA.

Also, Lansberg *et al.* [131] assume, as a first guess, that the β-dependence of q for the $\gamma \to \pi^-$ transition[5] is given by a simple linear law [6]

$$q(\beta) \;=\; 2(1-\beta)\,\theta(\beta) \quad .$$

The t-dependence comes solely from the Form Factors through the sum rules. Therefore, the resulting distribution $d(x,\xi)$, with $d = v, a$, must be normalized to 1 when integrated over x. This leads to a TDA whose dependence on the three kinematical variables is given by

$$D(x,\xi,t) \;=\; \Big(Q_d\, d^u(x,\xi) + Q_u\, d^d(x,\xi)\Big)\,\frac{\sqrt{2}f_\pi}{m_\pi} F_D\,(t) \quad , \tag{4.68}$$

D denoting either the vector or axial quantities.

In the same Reference the t-dependence coming from the Form Factors is considered negligible as we are concerned with small t region. In this way, we can use the values given at zero momentum transfer, see Section 4.3.4.

[5] See in Section 4.4 how to go link this transition to the $\pi^+ \to \gamma$.

[6] The parameterization is here given for the quark distribution, the antiquark would be $\bar{q}(\beta) = -q(-\beta)$.

As explained in Section 3.2.1, the reduction from the DD to *skewed* distributions requires a particular dependence on the skewness variable, imposed in the δ-function of the reduction formula. This choice leads to the identification of two kinematically different regions. The result obtained through the above-given ansatz is shown, for the u-quark and for a vector current, on Fig. 4.13. The shape of the vector u-quark TDA reasonably follows what we obtained in the NJL model, Fig. 4.10. The same ansatz is used for the axial TDA with the simple replacement $D = A$ in (4.68). Therefore the difference between the vector and axial TDA resulting from this ansatz resides in the ratio F_A^π/F_V^π and the charge combination. The total γ-π^- distribution does, in turn, change according to the charge combinations involved in the transition, see Section 4.4. Also, this parameterization from the phenomenology of GPDs does not include the term compensating for the gauge invariance in (4.61). However, this contribution is closely related to the pion pole whose importance in fulfilling the sum rule for the axial current has been highly emphasized in the previous Sections. We conclude that the axial TDA proposed by [131] considerably and conceptually differs from the one obtained in the NJL model.

Another (semi-)phenomenological approach including, this time, the phenomenology of photon distributions has been proposed in Ref. [199]. The t-dependent double distributions defined in Eqs. (4.56, 4.61) are calculated in a simple quark model. In doing so, Tiburzi determines the t-dependence of the distributions and reproduces the Form Factors. His intermediate results, in agreement with the results of Ref. [44], are $F_A(0)/F_V(0) = 0.98$ and $F_A(0) \sim 0.026$. However the partonic content of the model has been modified to give reasonable phenomenology while evolved. But positivity bounds for the pion-photon Transition Distribution Amplitudes are investigated instead. The positivity constraints are an application of the Schwartz inequality in the Hilbert space [80, 164, 166, 167, 168, 176]. Basically, in the $[-1, -\xi]$ and $[\xi, 1]$ regions, we can find a bound of the type, for the pion GPD,

$$\theta(1-x)\theta(x-\xi)\left|H_q^{\pi^+}(x,\xi,t)\right| \leq \sqrt{q^{\pi^+}\left(x_{\text{in}}\right)\, q^{\pi^+}\left(x_{\text{out}}\right)} \quad , \tag{4.69}$$

where the momentum fractions of the quark before and after the scattering are

$$x_{\text{in}} = \frac{x+\xi}{1+\xi} \quad , \qquad x_{\text{out}} = \frac{x-\xi}{1-\xi} \quad .$$

The author of Ref. [199] provides for some estimates of the TDAs on the basis of positivity bounds. The latters, determined using the technique described in Ref. [164], involve the u-quark and d-antiquark distributions, the first one related to the pion and the second to the photon.

The Double Distributions obtained in the simple quark model are modified in order to saturate those constraints. The modifications of the model are motivated by the apparition of pion and photon parton distributions in the new realistic double distributions. Since the evolved PDFs are well-known, this allows one to establish the renormalization scale of the model avoiding evolution. For the pion, a simple analytic parameterization of the valence and sea quark has been chosen following Ref. [99]. The real photon distribution is parameterized in a vector-meson dominance fashion [100]. From the perspective of model building, this comes out to be an attempt to satisfy the known constraints and generate an input distribution at a moderately low scale.

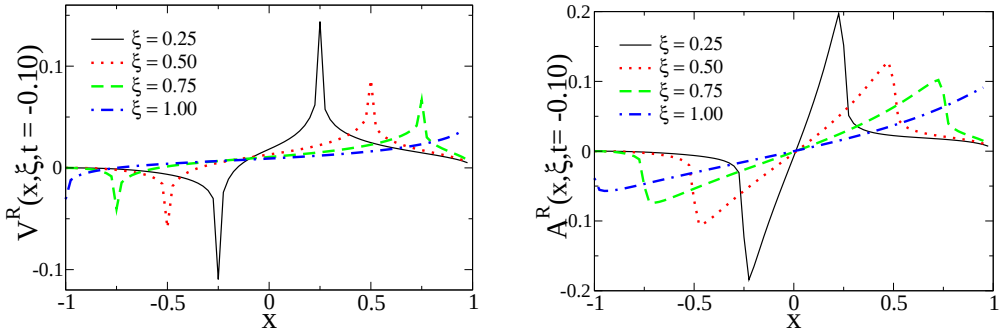

Figure 4.14: The vector and axial TDAs in the approach of Ref. [199].

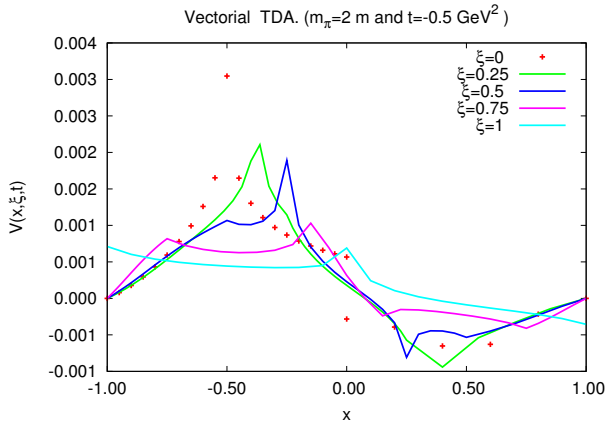

Figure 4.15: The vector TDA for $m_\pi = 2m$ and for $t = -0.5$ GeV^2.

Thus the values of the vector and axial Form Factor, as given by [11], are used in order to determine the empirical constants of the parametrization. In the same way, the constituent quark mass parameter m is obtained (fitted) requiring that the model pion-photon transition Form Factor comes close to the experimentally parameterized form. The value $m = 0.2$ GeV is obtained. The resulting TDAs, illustrated on Fig. 4.14, do not satisfy the isospin relation (4.53) due to the different choice of the u-quark and d-antiquark distributions used in the saturation of the positivity bounds. We have studied the positivity bounds (4.69) for GPDs in the NJL model and noticed that it is actually an upper bound that is sometimes very higher than the value of the GPD itself.

Moreover the TDAs shown by Tiburzi are rather peaked at $x = \xi$, what is not reproduced in the NJL model calculation. Rather, at weak binding when $m_\pi = 2m$, the latter presents peaks at $x = \frac{1}{2}(1-\xi)$ and $x = \frac{1}{2}(1+\xi)$ for the vector TDA Fig. 4.15. This is what one expects from a free quark picture. This has already been observed for the GPDs in the NJL model [153] and in a previous work of the same Tiburzi [194]. Given the previous argument, the position of the peaks obtained by Tiburzi is not understandable in the NJL model.

4.7.3 Model Calculations of the TDAs

Other model calculations of the pion-photon TDAs have already been done, respectively, in the Spectral Quark Model (SQM) [44] and a non-local Chiral Quark Model (χQM) [127]. The Double Distributions defined through the α-representation of Section 4.6 have been used in both calculations. We here after comment and compare their results.

The vector and axial TDAs calculated in the SQM, NJL model and non-local χQM are compared in Fig. 4.17.

The authors of the first reference use the asymmetric notation (F.8, F.7). The comparison is here awkward since the authors define, by turns,

$$\zeta = (p_\gamma - p_\pi)^+ / p_\pi^+ \quad ; \quad -\zeta = (p_\gamma - p_\pi)\cdot n$$

We nevertheless decide to use the standard relation between their asymmetric notations and the symmetric ones (F.8) [81]. Their functions $V_{\rm SQM}$ and $A_{\rm SQM}$ correspond, respectively, to the v and a given in Eqs. (4.23, 4.33). They are obtained through the reduction formulae, e.g. (4.57) for the vector TDA. As for the axial TDA, the decomposition (4.61) is not exactly adopted: Broniowski *et al. structurally* isolate the pion pole by neglecting the whole $\Delta\cdot z$ structure instead. In so doing they select from the trace only the piece proportional to $(\vec{\varepsilon}^{\perp}\cdot\vec{\Delta}^{\perp})\,p^\mu$ of the tensorial decomposition

$$\int \frac{dz^-}{2\pi} e^{ixp^+z^-} \,\langle\gamma\,(p_\gamma)|\,\bar q\left(-\frac{z}{2}\right)\not{n}\gamma_5\tau^- q\left(\frac{z}{2}\right)|\pi\,(p_\pi)\rangle\Big|_{z^+=z^\perp=0}$$
$$= \frac{1}{p^+} e\,\left(\vec{\varepsilon}^{\perp}\cdot\vec{\Delta}^{\perp}\right)\,\frac{A^{\pi^+}\,(x,\xi,t)}{\sqrt{2}f_\pi} + \dots \quad ,$$

where, here, A is seen as $\bar A$ (4.19) to which the pion resonance has been *structurally* subtracted. Therefore the piece proportional to $(\varepsilon\cdot\Delta)\Delta^\mu$ leads to both D-term like structures, one being the resonant pion pole (4.14), and is represented by the ellipses.

The normalization condition is different from the one used in the NJL model calculation and the results quoted by these authors must be multiplied, for the vector TDA, by a factor

$$48\pi^2\,\frac{\sqrt{2}f_\pi}{m_\pi}\,F_V(0) \sim 10$$

before comparison. From Fig. 4.17 we conclude that there is a qualitative and quantitative agreement, for the vector TDA, between the results of Ref. [44] and those obtained in the NJL model.

Regarding the axial TDA we observe, in addition to the normalization factor

$$48\pi^2\,\frac{\sqrt{2}f_\pi}{m_\pi}\,F_A(0) \quad \sim \quad 10 \quad ,$$

a change in the global sign due to different definitions. In the first version of [44] the axial TDA for positive values of ξ is given[7]. It coincides with the results in the NJL model, as observed in Fig. 4.17. Surprisingly, the result presented in Ref. [44] coincides with our result for negative ξ. It is perhaps due to the change in the definition of ξ mentioned above. Rather, one might call into question the selection procedure of the structure dependent quantities.

In Ref. [127] the TDAs are calculated in three different models. The first one is a local model whose pole structure has some similarity with the one of the NJL model. The two other models, i.e. semi-local and fully non-local, follow the results of the local one. The same structure decomposition as in the SQM is followed. The most prominent difference between the results obtained in the non-local and the NJL models is the appearence of important odd powers in ξ in the polynomial expansion of the vector TDA. We know from Ref. [155] that, for non-local models, there are

[7] There is a typographic error in Eq. (23) of the first version of this reference, where a factor $M_V^2/6$ must be dropped.

additional contributions to those calculated in Ref. [127]. In the case of PDFs, disregarding these contributions can produce small isospin violations [156]. It can therefore be considered that, on that point, the results of Ref. [127] must be confirmed.

For numerical comparison, the results obtained in [127] must be corrected by a factor

$$2\pi^2 \frac{\sqrt{2} f_\pi}{m_\pi} F_V(0) \quad \sim \quad 0.45 \quad ,$$

due to the use of a different normalization condition. We observe, see Fig. 4.17, that our results in the NJL model coincide with the results of the latter reference. [8]

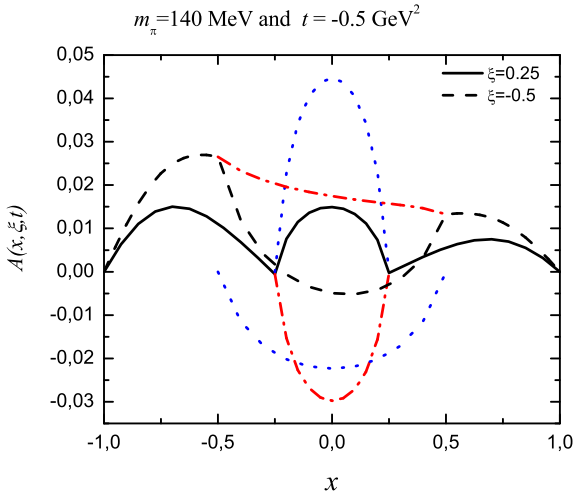

Figure 4.16: Contributions to the axial $\pi^+ \to \gamma$ TDA for both positive ($\xi = 0.25$, plain line) and negative ($\xi = -0.5$, dashed line) values of the skewness variable and for $m_\pi = 140$ MeV and $t = -0.5$ GeV^2. In each case, and in the ERBL region, the contribution coming from the first diagram of Fig. 4.8 is represented by the dashed-dotted lines and the non-resonant part of the second diagram of Fig. 4.8 is represented by the dotted lines.

Regarding our axial TDA, it is worth noticing that it differs from the previous calculations [199, 44, 127] due to the effect of the non-resonant part of the second diagram of Fig. 4.8. This contribution, corresponding to the last term of Eq. (4.35), is proportional to $\left(t - m_\pi^2\right)^{-1}$ but with zero value for the residue. The presence of this term is crucial in order to obtain the axial Form Factor using the sum rule as shown by the reduction formula (4.62). Furthermore this term is dominant in the ERBL region as we can infer from Fig. 4.16.

It can eventually be concluded that there is no disagreement between the different studies concerning the π-γ TDAs besides the ambiguity in the definition of the skewness variable. Calculations of Refs. [44, 127] are performed in the chiral limit, where ξ runs from -1 to 1. The symmetric nature of this interval makes difficult to check the sign of ξ. On the other hand, the NJL calculation is given for the physical pion mass. In this case, the kinematics of the process imposes $t/(2m_\pi^2 - t) < \xi < 1$. From Eqs. (4.34, 4.35) we observe that there is a pole in the axial TDA for the limit value $\xi = t/(2m_\pi^2 - t)$, preventing us from going through unphysical values of ξ.

Moreover, the sum rules (4.15, 4.16) for both the vector and axial TDAs are here satisfied for physical values of ξ, and broken in the unphysical regions $\xi < t/(2m_\pi^2 - t)$ and $\xi > 1$. We therefore conclude that the choice of sign in our calculation in the NJL model is consistent and gives a guideline for comparing with other models.

[8] For the axial TDA, there is a change in the definition of the skewness variable between the caption of Figs. 3, 5 and Fig. 9 of Ref. [127]. The agreement is valid if the convention of the caption of their Fig. 9 is chosen.

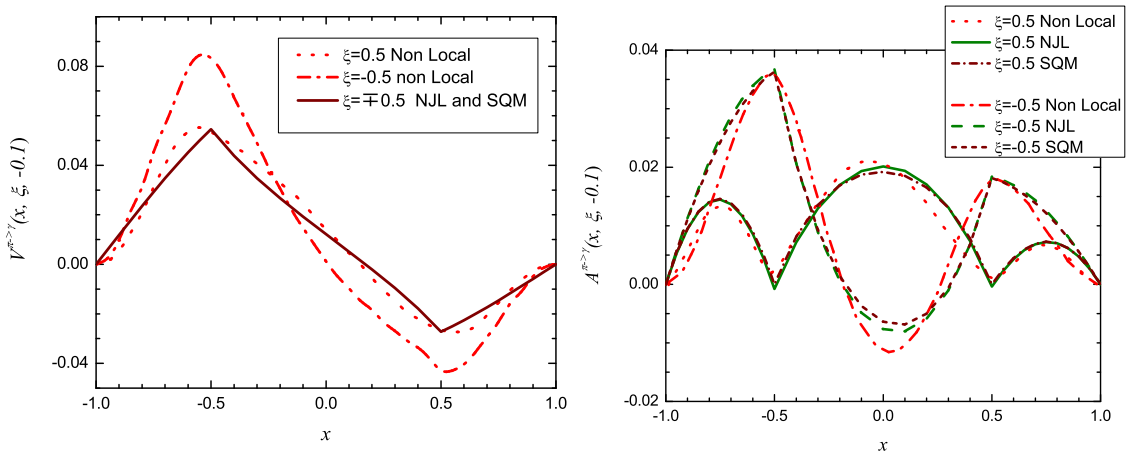

Figure 4.17: Comparison of the $\pi^+ \to \gamma$ TDAs for $t = -0.1$ GeV^2 of Refs. [44, 127] for $m_\pi = 0$ MeV and Ref. [67] for $m_\pi = 140$ MeV. On the left, we have: the vector TDA for $\xi = \pm 0.5$ as a single (solid) curve for the results of both the NJL model and SQM (these four curves are indistinguishable); the result of the non-local χQM calculation for $\xi = 0.5$ (dotted line) and for $\xi = -0.5$ (dashed-dotted line). On the right, we have the results of the axial TDA with the choice for the sign of ξ as discussed in the text.

4.8 Discussion about the Results

In this Chapter we have defined the pion-photon vector and axial Transition Distribution Amplitudes using the Bethe-Salpeter amplitude for the pion. In order to make numerical predictions we have used the Nambu-Jona Lasinio model. The Pauli-Villars regularization procedure is applied in order to preserve gauge invariance.

We know from PCAC that the axial current couples to the pion. Therefore, in order to properly define the axial TDA, i.e. with all the structure of the incoming hadron being included in $A\,(x, \xi, t)$, we need to extract the pion pole contribution. In so doing, we found that the axial TDA had two different contributions, the first one related to a direct coupling of the axial current to a quark of the incoming pion and to a quark coupled to the outcoming photon and a second related to the non-resonant part of a quark-antiquark pair coupled with the quantum numbers of the pion.

The use of a fully covariant and gauge invariant approach guaranties that we will recover all fundamental properties of the TDAs. In this way, we have the right support, $x \in [-1, 1]$, and the sum rules and the polynomiality expansions are recovered. We want to stress that these three properties are not inputs, but results in our calculation. The value we found for the vector Form Factor in the NJL model is in agreement with the experimental result [11] whereas the value found for the axial Form Factor is two times larger than in [11]. This discrepancy is a common feature of quark models [44]. Also the neutral pion vector Form Factor $F_{\pi\gamma^*\gamma}(t)$ is well described. These results allow us to assume that the NJL model gives a reasonable description of the physics of those processes at this energy regime.

Turning our attention to the polynomial expansion of the TDAs, we have seen that, in the chiral limit, only the coefficients of even powers in ξ were non-null for the vector TDA. This result is quoted as the recovery of the so-called α-symmetry of the Double Distributions. No constraint is obtained for the axial TDA. Nevertheless, the NJL model provides simple expressions for the

coefficients of the polynomial expansions in the chiral limit, Eqs. (4.41) and (4.43).

We have obtained quite different shapes for the vector and axial TDAs. This is in part, at least for the DGLAP regions, imposed by the isopin relation (4.53). We have pointed out the importance of the non-resonant part of the qq interacting pair diagram for the axial TDA in the ERBL region.

It is interesting to inquire about the domain of validity of the isospin relations (4.53). These relations are obtained from the isospin trace calculation involved in the diagram (a) of Fig. 4.8. Due to the simplicity of the isospin wave function of the pion these results are more general than the NJL model and could be considered as a result of the diagrams under consideration. These diagrams are the simplest contribution of handbag type.

Also, in the last Section, we have presented the different approaches proposed to gather information about the pion-photon transition distribution amplitudes. The model calculations are in good agreement one to others. On the other hand, the phenomenological approaches are either based on GPD's phenomenology or pion and photon PDF's. It is unfortunately the best we can do for now.

The Transition Distribution Amplitudes proposed by the authors of [165] open the possibility of enlarging the present knowledge of hadron structure for they generalize the concept of GPDs for non-diagonal transitions. Calculated here, as a first step, for pion-photon transitions, these new observables lead to interesting estimates of cross section for exclusive meson pair production in $\gamma^*\gamma$ scattering [131] as we will see in the next Chapter.

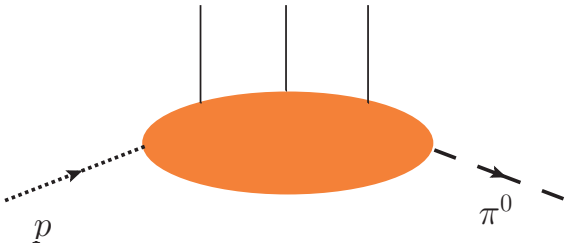

Figure 4.18: Baryonic $p \to \pi^0$ TDA.

Transition Distribution Amplitudes have also been extended to baryonic transitions [133, 134, 135, 165]. For instance, the nucleon-to-pion TDAs describe exactly how a baryon can turn into a meson, namely the transition from a baryonic to a mesonic state. The leading twist TDAs for the $p \to \pi^0$ transition, depicted in Fig. 4.18, are defined from the correlator

$$\langle \pi^0(p_\pi)|\epsilon^{ijk}\, u_i^\alpha(z_1 n)\, u_j^\beta(z_2 n)\, u_k^\gamma(z_3 n)|p(p_1,s_1)\rangle \quad ,$$

the latter matrix element being also related to the baryonic DAs.

There are 8 leading-twist TDAs for the $p \to \pi^0$ transition, namely, two vector $V_i^{p\pi^0}(x_i,\xi,\Delta^2)$, two axial $A_i^{p\pi^0}(x_i,\xi,\Delta^2)$ and four tensor $T_i^{p\pi^0}(x_i,\xi,\Delta^2)$ ones.

The peculiarity of the baryonic TDAs is that, for both the meson and photon cases, 3 quarks are exchanged in the t-channel, satisfying the relation $x_1 + x_2 + x_3 = 2\xi$ $(\xi \geq 0)$. The interplay of the variables implies 3 kinematical regions; one DGLAP region, $x_i \geq 0$, and two ERBL regions, $x_1 \geq 0; x_2 \geq 0; x_3 \leq 0$ and $x_1 \geq 0; x_2 \leq 0; x_3 \leq 0$.

A calculation in the Meson-Cloud model of Ref. [158] has been performed in the ERBL region [159, 162, 163], where the pion cloud contribution -as coming from a higher order in the Fock

state expansion- plays an important role and could therefore be tested. It is so far the only non-perturbative approach to these new distributions.
The experimental importance of baryonic TDAs will be shortly overviewed in the next Chapter.

5 Exclusive meson production in $\gamma^*\gamma$ scattering

This Chapter is devoted to the applications of the results for the photon-pion Transition Distribution Amplitudes displayed in the previous Chapter. In particular, we discuss the results of Ref. [70].

Cross section estimates for the processes

$$\gamma_L^*\gamma \to \pi^+\pi^- \quad , \quad \gamma_L^*\gamma \to \rho^+\pi^- \quad , \tag{5.1}$$

factorized according to Fig. 4.1, have been proposed in Ref. [131] using for the TDA the t-independent double distributions (4.66), in a first approach, and, in a second, the t-dependent Double Distribution (4.64) obtained through diagrammatic analysis.

To implement these analyses, in this Chapter, we display the cross section for the processes (5.1) with the large-distance part calculated in models. In a previous Section we have concluded that there is a clear agreement between the different model calculations of the pion-photon TDAs, we are allowed to analyze the result of a single model, e.g. the NJL model. Furthermore, this choice allows us to keep trace of the pion pole contribution in order to include it in our analysis.

5.1 Processes and Kinematics

The $\gamma^*\gamma \to M^+\pi^-$ process, with $M^+ = \rho_L^+$ or π^+, is a subprocess of the

$$e\,(p_e) + \gamma\,(p_\gamma) \to e\,\left(p_e'\right) + M^+\,(p_M) + \pi^-\,(p_\pi) \quad , \tag{5.2}$$

process. We follow all the definitions of the kinematics given in Ref. [131], [1] with the exception that our n^μ vector is defined following (A.9), which is twice the n^μ vector used in Ref. [131]. In particular, for massless pions,[2] we have,

[1] In Section III.A and Fig. 3.

[2] The pion mass is set to $m_\pi = 0$ MeV throughout the Chapter.

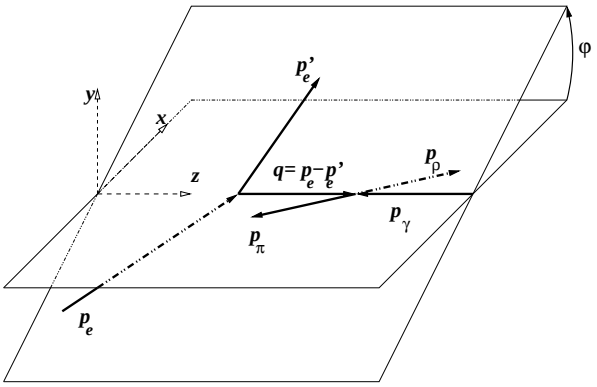

Figure 5.1: Kinematics for the processes (5.1) [131].

$$
\begin{aligned}
Q^2 &= -q^2 = -\left(p_e - p_e'\right)^2 \quad , \\
W^2 &= \left(q + p_\gamma\right)^2 \quad , \\
s_{e\gamma} &= \left(p_e + p_\gamma\right)^2 \quad , \qquad (5.3)
\end{aligned}
$$

with p_e and p_e', respectively, the momentum of the incoming and outgoing electron;

$$
\begin{aligned}
p_\gamma &= (1+\xi)\bar{p} \quad , \\
p_\pi &= (1-\xi)\bar{p} + \frac{\vec{\Delta}^{\perp 2}}{2\,(1-\xi)} n + \vec{\Delta}^{\perp}, \\
q &= -\frac{Q^2}{Q^2+W^2}\,(1+\xi)\,\bar{p} + \frac{Q^2+W^2}{1+\xi} n \quad , \qquad (5.4)
\end{aligned}
$$

where $\Delta_T = (0, \vec{\Delta}^{\perp}, 0)$, and therefore $\Delta_T^2 = -\vec{\Delta}^{\perp 2}$. Notice that

$$\vec{\Delta}^{\perp 2} = (-t)(1-\xi)/(1+\xi) \quad ,$$

with $t < 0$.

It is worth noticing that, even if the skewness variable is not constrained to be positive but rather to belong to $\xi \in [-1, 1]$, the external kinematics of the process (5.1) restrict ξ. Effectively, the kinematics (5.4) have been given with the photon momentum expressed in terms of the momentum transfer squared Q^2 and the center of mass energy squared of the $\gamma^*\gamma$ system W^2, through which we can determine the skewness variable, i.e.

$$
\begin{aligned}
y &= \frac{q \cdot p_\gamma}{p_\gamma \cdot p_e} = \frac{1+\xi}{2\xi}\frac{Q^2}{s_{e\gamma}} = \frac{Q^2+W^2}{s_{e\gamma}} \\
\Rightarrow \xi &= \frac{Q^2}{Q^2+2W^2} \quad .
\end{aligned}
$$

The momentum transfer therefore reads

$$q \;=\; -2\xi\bar{p} + \frac{Q^2}{4\xi} n \quad , \qquad (5.5)$$

The terms contributing to the cross section are selected by multiplying the amplitudes by the longitudinal polarization of the incoming photon $\varepsilon_{L\mu}$. An expression for $\varepsilon_{L\mu}$ is found knowing that $\varepsilon_L^2 = 1$ and that $\varepsilon_L . q = 0$. For q as given by (5.5), we find

$$\varepsilon_L = \left(\frac{2\xi}{Q}\bar{p} + \frac{Q}{2\xi} n\right) \quad , \qquad (5.6)$$

following Ref. [131] for the convention for the overall sign. The real photon polarization is defined by the condition $\varepsilon^- = 0$ together with the gauge condition $\varepsilon^+ = 0$. The kinematics are illustrated on Fig. 5.1.

5.2 Cross Sections

The differential cross section for the kinematical variables Q^2, t, ξ and the angle φ between the hadronic, where takes place the subprocess $\gamma_L^* \gamma \to M^+ \pi^-$ with M being either ρ_L or π, and leptonic planes reads

$$\frac{d\sigma^{e\gamma \to eM^+\pi^-}}{dQ^2 dt d\xi d\varphi} = \frac{1}{32\,(2\pi)^4\, s_{e\gamma}^2}\,\frac{1}{\xi(1+\xi)}\,|\mathcal{M}^{e\gamma\to eM^+\pi^-}|^2 \quad . \tag{5.7}$$

The square amplitude for the process $e\gamma \to eM^+\pi^-$ is obtained through the square amplitude for the subprocess $\gamma_L^*\gamma \to M^+\pi^-$ and the contribution of the fermionic line from which the highly virtual photon is emitted

$$|\mathcal{M}^{e\gamma\to eM^+\pi^-}|^2 = \frac{4\pi\,\alpha_{elm}}{2Q^4}\,\mathbb{T}\mathrm{r}\left(\not{p}'_e \not{\epsilon}_L\,(q)\,\not{p}_e \not{\epsilon}_L^*\,(q)\right)|\mathcal{M}^{M^+\pi^-}|^2 \quad . \tag{5.8}$$

Using Eq. (5.6), we find that the trace yields

$$16\xi\, s_{e\gamma}/(Q^2\,(1+\xi)^2)\{2\xi\, s_{e\gamma} - (1+\xi)Q^2\} \quad .$$

And the amplitude for the subprocess is the factorized amplitude of Fig. 4.1. It reads

$$\mathcal{M}^{\rho_L^+\pi^-}(Q^2,\xi,t) = -\int_{-1}^{1} dx \int_0^1 dz\,\frac{f_\rho}{\sqrt{2}\,f_\pi}\,\phi_\rho(z)\,M_h^V(z,x,\xi)\,V(x,\xi,t) \quad , \tag{5.9}$$

$$\begin{aligned}\mathcal{M}^{\pi^+\pi^-}(Q^2,\xi,t) &= \int_{-1}^{1} dx \int_0^1 dz\,\phi_\pi(z)\,M_h^A(z,x,\xi) \\ &\left[A^{\gamma\to\pi^-}(x,\xi,t) - \frac{4f_\pi^2}{m_\pi^2 - t}\,\epsilon(\xi)\,\phi^\pi\left(\frac{x+\xi}{2\xi}\right)\right]\end{aligned} \tag{5.10}$$

where z is the light-cone momentum fraction carried by the quark entering the M^+ and $f_\rho = 0.216$ GeV. The hard parts are defined as in [131]

$$\begin{aligned}M_h^V(z,x,\xi) &= 8\pi^2\alpha_{elm}\alpha_s\,\frac{C_F}{N_c\,Q}\,\epsilon^{+\nu\rho\sigma}\,P_\rho\,(p_\pi - p_\gamma)_\sigma\,\frac{1}{z(1-z)}\left(\frac{Q_u}{x-\xi+i\epsilon} + \frac{Q_d}{x+\xi-i\epsilon}\right) \quad , \\ M_h^A(z,x,\xi) &= 4\pi^2\alpha_{elm}\alpha_s\,\frac{C_F}{N_c}\,\frac{(\vec{\varepsilon}^{\perp}.\vec{\Delta}^{\perp})}{Q}\,\frac{1}{z(1-z)}\left(\frac{Q_u}{x-\xi+i\epsilon} + \frac{Q_d}{x+\xi-i\epsilon}\right) \quad .\end{aligned} \tag{5.11}$$

The pion DA is chosen to be the usual asymptotic normalized meson DA, i.e. $\phi_\pi(z) = 6z(1-z)$, what cancels the z-dependence of the hard amplitude. The integral over x remains which contains the model-dependent TDA. Separating the real and imaginary parts of the amplitude, but only for the structure dependent part, this integral is defined

$$\begin{aligned}I_x^D &= Q_u \int_{-1}^{1} dx \frac{D(x,\xi,t) - D(\xi,\xi,t)}{x-\xi} + Q_d \int_{-1}^{1} dx \frac{D(x,\xi,t) - D(-\xi,\xi,t)}{x+\xi} \\ &+ Q_u\,D(\xi,\xi,t)\left(\ln\frac{1-\xi}{1+\xi} - i\pi\right) + Q_d\,D(-\xi,\xi,t)\left(\ln\frac{1+\xi}{1-\xi} + i\pi\right) \quad ,\end{aligned} \tag{5.12}$$

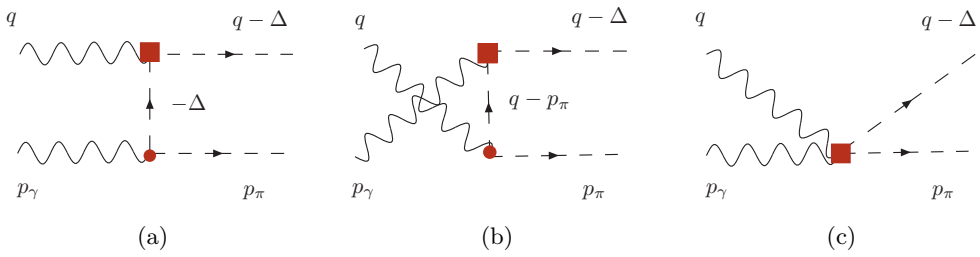

Figure 5.2: Pion Compton Scattering. The direct and the cross contributions, respectively (a) and (b), as well as the seagull contribution (c). The dot vertex is the usual $\pi\pi\gamma$-vertex and the square vertex is the Brodsky-Lepage vertex.

where D stands for V, A. This non-perturbative part will be given by the TDAs evaluated in the NJL model of Section 4.3.

As for the pion pole contribution, the expression for the amplitude (5.10) suggests that the pion amplitude is defined by performing the entire integral procedure just as for the TDAs. The pion pole term becomes proportional to the electromagnetic pion Form Factor studied in Section 2.7

$$I^{\pi} = -\frac{1}{\alpha_s}\,\frac{3}{4\pi}\,\frac{Q^2\,F_{\pi}\left(Q^2\right)}{t-m_{\pi}^2} \quad . \tag{5.13}$$

In this case we would use the asymptotic form for the pion DA by consistency. If we use $\phi_{\pi}\left(z\right) = 6z\left(1-z\right)$ with $z = \left(x+\xi\right)/2\xi$, we obtain the Brodsky-Lepage pion Form Factor (2.40)

$$Q^2\,F_{\pi}\left(Q^2\right) = 16\pi\;\alpha_s\;f_{\pi}^2 \quad . \tag{5.14}$$

Therefore the pion pole contribution to the amplitude (5.10) becomes

$$\mathcal{M}_{\pi} \;\;=\;\; -4\pi\,\alpha_{elm}\,2\,\frac{Q^2\,F_{\pi}(Q^2)}{t-m_{\pi}^2}\,\frac{\vec{\varepsilon}^{\perp}.\vec{\Delta}^{\perp}}{Q} \quad . \tag{5.15}$$

In an alternative way, the analyses of the pion Compton scattering yields the same result. For the sake of generality, we choose, for the purpose of that calculation, the general expression for ε given by $\varepsilon = \vec{\varepsilon}^{\perp} + \alpha\bar{p}$. Since it does not depend on α, we can state that the result obtained is independent of the gauge's choice. Therefore, in the $\alpha = 0$ gauges, only the direct diagram (a) of Fig. 5.2 does contribute to the cross section. Both the crossed (b) and the seagull (c) diagrams are higher-twist. Contrarily to the amplitudes involving the TDAs, the pion amplitude is model-independent thanks to the asymptotic expression of the pion DA that will be henceforth adopted.

An analysis of Eq. (5.11) including the isospin decomposition (4.23, 4.33) shows that only the direct terms of the charge combinations, i.e. $\propto Q_q^2$, contribute to the amplitude $\mathcal{M}^{\rho_L^+\pi^-}$. A similar analysis for the pion production but at zero momentum transfer indicates that the cross terms, i.e. $\propto Q_u Q_d$, cancel out.

Going back to the differential cross section Eq. (5.7), we average over the real photon polarization, which give an overall $\vec{\Delta}_{\perp}^2/2$ factor. The integration over φ being straightforward, we are left

with[3]

$$\frac{d\sigma^{e\gamma\to e\rho_L^+\pi^-}}{dQ^2dtd\xi} = 2\pi\,\frac{32\pi}{9}\,\frac{\alpha_{elm}^3\alpha_s^2}{s_{e\gamma}\,Q^8}\left(\frac{f_\rho}{\sqrt{2}\,f_\pi}\right)^2(-t)\,\frac{1-\xi}{(1+\xi)^4} \\ \left(2\xi\,s_{e\gamma}\,-\,(1+\xi)Q^2\right)\left\{\left(\Re\,I_x^V\right)^2+\left(\Im\,I_x^V\right)^2\right\}\quad , \tag{5.16}$$

$$\frac{d\sigma^{e\gamma\to e\pi^+\pi^-}}{dQ^2dtd\xi} = 2\pi\,\frac{32\pi}{9}\,\frac{\alpha_{elm}^3\alpha_s^2}{s_{e\gamma}\,Q^8}\,(-t)\,\frac{1-\xi}{(1+\xi)^4} \\ \left(2\xi\,s_{e\gamma}\,-\,(1+\xi)Q^2\right)\left\{\left(\Re\,I_x^A-\,72\,\frac{f_\pi^2}{t-m_\pi^2}\right)^2+\left(\Im\,I_x^A\right)^2\right\}\quad . \tag{5.17}$$

From Eq. (5.17) it can be observed that

$$\xi \geq Q^2/\left(2\,s_{e\gamma}-Q^2\right)\quad . \tag{5.18}$$

In other words, there is a (positive) lower limit on the value of ξ. Let us now proceed to evaluate these integrals.

5.3 Results from the Phenomenological Parameterization

The first estimates for the cross sections of meson production have been given for the phenomenological parameterization of the Double Distribution (4.66), what is referred to as Model 1. The t-dependent Double Distribution (4.64) are considered for the vector TDA and is called Model 2. In none of these approaches the pion pole contribution to the cross section for the pion production is taken into account. It means that the term proportional to the pion decay constant is not present in the expression for the cross section (5.17).

Also, no QCD evolution is taken into account, the effects of which are supposedly less important than the uncertainty of the modeling of the TDAs.

For the vector TDA both the real and imaginary part of the amplitude contribute significantly to the cross section. Since we are dealing with t-independent DDs, the t-dependence comes solely from the overall $-t$ factor in the trace.

In order to numerically estimate the cross sections, the strong coupling constant is fixed to a value of $\alpha_s \simeq 1$. This large value of α_s is indicated from the analyses of the electromagnetic Form Factor [38]. On the left panel of Fig. 5.3, the cross section for the $\pi\rho$ production is plotted for $Q^2 = 4$ GeV^2 and $s_{e\gamma} = 40$ GeV^2. The high-ξ behavior is similar for both model while the intermediate-ξ region is sensitive to specific models for the TDAs. On the other hand, as it is shown in Ref. [131], the Q^2 behavior at fixed ξ is model independent, what constitutes a crucial test for the validity of the approach.

Turning our attention to the $\pi\pi$ production, we should compare the estimates with the cross section for the Bremsstrahlung process in the same kinematical regime. It is shown in Ref. [131] that the process where the $\pi^+\pi^-$ is produced by a photon radiated from the leptonic line does not

[3] A factor 1/4 is missing in Eq. (23) of Ref. [131]. This typo does not affect to the numerical results reported in that reference [136].

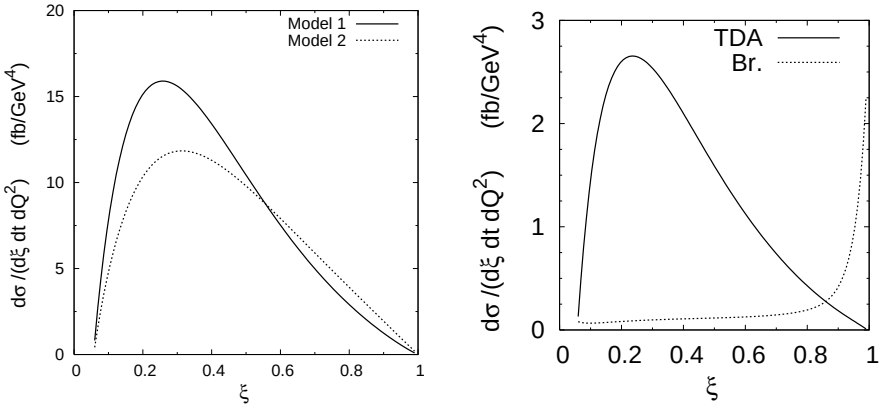

Figure 5.3: The cross section for $\pi\rho$ production (on the left) in a t-independent parameterization (Model 1) and a t-dependent one (Model 2) ; and for $\pi\pi$ on the right [131].

interfere much with the $\pi\pi$ production from $\gamma^*\gamma$ for reasonable values of ξ and with the exception of small values of $s_{e\gamma}$. In other words, the hard hadronic process dominates the Bremsstrahlung contribution in the kinematical region under scrutiny. This statement is illustrated on the right panel of Fig. 5.3. The axial TDA is given for the Model 1 and the dotted line represents the contribution of the Bremsstrahlung.

A general observation is that both the cross sections for $\rho_L^+\pi^-$ and $\pi^+\pi^-$ are rather small. In the next Section, we will see how these results are enhanced by the pion pole amplitude for the pion production as well as by QCD evolution for the rho production.

5.4 Results from the TDAs in the NJL Model

For the nonperturbative part of the process we use the TDAs evaluated in the NJL model.

The kinematics of the process restrict the domain of relevance of the variables (ξ, t), which, in turn, define the shape and the magnitude of the distributions. The restriction (5.18) on the value of the skewness variable is indeed particularly interesting because the value of ξ defines the shape of the TDAs. In particular, the shape of the axial TDA calculated in models radically changes according to the sign of the skewness variable; $A(x, \xi, t)$ has, at $x = \pm\xi$, its maximum values for $\xi > 0$ (see right panel of Fig. 4.12) while it has its minimum values for $\xi < 0$. However the vector TDA has its maximum and minimum values at $x = \pm\xi$ (see left panel of Fig. 4.12) independently of the sign of the skewness variable.
On the other hand, the magnitude of the distributions is controlled by the t-dependence. This can be easily understood because the TDAs, that must satisfy the sum rules (4.15, 4.16), are expected to decrease at least as t^{-1}. The t-behavior of the cross sections will therefore be dictated by both the overall $(-t)$ factor coming from the trace and the TDAs.

The value $\alpha_s \simeq 1$ chosen in Ref. [131] is also adopted here. Using this value for α_s we have evaluated the cross section for ρ production. In Fig. 5.6 we plot this cross section as a function of ξ. As we observe, the cross section is largely dominated by the imaginary part of the integral (5.16).

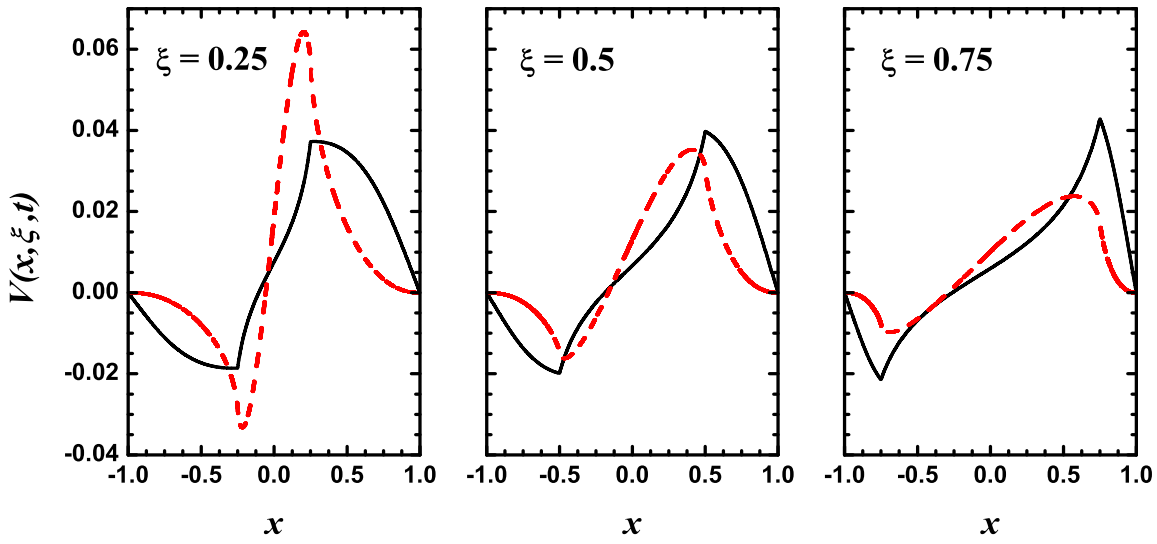

Figure 5.4: The functions $V^{\gamma\to\pi^-}(x,\xi,t)$ and for $\xi = 0.25$, 0.5, 0.75 and for $t = -0.5$ GeV^2. In each figure, the solid line corresponds to the NJL model prediction and the dashed line to its LO evolution.

Comparing with the previous results shown on Fig. 5.3, we observe that our predictions are higher by a factor 2 or 3.

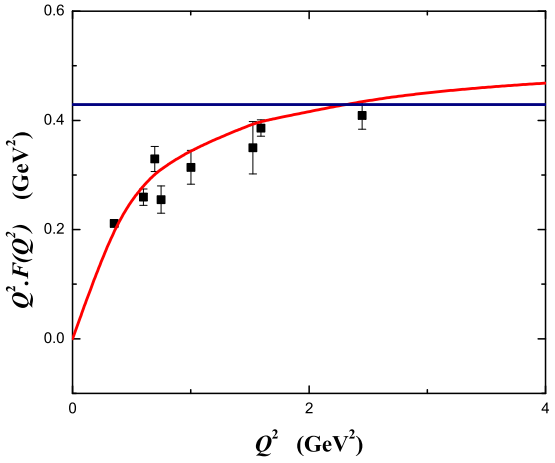

Figure 5.5: Electromagnetic Pion FF. The Brodsky-Lepage asymptotic FF for $\alpha_s = 1$ and $Q^2 = 2.45$ GeV^2 (blue line) and the experimental data given in Table 5.1. The red curve represents a fit in the monopole form $Q^2/(1 + 0.44\,Q^2/0.2336)$.

The cross section for pion production at $Q^2 = 4$ GeV^2 as a function of ξ is given in Fig. 5.7 (left). This cross section is dominated by the pion pole contribution which is determined by the Brodsky-Lepage pion Form Factor. Alternatively, if the pion Form Factor is experimentally known, we can infer phenomenologically this contribution. And hence the axial TDA could be extracted from the interference term. The latter shows already an impressive enhancement with respect to the cross section shown in the right panel of Fig. 5.3.

From Ref. [109] we know that the pion Form Factor at $Q^2 = 2.45$ GeV^2 is 0.167 ± 0.010. The pion Form Factor is shown on Fig. 5.5 for the different experimental results, see Ta-

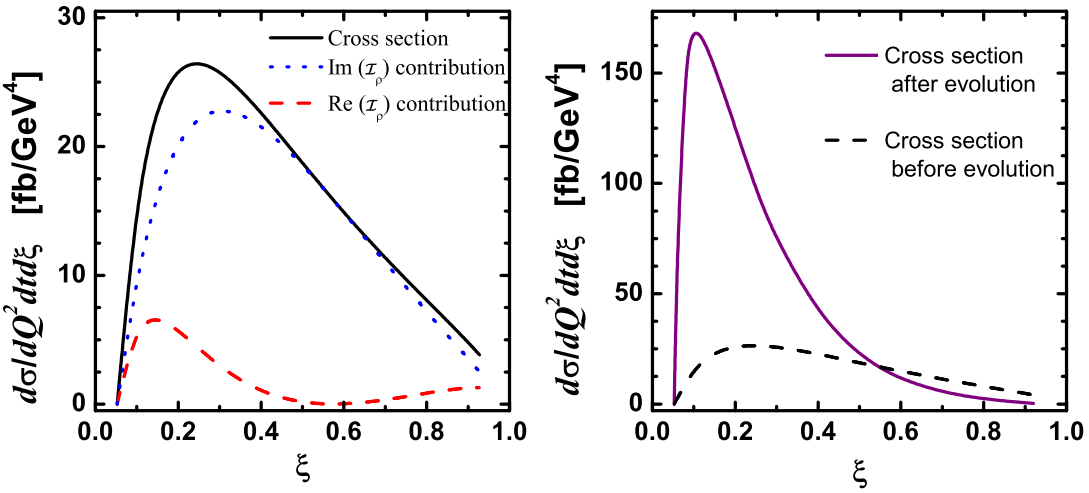

Figure 5.6: $e\gamma \to e'\rho_L^+\pi^-$ differential cross section plotted as a function of ξ for $Q^2 = 4\,\mathrm{GeV}^2$, $s_{e\gamma} = 40\,\mathrm{GeV}^2$, $t = -0.5\,\mathrm{GeV}^2$. In the first layer, the dotted (dashed) line is the contribution to the cross section coming from the imaginary (real) part of the integral given in Eq. (5.16). In the second layer we give the cross sections before and after evolution.

ble 5.1. In Fig. 5.7 (right) we depict, for each contribution, the prediction using the interval defined by the experimental value of the Form Factor (filled areas), including also the theoretical prediction using the Brodsky-Lepage pion Form Factor (lines). We observe an unexpectedly huge enhancement of the total cross section of a factor of about 60.

The t-dependence of the cross section for pion production includes a strong dependence on t coming from the pion pole. Neglecting the pion mass in (5.17), we observe that the pion pole contribution to I_π is proportional to t^{-1}. Therefore, the cross section grows as t^{-1} for small t values. For large t values we expect, as in the ρ production case, a decreasing as t^{-1}.

	Q^2 [GeV^2]	$F^\pi(Q^2)$	$F^\pi(Q^2)$+ error	$F^\pi(Q^2)$- error
DESY [1]	0.351405	0.211314		
DESY [37]	0.695093	0.329482	0.353265	0.306529
JLab [193]	0.599788	0.259397	0.274914	0.246048
	0.748309	0.254932	0.280412	0.230928
	1.00094	0.313972	0.345017	0.284536
	1.52456	0.34985	0.397251	0.309278
JLab [109]	1.59404	0.385976	0.408247	0.368385
	2.44972	0.405233	0.434364	0.38488

Table 5.1: The experimental results for the pion Form Factor. The last two columns represent the upper and the lower limit of the error bars.

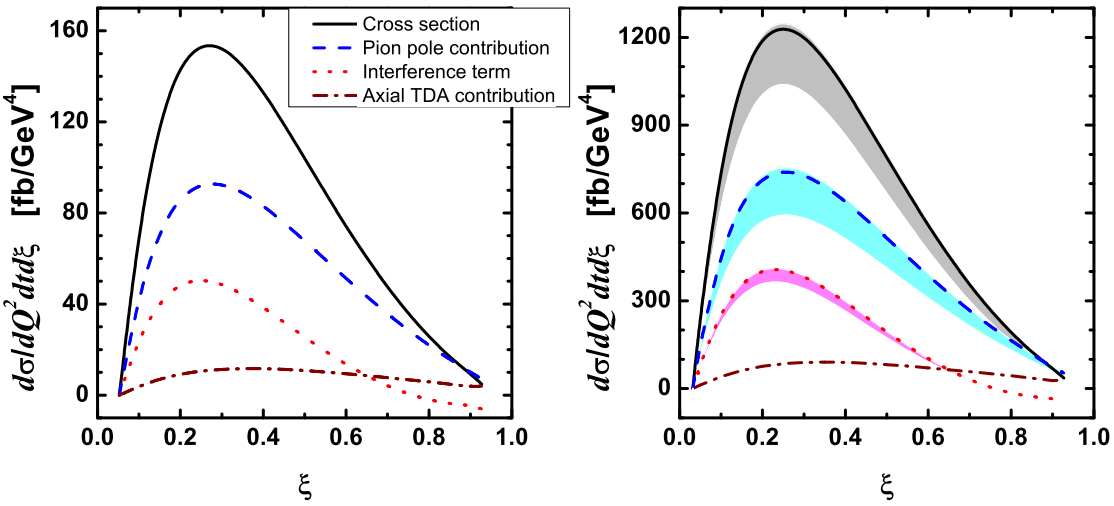

Figure 5.7: $e\gamma \to e'\pi^+\pi^-$ differential cross section plotted as a function of ξ for $s_{e\gamma} = 40\,\mathrm{GeV}^2$, $t = -0.5\,\mathrm{GeV}^2$, $Q^2 = 4\,\mathrm{GeV}^2$ (left) and $Q^2 = 2.45\,\mathrm{GeV}^2$ (right). The dashed (dashed-dotted)[dotted] line is the contribution to the cross section coming from the pion fom factor (axial TDA) [interference term between the pion Form Factor and A]. The pion pole contribution is calculated using the Brodsky-Lepage pion Form Factor. The filled areas in the right layer correspond to the same contributions but with the experimental value for the pion Form Factor $F_\pi = 0.167 \pm 0.010$ [109].

5.4.1 QCD Evolution

We have also studied the effect of the QCD evolution on our estimates, using for this purpose the code of Freund and McDermott [94]. The same procedure as for the Distribution Amplitude and the GPDs is followed. The value of Q_0 for the LO evolution in the NJL model is given by Eq. (2.30).

Turning our attention to the vector TDA evolved at LO to a scale of 4 GeV^2 (Fig. 5.4), we observe that the value of $V(x,\xi,t)$ at $x = \pm\xi$ grows for small values of ξ and decreases for large ξ values in comparison with the TDA at the scale of the model. This implies that the cross section for ρ production, which is largely dominated by the imaginary part, will grow appreciably in the small ξ region. In Fig. 5.6 we compare the cross section after evolution, calculated only through contribution of the imaginary part of I^V with the one obtained before evolution. We observe that this cross section is multiplied by a factor about 5 in the $\xi \sim 0.2$ region. In the case of the axial TDA, the cross section is dominated by the pion Form Factor contribution, therefore the effect of the evolution is expected to be small.

5.5 The Experimental Situation

In the previous Section we have looked at the expected cross section for π-π and π-ρ production in exclusive $\gamma^*\gamma$ scattering in the forward kinematical region using realistic models for the description of the pion. First we confirm the previous estimates for ρ production, even if our results for the

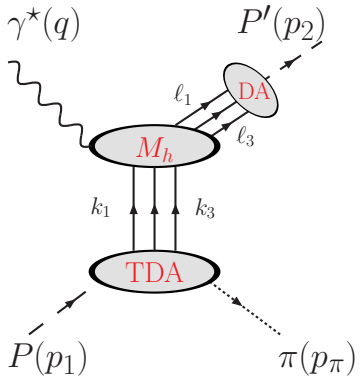

Figure 5.8: The factorization of the process $\gamma^* P \to P'\pi^0$ into proton DA, hard subprocess amplitude M_h and proton-pion TDA. Figure from [135].

cross section are a factor 2 larger than the one obtained in Ref. [131]. Second, in comparison with this previous evaluation of the cross sections, we have improved in considering the effect of evolution on the vector current. In doing so, an additional factor 5 appears in the small ξ region, leading to a cross section for ρ production of one order of magnitude larger than the previous calculation. We have also improved in including the pion pole term in the tensor decomposition of the axial current. Then an even larger enhancement factor, of about 60 in this case, is found in the cross section for pion production. The interference term becomes a factor 15 larger than the pure TDA contribution, making the axial TDA more accessible experimentally.

Data have been collected at LEP and CLEO on these reactions with some phenomenological success, even if mainly on $\rho\rho$ final states in a different factorization regime [16, 17]. More data are obviously needed and are eagerly waited for in the TDA region, and much hope comes from the high luminosity electron colliders.

5.6 Backward Pion Electro-production

Recently Pire and collaborators have shown in a series of articles [165, 133, 134, 135] that the TDAs represent the ideal framework through which it is possible to describe the backward pion electro-production, e.g., $ep \to e'p'\pi^0$, as well as the meson production via a nucleon-antinucleon Drell-Yan process, e.g., $\bar{N}N \to \gamma^*\pi$, in the forward kinematics.

These processes are experimentally more accessible then the ones previously analyzed. For instance, the $\bar{p}p$ annihilation, e.g. $\bar{p}p \to \gamma\gamma$, the meson production channel $\bar{p}p \to \gamma\pi^0$, that will be intensively studied at GSI-HESR antiproton program by the planned FAIR project, [4] and by the meson photo-production process, $p\gamma \to \pi^0 p$, with forthcoming data from JLab.

In Ref. [135], a soft-pion limit for the baryonic TDA is used to give an estimate of the differential cross section for $\gamma^* P \to P'\pi^0$. However, the lack of knowledge of the TDAs unfortunately prevents from giving an accurate estimate of the latter quantity. Data should be available, at higher energies, as for instance at HERMES and with CEBAF at 12 GeV [178]. The calculation of the cross

[4] A great wealth of up-to-date informations about the experiments that will be performed at GSI-HESR can be found at this web-page: http://www.gsi.de/zukunftspro jekt/indexe.html.

section [135], in an admittedly quite narrow range of the parameters, can thus serve as a reasonable input to the feasibility study of backward pion electroproduction at CEBAF at 12 GeV, in the hope to reach the scaling regime, in which we are interested.

6 Peeping through Spin Physics: the Sivers Function

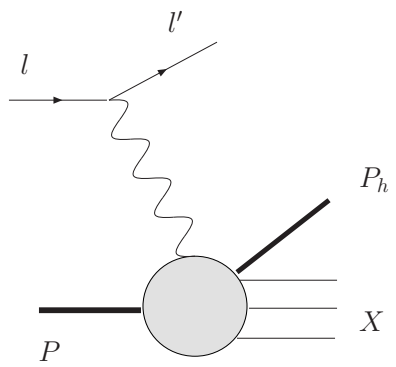

Figure 6.1: Semi-Inclusive Deeply Inelastic Scattering.

The partonic structure of transversely polarized hadrons is one of their less known features. A review [27] on the transverse polarization of quarks in hadrons gathered all the knowledge which is, nevertheless, appreciably growing on both the theoretical and experimental sides. Experiments for the determination of the transversity properties are progressing very fast and the relevant experimental effort has motivated a strong theoretical activity.

When extending our analyses to *unintegrated* parton distributions (1.28), we have to deal with the intrinsic transverse motion of quarks. This supplementary degree of freedom implies the existence of new parton distribution functions, i.e. (1.28). Besides their dependence on k_T, the additional parton distributions can either be chiral-even or odd. In the former case, the distributions can be probed in fully inclusive DIS. The conservation of chirality does however not allow the identification, through the optical theorem, of chiral-odd distributions, for helicity must be flipped twice as shown on Fig. 6.2. The *Transverse Momentum Dependent* Parton Distributions (TMD) studied in the context of transversely polarized nucleons do flip helicity and cannot be accessed through DIS.

Semi-inclusive deep inelastic scattering (SIDIS), i.e. the process depicted on Fig. 6.1

$$e(l)\, N(\mathcal{P}) \to e'(l')\, h(\mathcal{P}_h)\, X(\mathcal{P}_x) \quad , \tag{6.1}$$

with the detection in the final state of a produced hadron h in coincidence with the scattered electron e', is one of the proposed processes to access the parton distributions of transversely polarized hadrons. [1] For several years it has been known that SIDIS off a transversely polarized target shows azimuthal asymmetries, the so called *single spin asymmetries* (SSAs) [61, 189, 190].

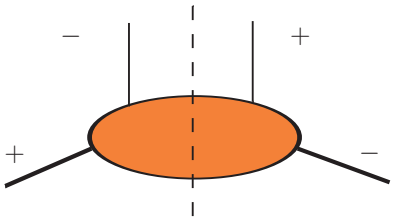

Figure 6.2: Representation of a chirally odd distribution. The corresponding handbag diagram is forbidden by conservation of chirallity.

As a matter of fact, it is predicted that the number of produced hadrons in a given direction or in the opposite one in the hadronic plane, with respect to the reaction plane, depends on the orientation of the transverse spin of a polarized target with respect to the direction of the unpolarized beam, [2]

$$A_{UT}(\phi_h, \phi_S) \equiv \frac{d\sigma(\phi_h, \phi_S) - d\sigma(\phi_h, \phi_S + \pi)}{d\sigma(\phi_h, \phi_S) + d\sigma(\phi_h, \phi_S + \pi)} \neq 0 \quad . \tag{6.2}$$

It can be shown that the SSA in SIDIS off transverse polarized targets is essentially due to two different physical mechanisms, whose contributions can be technically distinguished [24, 35, 128, 149].

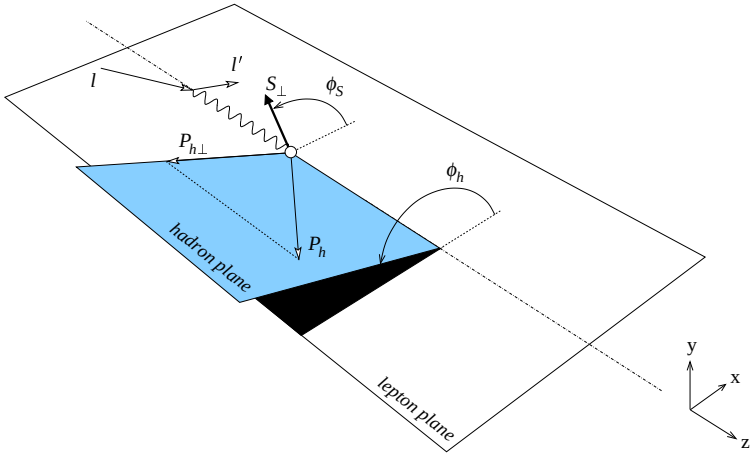

Figure 6.3: SIDIS kinematics in the $\gamma^* p$ frame as defined in the Trento conventions [23].

One of the two different mechanism has been proposed by Collins [61] and is therefore referred to after his name. It is due to parton final state interactions in the production of a spinless hadron by a transversely polarized quark, and will not be discussed here.

The other is the Sivers mechanism, producing a term in the SSA which is given by the product of the unpolarized fragmentation function with the Sivers Parton Distribution [189, 190], describing the modulation of the number density of unpolarized quarks in a transversely polarized target due to the correlation between the transverse spin of the target and the intrinsic transverse parton momentum.

[1] In this case, we can define two different *transverse directions*. In general, a quantity which is transverse in a frame where P and h have no transverse components (thus $\vec{P}_T = \vec{h}_T = 0$), is indicated with a subscript T, so that T means transverse with respect to $\vec{h}$, while those with a subscript $\perp$ are defined in a frame where q and P have no transverse components (standard DIS frame), so that $\perp$ means transverse with respect to $\vec{q}$ (thus $\vec{q}_\perp = \vec{P}_\perp = 0$) [149]. There is no such distinction in DIS, so that $T = \perp$ and they can be used equivalently.

[2] Here U means Unpolarized beam, T means Transversely polarized target and it is assumed that the produced hadron is spinless, or that its polarization is not detected.

The Sivers function, $f_{1T}^{\perp q}(x, k_T)$, is the quantity of interest of this Chapter. It is formally defined through the $\Phi^{[\gamma^+]}$ of the decomposition (1.28). Namely, [23, 102],

$$\begin{aligned}\Phi^{[\gamma^+]\,q}(x, \vec{k}_T, S) &= f_1^q(x, k_T) - \frac{\epsilon_T^{ij} k_{Ti} S_{Tj}}{M} f_{1T}^{\perp q}(x, k_T) \\ &= \frac{1}{2}\int \frac{d\xi^- d^2\vec{\xi}_T}{(2\pi)^3} e^{-i(x\xi^- P^+ - \vec{\xi}_T\cdot\vec{k}_T)} \langle P, S|\hat{O}_q|P, S\rangle \quad , \end{aligned} \tag{6.3}$$

with the operator defined by [121, 29]

$$\hat{O}_q = \bar{\psi}_q(0, \xi^-, \vec{\xi}_T)\mathcal{L}^\dagger_{\vec{\xi}_T}(\infty, \xi^-)\gamma^+\mathcal{L}_0(\infty, 0)\psi_q(0, 0, 0) \ , \tag{6.4}$$

where $\psi_q(\xi)$ is the quark field and the gauge link has been defined as follows,

$$\mathcal{L}_{\vec{\xi}_T}(\infty, \xi^-) = P\exp\left(-ig\int_{\xi^-}^{\infty} A^+(\eta^-, \vec{\xi}_T)d\eta^-\right) \quad . \tag{6.5}$$

The number density of unpolarized quarks in a transversely polarized target is effectively modulated by the quantity

$$\begin{aligned}&\Phi^{[\gamma^+]\,q}(x, \vec{k}_T, S_j =\uparrow) - \Phi^{[\gamma^+]\,q}(x, \vec{k}_T, S_j =\downarrow) \\ &= -2\,\epsilon^{ij}\,\frac{k_i}{M}\,f_{1T}^{\perp q}(x, k_T) \quad , \end{aligned} \tag{6.6}$$

with i, j being either x, y and $S =\uparrow / \downarrow$ standing for S in a transverse direction, in opposition with the helicity $S = \pm$.

The Sivers function contributes with a $\sin(\phi_h - \phi_S)$ weighting function to the cross section of SIDIS with unpolarized beam off a transversely polarized proton (6.2), with the angles ϕ_h, ϕ_S defined in Fig. 6.3. The Sivers asymmetry, according to the "Trento convention" [23], is defined in terms of the experimental cross sections,

$$A_{UT}^{Sivers} = \frac{\int d\phi_S d\phi_h \sin(\phi_h - \phi_S) d^6\sigma_{UT}}{\int d\phi_S d\phi_h d^6\sigma_{UU}} \quad . \tag{6.7}$$

The cross sections themselves can be written, through the factorization theorems, as a convolution of k_T-dependent distribution and fragmentation functions [149] as shown on Fig. 6.4; the former being here the Sivers function.

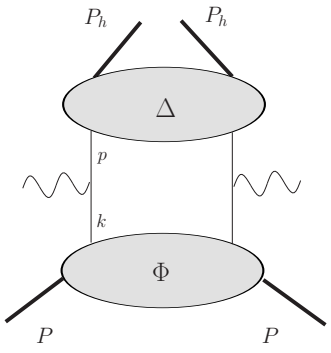

Figure 6.4: Factorization in SIDIS.

Recently, the first data of SIDIS off transversely polarized targets have been published, by the HERMES Collaboration [5] for the proton and by the COMPASS Collaboration [7] for the deuteron. It has been found that, while the Sivers effect is sizable for the proton, it becomes negligible for the deuteron, so that apparently the neutron contribution cancels the proton one, showing a strong flavor dependence of the mechanism.

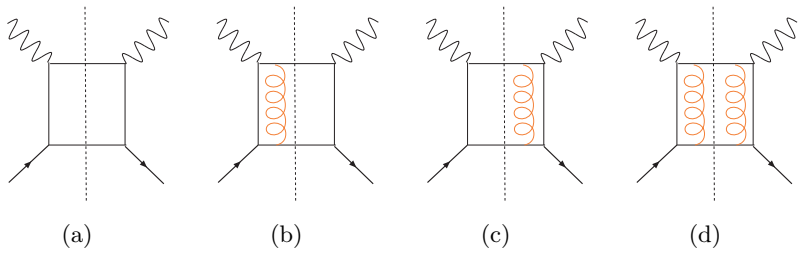

Figure 6.5: The expansion of the gauge link: $(a) + (b) + (c) + (d) + \ldots$.

Different parameterizations of the available SIDIS data have been published [19, 63, 20], still with large uncertainties. Deeper analyses are in progress, e.g., [74, 75]. New data will be soon available, e.g., thanks to the improvement of the CEBAF accelerator at 12 GeV at JLab [54] or the improvement of the experiments at HERMES [184], that will reduce the errors on the extracted Sivers function and will help discriminate between different theoretical predictions.

6.1 The Gauge Link

The Sivers function is a Transverse Momentum Dependent PD and vanishes if integrated over the transverse momentum. It is a time-reversal odd object [27] and for this reason, for several years, it was believed to vanish due to time reversal invariance. However, this argument was invalidated by a calculation in a spectator model [41], following the observation of the existence of leading-twist Final State Interactions (FSI) [42]. The current wisdom is that a non-vanishing Sivers function is generated by the gauge link in the definition of TMD parton distributions [62, 121, 29], whose contribution does not vanish in the light-cone gauge, [3] as happens for the standard parton distribution functions.

Technically, Final State Interactions are reflected in the expansion of the gauge link (6.5) as shown on Fig. 6.5. It is hence clear by the identification of the Sivers function in (6.6) that, if the Sivers function were defined without the gauge link, it would be identically zero.

To the first non trivial order, i.e. $(b) - (c)$ of Fig. 6.5, giving a contribution to the asymmetry, the Sivers function is obtained for the flavor α, as follows,

$$f_{1T}^{\perp\alpha}(x, k_T) = \Im\left\{\frac{M}{2k_x}\int \frac{d\xi^- d^2\vec{\xi}_T}{(2\pi)^3} e^{-i(x\xi^- P^+ - \vec{\xi}_T\cdot\vec{k}_T)}\langle\hat{O}^\alpha\rangle\right\} \quad , \tag{6.8}$$

where, in a helicity basis, the operator reads

$$\langle\hat{O}^\alpha\rangle \;=\; \langle PS_z = +|\bar{\psi}_{\alpha i}(\xi^-, \vec{\xi}_T)(ig)\left\{\int_{\xi^-}^{\infty} A_a^+(0, \eta^-, \vec{\xi}_T)d\eta^- T_{ij}^a\right\}\gamma^+\psi_{\alpha j}(0)|PS_z = -\rangle + \text{h.c.} \quad . \tag{6.9}$$

[3] The gauge link is usually taken in a non-singular gauge, i.e. not in the light-cone gauge, for further details we refer to Ref. [29].

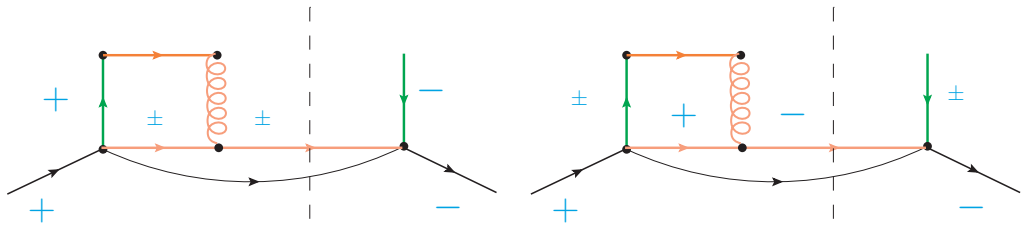

Figure 6.6: Contributions to the Sivers function in quark models. The $+, -$ signs represent the helicities.

6.2 Final State Interactions at the Quark Level

In this theoretical and experimental scenario, due to the lack of correct QCD calculations of Parton Distributions, it becomes important to perform model calculations of the Sivers function. Several estimates exist, in a quark-diquark model [41, 121, 22, 25]; in the MIT bag model, in its simplest version [206] and introducing an instanton contribution [56]; in a light-cone model [142]; in a nuclear-style framework, relevant to establish the arising of the Sivers function in proton-proton collisions [32]; in the Constituent Quark Model (CQM) of Isgur and Karl (IK) [66].

Constraints on the Sivers function are obtained from *first principles*, following the example of, e.g., sum rules in GPDs. A model independent constraint on calculations of $f_{1T}^{\perp\mathcal{Q}}(x, k_T)$ is the Burkardt sum rule [49, 50]. It states that the total average transverse momentum of the partons in a hadron, $\langle \vec{k}_T \rangle$, which can be defined through the first moments of $f_{1T}^{\perp\mathcal{Q}}(x, k_T)$, for all the partons in the target, has to vanish. If the proton is polarized in the positive x direction, the Burkardt sum rule reads,

$$\sum_{\mathcal{Q}=u,d,s,g..} \langle k_y^{\mathcal{Q}} \rangle = -\int_0^1 dx \int d\vec{k}_T \frac{k_y^2}{M} f_{1T}^{\perp\mathcal{Q}}(x, k_T) = 0 \quad . \tag{6.10}$$

The Burkardt sum rule remains unchanged under evolution.
To distinguish between the model estimates, data and model independent relations, such as this one, can be used.

It is also difficult to relate the Sivers Function to the target helicity-flip, impact parameter dependent (IPD), generalized parton distribution E (1.13). Although simple relations or ansatze between the two quantities are found in models [52, 144], a clear model independent formal relation is still to be proven, as shown in Ref. [146]. However some *gross* features, such as the sign of the Sivers function, can be deduced from the results for the IPD parton distributions.

In the context of Constituent Quark Model for the proton, one expects, as a consequence of the Burkardt sum rule, the u and the d Sivers functions to contribute with a similar magnitude but opposite sign.

In this Section, we analyze the Sivers functions in two such models; the MIT bag model and the CQM of Isgur and Karl. The gluon exchange is here treated in a perturbative way; both models moreover assume an $SU(6)$ proton wave function, even if only in the first order of the IK wave expansion

If an $SU(6)$ state is assumed, any model calculation of Parton Distributions gives u and d

parton distributions which are proportional to each other [113, 115]. In the case of $f_{1T}^{\perp\mathcal{Q}}$ one is not investigating single particle properties but two-body ones, due to the two-body Final State Interaction operator generated by the gauge-link. There is therefore in principle no reason to have proportionality, which is a good sign that the results in such models might a priori fulfill the Burkardt sum rule (6.10). [4]

The diagrammatic representation of the leading-twist Final State Interactions contributing to a non-zero Sivers function (6.8) in those models is depicted in Fig. 6.6. As it has been mentioned above, helicity has to flip twice: both at the nucleon state and at the quark level. At the quark level, it is the presence of a 2-body *light-like* gluon interaction that enables a spin-flip. By symmetry among the active quarks, the quark interacting with the virtual photon (green quark line) can either flip its helicity or not. The first case is represented on the left panel of Fig. 6.6, while the second case implies that the "active-but-non-interacting-with-the-photon" quark flips in turn as shown on the right panel.

Let us now concentrate on the results of these two model calculations. Historically the first calculation performed in the MIT bag model has been undertaken by Yuan [206] whose conclusions were followed by the whole Community. Our CQM calculation has led us to satisfactory Sivers functions [66] even if non complying with the conclusions of Ref. [206]. This is why we "peeped through" the first calculation in the bag model. A more physical picture of the Sivers function as allowing symmetry between the two active quarks 6.6 was revealed [72]. Therefore, the results of Refs. [66, 72] are presented here as illustrations of 1 and 3-body approaches of the Sivers function.

6.2.1 1-body Model

Here we revise the first formal calculation of the Sivers function that was performed in the MIT bag model [206]. The details of the calculation are given in Ref. [72] with the formalism developed in Ref. [206].

The expression (6.8) is written inserting the bag model wave function in momentum space, $\varphi(k)$. [5] Using Fig. 6.7 for the definition of the quark helicity and momentum labels, the Sivers function in the bag model

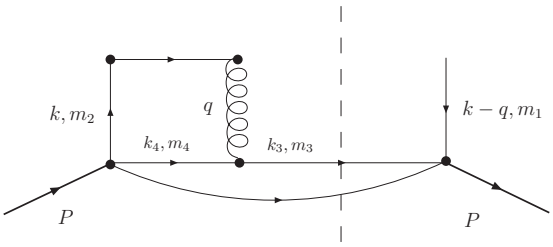

Figure 6.7: The quark helicity and momentum label for the bag calculation.

[4] A proportionality of -1 would nevertheless be more than acceptable for the fulfillment of the sum rule.

[5] The expression for the wave function of the MIT bag model in momentum space is

$$\varphi_m(\vec{k}) \quad = \quad i\sqrt{4\pi}\, N\, R_0^3 \begin{pmatrix} t_0(|\vec{k}|)\chi_m \\ \vec{\sigma}\cdot\hat{k}\, t_1(|\vec{k}|)\,\chi_m \end{pmatrix} \quad , \tag{6.11}$$

with the normalization factor $N = \left(\frac{\omega^3}{2R_0^3\,(\omega-1)\sin^2\omega}\right)^{1/2}$ where $\omega = 2.04$ for the lowest mode and R_0 is the bag radius. The two last quantities are related through the relation $R_0 M_P = 4\omega$. The functions $t_i(k)$ are defined as $t_i(k) = \int_0^1 u^2\, du\, j_i(ukR_0) j_i(u\omega)$.

can be written [206]

$$f_{1T}^{\perp\alpha}(x,k_\perp) = -2g^2\frac{ME_P}{k^y}\int\frac{d^2q_\perp}{(2\pi)^5}\frac{i}{q^2}\sum_{\beta,m_1,m_2,m_3,m_4} T^a_{ij}T^a_{kl}\langle PS_x|b^{i\dagger}_{\alpha m_1}b^j_{\alpha m_2}b^{k\dagger}_{\beta m_3}b^l_{\beta m_4}|PS_x\rangle$$
$$\times\varphi^\dagger_{m_1}(\vec{k}-\vec{q}_\perp)\gamma^0\gamma^+\varphi_{m_2}(\vec{k})\int\frac{d^3k_3}{(2\pi)^3}\varphi^\dagger_{m_3}(\vec{k_3})\gamma^0\gamma^+\varphi_{m_4}(\vec{k_3}-\vec{q}_\perp) \quad , \qquad (6.12)$$

where M is the proton mass, E_p its energy, $b^i_{\mathcal{Q},m}$ is the annihilation operator for a quark with flavor $\mathcal{Q}$, helicity m, and color index i, and T^a_{ij} is a Gell-Mann matrix.

Performing the integral over k_3 and then $q_\perp$ and calculating the appropriate flavor-color factors, we find that there is actually no proportionality between the u and the d quark distributions. Numerical results are shown in Fig. 6.8 for the first moment of the Sivers function (plain curves),

$$f_{1T}^{\perp(1)\mathcal{Q}}(x) = \int d^2\vec{k}_T\frac{k_T^2}{2M^2}f_{1T}^{\perp\mathcal{Q}}(x,k_T) \quad . \qquad (6.13)$$

The obtained Burkardt sum rule is

$$\sum_{\mathcal{Q}=u,d,s,g..}\langle k_y^{\mathcal{Q}}\rangle = -0.78\,\mathrm{MeV} \quad .$$

To have an estimate of the quality of the agreement of this result with this sum rule, we consider the ratio

$$r = \frac{\langle k_x^d\rangle+\langle k_x^u\rangle}{\langle k_x^d\rangle-\langle k_x^u\rangle}\simeq 0.05 \quad ,$$

i.e., the Burkardt sum rule seems to be violated by 5 %.

In order to compare the results with the data, one should realize that one step of the analysis is still missing. The scale of the model is much lower than the one of the HERMES data, which is $Q^2 = 2.5$ GeV^2. For a proper comparison, the QCD evolution from the model scale to the experimental one would be necessary [116]. Unfortunately, the evolution of TMDs is still to be understood. In order to have an indication of the effect of the evolution, we perform a NLO evolution of the model results assuming, for the moments of the Sivers function, Eq. (6.13), the same anomalous dimensions of the unpolarized PDFs. [6] The parameters of the evolution have been fixed in order to have a fraction $\simeq 0.55$ of the momentum carried by the valence quarks at 0.34 GeV^2, as in typical parameterizations of PDFs , starting from a scale of $\mu_0^2 \simeq 0.1$ GeV^2 with only valence quarks.

The results show an impressive improvement of the agreement with data once the results of Ref. [206] are evolved in the way just described. The data, represented by the dashed bands, are perfectly described for both flavors. Although one should not forget that the performed evolution is not really correct, the analysis shows that, after evolution, model calculations can be consistent with the available data.

[6] Important progress concerning the evolution of the first moment of the Sivers function have been made recently, see [122, 205].

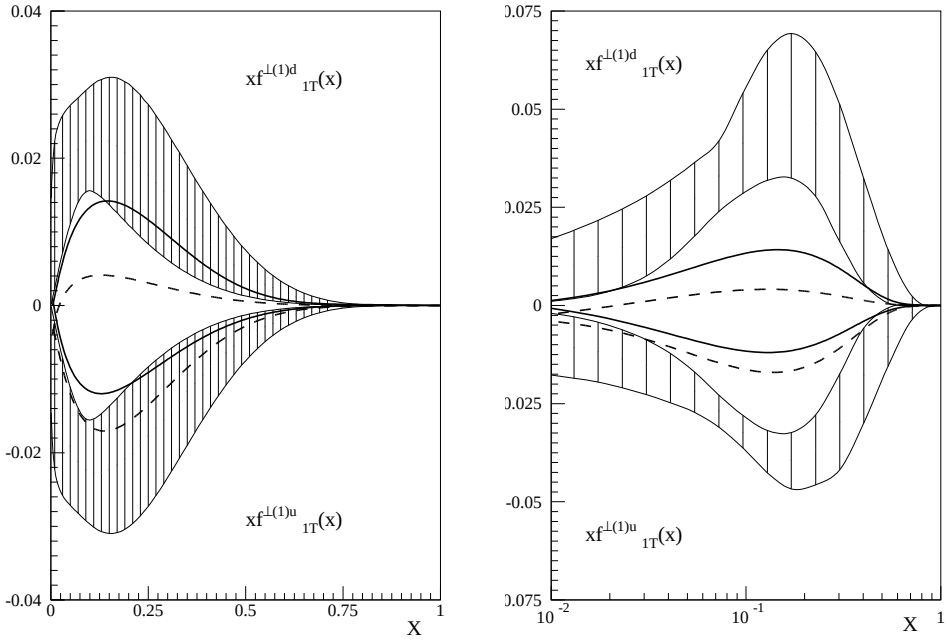

Figure 6.8: The (evolved) u and d Sivers functions obtained in the MIT Bag model and compared with the extraction from the data; respectively from (a) [63] and (b) [20]. The plain curves represent the results obtained through Eq. (6.12) [72], whereas the dotted curves represent the results of Ref. [206].

The slight violation of the Burkardt sum rule, which is a momentum property, is probably due to the fact that the proton state is not a momentum eigenstate in the MIT bag model.

6.2.2 3-body Model

The Constituent Quark Model (CQM) has a long story of successful predictions in low energy studies of the electromagnetic structure of the nucleon. The Isgur-Karl model [110, 111] is chosen to perform a calculation, in order to describe the performances of the approach developed in the context of CQM in Ref. [66]. A difference with respect to calculations of PDFs and GPDs is that, in the calculation of TMDs, the leading-twist contribution to the one-gluon-exchange (OGE) Final State Interaction has to be evaluated. This is done

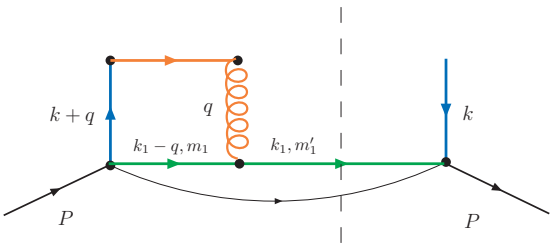

Figure 6.9: The quark helicity and momentum label for the CQM calculation.

through a non-relativistic reduction of the relevant operator, according to the philosophy of Constituent Quark Models [78]. [7]

The expression (6.8) is developed by inserting proper complete sets of intermediate one-quark states, using translational invariance and the definition of the gluon field as explained in Ref. [66] plus the definition of the labels of Fig. 6.9, one is left with the following expression for the Sivers function,

$$\begin{aligned} & f_{1T}^{\perp\alpha}(x,k_T) \\ & = \Im\left\{ ig^2 \frac{M}{2k_x} \int d\tilde{k}_1 d\tilde{k}_3 \frac{d^4q}{(2\pi)^3} \delta(q^+)\delta(k_3^+ + q^+ - xP^+)\delta(\vec{k}_{3T} + \vec{q}_T - \vec{k}_T)(2\pi)\delta(q_0) \right. \\ & \left. \sum_{\beta,m_1,m_1',m_3,m_3'} \langle PS_z = +|T_{ij}^a T_{kl}^a \; b_{m_1}^{\alpha i\dagger}(\tilde{k}_1) b_{m_3}^{\beta k\dagger}(\tilde{k}_3) b_{m_1'}^{\alpha j}(\tilde{k}_1 - \tilde{q}) b_{m_3'}^{\beta l}(\tilde{k}_3 + \tilde{q}) \; V(\vec{k}_1, \vec{k}_3, \vec{q}) | PS_z = -\rangle \right\} , \end{aligned} \tag{6.15}$$

with the interaction determined by

$$V(\vec{k}_1, \vec{k}_3, \vec{q}) = \frac{1}{q^2} \bar{u}_{m_3}(\vec{k}_3)\gamma^+ u_{m_3'}(\vec{k}_3 + \vec{q}) \bar{u}_{m_1}(\vec{k}_1)\gamma^+ u_{m_1'}(\vec{k}_1 - \vec{q}) \; . \tag{6.16}$$

For an easy presentation, the quantity which is usually shown for the results of calculations or for data of the Sivers function is its first moment (6.13). The results of the CQM approach are given by the red curves in Fig. 6.10 for the u and the d flavor following the example of Fig. 6.8 in the bag calculation. They are compared with a parameterization of the HERMES data, corresponding to an experimental scale of $Q^2 = 2.5$ GeV^2 [63]. The two dashed curves represent the best fit proposed in Ref. [63] plus 30 % and minus 30 %, respectively. Such an interval gives a rough estimate of the experimental errors and theoretical uncertainties in the extraction of the Sivers function from data.
The evolved results are given by the blue curves in Fig. 6.10 for the u and the d flavors. As it is clearly seen, the agreement with data improves dramatically and their trend is reasonably reproduced at least for $x \geq 0.2$.

Within our scheme, at the scale of the model, the Burkardt sum rule is

$$\langle k_x^u \rangle + \langle k_x^d \rangle \quad = \quad -0.40\,\mathrm{MeV} \quad ,$$

obtaining $r \simeq 0.02$, so that we can say that our calculation fulfills the Burkardt sum rule to a precision of a few percent.

[7] In this model the proton wave function is obtained in a OGE potential added to a confining harmonic oscillator; including contributions up to the $2\hbar\omega$ shell, the proton state is given by the following admixture of states

$$|N\rangle = a|^2S_{1/2}\rangle_S + b|^2S'_{1/2}\rangle_S + c|^2S_{1/2}\rangle_M + d|^4D_{1/2}\rangle_M \; , \tag{6.14}$$

where the spectroscopic notation $|^{2S+1}X_J\rangle_t$, with $t = A, M, S$ being the symmetry type, has been used. The coefficients were determined by spectroscopic properties to be $a = 0.931$, $b = -0.274$, $c = -0.233$, $d = -0.067$ [97].

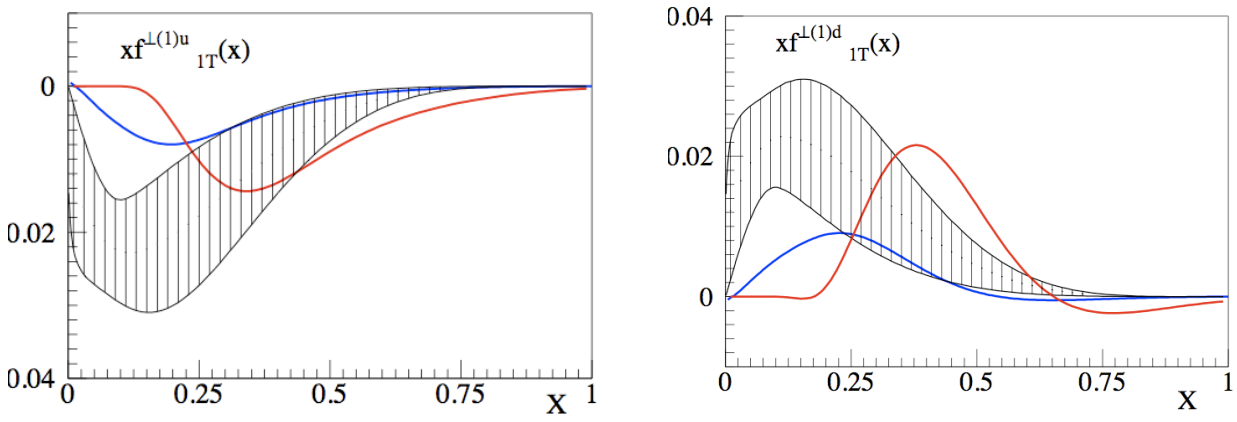

(a) (b)

Figure 6.10: The Sivers functions obtained in the IK model and compared with the extraction from the data [63].The red curves represent the results before evolution, whereas the blue curves are after evolution to the scale of the data.

6.3 The Way to a Conclusion

With respect to Ref. [206], the results in the MIT bag model (Fig. 6.8) show an impressive improvement of the agreement with data once the full contribution, i.e. coming from both diagrams 6.6, is taken into account. The data are described rather well for both flavors. Comparing this encouraging outcome with that of the IK model, one can notice that the Burkardt SR is better fulfilled in the CQM.

In closing our analyses of the Sivers functions in a 1 versus 3-body model, we can say that, for the first time, it has been established that correct model calculations provide phenomenological successful interpretations of the Sivers function, which are consistent with each other.

Let us compare our approach with other calculations mentioned above.
The first version of the MIT bag model calculation [206] has non-vanishing u and d-quarks contribution of opposite sign which are proportional in magnitude. The d-quark contribution is much smaller than the one obtained in the revised version of the bag model as well as the one of the CQM and therefore does not satisfy the Burkardt sum rule. The MIT bag model modified by instanton effects [56] has u and d-quark contributions of the same sign and therefore does not satisfy the Burkardt sum rule.
The diquark model with scalar diquarks [22] has no contribution for the d-quark and therefore does not satisfy the Burkardt sum rule, Eq. (6.10). The diquark model with axial-vector diquarks has contributions to both u and d-quarks and with opposite sign, but with the magnitude of the d 10 times smaller than that of the u. The Burkardt sum rule is not satisfied. The results are improved in the version of Ref. [25].

As a summary, we can say that the calculations presented here [66, 72], despite the naive wave functions used, are in better agreement with the data with respect to the other approaches, and fulfill the Burkardt sum rule. The model calculations have still to be improved and their evolution properly undertaken. So have to be the extraction of the data as well as the experiments. Much

efforts in that direction is being put from the whole *Transversity* community. [8]

[8] We cite, e.g., the latest workshop "Transversity 2008: 2nd International Workshop On Transverse Polarization Phenomena In Hard Processes", 28-31 May 2008, Ferrara, Italy.

7 Conclusion and Future Perspectives

Our main source of information about the internal pion and nucleon structure is provided by Deep Inelastic Scattering. Unpolarized DIS has revealed the partonic distributions of the hadrons. It has shown that the quarks carry only about half of the total hadron's momentum. Polarized DIS has provided information about spin distributions, telling us that only a small fraction of the spin of the proton is carried by the intrinsic spin of the quarks.

In the last decade, a theoretical treatment of semi-inclusive as well as exclusive deep reactions has been developed, increasing our knowledge on the structure of hadrons. For instance, Semi-Inclusive Deep Inelastic Scattering allows to obtain information also on chiral-odd Parton Distributions. In a transversely polarized hadron, the transversity distribution tells us what is the number density of quarks with polarization parallel to that of the hadron, minus the number density of quarks with antiparallel polarization. Moreover, the complete study of the features of the produced hadron in SIDIS requires that we take into account the transverse motion of quarks. The theoretical tools for the description of this process are therefore the *Transverse Momentum Dependent* PDs. Among this class of distributions, the Sivers function is the object of important theoretical studies as it has been proposed to explain single-spin asymmetries in SIDIS.

On the other hand, exclusive electroproduction of photons (Deep Virtual Compton Scattering) have been the most studied processes. Under the conditions of large virtuality Q^2 of the exchanged photon and low momentum transfer t, i.e. near the forward direction, the amplitude of the reaction factorizes into a hard and a soft part. This soft part have opened new windows on the structure of hadrons.

The theoretical tools for the understanding of theses processes are the *Generalized Parton Distributions*. The GPDs connect in different limits to other well known physical quantities: in the limit of low momentum transfer, $t \to 0$, they connect to the usual Parton Distributions. Integrated over the momentum fraction of the quark, GPDs lead to the electromagnetic hadron's Form Factors. Moreover, through Ji's sum rule, a particular combination of moments of GPDs can be related to the spin of the proton.

Exclusive hadron production in $\gamma^*\gamma$ scattering at small momentum transfer and large invariant mass is also assumed to factorize into hard and soft parts. The soft part provides for additional information on hadron structure through the *Transition Distribution Amplitudes*.

In this thesis, we have considered some of the distributions that we have just described. Throughout the Chapters 2, 3, 4 & 5, the partonic structure of the pion has been scrutinized under the Nambu - Jona-Lasinio description of the pion. In Chapters 2 & 3, we have reviewed the previous situation; whereas, in Chapters 4 & 5, we have presented our results on the Transition Distribution Amplitudes.

In Chapter 2, the *Distribution Amplitude* and the *Parton Distribution Function* of the pion have been presented together with their relation through the Soft Pion Theorems. The study of these well-known quantities have provided for a way to set the scene for the subsequent and original part of the manuscript. To be specific, more than a simple illustration of the formalism in which we were to be working, the calculation of the pion DA has allowed for a first criticism of the choice of the NJL model. This has been done, among other things, by determining the scale of validity of this quark model Q_0 by evolving according to the QCD evolution equations. In particular, the Parton Distribution Functions of the pion have been found to be in a surprisingly good agreement with the data, once evolved to Leading-Order. We have also considered the Next-to-Leading-Order evolution, and we have reached the conclusion that the effect of the NLO evolution has been compensated at LO in the adaptation of the low model's scale Q_0. On the other hand, the Distribution Amplitude of the pion calculated in the NJL model have been found to be in a good although less impressive agreement with the data.

The conclusions that we can draw from the analysis of the pion PDF and DA also follow from the questions of the support property as well as the end-point behavior. First, we conclude that the conservation of covariance on the light-cone is a must-have feature of the model that one would have chosen for the analyses of distribution functions. We have actually learned that the support property is closely related to this symmetry, which is respected in the NJL model. Second, we emphasize the importance of perturbative QCD when going to higher energies in which the experiments are performed. We therefore advocate discarding some models only after having evolved their results to a perturbative scale.

Given the symmetries it respects, and the good results it has led to, the NJL model, with all its merits and faults, can be considered as a realistic model for the pion not only for low energy observables, but also for the determination of the Parton Distributions. The emergent image of the pion is that it is basically determined by the chiral symmetry.

Chapter 3 has been devoted to the *Generalized Parton Distributions* of the pion. In particular, the results of Ref. [153] have been displayed together with the parameterization of GPDs via Double Distributions [171]. The expected support and the polynomiality for the GPD of the pion have been obtained. There is no relevant discrepancy between the results obtained in the NJL model and the other calculations, e.g. [45, 171], before and after QCD evolution. The agreement after evolution gives us confidence on the evolution code [94] that we have used.

In Chapter 4, we have principally presented our results for the pion-photon vector and axial *Transition Distribution Amplitudes*, respectively $V(x,\xi,t)$ and $A(x,\xi,t)$ [67, 68, 69]. We have

used the formalism developed in Chapter 2: the Bethe-Salpeter amplitude for the pion has been constructed with the quark-pion vertex function coming from the Nambu-Jona Lasinio model. This technique allows for numerical predictions. Also, the Pauli-Villars regularization procedure has been applied in order to preserve gauge invariance.

The definition of these pion-photon TDAs have been displayed in Section 4.2. The Partial Conservation of the Axial Current tells us that the axial current couples to the pion. Therefore, in order to properly define the axial TDA, namely with all the structure of the incoming hadron included in $A(x,\xi,t)$, the pion pole contribution must be extracted. By doing so, we have found that the axial TDA had, in the NJL model and the handbag approximation, two different contributions: the first one is related to a direct coupling of the axial current to a quark of the incoming pion and to a quark coupled to the outgoing photon. The second one is related to the non-resonant part of a quark-antiquark pair coupled with the quantum numbers of the pion. The presence of the latter contribution guarantees the gauge invariance of the axial TDA.

The use of a fully covariant and gauge invariant approach guarantees that all the fundamental properties of the TDAs will be recovered. In this way, the right support, $x \in [-1,1]$, has been obtained and the sum rules, together with the polynomiality expansions, have been recovered. We want to stress that these three properties are not inputs, but they are results springing from our calculation [67]. The value obtained in the NJL model for the vector Form Factor is in agreement with the experimental result provided in the Particle Data Group [11], whereas the value found for the axial Form Factor is two times larger than the ones found in the PDG [11]. This discrepancy is a common feature of quark models as it has been obtained in different calculations [44, 127]. Also, the neutral pion vector Form Factor $F_{\pi\gamma^*\gamma}(t)$ is well described, reproducing the value given by the anomaly [39]. These results allow us to assume that the NJL model gives a reasonable description of the physics of those processes at this energy regime.

Turning our attention to the polynomial expansion of the TDAs, it has been shown that, in the chiral limit, only the coefficients of even powers in ξ were non-null for the vector TDA [67]. No constrain has been obtained for the axial TDA. Nevertheless, the NJL model have provided for simple expressions for the coefficients of the polynomial expansions in the chiral limit (4.43).

We have obtained quite different shapes for the vector and axial TDAs. At least for the DGLAP regions, this is in part due to the isospin relation

$$V(x,\xi,t) = -\frac{1}{2}V(-x,\xi,t)\,, \qquad A(x,\xi,t) = \frac{1}{2}A(-x,\xi,t)\,, \qquad\qquad |\xi| < x < 1 \quad .$$

The difference in the shapes is also due to the non-resonant part of the qq interacting pair diagram for the axial TDA in the ERBL region. It is interesting to inquire about the domain of validity of the previous relations. These relations are obtained from the isospin trace calculation involved in the central diagram of Fig. 4.8. Due to the simplicity of the isospin wave function of the pion, these results are more general than the NJL model, and therefore more general than a result of the diagrams under consideration, which are the simplest contributions of the handbag type.

Since there exist other model calculations as well as phenomenological approaches of the pion-photon TDAs [44, 127, 131, 199], a qualitative comparison and/or criticism of our approach was in order. This has been done in Section 4.7, where the Double Distributions for the TDAs have been defined. We have concluded that there is no disagreement between the different studies concerning the π-γ TDAs, besides some ambiguities in the definition of the skewness variable.

The TDAs, calculated, as a first step, for pion-photon transitions, have led to interesting estimates of cross section for exclusive meson pair production in $\gamma^*\gamma$ scattering. These processes involve

photon-pion transitions. Also, the symmetries relating the different transitions, e.g., $\pi^+ \to \gamma$ to $\gamma \to \pi^-$ have been displayed. In Chapter 5 we have presented our results for a phenomenological application of the TDAs [70]. We have examined the expected cross section for π-π and π-ρ production in exclusive $\gamma^*\gamma$ scattering in the forward kinematical region, by using realistic models for the description of the pion. First, we have confirmed the previous estimates for ρ production obtained in Ref. [131], even if our results for the cross section are larger of a factor 2. Second, in comparison with this previous evaluation of the cross sections, we have improved our findings by considering the effect of QCD evolution on the vector current. By so doing, an additional factor 5 has appeared in the small ξ region, leading to a cross section for ρ production of one order of magnitude larger than the previous calculation. We have also ameliorated by including the pion pole term in the tensorial decomposition of the axial current. Then, an even larger enhancement factor, of about 60 in this case, has been found in the cross section for pion production. The interference term has become larger by a factor 15 with respect to the pure TDA contribution, making the axial TDA more accessible experimentally.

Besides the structure of the pion, we have also been interested in semi-inclusive processes involving Parton Distributions of the proton. Since the features of the proton are rather different than the pion's one, the description of the proton requires the use of models whose properties are adequate for that problem. In particular, we have used two models for the proton which do not include the realization of the chiral symmetry but rather confinement: the NR Constituent Quark Model of Isgur-Karl as well as the MIT bag model.

We now draw some conclusions on this part of the thesis, which discusses the Sivers function. In Chapter 6 we have presented our results for the calculation of the Sivers function in the two models described above. The formalism that we have developed in Ref. [66] for the evaluation of the Sivers function is rather general as it can be used in any Constituent Quark Model. The crucial ingredient of this calculation has been the Non Relativistic reduction of the leading twist part of the One-Gluon Exchange diagram in the final state. It has been shown that the Isgur-Karl model, based also on a OGE contribution to the Hamiltonian, is a proper framework for the estimate of the Sivers function. The obtained results show a sizable effect, with an opposite sign for the u and d flavors. This is in agreement with the pattern found from an analysis of impact parameter dependent GPDs in the IK model [93] and allows for the fulfillment of the Burkardt sum rule. More precisely, this sum rule is verified with a precision of a few percents. The connection of the Sivers function with Impact Parameter Dependent PDs deserves a careful analysis and will be discussed elsewhere. In particular, some future directions of work are given in a next Section.

The Sivers function calculated in the MIT bag model has been revised [72], and now it fulfills the Burkardt sum rule to a level of 5%. Comparing this encouraging outcome with that of the CQM, one can say that the Burkardt sum rule is better fulfilled in the CQM. Most probably this has to do with the fact that the Burkardt sum rule is associated with transverse momentum conservation. The evolved Sivers functions, as obtained in both models, show an impressive agreement with data. We would like to remark that the data are described rather well for both flavors.

In conclusion, we want to stress that we have established, for the first time, that correct model calculations provide phenomenological successful interpretations of the Sivers function, which are consistent with each other.

In what follows, we present the possible future directions for both lines of work, trying to merge

Spin Physics together with pion structure in the very last Section.

The Future of Transition Distribution Amplitudes

In Chapters 4 and 5, we have introduced the concept of *Transition Distribution Amplitudes* as an extension of Distribution Amplitudes as well as of Generalized Parton Distributions. We have presented the results in a model calculation, namely in the NJL model, and compared with different model calculations carried out until now. The mesonic TDAs have been applied in the estimation of the cross section for meson pair production in two-photon processes, awaiting experimental data.

A glimpse of distribution parameterizations have been given including phenomenological modeling. In this short Section, we mention some other approaches and applicability frameworks for TDAs.

Besides the parameterization through the Radyushkin's Double Distribution, there exists the so-called Dual Representation [170, 172]. Duality comes by representing the parton distributions as an infinite series of distribution amplitudes in the t-channel, obtained by decomposing the GPDs in t-channel partial waves. This representation leads to an alternative parameterization of GPDs with respect to (4.66).

A further study of the TDAs as parameterizing the processes (5.1) through this representation should lead to interesting, model-independent results. The latter could, in turn, be compared with the model-dependent estimations of the cross sections given in Section 5.4. The inclusion of the pion pole contribution renders more appealing the modeling. Moreover, its study is justified, from the experimental point of view, by the enhancement of the cross section for $\pi^+\pi^-$ production in $\gamma^*\gamma$ scattering due to the presence of the pion pole amplitude.

Among the processes involving the TDAs as the large-distance part, the process $\gamma^*\gamma \to \pi\pi$ is particularly interesting because different kinematical regimes lead to different mechanisms. This implies a description of the process through either the pions GDA or the pion-photon TDAs [13]. As it is depicted on Fig. 7, there is a duality in the factorization mechanisms in describing the fusion of a real photon with highly-virtual and longitudinally polarized photon. According to the kinematical regime, i.e.,

(a) $s \ll Q^2$ while t is of order Q^2;

(b) $t \ll Q^2$ while s is of order Q^2;

(c) $s, t \ll Q^2$;

(d) $s, t \sim Q^2$;

the process will factorize following the GDA[1] (regime (a)) or the TDA (regime (b)) mechanism. In addition there exists a kinematical domain, namely the regime (c), in which both mechanisms act in parallel, giving rise to duality in this region. The model-dependency of the GDA and its impact on duality is nevertheless pointed out. The regime (d) corresponds to the large angle scattering *à la* Brodsky-Lepage.

This interplay between kinematical regimes leads us to think that it would be interesting to deepen our understanding of the description of this process through the analysis of the twist-3 pion

[1]The twist-3 GDA here is selected by the $\gamma^*_L\gamma_T$ initial state.

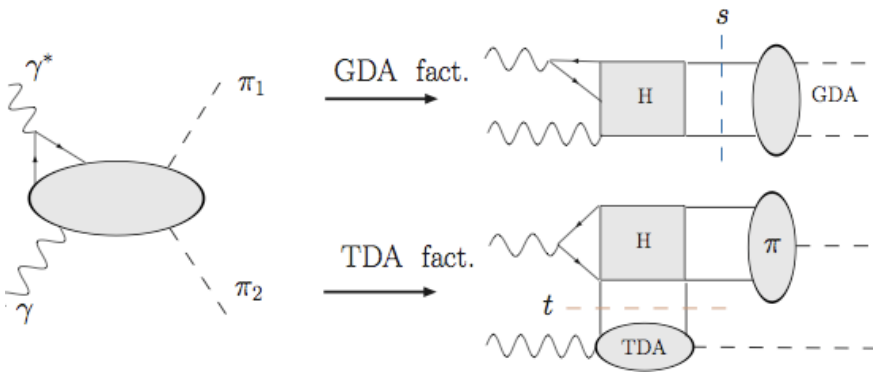

Figure 7.1: GDA vs. TDA factorization. From Ref. [13].

GDA, e.g. in the NJL model.

In conclusion, the meson-photon transitions lead to many possible applications that represent a natural follow-up of the work displayed in this thesis.

The Internal Spin Structure of the Pion

Complementarily to what has been explained in the previous Chapter, it has been shown that, even if the target is unpolarized, the momentum distribution of its quarks ejected in SIDIS can already exhibit a left-right asymmetry of the intrinsic transverse quark momentum k_T relative to their own transverse spin s_T [35]. The Boer-Mulders function is defined as the modulation of the probability density due to the correlation between these two variables, via the $\Phi^{[\sigma^{+j}\gamma_5]}$ of the decomposition (1.28),

$$\Phi^{[\sigma^{+j}\gamma_5]\,q}(x,\vec{k}_T,s) \quad = \quad f_1^q(x,k_T) - \frac{\epsilon_T^{ij} s_{Ti} k_{Tj}}{M} h_1^{\perp q}(x,k_T) \tag{7.1}$$

Like the Sivers function, the function $h_1^{\perp q}(x,k_T)$ requires the presence of Final State Interactions to allow different orbital angular momentum combinations.

Obviously, one of the outlooks of this thesis would be to calculate the Boer-Mulders function in both the 1 and 3-body models in which we already have calculated the Sivers function. This calculation is going to be completed very soon [73].

Another future perspective is related to the first part of this thesis, and it concerns the non trivial spin structure of the pion.

Since the pion has spin zero, its longitudinal spin structure in terms of quark and gluon degrees of freedom is trivial. However, it would be of interest to investigate the transverse spin structure of the pion, which, in the case of a spinless hadron, would come from a modulation of the number density due to the interplay between the transverse spin of the quarks and another intrinsic variable. The latter is namely either the momentum k_T or the Impact parameter $b_\perp$, which gives the distance between the center of momentum of the hadron in the plane transverse to its motion as shown on Fig. 7.2.

Following the example of the intuitive determination of the sign of the Sivers function from the E GPD (1.13), one expects that the sign of the Boer-Mulders function can be related to the distribution of transversely polarized quarks in the Impact Parameter space [51].

Little is known about both the Impact Parameter Dependent (IPD) distribution under scrutiny and the Boer-Mulders function. This holds both from the experimental and theoretical point of views. However, what motivates our project is the existence of the first lattice results for the Form Factors in momentum space of the concerned pion GPD [43].
Our proposal idea is basically to apply the formalism developed in Chapter 2 for the calculation of pion distribution in the NJL model to the calculation of the pion IPD distribution of transversely polarized quarks. In this way, we hope to gain some insight about the possible ansatz linking the pion GPD calculated in the impact parameter space, i.e. correlations between the impact parameter and the intrinsic transverse spin of the quarks, to the Boer-Mulders function. However, such relations involve a non trivial association of a spatial variable $b_\perp$ and a momentum $k_\perp$. It is henceforth a tantalizing goal to obtain model independent relations. So that one should restrain itself to global considerations, such as the relative signs. The latter can be afterwards compared with the result in the Lattice.

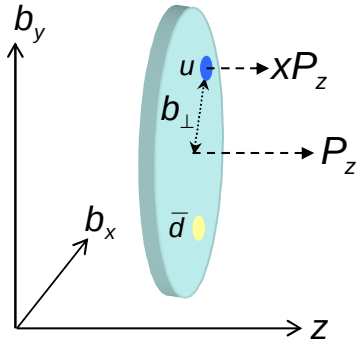

Figure 7.2: Illustration of the GPDs of the π^+ in the impact parameter space.

The IPD distributions have been proven to be related to the GPDs at zero skewness [47]. The Fourier transform of the charge density defined with respect to the impact parameter can be associated, without ambiguity, with the charge density as a function of the impact parameter in the Infinite Momentum Frame [47]. The same can be done for the GPDs, but only for $\xi = 0$. In other words, the GPDs at zero skewness allow a simultaneous measurement of the light-cone momentum and transverse position, i.e. impact parameter, distributions of partons in a hadron

$$F(x;\vec{b}_\perp) \;=\; \int \frac{d^2\Delta_\perp}{(2\pi)^2}\, e^{-i\vec{\Delta}_\perp\cdot\vec{b}_\perp}\, F(x,\xi=0-;\vec{\Delta}_\perp^{\,2}) \quad . \tag{7.2}$$

We now consider the transverse quark polarization, which is the only one allowed since the helicity-flip of the state is forbidden for the pion. Quarks with transverse polarization s_T are projected out by the operator $\frac{1}{2}\bar{q}\,[\gamma^+ - s^j\, i\sigma^{+j}\gamma_5]q$. Their density is therefore

$$\frac{1}{2}\left[F^\pi(x;\vec{b}_\perp) + s^i\, F_T^{i\,\pi}(x;\vec{b}_\perp)\right] \quad ,$$

i.e. a combination of the unpolarized (3.1) and polarized one. The latter IPD parton distribution is given by the chiral-odd twist-2 pion GPD, which is allowed by flipping the quarks' helicity. It is

defined as

$$F_T^{j\pi}(x,\xi,t) = \frac{-i}{2}\int \frac{dz^-}{2\pi}\, e^{ixz^-p^+} \left\langle \pi(P') \left| \bar{q}\left(-\frac{z}{2}\right) \sigma^{+j}\gamma_5\, q\left(\frac{z}{2}\right)\right| \pi(P)\right\rangle |_{z^\perp=z^+=0} \quad ,$$

$$= \frac{1}{2\,p^+}\,\frac{\epsilon^{+j\alpha\beta}\Delta_\alpha p_\beta}{\Lambda}\,\tilde{H}_T^\pi(x,\xi,t) \quad , \tag{7.3}$$

where a natural choice for some hadronic scale, say Λ, would be m_N in the nucleon case. [2]This scale is rather chosen to be $\Lambda = 4\pi\, f_\pi$ in Ref. [53] in order to avoid discussion within the chiral limit. However, the chiral limit has been studied in Ref. [83] showing that the choice $\Lambda = m_\pi$ is totally justified.

The Fourier transform (7.2) of the chiral-odd distribution $F_T^{j\pi}(x,\xi,t)$ leads to a derivative of the IPD distribution with respect to b^2;

$$\frac{1}{p^+}\left(H^\pi(x;\vec{b}_\perp) + \epsilon^{ij}\, s^i\, b^j\, \frac{2}{m_\pi}\,\frac{\partial}{\partial b^2}\,\tilde{H}_T^{\pi^+}(x;\vec{b}_\perp)\right) \quad .$$

The dipole term, as expected, leads to a dependence on the direction of $b_\perp$ for fixed s_T. The sign of this contribution seems to be opposite the the one of the Boer-Mulders function (def-bm). In other words, the IPD $\tilde{H}_T^{\pi^+}$ describes a sideways shift in the distribution of transversely polarized quarks in an unpolarized proton which has the opposite sign than the Boer-Mulders function.

In order to give such an estimation in the NJL model, the chiral-odd pion GPD defined in Eq. (7.3) has to be calculated using the formalism described in Section 2.1. In particular, the result reads

$$\tilde{H}_T^{\pi^+}(x,\xi,t) = i\,8m^3 N_c\, g_{\pi qq}^2\, \tilde{I}_3^{GPD}(x,\xi,t) \quad . \tag{7.4}$$

After that, the procedure is as described above: we first Fourier transform to the Impact Parameter space, and then match the sign conventions with the one used by, e.g., the Lattice Collaborations to finally yield our prediction for the sign of the Boer-Mulders function for SIDIS off pions.

A study of the Boer-Mulders function in the quark-spectator-antiquark *NJL-like* model is provided in Ref. [143]. The sign for the Boer-Mulders function is found to be negative. On the other hand, a naïve approach of IPD pion distribution function has been given in Ref. [53], where a positive sign for the distribution function was found. We thus expect a negative $h_{1\,\pi}^\perp$, a result that our calculation should either confirm or invalidate [71].
Lattice calculations nevertheless yield the same sign. For example, the latest lattice calculations [43] give access to x-moments of the quark spin densities $\rho^n(\vec{b}_\perp^{\,2}, s_\perp)$. They are obtained from the generalized Form Factors in momentum space by applying the Fourier transform (7.2). In turn, the generalized Form Factors are obtained through the usual recipe of taking the Mellin moments of the GPDs. The results are shown on Fig. 7.3.

[2] Note that, by analogy to the nucleon case, the standard nomenclature is E_T^π or $\bar{E}_T^\pi$ instead of $\tilde{H}_T^\pi$.

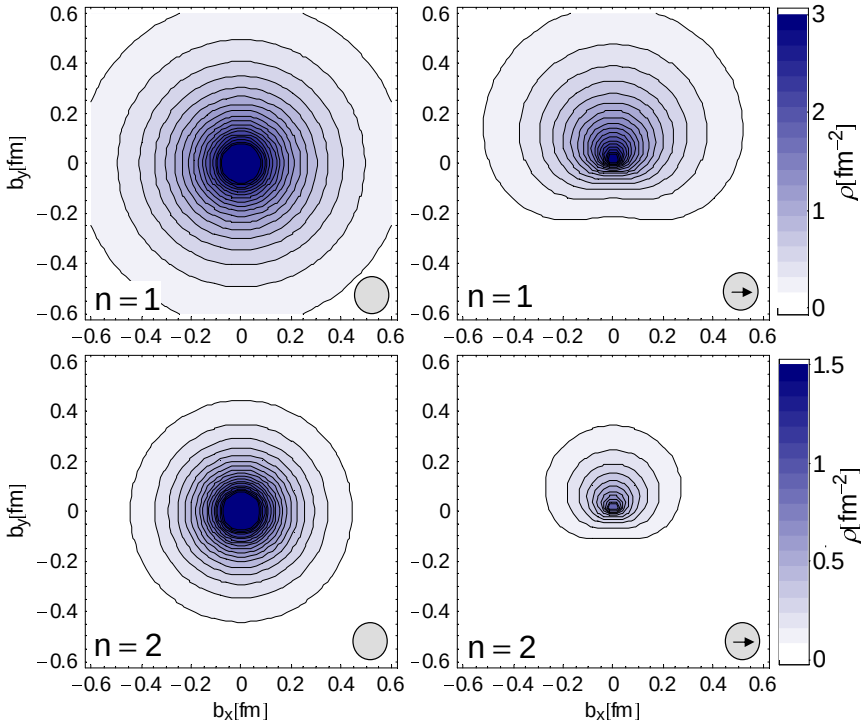

Figure 7.3: The lowest moment of the densities of unpolarized (left) and transversely polarized (right) up quarks in a π^+ in the lattice [43]. The quark spin is oriented in the transverse plane, as indicated by the arrow.

A Final Word...

We conclude this extended outlook by saying that the possibilities of learning something more about the partonic structure of pions and protons seem to be infinite! Hopefully, we will be able to unveil many secrets of the hadron's spin structure by performing simple and intuitive calculations, which can be implemented by phenomenological insights.

A Notations and Conventions

In this work, natural units are adopted,

$$\hbar = c = 1 \quad . \tag{A.1}$$

The metric tensor is

$$g^{\mu\nu} \quad = \quad g_{\mu\nu} = \mathrm{diag}(+1, -1, -1, -1) \quad . \tag{A.2}$$

A.1 Light-Cone Vectors

Here we first define the vector components in terms of light-cone variables and then, the Sudakov parametrization [28].
A four-vector is generically written as

$$a^{\mu} \quad = \quad (a^0, a^1, a^2, a^3) \quad . \tag{A.3}$$

We define the light-cone components

$$a^{\pm} \quad = \quad \frac{1}{\sqrt{2}}(a^0 \pm a^3) \quad , \tag{A.4}$$

hence a^{μ} has the form

$$a^{\mu} \quad = \quad (a^+, \vec{a}^{\perp}, a^-) \quad , \tag{A.5}$$

with $\vec{a}^{\perp} = (a^1, a^2)$.

The scalar product of two vectors is

$$a.b = a^+b^- + a^-b^+ - \vec{a}^{\perp}.\vec{b}^{\perp} \quad , \tag{A.6}$$

while the norm is

$$a^2 = 2a^+a^- - \vec{a}^{\perp 2} \quad . \tag{A.7}$$

We introduce the light-like vectors, i.e. vectors which norm is zero,

$$\begin{aligned} \bar{p}^{\mu} &= \frac{p^+}{\sqrt{2}}(1,0,0,1) \quad , \\ &= p^+\,(1,\vec{0}^{\perp},0) \quad , \\ n^{\mu} &= \frac{1}{p^+\sqrt{2}}(1,0,0,-1) \quad , \\ &= \frac{1}{p^+}(0,\vec{0}^{\perp},1) \quad , \end{aligned} \tag{A.8}$$

and those vectors have the following properties

$$\begin{aligned} \bar{p}^2 = n^2 &= 0 \quad , \\ \bar{p}.n &= 1 \quad , \\ n^+ = p^- &= 0 \quad . \end{aligned} \tag{A.9}$$

It is convenient to introduce the light-cone decomposition (also called Sudakov decomposition) for a vector

$$\begin{aligned} a^{\mu} &= \alpha\bar{p}^{\mu} + a^{\perp\mu} + \beta n^{\mu} \quad , \\ &= (a.n)\bar{p}^{\mu} + a^{\perp\mu} + (a.\bar{p})n^{\mu} \quad , \end{aligned} \tag{A.10}$$

with $a^{\perp\mu} = (0, \vec{a}^{\perp\mu}, 0)$.

In a "light-cone basis" the metric tensor $g^{\mu\nu}$ has non-zero components $g^{+-} = g^{-+} = 1$ and $g^{11} = g^{22} = -1$. Moreover we can construct the perpendicular metric tensor

$$g^{\mu\nu\perp} = g^{\mu\nu} - (\bar{p}^{\mu}n^{\nu} + \bar{p}^{\nu}n^{\mu}) \quad . \tag{A.11}$$

A.2 Pauli Matrices

The Pauli matrices will often be used in the form $\vec{\tau}$, where

$$\underline{\tau} = (\tau^+, \tau^3, \tau^-) \quad , \tag{A.12}$$

with

$$\tau^{+} = \frac{1}{2}(\tau^{1} + i\tau^{2}) \quad \text{and } \tau^{-} = \tfrac{1}{2}(\tau^{1} - i\tau^{2}) \quad , \tag{A.13}$$

where $\tau^{i} = \sigma^{i}$, i.e. the usual Pauli matrices. In the text, the notation $\vec{\tau}$ refers to

$$\vec{\tau} \;=\; (\tau^{\pi^{+}}, \tau^{\pi^{0}}, \tau^{\pi^{-}}) \quad , \tag{A.14}$$

with

$$\tau^{\pi^{+}} = \frac{1}{\sqrt{2}}(\tau^{1} + i\tau^{2}) \quad \text{and } \tau^{-} = \tfrac{1}{\sqrt{2}}(\tau^{1} - i\tau^{2}) \quad . \tag{A.15}$$

Hence, we have the following results

$$\tau^{+} = \begin{pmatrix} 0 & 1 \\ 0 & 0 \end{pmatrix} \quad , \quad \tau^{-} = \begin{pmatrix} 0 & 0 \\ 1 & 0 \end{pmatrix}, \tag{A.16}$$

$$\tau^{-}\tau^{+} = \begin{pmatrix} 0 & 0 \\ 0 & 1 \end{pmatrix} \quad , \quad \tau^{+}\tau^{-} = \begin{pmatrix} 1 & 0 \\ 0 & 0 \end{pmatrix} \quad . \tag{A.17}$$

Therefore, the following relation can be written

$$\begin{aligned} (\tau^{\pi^{+}}, \tau^{\pi^{0}}, \tau^{\pi^{-}}) \;&=\; (\sqrt{2}\tau^{+}, \tau^{3}, \sqrt{2}\tau^{-}) \quad , \\ &=\; \left(\sqrt{2}\begin{pmatrix} 0 & 1 \\ 0 & 0 \end{pmatrix}, \begin{pmatrix} 1 & 0 \\ 0 & -1 \end{pmatrix}, \sqrt{2}\begin{pmatrix} 0 & 0 \\ 1 & 0 \end{pmatrix}\right) \quad . \end{aligned} \tag{A.18}$$

B Discrete Symmetries

In this Chapter, we treat the discrete symmetries that link the distributions for a same kind of particle among themselves. General relations are given and then applied to the particular cases of pion DAs and TDAs.

For a generic particle $\mathcal{P}$ with momentum $\vec{p}$, spin projection s_z and charge Q_i, we write the particle state $|\mathcal{P}(\vec{p}, s_z, Q_i)\rangle$. Parity, time reversal invariance and charge conjugation act on this generic state in the following way

$$\begin{aligned} P|\mathcal{P}(\vec{p}, s_z, Q_i)\rangle &= \eta_P|\mathcal{P}(-\vec{p}, s_z, Q_i)\rangle \quad , \\ T|\mathcal{P}(\vec{p}, s_z, Q_i)\rangle &= \eta_T\,(-1)^{s-s_z}|\mathcal{P}(-\vec{p}, -s_z, Q_i)\rangle \quad , \\ C|\mathcal{P}(\vec{p}, s_z, Q_i)\rangle &= \eta_C|\mathcal{P}(\vec{p}, s_z, -Q_i)\rangle \quad , \end{aligned} \tag{B.1}$$

with η_P, η_T, η_C the respective phases. For the π^+, which is $J^{PC} = 0^{-+}$, are $\eta_P = \eta_T = -1, \eta_C = 1$.

In the light-front, the T symmetry as defined by the second expression of Eq. (B.1) changes x^+ to $-x^-$ and vice versa. It is therefore useful to define the V symmetry has the combination P_zT, what gives

$$V|\mathcal{P}(\vec{p}, s_z, Q_i)\rangle = \eta_V\,(-1)^{s-s_z}|\mathcal{P}(\vec{p}, -s_z, Q_i)\rangle \quad , \tag{B.2}$$

with $\eta_V = \eta_P\eta_T$.

The distribution functions for a generic transition between the state $\mathcal{P}(\vec{p}, s_z, Q_i)$ to the state

$\mathcal{P}'(\vec{p}', s'_z, Q_i)$ are associated to

$$\begin{aligned}&\frac{1}{2P^+}\,\mathcal{G}^{\mathcal{P}\to\mathcal{P}'}_{q\to q'}(x,\vec{p},s_z,\vec{p}',s'_z)\\&=\frac{1}{2}\int\frac{dz^-}{2\pi}\,e^{ixP^+z^-}\,\langle\mathcal{P}'(\vec{p}',s'_z,Q_i)|\bar{\psi}_{q'}\left(-\frac{z^-}{2}\right)\Gamma\psi_q\left(\frac{z^-}{2}\right)|\mathcal{P}(\vec{p},s_z,Q_i)\rangle,\end{aligned}\tag{B.3}$$

where $\mathcal{P}$ and $\mathcal{P}'$ can be different particles as well as the vacuum.

Let us now apply the definitions of the discrete symmetries to the generic distribution (B.3) :

- Time reversal, as given in its light-cone version by Eq. (B.2), transforms our generic distribution in the following way

$$\mathcal{G}^{\mathcal{P}\to\mathcal{P}'}_{q\to q'}(x,\vec{p},s_z,\vec{p}',s'_z) \;=\; \left(\zeta_V\,\eta_V\eta'_V(-1)^{s+s'-s_z-s'_z}\right)^*\mathcal{G}^{\mathcal{P}'\to\mathcal{P}}_{q'\to q}(x,\vec{p}',-s'_z,\vec{p},-s_z)\quad,$$

  with ζ_V related to the nature of the current, i.e. $\zeta_V=1$ for $\Gamma=1,i\gamma_5,\gamma_\mu$ while $\zeta_V=-1$ for $\Gamma=\gamma_\mu\gamma_5,\sigma_{\mu\nu}$.

- Similarly, applying charge conjugation, Eq. (B.1), we find

$$\mathcal{G}^{\mathcal{P}\to\mathcal{P}'}_{q\to q'}(x,\vec{p},s_z,\vec{p}',s'_z) \;=\; \zeta_C\,\eta_C\eta'_C\,\mathcal{G}^{\bar{\mathcal{P}}\to\bar{\mathcal{P}}'}_{\bar{q}\to\bar{q}'}(-x,\vec{p},s_z,\vec{p}',s'_z)\quad,$$

  with $\zeta_C=1$ for $\Gamma=1,i\gamma_5,\gamma_\mu\gamma_5$ while $\zeta_C=-1$ for $\Gamma=\gamma_\mu,\sigma_{\mu\nu}$.

- By applying both the above results, we obtain, for the CPT symmetry

$$\mathcal{G}^{\mathcal{P}\to\mathcal{P}'}_{q\to q'}(x,\vec{p},s_z,\vec{p}',s'_z) \;=\; \zeta_{CPT}\,\mathcal{G}^{\bar{\mathcal{P}}'\to\bar{\mathcal{P}}}_{\bar{q}'\to\bar{q}}(-x,\vec{p}',-s'_z,\vec{p},-s_z)\quad,$$

  where $\zeta_{CPT}=\zeta_C\zeta_V$.

- Let us finally give the hermitian of the generic transition (B.3)

$$\left(\mathcal{G}^{\mathcal{P}\to\mathcal{P}'}_{q\to q'}(x,\vec{p},s_z,\vec{p}',s'_z)\right)^* \;=\; \mathcal{G}^{\mathcal{P}'\to\mathcal{P}}_{q'\to q}(x,\vec{p}',s'_z,\vec{p},s_z)\quad.$$

We can now go to particular distribution functions:

- **Pion Distribution Amplitude**

  The pion DA would be

$$\begin{aligned}\mathcal{G}^{\pi^+\to 0}_{u\to d}((x-1/2),\vec{p},0) &= \int\frac{dz^-}{2\pi}e^{i(x-\frac{1}{2})p^+z^-}\,\langle 0|\,\bar{q}\left(-\frac{z}{2}\right)\gamma^+\gamma_5\tau^-q\left(\frac{z}{2}\right)|\pi^+(p)\rangle\Big|_{z^+=z^\perp=0}\\&= i\sqrt{2}f_\pi\,\phi^{\pi^+}(x)\quad.\end{aligned}\tag{B.4}$$

The hermitian conjugate of $\mathcal{G}^{\pi^+\to 0}((x-\frac{1}{2}),\vec{p},0)$ is given by

$$\mathcal{G}^{0\to\pi^+}_{d\to u}((x-1/2),0,\vec{p}) \;=\; -i\sqrt{2}f_\pi\left(\phi^{\pi^+}(x)\right)^* \quad .$$

Using the relations Eq. (B.1), the time reversal invariance leads to

$$\left(\phi^{\pi^+}(x)\right)^* \;=\; \phi^{\pi^+}(x) \quad ;$$

charge conjugation to

$$\phi^{\pi^-}(x) \;=\; \phi^{\pi^+}(1-x) \quad ; \tag{B.5}$$

and CPT to

$$\left(\phi^{\pi^-}(1-x)\right)^* \;=\; \phi^{\pi^+}(x) \quad .$$

- **Vector Pion Transition Distribution Amplitudes**

The π^+-γ and γ-π^- vector TDAs are defined

$$\begin{aligned}
\mathcal{G}^{\pi^+\to\gamma}_{u\to d}(x,\vec{p},\vec{p}',\varepsilon) &= \int\frac{dz^-}{2\pi}e^{ixP^+z^-}\left\langle\gamma(p_\gamma\varepsilon)\left|\bar{q}\left(-\frac{z}{2}\right)\gamma^+\tau^-q\left(\frac{z}{2}\right)\right|\pi^+(p_\pi)\right\rangle|_{z^+=z^\perp=0}\\
&= \frac{1}{P^+}i\,e\,\varepsilon_\nu\,\epsilon^{+\nu\rho\sigma}\,P_\rho\,(p_\gamma-p_\pi)_\sigma\,\frac{V^{\pi^+\to\gamma}(x,\xi,t)}{\sqrt{2}f_\pi} \quad ,\\
\mathcal{G}^{\gamma\to\pi^-}_{\bar{d}\to\bar{u}}(x,\vec{p}',\vec{p},\varepsilon) &= \int\frac{dz^-}{2\pi}e^{ixP^+z^-}\left\langle\pi^-(p_\pi)\left|\bar{q}\left(-\frac{z}{2}\right)\gamma^+\tau^-q\left(\frac{z}{2}\right)\right|\gamma(p_\gamma\varepsilon)\right\rangle|_{z^+=z^\perp=0}\\
&= \frac{1}{P^+}i\,e\,\varepsilon_\nu\,\epsilon^{+\nu\rho\sigma}\,P_\rho\,(p_\pi-p_\gamma)_\sigma\,\frac{V^{\gamma\to\pi^-}(x,-\xi,t)}{\sqrt{2}f_\pi} \quad .
\end{aligned}$$

The skewness variable is defined as

$$\xi \;=\; (p_\pi-p_\gamma)^+/2P^+ \quad .$$

The hermitian conjugate of the $\pi^+\to\gamma$ vector TDA is given by

$$\left(\mathcal{G}^{\pi^+\to\gamma}_{u\to d}(x,\vec{p},\vec{p}',\varepsilon)\right)^* \;=\; \mathcal{G}^{\gamma\to\pi^+}_{d\to u}(x,\vec{p}',\vec{p},\varepsilon) \quad ;$$

$$\Rightarrow\boxed{\left(V^{\pi^+\to\gamma}(x,\xi,t)\right)^* = V^{\gamma\to\pi^+}(x,-\xi,t)} \quad .$$

Time reversal invariance leads to

$$\mathcal{G}^{\pi^+\to\gamma}_{u\to d}(x,\vec{p},\vec{p}',\varepsilon) \;=\; \eta_V\,\mathcal{G}^{\gamma\to\pi^+}_{d\to u}(x,\vec{p}',\vec{p},\varepsilon) \quad ,$$

$$\begin{aligned} i\,e\,\varepsilon_\nu\,\epsilon^{\mu\nu\rho\sigma}\,n_\mu \quad & P_\rho\,\frac{(p_\gamma-p_\pi)_\sigma}{\sqrt{2}f_\pi}\,V^{\pi^+\to\gamma}(x,\xi,t) \\ & = -i\,e\,\varepsilon_\nu\,\epsilon^{\mu\nu\rho\sigma}\,n_\mu P_\rho\,\frac{(p_\pi-p_\gamma)_\sigma}{\sqrt{2}f_\pi}\,V^{\gamma\to\pi^+}(x,-\xi,t) \quad , \end{aligned}$$

$$\boxed{V^{\pi^+\to\gamma}(x,\xi,t) = V^{\gamma\to\pi^+}(x,-\xi,t)} \quad ;$$

charge conjugation to

$$\mathcal{G}^{\pi^+\to\gamma}_{u\to d}(x,\vec{p},\vec{p}',\varepsilon) \;=\; \zeta_C\,\eta_C\,\mathcal{G}^{\pi^-\to\gamma}_{\bar{u}\to\bar{d}}(-x,\vec{p},\vec{p}',\varepsilon) \quad ,$$

$$\begin{aligned} i\,e\,\varepsilon_\nu\,\epsilon^{\mu\nu\rho\sigma}\,n_\mu \quad & P_\rho\,\frac{(p_\gamma-p_\pi)_\sigma}{\sqrt{2}f_\pi}\,V^{\pi^+\to\gamma}(x,\xi,t) \\ & = +i\,e\,\varepsilon_\nu\,\epsilon^{\mu\nu\rho\sigma}\,n_\mu P_\rho\,\frac{(p_\gamma-p_\pi)_\sigma}{\sqrt{2}f_\pi}\,V^{\pi^-\to\gamma}(-x,\xi,t) \quad , \end{aligned}$$

$$\boxed{V^{\pi^+\to\gamma}(x,\xi,t) = V^{\pi^-\to\gamma}(-x,\xi,t)} \quad ;$$

and CPT to

$$\mathcal{G}^{\pi^+\to\gamma}_{u\to d}(x,\vec{p},\vec{p}',\varepsilon) \;=\; \zeta_{CPT}\,\eta_C\eta_V\,\mathcal{G}^{\gamma\to\pi^-}_{\bar{d}\to\bar{u}}(-x,\vec{p}',\vec{p},\varepsilon) \quad ,$$

$$\begin{aligned} i\,e\,\varepsilon_\nu\,\epsilon^{\mu\nu\rho\sigma}\,n_\mu \quad & P_\rho\,\frac{(p_\gamma-p_\pi)_\sigma}{\sqrt{2}f_\pi}\,V^{\pi^+\to\gamma}(x,\xi,t) \\ & = -i\,e\,\varepsilon_\nu\,\epsilon^{\mu\nu\rho\sigma}\,n_\mu P_\rho\,\frac{(p_\pi-p_\gamma)_\sigma}{\sqrt{2}f_\pi}\,V^{\gamma\to\pi^-}(-x,-\xi,t) \quad , \end{aligned}$$

$$\boxed{V^{\pi^+\to\gamma}(x,\xi,t) = V^{\gamma\to\pi^-}(-x,-\xi,t)} \quad .$$

- **Axial Pion Transition Distribution Amplitudes**

The π^+-γ and γ-π^- axial TDAs are defined So that

$$\begin{aligned} & e\,\left(\vec{\varepsilon}^{\,\perp}\cdot(\vec{p}^{\,\perp}_\gamma-\vec{p}^{\,\perp}_\pi)\right)\frac{A^{\pi^+\to\gamma}(x,\xi,t)}{\sqrt{2}f_\pi} \\ & = \mathcal{G}^{\pi^+\to\gamma}_{u\to d}(x,\vec{p},\vec{p}',\varepsilon) + i\mathcal{G}^{\pi^+\to 0}_{u\to d}\left(\frac{x}{2\xi},\vec{p},0\right)\,2e\,\epsilon(\xi)\,\frac{\varepsilon\cdot(p_\gamma-p_\pi)}{m_\pi^2-t} \quad , \end{aligned}$$

$$\begin{aligned} & e\,\left(\vec{\varepsilon}^{\,\perp}\cdot(\vec{p}^{\,\perp}_\pi-\vec{p}^{\,\perp}_\gamma)\right)\frac{A^{\gamma\to\pi^-}(x,-\xi,t)}{\sqrt{2}f_\pi} \\ & = \mathcal{G}^{\gamma\to\pi^-}_{\bar{d}\to\bar{u}}(x,\vec{p}',\vec{p},\varepsilon) - i\mathcal{G}^{0\to\pi^-}_{\bar{d}\to\bar{u}}\left(\frac{x}{2\xi},\vec{p},0\right)\,2e\,\epsilon(-\xi)\,\frac{\varepsilon\cdot(p_\pi-p_\gamma)}{m_\pi^2-t} \quad , \end{aligned}$$

with $\epsilon(\xi) = 1$ for $\xi > 0$ and $\epsilon(\xi) = -1$ for $\xi < 0$.
The skewness variable is defined as

$$\xi \;=\; (p_\pi - p_\gamma)^+ / 2P^+ \quad .$$

Combining the results for $\mathcal{G}_{u\to d}^{\pi^+\to\gamma}(x,\vec{p},\vec{p}',\varepsilon)$ and for $\mathcal{G}_{u\to d}^{\pi^+\to 0}\left(\frac{x}{2\xi},\vec{p},0\right)$ we find the expressions for the axial TDAs.
The hermitian conjugate of the $\pi^+ \to \gamma$ axial TDA is given by

$$\begin{aligned}
&\left(e\,\left(\vec{\varepsilon}^{\perp}\cdot(\vec{p}_\gamma^{\perp}-\vec{p}_\pi^{\perp})\right)\frac{A^{\pi^+\to\gamma}(x,\xi,t)}{\sqrt{2}f_\pi} + e\,(\varepsilon\cdot(p_\gamma-p_\pi))\,\frac{2\sqrt{2}f_\pi}{m_\pi^2-t}\,\epsilon(\xi)\,\phi\left(\frac{x+\xi}{2\xi}\right)\right)^* \\
&= e\,\left(\vec{\varepsilon}^{\perp}\cdot(\vec{p}_\pi^{\perp}-\vec{p}_\gamma^{\perp})\right)\frac{A^{\gamma\to\pi^+}(x,-\xi,t)}{\sqrt{2}f_\pi} + e\,(\varepsilon\cdot(p_\pi-p_\gamma))\,\frac{2\sqrt{2}f_\pi}{m_\pi^2-t}\,\epsilon(-\xi)\,\phi\left(\frac{x+\xi}{2\xi}\right) \quad ,
\end{aligned}$$

$$\Rightarrow \boxed{\left(A^{\pi^+\to\gamma}(x,\xi,t)\right)^* = A^{\gamma\to\pi^+}(x,-\xi,t)} \quad .$$

Time reversal invariance leads to

$$\boxed{A^{\pi^+\to\gamma}(x,\xi,t) = A^{\gamma\to\pi^+}(x,-\xi,t)} \quad ;$$

charge conjugation to

$$\boxed{A^{\pi^+\to\gamma}(x,\xi,t) = A^{\pi^-\to\gamma}(-x,\xi,t)} \quad ;$$

and CPT to

$$\boxed{A^{\pi^+\to\gamma}(x,\xi,t) = A^{\gamma\to\pi^-}(-x,-\xi,t)} \quad .$$

Those relations remain unchanged under evolution.

C The Nambu - Jona-Lasinio Model

A pre-QCD model for the pion was introduced in 1961 by Y. Nambu and G. Jona-Lasinio with nucleon degrees of freedom [151, 152]. This study was motivated by the theory of superconductivity of Bardeen, Cooper and Schrieffer (BCS) and so built in analogy with it. The basic idea of the theory is that the mass of the "Dirac particles", in the case of the original paper of Nambu and Jona-Lasinio a nucleon, could be due to some interaction between massless fermions that have the same quantum numbers excepted chirality. In the same fashion as in the theory of superconductivity, the gap is caused by nucleon-nucleon interaction. Therefore, starting from a massless nucleon, i.e. an eigenstate of chirality, we arrive to a massive nucleon. This is the "solid state physics" formulation of the chiral symmetry breaking.

The lagrangian was contructed to conserve chirality and "nucleon number". In quark language, more precisely in a two-flavor quark model, it has to be understood as $SU_V(2) \times SU_A(2) \times U_V(1)$ in the second version of the model which exclude $U_A(1)$ in accordance with experiment. Transformations under the isospin $SU_V(2)$ symmetry and the chiral $SU_A(2)$ symmetry are respectively given by

$$\psi \to e^{-i\tau.\frac{\omega}{2}}\psi \quad , \quad \psi \to e^{-i\tau.\frac{\theta}{2}\gamma_5}\psi \quad , \tag{C.1}$$

with ω and θ the respective generators.
The NJL lagrangian density in its 2-flavor version is

$$\mathcal{L}_{NJL} \;=\; i\bar{\psi}\,\partial\!\!\!/\,\psi + G\Big[(\bar{\psi}\psi)^2 + (\bar{\psi}i\gamma_5\vec{\tau}\psi)^2\Big] \quad , \tag{C.2}$$

with $\psi = \begin{pmatrix} u \\ d \end{pmatrix}$.

C.1 The Chiral Symmetry Breaking

Nowadays it makes sense to speak about quark degrees of freedom instead of nucleons. The quark mass topic is quite puzzling: quark models give us high values while chiral symmetry seems to impose small quark mass. This can be understood by considering the average interaction of a quark with the other quarks in the mean-field approximation. The concept of constituent quark mass can then be introduced in opposition to current quark mass. The quark self-energy in a mean-field approximation is given by the Hartree-Fock (HF) approximation, Fig. C.1. This consists in considering perturbations around the free "massive" lagrangian $\mathcal{L}_0'$, i.e.

$$\mathcal{L}_0' = \mathcal{L}_0 + \mathcal{L}_\Sigma \quad , \tag{C.3}$$

where the self-energy lagrangian $\mathcal{L}_\Sigma = -\Sigma\,\bar{\psi}\psi$ is chosen in such a way that the interaction lagrangian does not contain any self-energy effect.

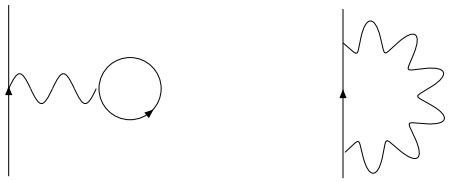

Figure C.1: The Hartree and Fock, respectively direct and exchange, contributions to the quark self-energy.

The total self-energy Σ is the sum of the scalar and pseudoscalar ones and is given by, in the HF approximation,

$$\begin{aligned} \Sigma &= \Sigma^s + \Sigma^{ps} \quad , \\ &= 2G\left\{\mathbb{T}\mathrm{r}\, iS(x,x) - iS(x,x) + (i\gamma_5\vec{\tau})\mathbb{T}\mathrm{r}\, iS(x,x)(i\gamma_5\vec{\tau}) - (i\gamma_5\vec{\tau})iS(x,x)(i\gamma_5\vec{\tau})\right\} \quad , \end{aligned} \tag{C.4}$$

where $S(x,x)$ is the quark propagator and satisfies

$$(i\,\partial\!\!\!/_x - m_0 - \Sigma)\,S(x,x') = \delta^4(x-x') \quad . \tag{C.5}$$

The current quark mass m_0 comes from $\mathcal{L}_0$.
Given the "observed" constituent quark mass m, the propagator $S(x,x)$ should also satisfy the following equation of motion

$$(i\,\partial\!\!\!/_x - m)\,S(x,x') = \delta^4(x-x') \quad , \tag{C.6}$$

so that $m - m_0 = \Sigma$. The solution of Eq. (C.5) in momentum space is then,

$$S(p) = \frac{p\!\!\!/ + m}{p^2 - m^2} \quad . \tag{C.7}$$

If we insert this result into the expression for the self-energy Eq. (C.4), performing the traces and noting that the integral odd in p does not contribute, we find

$$\Sigma = m - m_0 = 2iG\,(N_c N_f + \frac{1}{2}) \int \frac{d^4p}{(2\pi)^4} \frac{m}{p^2 - m^2} \quad . \tag{C.8}$$

At this point, it is a reasonable assumption to set the small current quark mass to $m_0 = 0$. Even if the exact chiral symmetry forbids mass terms in the Lagrangian, there exists a solution of the type $m \neq 0$ when the current quark mass is zero. Actually the equation Eq. (C.8) admits two solutions. The trivial one is $m = 0$ and is in agreement with symmetry requirements. The second and nontrivial one is

$$1 \;=\; 2iG\,N_c N_f \int \frac{d^4p}{(2\pi)^4}\frac{1}{p^2 - m^2} \quad . \tag{C.9}$$

This equation is called the self-consistency or gap equation in analogy with the nontrivial solution giving rise to the gap in the BCS theory. The non-trivial solution, as solution of the gap equation Eq. (C.9), exists if the value of the coupling strength G exceeds a critical value [151, 152].

Regarding the coefficient in front of the integral in (C.8), we observe that the first term, proportional to $G\,N_c$, comes from the direct diagram of Fig. C.1 (Hartree contribution), and that the second one, proportional to G, is the contribution of the exchange diagram (Fock contribution). We can understand the NJL model as an effective theory connected to QCD in the large N_c limit. In that case, $G\,N_c \sim \mathcal{O}(1)$ and $G \sim N_c^{-1}$. Therefore, since we can consider that we work in a N_c^{-1}-expansion, it is consistent to ignore the Fock contribution.

It would make sense to work out which of the two solutions is the ground-state solution. By analysing the vacua of both the trivial and non-trivial solutions, we can related them in a BCS variational vacuum fashion. The vacuum for the non-trivial solution $|0\rangle_m$ is expressed as a superposition of pairs of zero total momentum and zero total helicity over the trivial vacuum $|0\rangle_0$ [151, 152]. We consider the Dirac equation in both cases, and with similar initial conditions,

$$\begin{aligned} i\,\partial\!\!\!/\,\psi^0(x) &= 0 \quad , \\ (i\,\partial\!\!\!/ + m)\,\psi^m(x) &= 0 \quad , \end{aligned} \tag{C.10}$$

and decompose the respective fields into their Fourier's components

$$\psi^\alpha(x) \;=\; \sum_s \int \frac{d^4p}{(2\pi)^4}\left\{b^\alpha(\vec{p},s)u^\alpha(\vec{p},s)e^{ipx} + d^{\dagger\alpha}(\vec{p},s)v^\alpha(\vec{p},s)e^{-ipx}\right\} \quad , \tag{C.11}$$

for $\alpha = 0$ or m. The spinors for particles and antiparticles are respectively $u^\alpha(\vec{p},s)$ and $v^\alpha(\vec{p},s)$. The annihilation operators for particles and antiparticles are respectively $b^\alpha(\vec{p},s)$ and $d^\alpha(\vec{p},s)$. The annihilation operators for the fields ψ^0 and ψ^m are related to each other according to they have the same initial conditions. Therefore the vacua defined with respect to both fields, i.e.

$$\begin{aligned} b^0(\vec{p},s)|0\rangle_0 = d^0(\vec{p},s)|0\rangle_0 &= 0 \quad , \\ b^m(\vec{p},s)|0\rangle_m = d^m(\vec{p},s)|0\rangle_m &= 0 \quad , \end{aligned} \tag{C.12}$$

can also be related one to each other. It can be found [125]

$$|0\rangle_m \;=\; \prod_{p,s}\left\{\left(\cos\left[\frac{\phi(p)}{2}\right] + s\,\sin\left[\frac{\phi(p)}{2}\right]\right) b^{\dagger 0}(\vec{p},s)d^{\dagger 0}(-\vec{p},s)\right\}|0\rangle_0 \quad . \tag{C.13}$$

This is a BCS-like variational vacuum: a superposition of pairs of zero total momentum and zero total helicity. This is also called the Bogoliubov-Valatin approach because the operators that annihilate such a vacuum are found through a Bogoliubov-Valatin transformation [125]. The angle $\phi(p)$ is

determined by minimizing the vacuum energy $W[\phi(p)]_m =_m \langle 0|H|0\rangle_m$, obtaining $\tan[\phi(p)] = m/p$.

The energy difference of the two vacua $W_m - W_0$ is found to be negative [151, 152]. So $|0\rangle_m$ is the true vacuum and the nontrivial solution is the solution that minimizes the energy. In particular, minimizing the vacuum expectation value in the nontrivial solution case leads to the gap equation Eq. (C.9).

The true vacuum $|0\rangle_m$ is not invariant under $SU_A(2)$. The consequence is a (dynamical) breaking of the chiral symmetry $SU_A(2)$. In other words the interaction given by Eq. (C.2) between two massless quark with the same quantum numbers excepted chirality gives rise to the gap equation Eq. (C.9) and generates the constituent quark mass m.

C.2 Regularization

The gap equation Eq. (C.9),

$$1 \;=\; 2G\,N_c N_f\,I_1 \quad , \tag{C.14}$$

has not been resolved yet. In fact the integral I_1, given by Eq. (E.1), is divergent and we need to define a regularization scheme. The NJL interaction is a contact interaction that renders the theory nonrenormalizable. Therefore the parameters introduced by the regularization scheme are integrally part of the model in itself. The NJL model plus its regularization scheme is regarded as an effective theory of QCD.

Several regularization schemes have been studied. We mention the noncovariant 3-momentum cutoff scheme, the covariant 4-momentum cutoff scheme or the proper-time regularization [125].

In the study of PDFs, GPDs and TDAs, it is important to preserve Lorentz covariance and gauge invariance. The Pauli-Villars scheme fulfills these conditions. The idea of this scheme is to introduce the minimum number of regulating masses m_j and constants c_j in such a way that the result becomes finite. The following replacement is made

$$\int \frac{d^4p}{(2\pi)^4}\, f(p,m^2) \;\;\rightarrow\;\; \int \frac{d^4p}{(2\pi)^4} \sum_{j=0}^{2} c_j\, f(p,m_j^2) \quad , \tag{C.15}$$

with $m_j^2 = m^2 + j\Lambda^2$. We use the standard values given in [112] for the c_j coefficients, i.e. $c_0 = c_2 = 1$ and $c_1 = -2$. Λ and m are the regularization parameters. They are determined by calculating the pion decay constant f_π and the quark condensate [125]. For $f_\pi = 93\text{MeV}$ and $\langle \bar{u}u\rangle = \langle \bar{d}d\rangle = -(250\,\text{MeV})^3$, we obtain

$$\begin{aligned} m &= 241 \quad \text{MeV} \quad , \\ \Lambda &= 859 \quad \text{MeV} \quad . \end{aligned} \tag{C.16}$$

C.3 The Pion and the Sigma

In its two-flavor version, the NJL model Eq. (C.2) gives rise to 4 mesonic modes.

The scalar interaction is responsible for a isoscalar ($I = 0$) scalar $J^{PC} = 0^{++}$ mode. The scalar mode is associated with the σ-meson, also known as $f_0(600)$ [11]. The 0^{++} sector is both theoretically and experimentally complex. The scalar modes are difficult to solve because of their large decay widths.

The pseudoscalar channel is responsible for the isovector ($I = 1$) pseudoscalar $J^{PC} = 0^{-+}$ modes identified as the pions which are then the three Goldstone bosons coming from the chiral symmetry breaking.

There are two ways of expressing the pion. In the original paper [151, 152], Nambu and Jona-Lasinio consider the pion as a bound-state of two nucleons, what is nowadays reinterpreted as a bound-state of two quarks, and study it through the use of the Bethe-Salpeter (BS) equation in the ladder approximation. Another approach is to consider the effective interaction resulting from the exchange of a pion in the Random Phase Approximation (RPA). The two methods are identical.

Even though both approaches will be used in the next chapters, according to we are interested in pions as bound-states or in pion exchange, we choose to introduce here the pion as a bound-state through the Bethe-Salpeter equation.

The Bethe-Salpeter (BS) amplitude for the bound-state π with four-momentum P is given by

$$\vec{\chi}_P(x_1, x_2) \quad = \quad \langle 0|Tq(x_1)\bar{q}(x_2)|\vec{\pi}(P)\rangle \quad . \tag{C.17}$$

The NJL model contains a four-fermion interaction. In the ladder approximation, only direct diagrams are considered. In our case, this approximation is equivalent to considering the iteration of the simplest closed loop Fig. C.2 with the kernel $V(p, p'; P) = 2iG(i\,\gamma_5\vec{\tau})^2$. The equation of Bethe-Salpeter is easy to handle due to the point-like interaction of the NJL model.

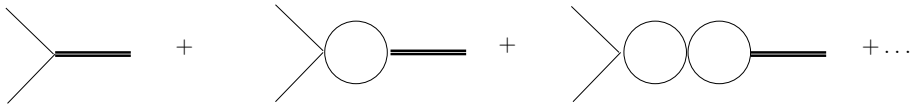

Figure C.2: Graphs corresponding to the BS equation in the ladder approximation. The thick line represents the bound-state.

The integral equation generated by the chain of diagrams Fig. C.2 is the Bethe-Salpeter equation [112]

$$iS^{-1}(p)\ \vec{\chi}_P(p)\ iS^{-1}(p-P) + \int \frac{d^4p''}{(2\pi)^4}\,\mathbb{T}\mathrm{r}\,\left(V(p,p'';P)\vec{\chi}_P(p'')\right) \quad = \quad 0 \quad , \tag{C.18}$$

here in momentum space. $S^{-1}(k) = \not{k} - m$ is the inverse of the Feynman quark propagator.

Solving the Bethe-Salpeter equation in the ladder approximation

$$iS^{-1}(p)\,\vec{\chi}_P(p)\,iS^{-1}(p-P) \quad = \quad G\gamma_5\vec{\tau}\int \frac{d^4p''}{(2\pi)^4}\,2\mathbb{T}\mathrm{r}\,\left(i\,\gamma_5\vec{\tau}.\vec{\chi}_P(p'')\right) \quad , \tag{C.19}$$

we find the expression for the Bethe-Salpeter amplitude

$$\vec{\chi}_P(p) \;=\; -g_{\pi qq}\, iS(p)\,\gamma_5\vec{\tau}\, iS(p-P) \quad . \tag{C.20}$$

Inserting the Bethe-Salpeter amplitude Eq. (C.20) back into the BS equation Eq. (C.18) gives a self-consistency condition

$$1 \;=\; 2G\,(-i)\int \frac{d^4p}{(2\pi)^4}\mathbb{T}\mathrm{r}\left(\gamma_5\tau^{\pi^-}\, S(p)\,\gamma_5\tau^{\pi^+}\, S(p-P)\right) \quad . \tag{C.21}$$

The integral represents the pseudoscalar proper polarization Π_{ps} shown in Fig. C.3. The mass of the pseudoscalar mode is obtained for $P^2 = m_\pi^2$. That is, the mass of the pion is found by solving the following equation

$$1 - 2G\,\Pi_{ps}(m_\pi^2) = 0 \quad . \tag{C.22}$$

We have completly defined the pion. By resolving Eq. (C.22) at $k^2 = m_\pi^2$, the mass m_π is found. Now we would like to show that the pion described in such a way is the researched Goldstone boson, i.e. that it has zero mass in absence of the current mass quarks. In order to solve such a problem, we allow a small current quark mass in the Lagrangian Eq. (C.2) of the type $-m_0\bar{\psi}\psi$ and solve Eq. (C.22).

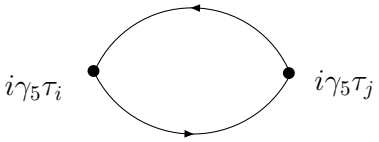

Figure C.3: The pseudoscalar proper polarization $\Pi_{ps}(k^2)$.

The proper polarization Fig. C.3 is explicitly given by

$$\begin{aligned}\Pi_{ps}(k^2) \;&=\; -i\int \frac{d^4p}{(2\pi)^4}\,\mathbb{T}\mathrm{r}\Big\{i\gamma^5\tau^{\pi^-}\, i\,\frac{\not{p}+\frac{1}{2}\not{k}+m}{(p+\frac{k}{2})^2-m^2}\; i\gamma^5\tau^{\pi^+}\, i\,\frac{\not{p}-\frac{1}{2}\not{k}+m}{(p-\frac{k}{2})^2-m^2}\Big\} \quad , \\ &=\; -i\,4N_cN_f\int \frac{d^4p}{(2\pi)^4}\,\frac{m^2-p^2+\frac{k^2}{4}}{[(p+\frac{k}{2})^2-m^2][(p-\frac{k}{2})^2-m^2]} \quad , \end{aligned} \tag{C.23}$$

where the change of variables $p = p + k/2$, with $P = k$, has been performed. We bring Eq. (C.23) into elementary integrals so that we can easily extract the pion mass m_π. The numerator can be reexpressed like $(m^2 - p^2 - \frac{k^2}{4}) + \frac{k^2}{2}$ and the denominator

$$\frac{1}{[(p+\frac{k}{2})^2-m^2][(p-\frac{k}{2})^2-m^2]} = \frac{1}{2[p^2+\frac{k^2}{4}-m^2]}\left(\frac{1}{[(p+\frac{k}{2})^2-m^2]}+\frac{1}{[(p-\frac{k}{2})^2-m^2]}\right) \quad . \tag{C.24}$$

So the pseudoscalar polarization Eq. (C.23) takes the form[1]

$$\Pi_{ps}(k^2) \;=\; 2N_cN_f[2I_1 - k^2 I_2(k^2)] \quad , \tag{C.25}$$

with I_1 and $I_2(k^2)$ respectively one and two-propagator integrals, see Appendix E. Moreover, the self-consistency condition Eq. (C.21) gives us the gap equation Eq. (C.14) when the mass of the bound-state is zero, i.e. $k^2 = 0$.

The first term on the right-hand side of Eq. (C.25) can be replaced by its expression in the gap equation Eq. (C.9). Adding a small current quark mass term to the gap equation, we find for I_1

$$8\,G\,N_cN_f\,I_1 \;=\; 1 - \frac{m_0}{m} \quad . \tag{C.26}$$

In doing so we obtain, using Eq. (C.22),

$$1 - 2G\Pi_{ps}(k^2) \;=\; \frac{m_0}{m} + 4\,G\,N_cN_f\,k^2\,I_2(k^2) \quad , \tag{C.27}$$

$$\;=\; 0 \quad . \tag{C.28}$$

For $k^2 = m_\pi^2$, we may deduce the mass of the pion

$$m_\pi^2 \;=\; -\frac{m_0}{m}\,\frac{1}{4\,G\,N_cN_f\,I_2(m_\pi^2)} \quad . \tag{C.29}$$

In the chiral limit, i.e. in the absence of current quark mass m_0, the mass of the pseudoscalar mode vanishes, as expected.

The quark-pion coupling constant $g_{\pi qq}$ has been determined by the standard normalization of the Bethe-Salpeter equation [112]

$$g_{\pi qq}^2 \;=\; \frac{-1}{12\left(I_2(m_\pi^2) + m_\pi^2\left(\frac{\partial I_2(P)}{\partial P^2}\right)|_{P^2=m_\pi^2}\right)} \quad , \tag{C.30}$$

with $I_2(p)$ given in Eq. (E.2).

Alternatively, we can determine the interaction properties of the bound-states in the NJL model through the study of $q\bar{q}$-scattering amplitudes [151, 152]. In the ladder approximation the bound-states are expected to be real stable particles. So should be the poles corresponding to the virtual exchange of, in the pseudoscalar channel example, pions. The bound-state is therefore the iteration of the bubble diagrams $\Pi_{ps}(k^2)$ in the pseudoscalar channel Eq. (C.3).

The scattering matrix Fig. C.4 generated by the exchange of a pion is then

$$iU_{ij}(k^2) \;=\; (i\gamma_5\tau^i)\left[2iG + 2iG(-i\Pi_{ps}(k^2))2iG + \ldots\right](i\gamma_5\tau^j) \quad ,$$

$$\;=\; (i\gamma_5\tau^i)\,\frac{2iG}{1 - 2G\Pi_{ps}(k^2)}\,(i\gamma_5\tau^j) \quad . \tag{C.31}$$

[1] A shift has been performed in order to obtain the $2I_1$ term. This still holds if one uses the Pauli-Villars regularization scheme. What is not obvious in other schemes.

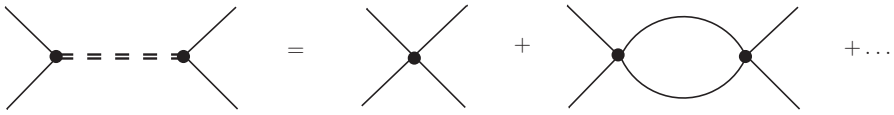

Figure C.4: Scattering matrix generated by the bubble diagram Fig. C.3.

The τ^i selects the appropriate channel. For exchanging a π^+, $\tau^i = \tau^{\pi^-}$ and $\tau^j = \tau^{\pi^+}$, vice versa for a π^- and $\tau^i = \tau^j = \tau^{\pi^0}$ for a π^0. This scattering matrix can be compared to the one coming from the minimal local interaction Lagrangian that describes the coupling of a pion field to quark fields. Namely, the effective pion exchange is

$$iU_{ij}(k^2) \;=\; (i\gamma_5\tau^i)\,\frac{-ig^2_{\pi qq}}{k^2-m^2_\pi}\,(i\gamma_5\tau^j) \quad . \tag{C.32}$$

Hence, in the light of Eq. (C.32), we can immediately determines the mass of the pion by finding the pole of Eq. (C.31) at $k^2 = m^2_\pi$. In other words, the self-consistency equation Eq. (C.21) of the Bethe-Salpeter equation comes to be the pole of Eq. (C.31)

$$1 - 2G\,\Pi_{ps}(k^2 = m^2_\pi) = 0 \quad . \tag{C.33}$$

In the same fashion, we can relate the quark-pion coupling constant to the residue at the pole Eq. (C.33)

$$g^2_{\pi qq} \;=\; \left(\frac{\partial\Pi_{ps}(k^2)}{\partial k^2}\right)^{-1}\Big|_{k^2=m^2_\pi} \quad . \tag{C.34}$$

With $\Pi_{ps}(k^2)$ given by Eq. (C.23), the expression Eq. (C.30) is recovered.

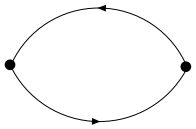

Figure C.5:

The mass of the scalar mode σ associated with the term $(\bar\psi\psi)^2$ can be obtained in the same fashion. The zero of the function $1-2G\Pi_s(k^2)$, with $\Pi_s(k^2)$ the scalar bubble diagram Fig. C.5, defines its mass m_σ. Also its coupling strength can be related to the residue of the pole at $k^2 = m^2_\sigma$.

The scalar loop is given as

$$\begin{aligned} -i\Pi_s(k^2) \;&=\; -\int \frac{d^4p}{(2\pi)^4}\,\mathbb{T}\mathrm{r}\Big\{\, i\,\frac{\not p + \frac{1}{2}\not k + m}{(p+\frac{k}{2})^2 - m^2}\;\; i\,\frac{\not p - \frac{1}{2}\not k + m}{(p-\frac{k}{2})^2 - m^2}\Big\} \quad , \\ &=\; -4N_cN_f\int \frac{d^4p}{(2\pi)^4}\,\frac{m^2 + p^2 - \frac{k^2}{4}}{[(p+\frac{k}{2})^2 - m^2][(p-\frac{k}{2})^2 - m^2]} \quad . \end{aligned} \tag{C.35}$$

Using the same trick as in the pseudoscalar case, i.e. writing Eq. (C.35) in terms of elementary integrals, we find

$$\Pi_s(k^2) \;=\; 2N_cN_f\,[2I_1 - (k^2 - 4m^2)\,I_2(k^2)] \quad . \tag{C.36}$$

As before the one-propagator integral is extracted from the gap equation and we find

$$1 - 2G\Pi_s(k^2) \;=\; \frac{m_0}{m} + 4\,G\,N_c N_f\,(k^2 - 4m^2)\,I_2(k^2) \quad , \tag{C.37}$$

which is exactly zero. On the pole $k^2 = m_\sigma^2$, we find

$$\begin{aligned} m_\sigma^2 \;&=\; -\frac{m_0}{m}\,\frac{1}{4\,G\,N_c N_f\,I_2(m_\sigma^2)} + 4m^2 \quad , \\ &\simeq\; 4m^2 + m_\pi^2 \quad . \end{aligned} \tag{C.38}$$

This result linking the pion and the sigma masses is independent of the regularization scheme employed. In the chiral limit, the mass of the σ-meson is non-zero and its value is

$$m_\sigma^2 \;=\; 4m^2 \quad . \tag{C.39}$$

We have described a model for the pion. In the NJL model the pion arises through the dynamical breaking of the chiral symmetry. As a consequence its mass m_π should be zero in the chiral limit.

The NJL Lagrangian contains a point-like interaction that renders the theory nonrenormalizable. The model should always be completed by a regularization scheme fulfilling the conditions imposed by the theory: the existence of a "gap" and, therefore, zero-modes or Goldstone bosons. Another shortcoming is that the model is not confining.
The Nambu - Jona-Lasinio model together with its regularization scheme is treated like an effective theory and should therefore be used in a characteristic scale imposed by the same regularization scheme.

C.4 Partial Conservation of the Axial Current

We showed in Section C.1 that the true vacuum is not invariant under $SU_A(2)$. One might wonder what happens for the axial transformations. Familiar conservation laws are derived from the conservation of the currents associated with manifest symmetries of the, e.g., strong interactions. So the vector $SU_V(2) \times U_V(1)$ transformations, which are manifest symmetries, imply baryon number and isospin conservation.

The $SU_A(2)$ symmetry being broken, we restore the chiral symmetry by assuming that the axial currents

$$A_\mu^a(x) \;=\; \bar{q}(x)\,\gamma_\mu\gamma_5\,\frac{\tau^a}{2}\,q(x) \quad , \tag{C.40}$$

are partially / approximately conserved. The symmetry is implemented in the Goldstone mode with the pion as massless particles. Besides the fact that it is spontaneously broken, the chiral symmetry is explicitly broken by the mass term in the Lagrangian. That is, when the current quark mass are non zero, the pion which is effectively massless, acquires a mass, just as explained in Section C.3.

Consider that the axial current matrix element between a pion state and the vacuum can be parameterized by

$$\langle 0|A_\mu^j(x)|\pi^k(p)\rangle \;=\; ip_\mu\delta^{jk}\,f_\pi\,e^{-ip\cdot x} \quad , \tag{C.41}$$

with f_π the pion decay constant. It is experimentally estimated to $f_\pi = 93$ MeV [11] through the decay $\pi^- \to \mu^- \nu$

$$\Gamma_{\pi^- \to \mu^- \nu} = \frac{G^2\, m_\mu^2 f_\pi^2\, (m_\pi^2 - m_\mu^2)^2}{4\pi\, m_\pi^3} \cos^2\theta_C \quad ,$$

with θ_C the Cabibbo angle and G the Fermi constant.

The conservation of the axial current implies that

$$\langle 0|\partial^\mu A_\mu^j(x)|\pi^k(p)\rangle = m_\pi^2\, \delta^{jk}\, f_\pi\, e^{-ip\cdot x} = 0 \quad .$$

It means that $m_\pi^2\, f_\pi = 0$, so that, m_π^2 is chosen to be zero since the Goldstone realization of the symmetry is in agreement with nearly massless pions.

Figure C.6: Axial current in the nucleon. On the right panel, the pion pole contribution.

However, when restoring the quark (current) mass term, the axial current is no longer exactly conserved. The pions acquire a mass as given by Eq. (C.29). Hence, it is worth finding an expression for the current conservation when extrapolating from $p^2 = 0$ to $p^2 = m_\pi^2$, with $m_\pi^2 \neq 0$. This can be done by identifying the divergence of the current with a smooth interpolating pion field π^j,

$$\partial^\mu A_\mu^j(x) = m_\pi^2\, f_\pi\, \pi^j(x) \quad . \tag{C.42}$$

This behavior of this interpolating field can be guessed from the analysis of the matrix element of the axial current between nucleon states[2], Fig. C.6. Current conservation in the exact chiral limit effectively implies the exchange of a massless particle, identified here, to be the pion. It therefore means that the matrix elements of the divergence of the axial current are dominated by a pion pole (on the right panel of Fig. C.6) for small momentum transfers $|q^2| < m_\pi^2$

$$\langle A(p+q)|\partial^\mu A_\mu^j|B(q)\rangle = \frac{\text{Res}}{q^2 - m_\pi^2} + \ldots \tag{C.43}$$

By consistency with the model calculation, it is important to evaluate the pion decay with the technology developed in the previous Sections of this Appendix. In the NJL model, the expression Eq. (C.41) becomes, see Fig. C.7

[2]See, for instance, classical notebooks Refs. [161, 112].

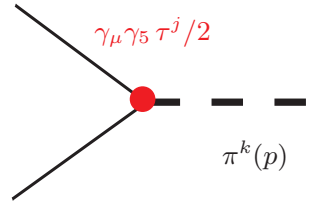

Figure C.7:

$$
\begin{aligned}
ip_\mu \delta^{jk} f_\pi \, e^{-ip\cdot x} &= \langle 0| \sum_c \bar{\psi}_c(x) \gamma_\mu \gamma_5 \frac{\tau^j}{2} \psi_c(x) |\pi^k(p)\rangle \quad , \\
&= -e^{-ip\cdot x} \int \frac{d^4k}{(2\pi)^4} \, \mathbb{T}\mathrm{r} \left(iS_F(k) \, ig_{\pi qq} i\gamma_5 \tau^j \, iS_F(-p+k) \gamma_\mu \gamma_5 \frac{\tau^j}{2} \right) \quad ,
\end{aligned}
\tag{C.44}
$$

which gives us the expression for f_π in terms of 2-propagator integrals

$$
f_\pi = -2N_c N_f \, g_{\pi qq} \, m \, I_2(m,p) \quad . \tag{C.45}
$$

D Transition Form Factors

In the NJL model, the vector form factor is

$$F_V^{\pi^+}(t) = \frac{8\,N_c}{3}\,m\,m_\pi\,\frac{g_{\pi qq}}{\sqrt{2}}\,I_3(p,p') \qquad . \tag{D.1}$$

In order to calculate the form factors we need the expression for the three-propagator integral. In the particular case where $p^2 = m_\pi^2$ and $p'^2 = 0$, the expression for $I_3(p,p')$ given by Eq. (E.4).

The axial form factor involves the three-propagator integral as well, but also the two-propagator integral given by Eq. E.2

$$F_A^{\pi^+}(t) = 4N_c\,m\,m_\pi\,g_{\pi qq}\sqrt{2}\,\left(I_3(p,p') + \frac{2}{m_\pi^2 - t}\left[I_2(m_\pi^2) - I_2(t)\right]\right) \qquad , \tag{D.2}$$

The $\pi^0 \to \gamma^*\gamma$ form factor can be obtained from the vector form factor through a isospin rotation

$$F_{\pi\gamma^*\gamma}(t) \;=\; \frac{\sqrt{2}}{m_\pi}\,F_V^{\pi^+}(t) \quad . \tag{D.3}$$

In the chiral limit and for $t = 0$ all the considered form factors have the simple expression:

$$\begin{aligned}\left.\frac{F_{\pi\gamma^*\gamma}(0)}{\sqrt{2}}\right|_{m_\pi\to 0} = \left.\frac{F_V^{\pi^+}(0)}{m_\pi}\right|_{m_\pi\to 0} = \left.\frac{F_A^{\pi^+}(0)}{m_\pi}\right|_{m_\pi\to 0} &= \frac{1}{\sqrt{2}\,4\pi^2 f_\pi}\left[1 - \frac{2m^2}{m^2+\Lambda^2} + \frac{m^2}{m^2+2\Lambda^2}\right] \\ &= 0.192 \times (1 - 0.108)\,\mathrm{GeV}^{-1} = 0.171\,\mathrm{GeV}^{-1}\end{aligned} \tag{D.4}$$

The first coefficient of the right hand side is what is expected from the axial anomaly contribution to $\pi \to \gamma^*\gamma$ decay. The term between brackets has a small correction to the expected value of 1 due to the finiteness of the regularization masses. In the NJL model not only the quarks, but also the counter-terms run in the triangle diagram of the axial anomaly. In a proper renormalizable theory this correction disappears in the limit $\Lambda \to \infty$.

E Elementary Integrals

Regularization of the following integrals is insured by the Pauli-Villars regularization scheme, i.e. see Section C.2.

E.1 One, two and three-propagator Integrals

The one-propagator integral I_1 is given by

$$\begin{aligned} I_1 &= i\int \frac{d^4k}{(2\pi)^4}\,\frac{1}{k^2-m^2+i\epsilon} \quad , \\ &= \frac{1}{(4\pi)^2}\,\sum_{j=0}^{2} c_j\, m_j^2\,\ln\frac{m_j^2}{m^2} \quad . \end{aligned} \tag{E.1}$$

The two-propagator integral $I_2(p)$ is given by, in a general case,

$$\begin{aligned} I_2(p^2) &= i\int \frac{d^4k}{(2\pi)^4}\,\frac{1}{(k^2-m^2+i\epsilon)((p+k)^2-m^2+i\epsilon)} \quad , \\ &= \frac{1}{(4\pi)^2}\,\sum_{j=0}^{2} c_j \left\{ \ln\frac{m_j^2}{m^2} + \sqrt{\frac{p^2-4m_j^2}{p^2}}\,\ln\frac{1-\sqrt{\frac{p^2}{p^2-4m_j^2}}}{1-\sqrt{\frac{p^2}{p^2-4m_j^2}}} \right\} \quad . \end{aligned} \tag{E.2}$$

In particular, for $0 < p^2 < 4m^2$, Eq. (E.2) becomes

$$I_2(p^2) = \frac{1}{(4\pi)^2}\,\sum_{j=0}^{2} c_j \left\{ \ln\frac{m_j^2}{m^2} + 2\sqrt{\frac{4m_j^2-p^2}{p^2}}\,\mathrm{arctg}\frac{1}{\sqrt{\frac{4m_j^2-p^2}{p^2}}} \right\} \quad . \tag{E.3}$$

The three-propagator integral $I_3(p_1, p_2)$ is given by

$$\begin{aligned} I_3(p_1,p_2) &= i\int \frac{d^4k}{(2\pi)^4}\,\frac{1}{(k^2-m^2+i\epsilon)((p_1+k)^2-m^2+i\epsilon)((p_2+k)^2-m^2+i\epsilon)} \quad , \\ &= \frac{1}{(4\pi)^2}\sum_{j=0}^{2} c_j \int_0^1 dz\,\frac{z}{\sqrt{D}}\ln\frac{E-\sqrt{D}}{E+\sqrt{D}} \quad , \end{aligned} \tag{E.4}$$

with, in the particular case where $p_1^2 = p_2^2 = m_\pi^2$,

$$\begin{aligned} D &= t^2z^4 - 4z^2t(m_j^2 + m_\pi^2 z(z-1)) \quad ; \\ E &= z^2t - 2m_j^2 - 2m_\pi^2 z(z-1) \quad ; \end{aligned} \tag{E.5}$$

and with, in the particular case where $p_1^2 = m_\pi^2$ and $p_2^2 = 0$, we obtain

$$D = t^2z^4 + z^2(1-z)^2m_\pi^4 + 2\,t\,z^2(m_\pi^2 z(1-z) - 2m_j^2) \quad , \tag{E.6}$$

$$E = z^2t + z(1-z)m_\pi^2 - 2m_j^2 \quad . \tag{E.7}$$

E.2 Light-front Integrals

E.2.1 Two-propagator light-front integrals

We can now calculate the three 2-propagator integrals, $\tilde{I}_{2,\Delta}(x,\xi,t)$, $\tilde{I}_{2,P'}$ and $\tilde{I}_{2,P}(x,\xi)$ defined as

$$\begin{aligned} \tilde{I}_{2,\Delta}(x,\xi,t) &= i\,p^+ \int \frac{d^4k}{(2\pi)^4}\,\frac{\delta\left((x-1)p^+ + k^+\right)}{((P-k)^2-m^2+i\epsilon)((P'-k)^2-m^2+i\epsilon)} \quad , \\ \tilde{I}_{2,P'} &= i\,p^+ \int \frac{d^4k}{(2\pi)^4}\,\frac{\delta\left((x-1)p^+ + k^+\right)}{(k^2-m^2+i\epsilon)((P'-k)^2-m^2+i\epsilon)} \quad , \\ \tilde{I}_{2,P}(x,\xi) &= i\,p^+ \int \frac{d^4k}{(2\pi)^4}\,\frac{\delta\left((x-1)p^+ + k^+\right)}{(k^2-m^2+i\epsilon)((P-k)^2-m^2+i\epsilon)} \quad . \end{aligned} \tag{E.8}$$

The first step of this integration consists in decomposing the momenta in their light-cone components. The delta function selects the +-momenta carried by the quarks so that the integral over dk^+ is straightforward. The integral over dk^- is performed with the help of the Residue Theorem so that we are left with an integration over $dk^\perp$. The latter is straightforward.

GPDs' kinematics

The result is

$$\tilde{I}_{2,\Delta}(x,\xi,t) = \frac{1}{(4\pi)^2}\frac{1}{2\xi}\sum_{j=0}^{2} c_j \ln\frac{m_j^2 + \frac{t}{4}\frac{x^2-\xi^2}{\xi^2}}{m^2}\;\theta(x+\xi)\theta(\xi-x) \quad . \tag{E.9}$$

The same steps can be done with the $\tilde{I}_{2,P'}$ and $\tilde{I}_{2,P}(x,\xi)$ integrals:

$$\tilde{I}_{2,P'} = \frac{1}{(4\pi)^2}\frac{1}{1-\xi}\sum_{j=0}^{2} c_j \ln\frac{m_j^2 + m_\pi^2\frac{(x-\xi)(x-1)}{(1-\xi)^2}}{m^2}\ \theta(x-\xi)\theta(1-x) \quad . \tag{E.10}$$

The $\tilde{I}_{2,P}(x,\xi)$ integral is defined on $-\xi < x < 1$.

$$\tilde{I}_{2,P}(x,\xi) = \frac{1}{(4\pi)^2}\frac{1}{1+\xi}\sum_{j=0}^{2} c_j \ln\frac{m_j^2 + m_\pi^2\frac{(x+\xi)(x-1)}{(1+\xi)^2}}{m^2}\ \theta(x+\xi)\theta(1-x) \quad . \tag{E.11}$$

TDAs' kinematics

In the TDA's kinematics, the Eqs. (E.9, E.11) do not change but $\tilde{I}_{2,P'}$ becomes

$$\tilde{I}_{2,P'} = \frac{1}{(4\pi)^2}\frac{1}{1-\xi}\sum_{j=0}^{2} c_j \ln\frac{m_j^2}{m^2}\ \theta(x-\xi)\theta(1-x) \quad . \tag{E.12}$$

E.2.2 Three-propagator light-front integrals

The three-propagator light-front integral is given by

GPDs' kinematics

$$\begin{aligned}
&\tilde{I}_3^{GPD}(x,\xi,t)\\
&= i\,p^+\int \frac{d^4k}{(2\pi)^4}\,\frac{\delta\left((x-1)p^+ + k^+\right)}{(k^2-m^2+i\epsilon)((P-k)^2-m^2+i\epsilon)((P'-k)^2-m^2+i\epsilon)} \quad ,\\
&= \frac{1}{2\,(4\pi)^2}\sum_{j=0}^{2} c_j\\
&\quad\Big\{\theta(1-x)\theta(x-\xi)\frac{1}{\sqrt{D}}\ln\frac{-m_\pi^2 x(1-x)+m_j^2(1-\xi^2)-\frac{t}{2}(1-x)^2+(1-x)\sqrt{D}}{-m_\pi^2 x(1-x)+m_j^2(1-\xi^2)-\frac{t}{2}(1-x)^2-(1-x)\sqrt{D}}\\
&\quad+\theta(\xi-x)\theta(x+\xi)\frac{1}{\sqrt{D}}\ln\frac{-m_\pi^2\xi(\xi+x)+2m_j^2\xi(1+\xi)-\frac{t}{2}(1-x)(x+\xi)+(x+\xi)\sqrt{D}}{-m_\pi^2\xi(\xi+x)+2m_j^2\xi(1+\xi)-\frac{t}{2}(1-x)(x+\xi)-(x+\xi)\sqrt{D}}\Big\},
\end{aligned} \tag{E.13}$$

with

$$D = m_\pi^4\xi^2 + \frac{t^2}{4}(1-x)^2 - 4m_j^2\xi^2 m_\pi^2 + t m_\pi^2 x(1-x) - m_j^2 t(1-\xi^2) \quad . \tag{E.14}$$

TDAs' kinematics

In the TDA's kinematics, the skewness variable is bounded by $t/(2m_\pi^2 - t) < \xi < 1$. We therefore have to consider both the cases with positive and negative values of ξ.

For positive values of ξ, the three-propagator light-front integral becomes

$$\begin{aligned}
&\tilde{I}_3^{TDA}(x,\xi,t) \\
&= i\,p^+ \int \frac{d^4k}{(2\pi)^4} \frac{\delta\left((x-1)p^+ + k^+\right)}{(k^2 - m^2 + i\epsilon)((P-k)^2 - m^2 + i\epsilon)((P'-k)^2 - m^2 + i\epsilon)} \quad , \\
&= \frac{1}{(4\pi)^2} \sum_{j=0}^{2} c_j \\
&\quad \Big\{ \theta(x+|\xi|)\theta(|\xi|-x) \frac{1}{\sqrt{D}} \ln \frac{m_\pi^2(x-\xi) + t(x-1) + 4\xi\frac{1+\xi}{x+\xi}m_j^2 + \sqrt{D}}{m_\pi^2(x-\xi) + t(x-1) + 4\xi\frac{1+\xi}{x+\xi}m_j^2 - \sqrt{D}} \\
&\quad + \theta(x-|\xi|)\theta(1-x) \frac{1}{\sqrt{D}} \ln \frac{m_\pi^2(x-\xi) - t(x-1) + 2\frac{1-\xi^2}{x-1}m_j^2 - \sqrt{D}}{m_\pi^2(x-\xi) - t(x-1) + 2\frac{1-\xi^2}{x-1}m_j^2 + \sqrt{D}} \Big\} \quad , \qquad \text{(E.15)}
\end{aligned}$$

where we have introduced the Pauli-Villars regularization parameters and with

$$D = \left(m_\pi^2\,(x-\xi) + t(1-x)\right)^2 + 4\,m_j^2\,(2m_\pi^2\xi(1-\xi) - t(1-\xi^2)) \quad . \qquad \text{(E.16)}$$

On the other hand, for negative values of the skewness variable, the three-propagator light-front integral becomes

$$\begin{aligned}
&\tilde{I}_3^{TDA}(x,\xi,t) \\
&= i\,p^+ \int \frac{d^4k}{(2\pi)^4} \frac{\delta\left((x-1)p^+ + k^+\right)}{(k^2 - m^2 + i\epsilon)((P-k)^2 - m^2 + i\epsilon)((P'-k)^2 - m^2 + i\epsilon)} \quad , \\
&= \frac{1}{(4\pi)^2} \sum_{j=0}^{2} c_j \\
&\quad \Big\{ \theta(x+|\xi|)\theta(|\xi|-x) \frac{1}{\sqrt{D}} \ln \frac{-m_\pi^2(x+\xi) + t(x-1) - 4\xi\frac{1-\xi}{x-\xi}m_j^2 + \sqrt{D}}{-m_\pi^2(x+\xi) + t(x-1) - 4\xi\frac{1-\xi}{x-\xi}m_j^2 - \sqrt{D}} \\
&\quad + \theta(x-|\xi|)\theta(1-x) \frac{1}{\sqrt{D}} \ln \frac{m_\pi^2(x-\xi) - t(x-1) + 2\frac{1-\xi^2}{x-1}m_j^2 - \sqrt{D}}{m_\pi^2(x-\xi) - t(x-1) + 2\frac{1-\xi^2}{x-1}m_j^2 + \sqrt{D}} \Big\} \quad . \qquad \text{(E.17)}
\end{aligned}$$

F Double Distributions and the α-representation

This Appendix is based on the work by Broniowski, Ruiz Arriola and Golec-Bernat [45].

In this Appendix we aim to give an explicit calculation of the Double Distribution of the form given by reduction formula (3.25). This is conveniently done through the Feynman α-representation of the scalar propagators.
So the scalar propagator reads

$$S_k \;=\; \frac{1}{k^2-m^2+i\epsilon} = \int_0^\infty d\alpha e^{-\,\alpha(k^2-m^2+i\epsilon)} \quad .$$

The 3-propagator Integral

We write the 3-propagator integral in the asymmetric notation for it is more appropriate for our purposes, omitting to write the $+i\epsilon$. It reads [44]

$$\tilde{I}_3(X,\zeta,t) \;=\; i\int \frac{d^4k}{(2\pi)^4}\,\frac{\delta(X-k\cdot n)}{(k^2-m^2)\,((k+\Delta)^2-m^2)\,((k-p_\pi)^2-m^2)} \quad ,$$

with $\Delta = p_\gamma - p_\pi$. In terms of exponential representation of the propagator, the vector TDA becomes

$$\begin{aligned}\tilde{I}_3(X,\zeta,t) \;=\; & i\int \frac{d^4k}{(2\pi)^4}\int \frac{d\lambda}{2\pi}\,e^{i\lambda(k\cdot n-X)} \\ & \int_0^\infty d\alpha\int_0^\infty d\beta\int_0^\infty d\gamma\, e^{-\alpha\left(k^2-m^2\right)-\beta\left((k+\Delta)^2-m^2\right)-\gamma\left((k-p_\pi)^2-m^2\right)} \quad .\end{aligned}$$

We perform the following change of variables

$$s=\alpha+\beta+\gamma \quad , \quad y=\frac{\beta}{s} \quad , \quad z=\frac{\gamma}{s} \quad ,$$

with $a, b, c > 0$ so that we can constrain y, z to have support between $[0, 1]$ and also $y + z \leq 1$. The constrains on the limits for y, z are automatically imposed by the α-representation of the scalar propagator.

Concentrating on the argument of the exponential, we find

$$\begin{aligned} &-(\alpha+\beta+\gamma)(k^2-m^2) - \beta\,\Delta^2 - \gamma\,p_\pi^2 - 2\beta\,\Delta\cdot k + 2\gamma\,p_\pi\cdot k + i\lambda k\cdot n - i\lambda X \\ &= -s\left((k^2-m^2) + y\,\Delta^2 + z p_\pi^2 + 2y\,\Delta\cdot k - 2z\,p_\pi\cdot k - i\lambda\frac{k\cdot n}{s} + i\lambda\frac{X}{s}\right) \quad . \end{aligned} \tag{F.1}$$

The following change of variable is performed,

$$k = k' + z\,p_\pi - y\,\Delta + i\frac{\lambda n}{2s} \quad , \tag{F.2}$$

$$\begin{aligned} \Rightarrow \qquad k'^2 &= k^2 + z^2\,p_\pi^2 + y^2\,\Delta^2 - 2z\,p_\pi\cdot k + 2y\,\Delta\cdot k - i\lambda\frac{k\cdot n}{s} - 2\,zy\,p_\pi\cdot\Delta \\ &\quad + i\lambda z\frac{p_\pi\cdot n}{s} - i\lambda y\frac{\Delta\cdot n}{s} \quad . \end{aligned}$$

The argument of the exponential (F.1) becomes

$$\begin{aligned} -s\Big((k'^2-m^2) &+ \Delta^2\,y(1-y) + p_\pi^2\,z(1-z) + 2zy\,p_\pi\cdot\Delta \\ &- i\lambda z\frac{p_\pi\cdot n}{s} + i\lambda y\frac{\Delta\cdot n}{s} + i\lambda\frac{X}{s}\Big) \quad . \end{aligned} \tag{F.3}$$

The integral over dk is a Gaussian-integral when going to the Euclidean space. Rotating the contour of the k^0 integration by performing a Wick rotation, i.e. $k^0 \equiv ik_E^0$ while $\mathbf{k} = \mathbf{k}_E$, we are left with

$$\begin{aligned} \tilde{I}_3(X,\zeta,t) \;=\; & \frac{1}{(2\pi)^4}\int\frac{d\lambda}{2\pi}\int_0^\infty ds\,s^2\,\frac{\pi^2}{s^2}\int_0^1 dy\int_0^1 dz\,\theta(1-y-z) \\ & e^{-s\left(-m^2+\Delta^2\,y(1-y)+p_\pi^2\,z(1-z)+2zy\,p_\pi\cdot\Delta - i\lambda z\frac{p_\pi\cdot n}{s}+i\lambda y\frac{\Delta\cdot n}{s}+i\lambda\frac{X}{s}\right)} \end{aligned}$$

We can now perform the integral over $d\lambda$. The dependence upon λ comes only from the exponential

$$e^{-i\lambda(X+y\,\Delta\cdot n - z\,p_\pi\cdot n)} \quad .$$

The expression for the 3-propagator integral hence becomes

$$\begin{aligned}\tilde{I}_3(X,\zeta,t) &= \frac{1}{(4\,\pi)^2}\int_0^\infty ds\int_0^1 dy\int_0^1 dz\theta\,(1-y-z)\\ &\quad \delta\,(X-z\,p_\pi\cdot n-y\Delta\cdot n)\,e^{-sm^2}e^{-p_\pi^2 z(1-z)s}e^{-\Delta^2 y(1-y)s}e^{-2yzs\,p_\pi\cdot\Delta}\quad .\end{aligned}$$

In turn, the integral over ds gives

$$\begin{aligned}\tilde{I}_3(X,\zeta,t) &= \frac{1}{(4\,\pi)^2}\int_0^1 dy\int_0^1 dz\theta\,(1-y-z)\\ &\quad \frac{\delta\,(X-z\,p_\pi\cdot n-y\Delta\cdot n)}{m^2-p_\pi^2\,z(1-z)-\Delta^2\,y(1-y)-2\,yz\,p_\pi\cdot\Delta}\quad .\end{aligned}\tag{F.4}$$

The latter expression can be reduced to a Double Distribution following Eq. (3.25)

$$\tilde{I}_3(X,\zeta,t) = \frac{1}{(4\,\pi)^2}\int_0^1 dy\int_0^1 dz\,\delta\,(X-z\,p_\pi\cdot n-y\Delta\cdot n)\;\mathcal{I}_3(z,y,t)\quad ;\tag{F.5}$$

where the Double Distribution $\mathcal{F}_\pi^q(z,y,t)$ has be determined to be

$$\mathcal{I}_3(z,y,t) = \frac{\theta\,(1-y-z)}{m^2-p_\pi^2\,z(1-z)-\Delta^2\,y(1-y)-2\,yz\,p_\pi\cdot\Delta}\quad .\tag{F.6}$$

By definition, the DD is not constrained by the kinematics. When linking the 2-dimensional Fourier transform that defines the DD to the 1-dimensional Fourier transform defining the skewed parton distributions, one has to use the kinematics imposed by the process and to relate the two variables $p\cdot n$ and $\Delta\cdot n$. This is done through the δ-function in Eq. (F.5). In other words, the function $\tilde{I}_3$ depends also on the skewness variable.

So far, we have hardly used the typical kinematics of the transition and the result is somehow general. We can now apply the previous developments to the TDA's kinematics. We will use the asymmetric notation introduced by Radyushkin. The kinematics are slightly changed with respect to the one described in Section 4.2. In Ref. [44], the following conventions are used

$$n^2=0\,,\qquad p_\pi\cdot n=1\,,\qquad \Delta\cdot n=-\zeta\,,$$

$$p_\pi^2=m_\pi^2\,,\qquad \Delta^2=t\,,\qquad 2\,p_\pi\cdot\Delta=m_\pi^2+t\quad ,\tag{F.7}$$

with the *asymmetric* skewness variable a priori defined between $\zeta\in[0,1]$. The couple of symmetric variables (x,ξ) is related the the asymmetric ones (X,ζ) by

$$X=\frac{x+\xi}{1+\xi}\,,\qquad \zeta=\frac{2\xi}{1+\xi}\quad .\tag{F.8}$$

Also, in this asymmetric notation, one should change the couple of variables

$$(\beta,\alpha)\quad\longrightarrow\quad(z,(2y+z-1))\quad ,$$

what is equivalent to changing (x, ξ) for (X, ζ).

The expression (F.4) can be written in the form of a reduction formula for the TDA's kinematics

$$\tilde{I}_3(X,\zeta,t) \;=\; \frac{1}{(4\,\pi)^2}\int_0^1 dy \int_0^1 dz\,\delta\left(X-z-y\zeta\right)\,\mathcal{I}_3(z,y,t) \quad , \tag{F.9}$$

with the double distribution in the same kinematics

$$\mathcal{I}_3(z,y,t) \;=\; \frac{\theta\left(1-y-z\right)}{m^2-m_\pi^2\,z(1-z-y)-t\,y(1-y-z)} \quad . \tag{F.10}$$

Performing the z-integration, its value is set at $z = X - y\zeta$. In the TDA's kinematics, the value of the skewness variable is not constrained to be positive, see (4.9). This leads to two support decompositions according to the sign of ζ. For positive ζ values

$$\begin{aligned}\tilde{I}_3(X,\zeta,t) \;=\; & \frac{1}{(4\,\pi)^2}\left(\theta(X)\theta(\zeta-X)\int_0^{X/\zeta}+\theta(1-X)\theta(X-\zeta)\int_0^{(1-X)/(1-\zeta)}\right)\\ & \frac{dy}{m^2-m_\pi^2\,(X-y\zeta)(1-(X-y\zeta)+y)-t\,y(1-y+(X-y\zeta))} \quad (\zeta>0) \quad ;\end{aligned} \tag{F.11}$$

leading to a support $x \in [0, \zeta]$ and $x \in [\zeta, 1]$. On the other hand, for negative values of ζ, the support is decomposed in the following way

$$\begin{aligned}\tilde{I}_3(X,\zeta,t) \;=\; & \frac{1}{(4\,\pi)^2}\left(\theta(X)\theta(\zeta-X)\int_{X/\zeta}^{(1-X)/(1-\zeta)}+\theta(X)\theta(1-X)\int_0^{(1-X)/(1-\zeta)}\right)\\ & \frac{dy}{m^2-m_\pi^2\,(X-y\zeta)(1-(X-y\zeta)+y)-t\,y(1-y+(X-y\zeta))} \quad (\zeta<0) \quad ,\end{aligned} \tag{F.12}$$

which corresponds to a support in x between $[\zeta, 0]$ and $[0, 1]$.

The k^ν-dependent 3-propagator Integral

In the case of an integral proportional to the loop variable, i.e.

$$\tilde{I}_3^\nu(X,\zeta,t) \;=\; i\int\frac{d^4k}{(2\pi)^4}\,\frac{\delta(X-k\cdot n)\,k^\nu}{(k^2-m^2)\,((k+\Delta)^2-m^2)\,((k-p_\pi)^2-m^2)} \quad ,$$

the shifting operation changes to y, z dependence of the DD.

In the particular case of the axial TDA, the Dirac trace taken over the axial matrix element brings a factor of $-2\,k^\nu$ into the integral. The change of variable (F.2) produces a shift of

$$-\,2\,k^\nu \quad\longrightarrow\quad -\,(2k+2z\,p_\pi-2y\,\Delta)^\nu \quad .$$

Using the fact that the photon polarization implies $\varepsilon \cdot p_\gamma = 0$, we obtain $\varepsilon \cdot p_\pi = -\varepsilon \cdot \Delta$;

$$\begin{aligned} \varepsilon \cdot \tilde{I}_3(X,\zeta,t) &= i \int \frac{d^4k}{(2\pi)^4} \int_0^\infty ds\, s^2 \int_0^1 dy \int_0^1 dz\, \theta(1-y-z) \\ &\quad \varepsilon_\nu \left(2k^\nu - (2y+2z)\,\Delta^\nu\right) \\ &\quad e^{-s\left((k^2-m^2)+\Delta^2\, y(1-y)+p_\pi^2\, z(1-z)+2zy\, p_\pi\cdot\Delta - i\lambda z \frac{p_\pi\cdot n}{s} + i\lambda y \frac{\Delta\cdot n}{s} + i\lambda \frac{X}{s}\right)} \quad . \end{aligned} \tag{F.13}$$

The Gaussian integration over dk carries out a $\left(\sqrt{\pi/s}\right)^4$. The term proportional to k cancels out. The following steps are as described in above for $\tilde{I}_3$, we obtain

$$\varepsilon \cdot \tilde{I}_3(X,\zeta,t) = \frac{\varepsilon\cdot\Delta}{2\pi^2} \int_0^1 dy \int_0^1 dz\, \delta\left(X - z - y\zeta\right)\, (2y+2z)\, D(z,y,t) \quad , \tag{F.14}$$

with the double distribution $D(z,y,t)$ defined by Eq. (F.10).

Polynomiality Property

Turning our attention to the polynomiality condition (4.39) resulting from Lorentz invariance, we find that it is an inherent property of the Double Distribution parameterization,

$$\begin{aligned} \int_0^1 dX\, X^{n-1}\, \tilde{I}_3(X,\zeta,t) &= \frac{1}{2\,\pi^2} \int_0^1 dy \int_0^1 dz\, \theta(z+y\zeta)\, \theta(1-z-y\zeta)\, (\zeta\, y + z)^{n-1}\, \mathcal{I}_3(z,y,t) \quad , \\ &= \sum_{i=0}^{n-1} c_{n,i}(t)\, \zeta^i \quad . \end{aligned}$$

The latter expression implies the expression for the general form factors as follows

$$c_{n,i}(t) \propto \frac{1}{2\pi^2} \int_0^1 dy \int_0^1 dz\, y^i\, z^{n-1-i}\, \mathcal{I}_3(z,y,t) \quad . \tag{F.15}$$

Since the kinematical range for the skewness variable is $-1 \leq \zeta \leq 1$, the condition on the integration limits imposed by the θ-function are verified.

The expression (F.15) corresponds to the Double Distribution form of the General Moments (4.55), as expected.

Bibliography

[1] H. Ackermann *et al.*, "Determination Of The Longitudinal And The Transverse Part In Pi+ Electroproduction," Nucl. Phys. B **137**, 294 (1978).

[2] B. Aubert [The BABAR Collaboration], "Measurement of the gamma gamma* –¿ pi0 transition form factor," arXiv:0905.4778 [hep-ex].

[3] E. M. Aitala *et al.* [E791 Collaboration], "Direct measurement of the pion valence quark momentum distribution, the pion light-cone wave function squared," Phys. Rev. Lett. **86** (2001) 4768 [arXiv:hep-ex/0010043].

[4] A. Airapetian *et al.* [HERMES Collaboration], "Measurement of the beam spin azimuthal asymmetry associated with deeply-virtual Compton scattering," Phys. Rev. Lett. **87** (2001) 182001 [arXiv:hep-ex/0106068].

[5] A. Airapetian *et al.* [HERMES Collaboration], "Single-spin asymmetries in semi-inclusive deep-inelastic scattering on a transversely polarized hydrogen target," Phys. Rev. Lett. **94**, 012002 (2005) [arXiv:hep-ex/0408013].

[6] A. Aktas *et al.* [H1 Collaboration], "Measurement of deeply virtual Compton scattering at HERA," Eur. Phys. J. C **44** (2005) 1 [arXiv:hep-ex/0505061].

[7] V. Y. Alexakhin *et al.* [COMPASS Collaboration], "First measurement of the transverse spin asymmetries of the deuteron in semi-inclusive deep inelastic scattering," Phys. Rev. Lett. **94**, 202002 (2005) [arXiv:hep-ex/0503002].

[8] G. Altarelli, N. Cabibbo, L. Maiani and R. Petronzio, "The Nucleon as a bound state of three quarks and deep inelastic phenomena," Nucl. Phys. B **69**, 531 (1974).

[9] G. Altarelli and G. Parisi, "Asymptotic Freedom In Parton Language," Nucl. Phys. B **126** (1977) 298.

[10] D. Amrath, M. Diehl and J. P. Lansberg, "Deeply virtual Compton scattering on a virtual pion target," Eur. Phys. J. C **58** (2008) 179 [arXiv:0807.4474 [hep-ph]].

[11] C. Amsler *et al.* [Particle Data Group], Review of particle physics, Phys. Lett. **B667** (2008) 1.

[12] I. V. Anikin, D. Binosi, R. Medrano, S. Noguera and V. Vento, Eur. Phys. J. A **14** (2002) 95 [arXiv:hep-ph/0109139].

[13] I. V. Anikin, I. O. Cherednikov, N. G. Stefanis and O. V. Teryaev, "Duality between different mechanisms of QCD factorization in $\gamma^*\gamma$ collisions," arXiv:0806.4551 [hep-ph].

[14] I. V. Anikin, A. E. Dorokhov and L. Tomio, "Pion structure in the instanton liquid model," Phys. Part. Nucl. **31**, 509 (2000) [Fiz. Elem. Chast. Atom. Yadra **31**, 1023 (2000)].

[15] I. V. Anikin, B. Pire and O. V. Teryaev, "On the gauge invariance of the DVCS amplitude," Phys. Rev. D **62** (2000) 071501 [arXiv:hep-ph/0003203].

[16] I. V. Anikin, B. Pire and O. V. Teryaev, "On gamma gamma* production of two rho0 mesons," Phys. Rev. D **69** (2004) 014018 [arXiv:hep-ph/0307059].

[17] I. V. Anikin, B. Pire and O. V. Teryaev, "Search for isotensor exotic meson and twist 4 contribution to $\gamma^*\gamma \to \rho\rho$," Phys. Lett. B **626** (2005) 86 [arXiv:hep-ph/0506277].

[18] M. Anselmino *et al.* [TESLA-N Study Group], "TESLA: The superconducting electron positron linear collider with an integrated X-ray laser laboratory. Technical design report. Pt. 6: Appendices. Chapter 4: ELFE: The electron laboratory for Europe,"

[19] M. Anselmino, M. Boglione, U. D'Alesio, A. Kotzinian, F. Murgia and A. Prokudin, "Extracting the Sivers function from polarized SIDIS data and making predictions," Phys. Rev. D **72**, 094007 (2005) [Erratum-ibid. D **72**, 099903 (2005)] [arXiv:hep-ph/0507181].

[20] M. Anselmino *et al.*, "Sivers Effect for Pion and Kaon Production in Semi-Inclusive Deep Inelastic Scattering," Eur. Phys. J. A **39** (2009) 89 [arXiv:0805.2677 [hep-ph]].

[21] P. Aurenche, R. Baier, M. Fontannaz, M. N. Kienzle-Focacci and M. Werlen, "THE GLUON CONTENT OF THE PION FROM HIGH P(T) DIRECT PHOTON PRODUCTION," Phys. Lett. B **233** (1989) 517.

[22] A. Bacchetta, A. Schaefer and J. J. Yang, "Sivers function in a spectator model with axial-vector diquarks," Phys. Lett. B **578**, 109 (2004) [arXiv:hep-ph/0309246].

[23] A. Bacchetta, U. D'Alesio, M. Diehl and C. A. Miller, "Single-spin asymmetries: The Trento conventions," Phys. Rev. D **70**, 117504 (2004) [arXiv:hep-ph/0410050].

[24] A. Bacchetta, M. Diehl, K. Goeke, A. Metz, P. J. Mulders and M. Schlegel, "Semi-inclusive deep inelastic scattering at small transverse momentum," JHEP **0702**, 093 (2007) [arXiv:hep-ph/0611265].

[25] A. Bacchetta, F. Conti and M. Radici, "Transverse-momentum distributions in a diquark spectator model," Phys. Rev. D **78** (2008) 074010 [arXiv:0807.0323 [hep-ph]].

[26] J. Badier *et al.* [NA3 Collaboration], "Experimental Determination Of The Pi Meson Structure Functions By The Drell-Yan Mechanism," Z. Phys. C **18** (1983) 281.

[27] V. Barone, A. Drago and P. G. Ratcliffe, "Transverse polarisation of quarks in hadrons," Phys. Rept. **359** (2002) 1 [arXiv:hep-ph/0104283].

[28] V. Barone and E. Predazzi, "High-Energy Particle Diffraction," *Springer (2002) 407p*

[29] A. V. Belitsky, X. Ji and F. Yuan, "Final state interactions and gauge invariant parton distributions," Nucl. Phys. B **656**, 165 (2003) [arXiv:hep-ph/0208038].

[30] A. V. Belitsky and A. V. Radyushkin, "Unraveling hadron structure with generalized parton distributions," Phys. Rept. **418** (2005) 1 [arXiv:hep-ph/0504030].

[31] B. Betev *et al.* [NA10 Collaboration], "Observation Of Anomalous Scaling Violation In Muon Pair Production By 194-Gev/C Pi- Tungsten Interactions," Z. Phys. C **28** (1985) 15.

[32] A. Bianconi, "A nuclear-style mean field model for the Sivers effect in nucleon-hadron single spin asymmetries and Drell-Yan," arXiv:hep-ph/0702186.

[33] D. Binosi, J. Collins, C. Kaufhold and L. Theussl, "JaxoDraw: A graphical user interface for drawing Feynman diagrams. Version 2.0 release notes," arXiv:0811.4113 [hep-ph].

[34] J. D. Bjorken, J. B. Kogut and D. E. Soper, "Quantum Electrodynamics At Infinite Momentum: Scattering From An External Field," Phys. Rev. D **3** (1971) 1382.

[35] D. Boer and P. J. Mulders, "Time-reversal odd distribution functions in leptoproduction," Phys. Rev. D **57** (1998) 5780 [arXiv:hep-ph/9711485].

[36] S. Boffi and B. Pasquini, "Generalized parton distributions and the structure of the nucleon," Riv. Nuovo Cim. **30** (2007) 387 [arXiv:0711.2625 [hep-ph]].

[37] P. Brauel *et al.*, "Separation Of Sigma-L And Sigma-U In Pi+ Electroproduction Above The Resonance Region," Phys. Lett. B **69** (1977) 253.

[38] V. M. Braun, A. Lenz, G. Peters and A. V. Radyushkin, "Light cone sum rules for gamma* N $\to$ Delta transition form factors," Phys. Rev. D **73** (2006) 034020 [arXiv:hep-ph/0510237].

[39] S. J. Brodsky and G. P. Lepage, "Large Angle Two Photon Exclusive Channels In Quantum Chromodynamics," Phys. Rev. D **24** (1981) 1808.

[40] S. J. Brodsky, M. Burkardt and I. Schmidt, "Perturbative QCD constraints on the shape of polarized quark and gluon distributions," Nucl. Phys. B **441** (1995) 197 [arXiv:hep-ph/9401328].

[41] S. J. Brodsky, D. S. Hwang and I. Schmidt, "Final-state interactions and single-spin asymmetries in semi-inclusive deep inelastic scattering," Phys. Lett. B **530**, 99 (2002) [arXiv:hep-ph/0201296].

[42] S. J. Brodsky, P. Hoyer, N. Marchal, S. Peigne and F. Sannino, "Structure functions are not parton probabilities," Phys. Rev. D **65**, 114025 (2002) [arXiv:hep-ph/0104291].

[43] D. Brommel *et al.* [QCDSF Collaboration and UKQCD Collaboration], "The spin structure of the pion," Phys. Rev. Lett. **101** (2008) 122001 [arXiv:0708.2249 [hep-lat]].

[44] W. Broniowski and E. R. Arriola, "Pion photon transition distribution amplitudes in the spectral quark model," Phys. Lett. B **649** (2007) 49 [arXiv:hep-ph/0701243].

[45] W. Broniowski, E. R. Arriola and K. Golec-Biernat, "Generalized parton distributions of the pion in chiral quark models and their QCD evolution," Phys. Rev. D **77** (2008) 034023. [arXiv:0712.1012 [hep-ph]].

[46] D. A. Bryman, P. Depommier and C. Leroy, "Pi $\to$ E Neutrino, Pi $\to$ E Neutrino Gamma Decays And Related Processes," Phys. Rept. **88** (1982) 151.

[47] M. Burkardt, "Impact parameter dependent parton distributions and off-forward parton distributions for $\zeta \to 0$," Phys. Rev. D **62** (2000) 071503 [Erratum-ibid. D **66** (2002) 119903] [arXiv:hep-ph/0005108].

[48] M. Burkardt, "Impact parameter space interpretation for generalized parton distributions," Int. J. Mod. Phys. A **18** (2003) 173 [arXiv:hep-ph/0207047].

[49] M. Burkardt, "Sivers mechanism for gluons," Phys. Rev. D **69** (2004) 091501; [arXiv:hep-ph/0402014].

[50] M. Burkardt, "Quark correlations and single spin asymmetries," Phys. Rev. D **69** (2004) 057501 [arXiv:hep-ph/0311013].

[51] M. Burkardt, "Transverse deformation of parton distributions and transversity decomposition of angular momentum," Phys. Rev. D **72** (2005) 094020 [arXiv:hep-ph/0505189].

[52] M. Burkardt, "Chromodynamic lensing and transverse single spin asymmetries," Nucl. Phys. A **735**, 185 (2004) [arXiv:hep-ph/0302144] and Ref. therein.

[53] M. Burkardt and B. Hannafious, "Are all Boer-Mulders functions alike?," Phys. Lett. B **658** (2008) 130 [arXiv:0705.1573 [hep-ph]].

[54] e.g., V. D. Burkert, "CLAS12 and its initial physics program at the JLab 12 GeV Upgrade", Talk at the CLAS12 European Workshop February 25-28, 2009- Genova, Italy; or http://www.jlab.org/Hall-B/clas12/Documentation/

[55] S. Chekanov *et al.* [ZEUS Collaboration], "Measurement of deeply virtual Compton scattering at HERA," Phys. Lett. B **573** (2003) 46 [arXiv:hep-ex/0305028].

[56] I. O. Cherednikov, U. D'Alesio, N. I. Kochelev and F. Murgia, "Instanton contribution to the Sivers function," Phys. Lett. B **642**, 39 (2006) [arXiv:hep-ph/0606238].

[57] H. M. Choi, C. R. Ji and L. S. Kisslinger, "Skewed quark distribution of the pion in the light-front quark model," Phys. Rev. D **64** (2001) 093006 [arXiv:hep-ph/0104117].

[58] H. M. Choi, C. R. Ji and L. S. Kisslinger, "Continuity of skewed parton distributions for the pion virtual Compton scattering," Phys. Rev. D **66** (2002) 053011 [arXiv:hep-ph/0204321].

[59] F. E. Close, "An Introduction To Quarks And Partons," *Academic Press/london 1979, 481p*

[60] J. C. Collins, D. E. Soper and G. Sterman, "Factorization of Hard Processes in QCD," Adv. Ser. Direct. High Energy Phys. **5** (1988) 1 [arXiv:hep-ph/0409313].

[61] J. C. Collins, "Fragmentation of transversely polarized quarks probed in transverse momentum distributions," Nucl. Phys. B **396**, 161 (1993) [arXiv:hep-ph/9208213].

[62] J. C. Collins, "Leading-twist single-transverse-spin asymmetries: Drell-Yan and deep-inelastic scattering," Phys. Lett. B **536**, 43 (2002) [arXiv:hep-ph/0204004].

[63] J. C. Collins, A. V. Efremov, K. Goeke, S. Menzel, A. Metz and P. Schweitzer, "Sivers effect in semi-inclusive deeply inelastic scattering," Phys. Rev. D **73**, 014021 (2006) [arXiv:hep-ph/0509076].

[64] J. C. Collins, L. Frankfurt and M. Strikman, "Factorization for hard exclusive electroproduction of mesons in QCD," Phys. Rev. D **56** (1997) 2982 [arXiv:hep-ph/9611433].

[65] J. S. Conway *et al.*, "Experimental Study Of Muon Pairs Produced By 252-Gev Pions On Tungsten," Phys. Rev. D **39** (1989) 92.

[66] A. Courtoy, F. Fratini, S. Scopetta and V. Vento, "A quark model analysis of the Sivers function," Phys. Rev. D **78** (2008) 034002 [arXiv:0801.4347 [hep-ph]].

[67] A. Courtoy and S. Noguera, "The Pion-Photon Transition Distribution Amplitudes in the Nambu-Jona Lasinio Model," Phys. Rev. D **76** (2007) 094026 [arXiv:0707.3366 [hep-ph]].

[68] A. Courtoy and S. Noguera, "Pion-Photon TDAs in the NJL Model," Prog. Part. Nucl. Phys. **61**, 170 (2008) [arXiv:0803.3524 [hep-ph]].

[69] A. Courtoy and S. Noguera, "Pion-Photon Transition Distribution Amplitudes," AIP Conf. Proc. **1038** (2008) 249 [arXiv:0804.4337 [hep-ph]].

[70] A. Courtoy and S. Noguera, "Enhancement effects in exclusive $\pi\pi$ and $\rho\pi$ production in $\gamma^*\gamma$ scattering," Phys. Lett. **B675**(2009) 3842, [arXiv:0811.0550 [hep-ph]].

[71] A. Courtoy and S. Noguera, in preparation.

[72] A. Courtoy, S. Scopetta and V. Vento, "Model calculations of the Sivers function satisfying the Burkardt Sum Rule," Phys. Rev. D **79**, 074001 (2009) [arXiv:0811.1191 [hep-ph]].

[73] A. Courtoy, S. Scopetta and V. Vento, in preparation.

[74] U. D'Alesio and F. Murgia, "Azimuthal and Single Spin Asymmetries in Hard Scattering Processes," arXiv:0712.4328 [hep-ph], to be published in Prog. Part. Nucl. Phys..

[75] U. D'Alesio and F. Murgia, "Single spin asymmetries in inclusive hadron production from SIDIS to hadronic collisions: universality and phenomenology," arXiv:0712.4240 [hep-ph].

[76] R. M. Davidson and E. Ruiz Arriola, "Structure Functions Of Pseudoscalar Mesons In The SU(3) Njl Model," Phys. Lett. B **348** (1995) 163.

[77] R. M. Davidson and E. Ruiz Arriola, "Parton distributions functions of pion, kaon and eta pseudoscalar mesons in the NJL model," Acta Phys. Polon. B **33** (2002) 1791 [arXiv:hep-ph/0110291].

[78] A. De Rujula, H. Georgi and S. L. Glashow, "Hadron Masses In A Gauge Theory," Phys. Rev. D **12**, 147 (1975).

[79] M. Diehl, "Generalized parton distributions with helicity flip," Eur. Phys. J. C **19** (2001) 485 [arXiv:hep-ph/0101335].

[80] M. Diehl, T. Feldmann, R. Jakob and P. Kroll, "The overlap representation of skewed quark and gluon distributions," Nucl. Phys. B **596** (2001) 33 [Erratum-ibid. B **605** (2001) 647] [arXiv:hep-ph/0009255].

[81] M. Diehl, "Generalized parton distributions," Phys. Rept. **388** (2003) 41 [arXiv:hep-ph/0307382].

[82] M. Diehl and Ph. Hagler, "Spin densities in the transverse plane and generalized transversity distributions," Eur. Phys. J. C **44** (2005) 87 [arXiv:hep-ph/0504175].

[83] M. Diehl, A. Manashov and A. Schafer, "Generalized parton distributions for the nucleon in chiral perturbation theory," Eur. Phys. J. A **31** (2007) 335 [arXiv:hep-ph/0611101].

[84] P. A. M. Dirac, "Forms Of Relativistic Dynamics," Rev. Mod. Phys. **21** (1949) 392.

[85] Y. L. Dokshitzer, "Calculation Of The Structure Functions For Deep Inelastic Scattering And E+ E- Annihilation By Perturbation Theory In Quantum Chromodynamics. (In Russian)," Sov. Phys. JETP **46** (1977) 641 [Zh. Eksp. Teor. Fiz. **73** (1977) 1216].

[86] J. F. Donoghue, E. Golowich and B. R. Holstein, "Dynamics Of The Standard Model," Camb. Monogr. Part. Phys. Nucl. Phys. Cosmol. **2** (1992) 1.

[87] A. E.Dorokhov, A. E. Radzhabov and M. K. Volkov, "Pion Radii in the Nonlocal Chiral Quark Model," Eur. Phys. J. A **21**, 155-159 (2004).

[88] A. V. Efremov and A. V. Radyushkin, "Factorization And Asymptotical Behavior Of Pion Form-Factor In QCD," Phys. Lett. B **94** (1980) 245.

[89] R. K. Ellis, H. Georgi, M. Machacek, H. D. Politzer and G. G. Ross, "Factorization And The Parton Model In QCD," Phys. Lett. B **78** (1978) 281; "Perturbation Theory And The Parton Model In QCD," Nucl. Phys. B **152** (1979) 285.

[90] R. P. Feynman, "Very high-energy collisions of hadrons," Phys. Rev. Lett. **23** (1969) 1415.

[91] L. L. Frankfurt, M. V. Polyakov and M. Strikman, "N –¿ Delta DVCS, exclusive DIS processes and skewed quark distributions in large N(c) limit," arXiv:hep-ph/9808449.

[92] L. L. Frankfurt, P. V. Pobylitsa, M. V. Polyakov and M. Strikman, "Hard exclusive pseudoscalar meson electroproduction and spin structure of a nucleon," Phys. Rev. D **60** (1999) 014010 [arXiv:hep-ph/9901429].

[93] F. Fratini, Master Thesis, University of Perugia (2008) unpublished.

[94] A. Freund and M. F. McDermott, "Next-to-leading order evolution of generalized parton distributions for HERA and HERMES," Phys. Rev. D **65**, 056012 (2002) [Erratum-ibid. D **66**, 079903 (2002)]. [arXiv:hep-ph/0106115]. .See the web page http://durpdg.dur.ac.uk/hepdata/dvcs.html

[95] H. Fritzsch, M. Gell-Mann and H. Leutwyler, "Advantages Of The Color Octet Gluon Picture," Phys. Lett. B **47** (1973) 365.

[96] M. Gell-Mann, "A Schematic Model Of Baryons And Mesons," Phys. Lett. **8** (1964) 214.

[97] M. M. Giannini, "Electromagnetic excitations in the constituent quark model," Rept. Prog. Phys. **54**, 453 (1990).

[98] M. Gluck, E. Reya and A. Vogt, "Dynamical Parton Distributions Of The Proton And Small X Physics," Z. Phys. C **67** (1995) 433.

[99] M. Gluck, E. Reya and I. Schienbein, "Pionic parton distributions revisited," Eur. Phys. J. C **10** (1999) 313 [arXiv:hep-ph/9903288].

[100] M. Gluck, E. Reya and I. Schienbein, "Radiatively generated parton distributions of real and virtual photons," Phys. Rev. D **60** (1999) 054019 [Erratum-ibid. D **62** (2000) 019902] [arXiv:hep-ph/9903337].

[101] K. Goeke, M. V. Polyakov and M. Vanderhaeghen, "Hard exclusive reactions and the structure of hadrons," Prog. Part. Nucl. Phys. **47** (2001) 401 [arXiv:hep-ph/0106012].

[102] K. Goeke, S. Meissner, A. Metz and M. Schlegel, "Checking the Burkardt sum rule for the Sivers function by model calculations," Phys. Lett. B **637**, 241 (2006) [arXiv:hep-ph/0601133].

[103] K. J. Golec-Biernat and A. D. Martin, "Off-diagonal parton distributions and their evolution," Phys. Rev. D **59** (1999) 014029 [arXiv:hep-ph/9807497].

[104] V. N. Gribov and L. N. Lipatov, "Deep Inelastic E P Scattering In Perturbation Theory," Sov. J. Nucl. Phys. **15** (1972) 438 [Yad. Fiz. **15** (1972) 781].

[105] J. Gronberg *et al.* [CLEO Collaboration], Phys. Rev. D **57** (1998) 33 [arXiv:hep-ex/9707031].

[106] D. J. Gross and F. Wilczek, "ULTRAVIOLET BEHAVIOR OF NON-ABELIAN GAUGE THEORIES," Phys. Rev. Lett. **30** (1973) 1343.

[107] P. A. M. Guichon and M. Vanderhaeghen, "Virtual Compton scattering off the nucleon," Prog. Part. Nucl. Phys. **41**, 125 (1998) [arXiv:hep-ph/9806305].

[108] M. Guidal, "Generalized Parton Distributions And Deep Virtual Compton Scattering," Prog. Part. Nucl. Phys. **61** (2008) 89.

[109] T. Horn *et al* [Jefferson Lab F(pi)-2 Collaboration], "Determination of the Charged Pion Form Factor at Q2=1.60 and 2.45 (GeV/c)2," Phys. Rev. Lett. **97**, 192001 (2006) [arXiv:nucl-ex/0607005].

[110] N. Isgur and G. Karl, "P Wave Baryons In The Quark Model," Phys. Rev. D **18**, 4187 (1978);

[111] N. Isgur and G. Karl, "Positive Parity Excited Baryons In A Quark Model With Hyperfine Interactions," Phys. Rev. D **19**, 2653 (1979) [Erratum-ibid. D **23**, 817 (1981)].

[112] C. Itzykson and J. B. Zuber, "Quantum Field Theory" (MacGraw-Hill, New York, 1980)

[113] R. L. Jaffe, "Deep Inelastic Structure Functions In An Approximation To The Bag Theory," Phys. Rev. D **11** (1975) 1953.

[114] R. L. Jaffe, "Spin, twist and hadron structure in deep inelastic processes," arXiv:hep-ph/9602236.

[115] R. L. Jaffe and X. D. Ji, "Chiral odd parton distributions and polarized Drell-Yan," Phys. Rev. Lett. **67** (1991) 552.

[116] R. L. Jaffe and G. G. Ross, "Normalizing The Renormalization Group Analysis Of Deep Inelastic Leptoproduction," Phys. Lett. B **93**, 313 (1980).

[117] X. D. Ji, "Gauge invariant decomposition of nucleon spin," Phys. Rev. Lett. **78** (1997) 610 [arXiv:hep-ph/9603249].

[118] X. D. Ji, "Deeply-virtual Compton scattering," Phys. Rev. D **55** (1997) 7114 [arXiv:hep-ph/9609381].

[119] X. D. Ji and J. Osborne, "One-loop corrections and all order factorization in deeply virtual Compton scattering," Phys. Rev. D **58** (1998) 094018 [arXiv:hep-ph/9801260].

[120] X. D. Ji, "Off-forward parton distributions," J. Phys. G **24** (1998) 1181 [arXiv:hep-ph/9807358].

[121] X. D. Ji and F. Yuan, "Parton distributions in light-cone gauge: Where are the final-state interactions?," Phys. Lett. B **543**, 66 (2002) [arXiv:hep-ph/0206057].

[122] Z. B. Kang and J. W. Qiu, "Evolution of twist-3 multi-parton correlation functions relevant to single transverse-spin asymmetry," Phys. Rev. D **79**, 016003 (2009) [arXiv:0811.3101 [hep-ph]].

[123] N. Kivel and L. Mankiewicz, "Conformal string operators and evolution of skewed parton distributions," Nucl. Phys. B **557** (1999) 271 [arXiv:hep-ph/9903531].

[124] N. Kivel and L. Mankiewicz, "On scale dependence of QCD string operators," Phys. Lett. B **458** (1999) 338 [arXiv:hep-ph/9905342].

[125] S. P. Klevansky, "The Nambu-Jona-Lasinio model of quantum chromodynamics," Rev. Mod. Phys. **64** (1992) 649.

[126] J. B. Kogut and D. E. Soper, "Quantum Electrodynamics In The Infinite Momentum Frame," Phys. Rev. D **1** (1970) 2901.

[127] P. Kotko and M. Praszalowicz, "Pion-to-photon transition distribution amplitudes in the non-local chiral quark model," arXiv:0803.2847 [hep-ph].

[128] A. M. Kotzinian and P. J. Mulders, "Probing transverse quark polarization via azimuthal asymmetries in leptoproduction," Phys. Lett. B **406** (1997) 373 [arXiv:hep-ph/9701330].

[129] J. M. Laget *et al.*, "ELFE (Electron Laboratory for Europe): Physics motivations,"

[130] H. L. Lai *et al.*, "Improved parton distributions from global analysis of recent deep inelastic scattering and inclusive jet data," Phys. Rev. D **55** (1997) 1280 [arXiv:hep-ph/9606399].

[131] J. P. Lansberg, B. Pire and L. Szymanowski, "Exclusive meson pair production in gamma* gamma scattering at small momentum transfer," Phys. Rev. D **73** (2006) 074014 [arXiv:hep-ph/0602195].

[132] J. P. Lansberg, B. Pire and L. Szymanowski, "Backward DVCS and proton to photon transition distribution amplitudes," Nucl. Phys. A **782** (2007) 16 [arXiv:hep-ph/0607130].

[133] J. P. Lansberg, B. Pire and L. Szymanowski, "Transition Distribution Amplitudes," arXiv:0709.2567 [hep-ph].

[134] J. P. Lansberg, B. Pire and L. Szymanowski, "Production of a pion in association with a high-Q2 dilepton pair in antiproton-proton annihilation at GSI-FAIR," Phys. Rev. D **76** (2007) 111502 [arXiv:0710.1267 [hep-ph]].

[135] J. P. Lansberg, B. Pire and L. Szymanowski, "Hard exclusive electroproduction of a pion in the backward region," Phys. Rev. D **75** (2007) 074004, [Erratum-ibid. D **77** (2008) 019902] [arXiv:hep-ph/0701125].

[136] J. P. Lansberg, Private Communication.

[137] G. Laveissiere *et al.* [Jefferson Lab Hall A Collaboration], "Virtual Compton Scattering and Neutral Pion Electroproduction in the Resonance Region up to the Deep Inelastic Region at Backward Angles," Phys. Rev. C **79** (2009) 015201 [arXiv:0811.3867 [nucl-ex]].

[138] G. P. Lepage and S. J. Brodsky, "Exclusive Processes In Quantum Chromodynamics: Evolution Equations For Hadronic Wave Functions And The Form-Factors Of Mesons," Phys. Lett. B **87** (1979) 359;

[139] G. P. Lepage and S. J. Brodsky, SLAC-PUB-2294; "Exclusive Processes And The Exclusive Inclusive Connection In Quantum Chromodynamics,"

[140] G. P. Lepage and S. J. Brodsky, "Exclusive Processes In Perturbative Quantum Chromodynamics," Phys. Rev. D **22** (1980) 2157.

[141] L. N. Lipatov, "The parton model and perturbation theory," Sov. J. Nucl. Phys. **20**, 94 (1975) [Yad. Fiz. **20**, 181 (1974)].

[142] Z. Lu and B. Q. Ma, "Sivers function in light-cone quark model and azimuthal spin asymmetries in pion electroproduction," Nucl. Phys. A **741**, 200 (2004) [arXiv:hep-ph/0406171].

[143] Z. Lu and B. Q. Ma, "Non-zero transversity distribution of the pion in a quark-spectator antiquark model," Phys. Rev. D **70** (2004) 094044 [arXiv:hep-ph/0411043].

[144] Z. Lu and I. Schmidt, "Connection between the Sivers function and the anomalous magnetic moment," Phys. Rev. D **75**, 073008 (2007) [arXiv:hep-ph/0611158].

[145] L. Mankiewicz, G. Piller and A. Radyushkin, "Hard exclusive electroproduction of pions," Eur. Phys. J. C **10** (1999) 307 [arXiv:hep-ph/9812467].

[146] S. Meissner, A. Metz and K. Goeke, "Relations between generalized and transverse momentum dependent parton distributions," Phys. Rev. D **76**, 034002 (2007) [arXiv:hep-ph/0703176].

[147] M. Moreno, "Pion Radiative Decay, One Loop Models And Light Quarks," Phys. Rev. D **16** (1977) 720.

[148] D. Mueller, D. Robaschik, B. Geyer, F. M. Dittes and J. Horejsi, "Wave functions, evolution equations and evolution kernels from light-ray operators of QCD," Fortsch. Phys. **42** (1994) 101 [arXiv:hep-ph/9812448].

[149] P. J. Mulders and R. D. Tangerman, "The complete tree-level result up to order 1/Q for polarized deep-inelastic leptoproduction," Nucl. Phys. B **461** (1996) 197 [Erratum-ibid. B **484** (1997) 538] [arXiv:hep-ph/9510301].

[150] T. Muta, "Foundations of quantum chromodynamics. Second edition," World Sci. Lect. Notes Phys. **57** (1998) 1.

[151] Y. Nambu and G. Jona-Lasinio, "Dynamical model of elementary particles based on an analogy with superconductivity. I," Phys. Rev. **122** (1961) 345.

[152] Y. Nambu and G. Jona-Lasinio, "Dynamical model of elementary particles based on an analogy with superconductivity. II," Phys. Rev. **124** (1961) 246.

[153] S. Noguera, L. Theussl and V. Vento, "Generalized parton distributions of the pion in a Bethe-Salpeter approach," Eur. Phys. J. A **20** (2004) 483 [arXiv:nucl-th/0211036].

[154] S. Noguera, S. Scopetta and V. Vento, "Relativity and constituent quark structure in model calculations of parton distributions," Phys. Rev. D **70** (2004) 094018 [arXiv:hep-ph/0409059].

[155] S. Noguera, "Non local lagrangians. I: The pion," Int. J. Mod. Phys. E **16** (2007) 97 [arXiv:hep-ph/0502171].

[156] S. Noguera and V. Vento, "Pion parton distributions in a non local Lagrangian," Eur. Phys. J. A **28** (2006) 227 [arXiv:hep-ph/0505102].

[157] P. Pascual and R. Tarrach, "QCD: Renormalization For The Practitioner," Lect. Notes Phys. **194** (1984) 1.

[158] B. Pasquini and S. Boffi, "Virtual meson cloud of the nucleon and generalized parton distributions," Phys. Rev. D **73** (2006) 094001 [arXiv:hep-ph/0601177].

[159] B. Pasquini, M. Pincetti and S. Boffi, "Parton content of the nucleon from distribution amplitudes and transition distribution amplitudes," arXiv:0905.4018 [hep-ph].

[160] M. Penttinen, M. V. Polyakov and K. Goeke, "Helicity skewed quark distributions of the nucleon and chiral symmetry," Phys. Rev. D **62** (2000) 014024 [arXiv:hep-ph/9909489].

[161] M. E. Peskin and D. V. Schroeder, "An Introduction To Quantum Field Theory," *Reading, USA: Addison-Wesley (1995) 842 p*

[162] M. Pincetti, B. Pasquini and S. Boffi, "Nucleon to Pion Transition Distribution Amplitudes in a Light-Cone Quark Model," arXiv:0807.4861 [hep-ph].

[163] M. Pincetti, "Exploring the Partonic Structure of the Nucleon on the Light-Cone," Ph.D. Thesis, Pavia University, 2008.

[164] B. Pire, J. Soffer and O. Teryaev, "Positivity constraints for off-forward parton distributions," Eur. Phys. J. C **8** (1999) 103 [arXiv:hep-ph/9804284].

[165] B. Pire and L. Szymanowski, "Hadron annihilation into two photons and backward VCS in the scaling regime of QCD," Phys. Rev. D **71** (2005) 111501 [arXiv:hep-ph/0411387].

[166] P. V. Pobylitsa, "Inequalities for generalized parton distributions H and E," Phys. Rev. D **65** (2002) 077504 [arXiv:hep-ph/0112322];

[167] P. V. Pobylitsa, "Disentangling positivity constraints for generalized parton distributions," Phys. Rev. D **65** (2002) 114015 [arXiv:hep-ph/0201030];

[168] P. V. Pobylitsa, "Positivity bounds on generalized parton distributions in impact parameter representation," Phys. Rev. D **66** (2002) 094002 [arXiv:hep-ph/0204337].

[169] H. D. Politzer, "RELIABLE PERTURBATIVE RESULTS FOR STRONG INTERACTIONS?," Phys. Rev. Lett. **30** (1973) 1346.

[170] M. V. Polyakov, "Study of two-pion light-cone distribution amplitudes in the resonance region and at low energies," Nucl. Phys. B **555** (1999) 231 [arXiv:hep-ph/9809483].

[171] M. V. Polyakov and C. Weiss, "Skewed and double distributions in pion and nucleon," Phys. Rev. D **60** (1999) 114017 [arXiv:hep-ph/9902451].

[172] M. V. Polyakov and A. G. Shuvaev, "On 'dual' parametrizations of generalized parton distributions," arXiv:hep-ph/0207153.

[173] A. V. Radyushkin, "Scaling Limit of Deeply Virtual Compton Scattering," Phys. Lett. B **380** (1996) 417 [arXiv:hep-ph/9604317].

[174] A. V. Radyushkin, "Nonforward parton distributions," Phys. Rev. D **56** (1997) 5524 [arXiv:hep-ph/9704207].

[175] A. V. Radyushkin, "Symmetries and structure of skewed and double distributions," Phys. Lett. B **449** (1999) 81 [arXiv:hep-ph/9810466].

[176] A. V. Radyushkin, "Double distributions and evolution equations," Phys. Rev. D **59** (1999) 014030 [arXiv:hep-ph/9805342].

[177] A. V. Radyushkin and C. Weiss, "DVCS amplitude at tree level: Transversality, twist-3, and factorization," Phys. Rev. D **63** (2001) 114012 [arXiv:hep-ph/0010296].

[178] J. Roche, C. E. Hyde-Wright, B. Michel, C. Munoz Camacho, *et al.* [Hall A Collaboration], "Measurements of the electron-helicity dependent cross sections of deeply virtual Compton scattering with CEBAF at 12-GeV," arXiv:nucl-ex/0609015.

[179] E. Ruiz Arriola and W. Broniowski, "Pion light-cone wave function and pion distribution amplitude in the Nambu-Jona-Lasinio model," Phys. Rev. D **66** (2002) 094016 [arXiv:hep-ph/0207266].

[180] E. Ruiz Arriola, "Pion structure at high and low energies in chiral quark models. ((V))," Acta Phys. Polon. B **33** (2002) 4443 [arXiv:hep-ph/0210007].

[181] E. Ruiz Arriola and W. Broniowski, "Spectral quark model and low-energy hadron phenomenology," Phys. Rev. D **67** (2003) 074021 [arXiv:hep-ph/0301202].

[182] J. J. Sakurai, "Theory of strong interactions," Annals Phys. **11** (1960) 1.

[183] J. J. Sakurai, "Currents and Mesons," The University of Chicago Press, Chicago, Ill., 1969.

[184] G. Schnell, "Highlights from Hermes",Talk at the CLAS12 European Workshop February 25-28, 2009- Genova, Italy

[185] A. W. Schreiber, A. I. Signal and A. W. Thomas, "Structure Functions In The Bag Model," Phys. Rev. D **44** (1991) 2653.

[186] S. Scopetta, V. Vento and M. Traini, "Towards a unified picture of constituent and current quarks," Phys. Lett. B **421** (1998) 64 [arXiv:hep-ph/9708262].

[187] S. Scopetta, V. Vento and M. Traini, "Polarized structure functions in a constituent quark scenario," Phys. Lett. B **442** (1998) 28 [arXiv:hep-ph/9804302].

[188] A. I. Signal and A. W. Thomas, "CALCULATION OF QUARK DISTRIBUTION FUNCTIONS USING BAG MODEL WAVE FUNCTIONS," Phys. Rev. D **40** (1989) 2832.

[189] D. W. Sivers, "Single Spin Production Asymmetries From The Hard Scattering Of Point-Like Constituents," Phys. Rev. D **41**, 83 (1990).

[190] D. W. Sivers, "Hard scattering scaling laws for single spin production asymmetries," Phys. Rev. D **43**, 261 (1991).

[191] S. Stepanyan *et al.* [CLAS Collaboration], "First observation of exclusive deeply virtual Compton scattering in polarized electron beam asymmetry measurements," Phys. Rev. Lett. **87** (2001) 182002 [arXiv:hep-ex/0107043].

[192] P. J. Sutton, A. D. Martin, R. G. Roberts and W. J. Stirling, "Parton distributions for the pion extracted from Drell-Yan and prompt photon experiments," Phys. Rev. D **45** (1992) 2349.

[193] V. Tadevosyan *et al.* [Jefferson Lab F(pi) Collaboration], "Determination of the pion charge form factor for $Q^2 = 0.60-1.60\mathrm{GeV}^2$," Phys. Rev. C **75** (2007) 055205 [arXiv:nucl-ex/0607007].

[194] B. C. Tiburzi and G. A. Miller, "Exploring skewed parton distributions with two-body models on the light front. I: Bimodality," Phys. Rev. C **64** (2001) 065204 [arXiv:hep-ph/0104198].

[195] B. C. Tiburzi and G. A. Miller, "Exploring skewed parton distributions with two-body models on the light front. II: Covariant Bethe-Salpeter approach," Phys. Rev. D **65** (2002) 074009 [arXiv:hep-ph/0109174].

[196] B. C. Tiburzi and G. A. Miller, "Current in the light-front Bethe-Salpeter formalism. I: Replacement of non-wave function vertices," Phys. Rev. D **67** (2003) 054014 [arXiv:hep-ph/0210304].

[197] B. C. Tiburzi and G. A. Miller, "Current in the light-front Bethe-Salpeter formalism. II: Applications," Phys. Rev. D **67** (2003) 054015 [arXiv:hep-ph/0210305].

[198] B. C. Tiburzi and G. A. Miller, "Generalized parton distributions and double distributions for q anti-q pions," Phys. Rev. D **67** (2003) 113004 [arXiv:hep-ph/0212238].

[199] B. C. Tiburzi, "Estimates for pion photon transition distributions," Phys. Rev. D **72** (2005) 094001 [arXiv:hep-ph/0508112].

[200] M. Traini, A. Mair, A. Zambarda and V. Vento, "Constituent quarks and parton distributions," Nucl. Phys. A **614** (1997) 472.

[201] M. Vanderhaeghen, P. A. M. Guichon and M. Guidal, "Deeply virtual electroproduction of photons and mesons on the nucleon: Leading order amplitudes and power corrections," Phys. Rev. D **60**, 094017 (1999) [arXiv:hep-ph/9905372].

[202] A. Van Dyck, T. Van Cauteren and J. Ryckebusch, "Support of generalized parton distributions in Bethe-Salpeter models of hadrons," arXiv:0710.2271 [hep-ph].

[203] A. Van Dyck, "Generalized parton distributions of pseudoscalar mesons in a relativistic Bethe-Salepeter framework", Ph. D. Thesis, Ghent University, Belgium, 2008.

[204] A. Van Dyck, T. Van Cauteren, J. Ryckebusch and B. C. Metsch, "Generalized parton distributions of pseudoscalar mesons in a covariant constituent quark model," arXiv:0808.0429 [hep-ph].

[205] W. Vogelsang and F. Yuan, "Next-to-leading Order Calculation of the Single Transverse Spin Asymmetry in the Drell-Yan Process," arXiv:0904.0410 [hep-ph].

[206] F. Yuan, "Sivers function in the MIT bag model," Phys. Lett. B **575** (2003) 45 [arXiv:hep-ph/0308157].

[207] G. Zweig, "An SU(3) Model For Strong Interaction Symmetry And Its Breaking," "An SU(3) Model For Strong Interaction Symmetry And Its Breaking. 2"

Remerciements

Il est 14h27, nous avons du descendre la persienne de la salle de réunions du Département. Le soleil frappe déjà, le café devient trop chaud assis dans les fauteuils trop confortables.

De façon exceptionelle, mon humeur a changé aujourd'hui. Comme de coutûme, Joel, vers 13h06, a fait le tour des bureaux (où devrais-je dire, une sélection bien précise de bureaux) accompagné de son air enjoué ; et avec ce sourire qui ne s'en va jamais, s'est exclamé "Ya sé que me vas a decir que No, pero te hago la misma pregunta : Te vienes a comer?". Je devais effectivement être de meilleure humeur ; j'ai accepté d'aller jusqu'à Farmacia, trouver une table, attendre, crier pour s'entendre, se faire entendre. Vicent, Joel, Vincent et les postdocs attendent sur le palier pendant que Carlos réchauffe ses petits plats au micro-ondes. Je fais la file moi aussi ; on papotte laissant insouciamment tiédir le dîner. Il est alors 13h24, nous attendons Catalina.

Maintenant après ce café, somnolant, j'écris mes remerciements. Vicente passe dans le couloir, sort une blague à quelqu'un qui, sans doute, est à l'autre bout du couloir. Mais sa voix porte loin et la blague est plutôt destinée à tout le monde. Santiago vient chercher son courier en rigolant et me jette cet éternel "Qué hay?". Je sais déjà, que lorsque je me dirigerai vers mon bureau, une fois que j'en aurai assez de ce fauteuil trop confortable, je croiserai Joannis perdu dans ses pensées et récupérant sa balle orange, ou celle multicolore, qu'il aura lancée dans le couloir, négligemment.

Tel est le quotidien dans ce Département ; et dans beaucoup d'autres, sans doute. Car s'il est une chose que l'on apprend vite, c'est bien à associer à chaque personnage de l'une de nos "vies" à d'autres de périodes anciennes, vécues, nostalgiques mais aussi à venir. Pourtant chacun d'entre eux est irremplaçable.

Et écrivant cette dernière phrase, me prend cette idée saugrenue d'avoir désiré pouvoir écrire ces quelques lignes ailleurs, regardant, tour à tour, le jardin de Marie et Arthur, et leurs poules, et l'Opéra et la gare des Guillemins. Dans cet endroit magique, entre les murailles et les cerisiers, entre les repas dans le jardin et les sourires de ses gens, digne des paroles d'une chanson bucolique, j'ai oublié une partie consciente et entière de mon innocence. Et si la larme coule, c'est sans doute de bonheur du vécu avec eux.

Mais je divague, élucubre au lieu de conter les innombrables personnages qui ont fait des ces années passées à Valencia l'histoire de cette thèse. Car à chaque morceaux d'équation, à chaque pas et à chaque compilation de programme sont associés des moments d'intranquilité et puis, de satisfaction partagés, souvent inconsciemment, avec mon entourage. Je pense qu'Aymeric serait capable de reconstituer l'historique des passages délicats, de dresser l'inventaire des e-mails encourageants ou encore des referee reports. Bouteilles de vin, tâches ménagères, y a-t'il de plus beaux indices ? Il aura su parfois trouver la juste diversion, ou simplement il aura su souvent remettre dans leur contexte des détails sans importance à l'échelle d'une vie.

Et parlant de ces e-mails encourageants ou résignés, il me vient à l'esprit les e-mails de Sergio, ceux que Vicente qualifie de "emails para echarse a llorar". Les e-mails de Sergio entrent dans une toute autre catégorie : celle des e-mails déprimants et plein de l'envie de pouvoir partager avec nous ce sentiment de déception face à la non compréhension du moment. Et je nous imagine bien devant le tableau de son bureau écrivant les nouvelles idées, ou en long brainstorming quand l'équipe était

au complet. Ce brainstorming aurait sans doute terminé au Centodieci devant un aperitivo bien mérité.

Mais je divague encore.
Le parcours de ces 4 années est aussi ponctué de moments de semblant de vie sociale que nous avons réussi à recréer dans le Département, ... entre guiris ! Il est fort possible qu'aujourd'hui, justement aujourd'hui, l'envie me prenne de suggérer d'aller boire un verre. Et parmi les personnages non négligeables de l'histoire de cette thèse, il est impossible de ne pas mentionner les cacique con limón bus en compagnie de Cristina et Joannis. Ou encore le zumo de melocotón de Catalina. Autant d'acteurs de second rôle qui émèchent ajoutant la nécessaire touche de gaieté.

Mais, par dessus tout, cette thèse a été ponctuée de longs moments de solitude.
Car souvent perchée sur mon vélo, souriant à tout vent, il me plaît de regarder les gens sur les trottoirs (il faut dire que je connais le chemin par coeur). Max aurait dit que je souriais pour une raison que seule pouvait comprendre la toute petite aurore, la toute petite cachée derrière la montagne de points d'interrogation à laquelle a notablement contribué cette thèse. Mais il ne savait sans doute pas que, telle une nouvelle de Cortázar, l'histoire de cette raison résidait dans les jeux de regards. Le sourire d'un inconnu se reflète sur la vitre du métro ; il suffit d'une seconde, les règles s'imposent presque d'elles-même ; ça devient souvent un rayon de soleil qui illumine une journée. Mais parfois le jeu devient grisant. L'on s'y prend et s'y perd ; et se retrouve à vouloir déchiffrer, entre deux corrections grammaticales de mon anglais, les paroles d'un obscur *In power we entrust the love advocated*. Il faudra que je lui raconte comment, un beau jour, au bon détour du couloir, sans le vouloir, il m' a rappelé ce *Manuscrito hallado en un bolsillo*. [1]

J'essaye de réunir, avant de sombrer au confort du fauteuil, les vrais remerciements. Il est évident que mon directeur de thèse, Santiago, est premier sur la liste. Pour sa patience, ses conseils, le temps qu'il m'a consacré et ses anecdotes, je lui suis très reconnaissante. Le deuxième est sans dire Vicente, pour les calculs à vérifier (il faut se forger !), pour les conseils autres que concernant des restaurants et pour l'avoir entendu répéter des dizaines de fois, sans s'en lasser, que les femmes avaient de nos jours plus d'opportinutés que les hommes et qu'il faudrait savoir en tirer parti (point sur lequel je ne suis pas tout à fait d'accord, mais le débat n'a pas sa place ici). Mes remerciements vont aussi à Sergio pour son immense patience et pour l'engagement en ce qui concerne nos travaux.

Dans la "nouvelle génération" que j'ai cru un instant enjouée et passionée, je remercie les jeunes physiciens desquels j'ai partagé les intérêts et avec qui j'ai passé d'agréables moments à divaguer, encore une fois, sur la structure des hadrons. De Filippo, Annelies et Manuel, aucun n'aura poursuivi cette quête. Sommes-nous donc comme Don Quijote à nous battre contre des moulins ?

Il est quelques heures plus tard. Il me semble avoir oublié comment remercier. Mais cette bonne humeur me poursuit : avec ces dernières lignes, je finis ma thèse !

[1] Je ne pouvais pas écrire ces remerciements en anglais. Max ne pouvait pas me les corriger, évidemment !